May, 1981

LIDS-TH-1093

Research Supported By:

Department of Energy
Contract DE-AC01-78RA03395

NASA Ames Research Center
Grant NGL-22-009-124

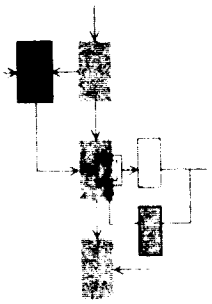

PRACTICAL ROBUSTNESS MEASURES IN MULTIVARIABLE CONTROL SYSTEM ANALYSIS

Norman August Lehtomaki

Laboratory for Information and Decision Systems

MASSACHUSETTS INSTITUTE OF TECHNOLOGY, CAMBRIDGE, MASSACHUSETTS 02139

May, 1981 LIDS-TH-1093

PRACTICAL ROBUSTNESS MEASURES IN MULTIVARIABLE CONTROL SYSTEM ANALYSIS

by

Norman August Lehtomaki

This report is based on the unaltered thesis of Norman August Lehtomaki, submitted in partial fulfillment of the requirements for the degree of Doctor of Philosopy at the Massachusetts Institute of Technology in May 1981. The research was conducted at the M.I.T. Laboratory for Information and Decision Systems with support provided by the U.S. Department of Energy under contract DE-AC01-78RA03395 and by the NASA Ames Research Center under grant NGL-22-009-124.

Laboratory for Information and Decision Systems
Massachusetts Institute of Technology
Cambridge, MA 02139

PRACTICAL ROBUSTNESS MEASURES IN MULTIVARIABLE CONTROL SYSTEM ANALYSIS

by

Norman August Lehtomaki

B.S.E.E., Michigan State University
(1974)

S.M., Massachusetts Institute of Technology
(1978)

E.E., Massachusetts Institute of Technology
(1979)

SUBMITTED IN PARTIAL FULLFILLMENT
OF THE REQUIREMENTS FOR THE
DEGREE OF

DOCTOR OF PHILOSOPHY

at the

MASSACHUSETTS INSTITUTE OF TECHNOLOGY

May 1981

Signature of the Author..Norman A. Lehtomaki.....
Department of Electrical Engineering and Computer Science, May 1, 1981

Certified by..Michael Athans.....
Michael Athans
Thesis Supervisor

Accepted by.....
Arthur C. Smith
Chairman, Departmental Graduate Committee

PRACTICAL ROBUSTNESS MEASURES IN MULTIVARIABLE CONTROL SYSTEM ANALYSIS

by

Norman August Lehtomaki

Submitted to the Department of Electrical Engineering and Computer Science on May 1, 1981 in partial fulfillment of the requirements for the Degree of Doctor of Philosophy.

ABSTRACT

The robustness of the stability of multivariable linear time-invariant feedback control systems with respect to model uncertainty is considered using frequency domain criteria. Available and new robustness tests are unified under a common framework based on the nature and structure of model errors. These results are derived using a multivariable version of Nyquist's stability theorem in which the minimum singular value of the return difference transfer matrix is shown to be the multivariable generalization of the distance to the critical point on a single-input, single-output (SISO) Nyquist diagram. Using the return difference transfer matrix a very general robustness theorem is presented from which all of the robustness tests dealing with specific model errors may be derived. These latter robustness tests regarding the stability of the feedback system under model variations may be divided into two categories: (a) those that use only the magnitude of the model error and (b) those that use some aspect of the model error structure, in addition to its magnitude. The robustness tests that explicitly utilize model error structure are able to guarantee feedback system stability in the face of model errors of larger magnitude than those robustness that do not utilize model error structure and thus represent an improvement of these latter robustness tests.

The robustness of Linear-Quadratic-Gaussian (LQG) control systems are analyzed via this robustness theory and multiloop stability margins are presented; in particular, a new type of margin, a crossfeed margin, is introduced. Other frequency domain analysis and design techniques are also briefly discussed and their relation to the present robustness analysis is examined.

Thesis Supervisor: Dr. Michael Athans
Title: Professor of Systems Science and Engineering

ACKNOWLEDGEMENTS

I would like to express my deep appreciation to Professor Michael Athans for his guidance throughout the course of this research. His thorough and painstaking reading and rereading of several drafts of this thesis and his valuable suggestions for its improvement are gratefully acknowledged.

Dr. Nils Sandell Jr., and Professor Gunter Stein deserve special thanks. Their contributions to the development of my understanding of the thesis subject have proved invaluable. This work has also benefitted greatly from the many technical discussions with Dr. David Castanon and Professor Bernard Levy. Their help is greatly appreciated.

I am also especially grateful to Dr. Sherman Chan for the many arguments and questions he advanced to clarify my muddled thinking on many particular aspects of this work. Two other classmates, Mr. James Lewis and Mr. Ricky Lee, have also had a great impact on the development of many of the ideas expressed in this work.

Mr. Norman Darling and Mr. Arthur Giordani are to be thanked for their fine art work. I am also deeply thankful for the diligent and excellent typing of Ms. Margaret Flaherty and Ms. Fifa Monserrate that enabled a timely completion of this manuscript.

Moreover, I would like to express my deepest gratitude and admiration for Darless, my wife. She encouraged me when I was discouraged, and worked very hard to relieve me of many of my responsibilities to allow me more time for this work. Most of all, I am thankful for her stedfast and abiding love.

This research was conducted at the MIT Laboratory for Information and Decisions Systems, with support provided by the U.S. Department of Energy under contract DE-AC01-78RA03395 and by the NASA Ames Research Center under grant NGL-22-009-124.

To My Parents

TABLE OF CONTENTS

TABLE OF CONTENTS (cont'd)

TABLE OF CONTENTS (cont'd)

LIST OF FIGURES

LIST OF FIGURES (cont'd)

1. INTRODUCTION

The importance of obtaining robustly stable feedback control systems has long been recognized by designers. Indeed, a principal reason for using feedback rather than open-loop control is the presence of model uncertainties. Any model is at best an approximation of reality, and the relatively low order, linear, time-invariant models most often used for controller synthesis are bound to be rather crude approximations.

More specifically, a given system model can usually be characterized as follows. There is a certain range of inputs typically bounded in amplitude and in a certain frequency range for which the model is a reasonable engineering approximation to the system. Outside of this range, due to neglected nonlinearities and dynamic effects, the model and system may behave in grossly different ways. Unfortunately, this range of permissible inputs is rarely spelled out explicitly along with the model, but is rather implicit in the technology that the model came from - there is no "truth in modelling" law in systems theory.

The term robustness as used in this thesis will refer to the extent to which a model of a open-loop system may be changed from the nominal design model without destabilizing the overall closed-loop feedback system designed to control the outputs of the open-loop system. We stress that in this definition, we implicitly assume that the dynamic compensator is fixed, that is, it does not change if, for whatever reason, one suspects that the actual open-loop dynamics are different from those used in the model. Real time changes in the compensator structure (gains or other changes) lead to adaptive control systems, a topic that will not

be addressed in this thesis. Thus, the term robustness refers the preservation of closed-loop system stability in the face of model uncertainty not accounted for in the compensator design.

Robustness issues are not new in control system design. In classical single-input, single-output (SISO) servomechanism designs, robustness specifications were often specified in terms of gain margin and phase margin requirements. However, for multiple-input, multiple-output (MIMO) control systems, similar robustness measures are not straight forward, and their interpretation must be done with care. Thus, the major theme of this thesis is to address robustness issues for MIMO control designs.

The robustness problem can be logically divided into three distinct questions:

(a) given a model of a feedback control system how close to instability is it?

(b) given the class of model errors for which the control system is stable, does this class include the model errors that can be reasonably expected for this particular system?

(c) how can a robust feedback system be designed?

Question (a) is an analysis problem that can be solved exactly by an appropriate mathematical formulation. This problem will be addressed extensively in this thesis and is by far the easiest of the three questions to answer. Question (b) cannot be answered without a proper understanding of the physics of the physical system to be controlled and the assumptions that were made in constructing a model to be used

in controller design. Even with a good understanding of modelling deficiencies it is difficult to characterize this knowledge in a form that is mathematically easy to deal with from the analysis point of view. Question (c) combines aspects of both questions (a) and (b) in that a designer must be able to tell if there exists a controller that would be able to tolerate the class of modelling errors he believes is reasonable for a given open-loop system design model.

However, the robustness properties of a feedback system cannot be optimized without regard to the deterministic and noise performance requirements for the control system. For open-loop stable systems, this is clearly demonstrated since the most robust control system is the open-loop system with no feedback. Of course, for this open-loop stable system the transient response to a step input command or the response to disturbances may not meet the performance specifications. This underscores the fact that there is a fundamental tradeoff between robustness, determinstic performance and stochastic performance (performance with respect to stochastic disturbance and/or sensor noise inputs). Specification of any one of these system characteristics may place constraints on the achievable performance or margin of stability for the other two system characteristics. For example, with linear-quadratic-gaussian (LQG) regulators one may obtain acceptable deterministic responses to command inputs and have an adequate margin of stability but the adequate robustness properties may be obtained at the expense of an increased response to process noise driving the open-loop plant if the deterministic performance must be maintained.

In signal-input, single-output (SISO) control system design these issues are well understood. The classical frequency domain techniques for SISO design naturally handle the robustness characterization[1]. These techniques employ various graphical means (e.g., Bode, Nyquist, inverse-Nyquist, Nichols diagrams) of displaying the system model in terms of its frequency response. From these plots, it is very very easy to determine (by inspection) the minimum change in model frequency response that leads to instability. From the same plots the system's transient response and response to various inputs can also be estimated. Thus, the classical control system designer can observe the fundamental tradeoffs that must be made from these plots.

This is in contrast to the multiple-input, multiple-output (MIMO) case where these tradeoffs are often obscured. Many design techniques for MIMO systems such as pole placement completely neglect the robustness issue in placing poles to obtain a good transient response. Other state space methods attempt to overcome this problem by using state-space models whose parameters may vary and then assuring that for a range of parameter values the closed-loop feedback system will be stable. However, these parameterized state-space models cannot characterize modelling errors arising from neglected dynamics and, therefore, omit an important class of variations in the nominal design model for stability analysis.[2] In short, many state space methods do not naturally lead to techniques that adequately account for modelling error.

---

[1] See the fundamental work of Bode [6], and any good classical textbook, but especially [9].

[2] If the dimension of parameterized state-space model is allowed to increase then neglected dynamics could be accounted for.

The presently available frequency domain MIMO design techniques [1,2,4,5,56] also have the problem that they do not ensure stability for a sufficiently large class of modelling errors. They basically treat a MIMO system as a series of single-loop design problems that are essentially decoupled. They give good stability margins in a coordinate system that makes the design problem simple but not in the coordinate system of the input and output of the physical plant, the coordinate system in which it is important to have robustness and good stability margins. For this reason, these methods may not detect small modelling errors that could potentially destabilize the closed-loop feedback system. The measures of the robustness of a MIMO feedback control system presented in this thesis do not suffer the above deficiency; they will always detect the near instability of a feedback control system. However, in many cases these robustness tests are conservative and therefore a significant section of this thesis is devoted to eliminating this conservatism. These results are derived in the frequency domain using a multivariable version of Nyquist's criterion, singular values and the singular value decomposition familar from numerical linear algebra [44]. The approach taken in this thesis is similar in nature to that of Doyle in [14] and to that of Safonov in [18].

1.1 Thesis Contributions

The main contributions of this thesis are:

(1) a simplified derivation of available and new robustness results for linear time-invariant systems.

(2) the unification of these robustness results under a common framework based on a classification of various types of modelling errors

(3) the reduction of conservatism of robustness results using only information about the magnitude of modelling error by including information about the structure of the modelling error.[1,2]

(4) the interpretation of robustness properties of LQG control systems via the framework based on model error type.

The results of this thesis summarize and extend the state of the art on the robustness of multivariable control system. However, the practical application of these results is far from trivial and requires sound engineering judgment about the nature of modelling errors based on the physics of the controlled system. However, it is hoped that practical experience with physical systems may provide further insight as to how to successfully apply these new results since engineering knowledge about modelling errors is not always easily interpreted in the mathematical framework required by these results.[3]

1.2 Summary of Thesis

In chapter 2 some matrix theory results that are useful in later chapters are collected to enable a clearer discussion of control related

---

[1] The original motivation for exploring this problem of conservatism that lead to the development of these results were discussions with Mr. James Lewis, a former classmate, working on MIMO control systems for automotive engines [42]. The application of then current robustness results proved conservative for an engine control system similar to one that had worked satisfactorily for years on production automobiles. This in turn lead to the question of how the robustness of a control system may be assessed when the sufficient conditions for stability are violated. The nature of the solution of this problem was first suggested by Dr. David Castanon.

[2] These results were further developed due to discussions with Dr. Sherman Chan, who raised many thought provoking questions with regard to their practical application.

[3] For an application of some of these results to control of multiterminal DC/AC power systems the reader is referred to [46].

robustness issues in those later chapters. The basic problem solved in Chapter 2 is that of finding the nearest singular complex matrix to a given nonsingular complex matrix under constraints on the class of singular matrices considered. This is done using singular values and the singular value decomposition of a matrix which are some of the fundamental mathematical tools explained in Chapter 2.

The structure of the matrix E of smallest norm that makes A+E singular, where A is a given nonsingular matrix, is given in the solution to Problem A. The main new matrix theory result is given in Problem B. Problem B poses the problem of finding the matrix of smallest norm that makes A+E singular but where E is constrained to be unlike in structure to the E matrix of Problem A. Problem C extends a special case of Problem B to include more complicated structural constraints on the matrix E.

Chapter 3 formulates the fundamental robustness theorem (Theorem 3.2) using a multivariable version of Nyquist's criterion from which all robustness tests for linear systems in this thesis may be derived. These robustness tests (Theorems 3.3 to 3.6 and 3.9) are formulated in terms of the size or magnitude of different types of modelling errors. They are first explained for SISO systems to demonstrate that the MIMO case simply generalizes the idea that if magnitude of the change in the Nyquist diagram of the nominal system, induced by modelling error, is less than the distance of the Nyquist diagram to the critical (-1,0) point, then the closed-loop system will remain stable. These tests, employing various model error criteria are then used to formulate multi-loop gain, phase and crossfeed stability margins. Corollaries 3.3 and 3.4

give bounds on the amount of cross coupling between feedback channels that the feedback system will tolerate; that is, they specify crossfeed margins. The various robustness tests employing different model error criteria are then related to the well-known small gain and passivity theorems [12] (Theorems 3.7 and 3.8). Extensions to simple nonlinear systems are also given. The chapter concludes with a discussion of the relative merits of the various results.

Chapter 4 begins with a discussion of how to distinguish between model errors that increase the margin of stability of the feedback system and those that decrease the margin of stability of the feedback system. This is first explained in the SISO case and generalized to the MIMO case by using the matrix theory results of chapter 2. The basic results involve defining the smallest error that destabilizes the feedback system. If this type of model error can be ruled out on physical grounds, the results describe the next smallest destabilizing model error and its minimum magnitude (Theorems 4.1 and 4.2). This extends the robustness tests of Chapter 3 enabling them to consider modelling errors of larger magnitude (that violate the original tests) by eliminating only those model errors, of smaller magnitude, that would destabilize the feedback system, on the grounds that they are not physically realistic or plausible types of modelling errors. The interpretation of the smallest destabilizing modelling errors is discussed via block diagrams and the singular value decomposition of the return difference transfer matrix. An example is also used to illustrate the nature of these results.

In Chapter 5 the robustness properties of LQG control systems are considered. Using the results of Chapter 3 and the multivariable Kalman inequality the robustness properties of LQ state feedback regulators are derived (Theorem 5.2). The multiloop gain, phase and crossfeed margins for LQ regulators (Corollaries 5.1 and 5.2) and some variations (Corollaries 5.3 and 5.4) of the LQ regulator with better margins hold in a coordinate system specified by the control weighting (R) matrix. It is shown that if R is not selected properly the gain, phase and crossfeed margins may become arbitrarily small. Using the results for the LQ state feedback regulator the stability margins for LQG regulators are explored (Theorem 5.4). In general there are no guaranteed stability margins for LQG control systems unless the Kalman filter embedded in the controller possesses the correct dynamic model of the perturbed system and then the stability margins for LQ regulators hold. This is not a practical assumption and robustness recovery procedures for asymptotically recovering the LQ guaranteed stability margins at either the input or output of the open-loop system are discussed. Next, the possibility of recovering stability margins at both input and output is discussed and related to the problem of obtaining a characterization of the expected model error.

Chapter 6, very briefly discusses current frequency domain techniques for MIMO design and robustness analysis (characteristic loci, inverse Nyquist array and principal gain and phase methodologies). These are placed in perspective with respect to the approach of this thesis.

Chapter 7 summarizes the key results, gives some conclusions, and outlines some future research directions.

1.3 Notation

The following conventions will be adopted in this thesis. All matrices will be denoted by capital letters[1], all scalars by lower case letters and all vectors by underlined lower case letters. Outside of the chapter in which they occur, all equation numbers, theorem and corollary numbers and figure numbers will be prefaced with the chapter number followed by a period and the number occuring within the chapter. Thus, for example, equation (32) of Chapter 3 will be referred to as (32) within Chapter 3 and as (3.32) outside of Chapter 3.

[1] One exception to this convention is the matrix functions $f(\cdot)$ and $h(\cdot)$ which take matrix arguments and are themselves matrices. These functions are found in Chapters 3 and 4 respectively.

Notation

s.t.	subject to
tr(A)	trace of the matrix A
A^H	complex conjugate transpose of the matrix A
A^*	complex conjugate of the matrix A
A^T	transpose of the matrix of A
det A	determinant of A
$<\cdot,\cdot>$	innerproduct
$\lambda_i(A)$	$i^{\underline{th}}$ eigenvalue of A
$\sigma_i(A)$	$i^{\underline{th}}$ singular value of A = $\lambda_i^{\frac{1}{2}}(A^HA)$
$\|\|\cdot\|\|_p$	$p^{\underline{th}}$ order norm
I	identity matrix
j	$\sqrt{-1}$
$\|\|\cdot\|\|_E$	Euclidean (or Frobenius) matrix norm
A^{-1}	inverse of the matrix A
$\mathbb{R}$	the real numbers
$\mathbb{C}$	the complex numbers
$\mathbb{C}^{n\times m}$	the space of nxm matrices with elements in $\mathbb{C}$
$a \in A$	a is an element of the set A
$\prod_{i=1}^{n} \alpha_i$	the product $(\alpha_1\alpha_2 \ldots \alpha_n)$
$\|x\|$	magnitude of the scalar x
A>B	A-B is positive definite
$A \geq B$	A-B is nonnegative definite
(A,B,C)	realization of the linear system specified by the time domain description $\dot{\underline{x}} = A\underline{x} + B\underline{u}$ $\underline{y} = C\underline{x}$

$\triangleq$	defined as
$G(s)$	loop-transfer matrix
$\tilde{G}(s)$	perturbed loop-transfer matrix
$L(s)$	multiplicative perturbation transfer matrix
$\phi_{OL}(s)$	open-loop characteristic polynomial
$\phi_{CL}(s)$	closed-loop characteristic polynomial
$\tilde{\phi}_{OL}(s)$	perturbed open-loop characteristic polynomial
$\tilde{\phi}_{CL}(s)$	perturbed closed-loop characteristic polynomial
$N(\Omega, f(s), C)$	number of clockwise encirclements of the point Ω by the locus of $f(s)$ as s traverses the closed contour C in the complex plane in a clockwise sense.
D_R	Nyquist contour of Fig. 3.10
Ω_R	segment of D_R for which $\mathrm{Re}[s] \leq 0$.
SISO	single-input, single-output
MIMO	multiple-input, multiple-output
ORHP (CRHP)	open-(closed) right-half-plane
OLHP (CLHP)	open-(closed) left-half-plane
LQ	linear-quadratic
LQG	linear-quadratic-Gaussian
KF	Kalman filter

2. MATRIX THEORY

2.1 Introduction

The purpose of this chapter is to introduce important tools from matrix theory and prove some results which form the backbone of the robustness theory of later chapters. The specific problem considered in this chapter is the following. Given a nonsingular complex matrix A, find the nearest (in some sense) singular matrix $\tilde{A}$ which belongs to a certain class of singular matrices. Essential use of the singular value decomposition for complex matrices is made in the solution of this problem as well as in the definition of an appropriate constraint set to which $\tilde{A}$ must belong.

It is thus necessary to review some preliminary definitions and properties of special complex matrices and different vector and matrix norms. After this preliminary review and some specialized results for 2x2 matrices the singular values of a complex matrix are defined and related to size of the error matrix E which is simply the difference $\tilde{A} - A$. Next the singular value decomposition (SVD) is presented and the expansion of an arbitrary matrix in the orthonormal basis generated by the SVD is discussed. In the final section of this chapter the structure of the error matrix E is studied via the SVD when E is both unconstrained and constrained to a certain set of matrices.

2.2 Preliminary Definitions and Properties

The following definitions and properties are elementary and can be found in the many books on linear algebra [44].

2.2.1 Vector and Matrix Norms

It is useful to have a single number to measure the size of a vector or matrix. This number is called a norm and is denoted by $||\cdot||$.

For vector norms the following relations must hold

$$||\underline{x}|| > 0 \quad \text{unless } \underline{x} = 0 \tag{1}$$

$$||\alpha\underline{x}|| = |\alpha| \; ||\underline{x}|| \quad \text{for any scalar } \alpha \tag{2}$$

$$||\underline{x} + \underline{y}|| \leq ||\underline{x}|| + ||\underline{y}|| \tag{3}$$

Three vector norms that are commonly used are given by

$$||\underline{x}||_p \triangleq (|x_1|^p + |x_2|^p + \ldots + |x_n|^p)^{1/p}; \quad (p = 1,2,\infty) \tag{4}$$

where x_i are the components of $\underline{x}$ and $||\underline{x}||_\infty$ is interpreted as $\max_i |x_i|$. The norm $||\underline{x}||_2$ is the usual Euclidean length of the vector $\underline{x}$.

Two vectors $\underline{x}$ and $\underline{y}$ are said to be orthogonal if their innerproduct, $\langle \underline{x},\underline{y} \rangle$, defined by

$$\langle \underline{x},\underline{y} \rangle \triangleq \underline{x}^H \underline{y} \tag{5}$$

is zero. The Schwartz inequality,

$$|\langle \underline{x},\underline{y} \rangle| \leq ||\underline{x}||_2 ||\underline{y}||_2 \tag{6}$$

bounding the magnitude of the innerproduct, is important in solving least squares and minimum norm problems of the type we are dealing with.

Turning to matrix norms, we denote the norm of a matrix A also by $||A||$ where the following relations must hold

$$||A|| > 0 \text{ unless } A = 0 \tag{7}$$

$$||\alpha A|| = |\alpha| \; ||A|| \text{ for any scalar } \alpha \tag{8}$$

$$||A+B|| \leq ||A|| + ||B|| \tag{9}$$

$$||AB|| \leq ||A||\ ||B|| \ . \tag{10}$$

Corresponding to each vector norm there is an associated induced matrix norm defined by

$$||A|| \triangleq \max_{\underline{x}\neq 0} \frac{||A\underline{x}||}{||\underline{x}||} \tag{11}$$

which satisfies the conditions (7) to (10) and is said to be subordinate to the vector norm. For the three vector norms given by (4) the three induced subordinate matrix norms are

$$||A||_1 = \max_j \sum_i |a_{ij}| \tag{12}$$

$$||A||_\infty = \max_i \sum_j |a_{ij}| \tag{13}$$

$$||A||_2 = \max_i \lambda_i^{1/2}\ (A^H A) \tag{14}$$

where $\lambda_i(A^H A)$ are necessarily real as shown later.

From the definition of these norms it is apparent that

$$||A\underline{x}||_p \leq ||A||_p\ ||\underline{x}||_p \ ; \quad p = 1,2,\infty \tag{15}$$

is satisfied for all $\underline{x}$. Any matrix norm which satisfies this inequality is said to be consistent or compatible. Another matrix norm which is used frequently that is compatible with the vector norm $||\cdot||_2$ is the Euclidean norm. The Euclidean norm for a matrix A is defined by

$$||A||_E = [\sum_i \sum_j |a_{ij}|^2]^{1/2} \tag{16}$$

The $||A||_2$ norm is referred to as the spectral norm. Some useful relationships involving the spectral and Euclidean norms that can be developed are

$$||A||_2 \leq ||A||_E \leq n^{1/2}||A||_2 \tag{17}$$

where A is an n x n matrix. These inequalities follow from the fact that A^HA is positive semidefinite and

$$\max_i \lambda_i(A^HA) \leq ||A||_E^2 = \mathrm{tr}(A^HA) \leq n \max_i \lambda_i(A^HA) \quad . \tag{18}$$

Also, if λ is an eigenvalue of A and $\underline{x}$ is a corresponding eigenvector, then for consistent matrix and vector norms

$$||A\underline{x}|| = |\lambda| \; ||\underline{x}|| \leq ||A|| \; ||\underline{x}|| \tag{19}$$

$$|\lambda| \leq ||A|| \; . \tag{20}$$

From this we can obtain

$$||A||_2^2 = \max_i \lambda_i(A^HA) \leq ||A^HA||_\infty \leq ||A||_1||A||_\infty \; . \tag{21}$$

2.2.2 Special Matrices

There are two types of matrices that will play a special role in the ensuing analysis. They are known as hermitian and unitary matrices and have special properties that make them useful.

Definition 1: A complex matrix A is hermitian if $A = A^H$.

Definition 2: A complex matrix U is unitary if $U^H = U^{-1}$.

Property 1: All of the eigenvalues of a hermitian matrix are real.

Property 2: All of the eigenvalues of a unitary matrix have unit magnitude.

Property 3: $||U||_2 = 1$ if U is unitary.

Property 4: If a matrix A is hermitian then there exists a unitary matrix U such that $A = U \Lambda U^H$ where Λ is a diagonal matrix of eigenvalues of A.

Note that Property 4 means that any hermitian matrix has a full linearly independent set of eigenvectors which are orthogonal to each other. For example, the columns of the U matrix in Property 4 are eigenvectors of the matrix A.

Definition 3: A complex matrix S is skew-hermitian if $A^H = -A$.

Property 5: All of the eigenvalues of a skew-hermitian matrix are purely imaginary.

Property 6: If S is skew-hermitian then jS is hermitian.

Property 7: The diagonal elements of a hermitian (skew-Hermitian) matrix are purely real (imaginary).

Rayleigh's Principle: If A is hermitian then

$$\min_{\underline{x} \neq 0} \frac{\underline{x}^H A \underline{x}}{\underline{x}^H \underline{x}} = \lambda_{min}(A) \tag{22a}$$

and

$$\max_{\underline{x} \neq 0} \frac{\underline{x}^H A \underline{x}}{\underline{x}^H \underline{x}} = \lambda_{max}(A) \tag{22b}$$

where the ratio $\underline{x}^H A \underline{x} / \underline{x}^H \underline{x}$ is known as Rayleigh's quotient which achieves its minimum (maximum) when $\underline{x}$ is an eigenvector corresponding to $\lambda_{min}(A)$ ($\lambda_{max}(A)$). Note that $||\underline{x}||_2 = 1$ can always be assumed and thus the Rayleigh quotient becomes simply $\underline{x}^H A \underline{x}$.

2.2.3 Some Useful Results Involving $||\cdot||_E$ and $||\cdot||_2$

Any complex matrix A can be decomposed into the sum of a hermitian and skew-hermitian matrix as

$$A = A_H + A_{SH} \tag{23}$$

where

$$A_H = \frac{1}{2}\,(A+A^H) \tag{24}$$

$$A_{SH} = \frac{1}{2}\,(A-A^H)\ . \tag{25}$$

A result we will use later is the following

$$||A||_E^2 = ||A_H||_E^2 + ||A_{SH}||_E^2 \tag{26}$$

which can be seen directly from the following equations

$$\begin{aligned} ||A||_E^2 &= \mathrm{tr}(A^H A) = \mathrm{tr}[(A_H - A_{SH})(A_H + A_{SH})] \\ &= \mathrm{tr}[A_H^H A_H] - \mathrm{tr}[A_{SH}A_H] + \mathrm{tr}[A_H A_{SH}] + \mathrm{tr}[A_{SH}^H A_{SH}] \\ &= \mathrm{tr}[A_H^H A_H] + \mathrm{tr}[A_{SH}^H A_{SH}] \end{aligned} \tag{27}$$

where we have used the fact that $\mathrm{tr}(AB) = \mathrm{tr}(BA)$. Some very specialized formulas for 2x2 matrices that are useful in deriving results in section 2.4 are the following. If A is hermitian then

$$||A||_2^2 = \lambda_{max}(A^H A) = \lambda_{max}(A^2) = \max_i |\lambda_i(A)|^2 \tag{28}$$

or

$$||A||_2 = \max_i |\lambda_i(A)|\ . \tag{29}$$

For any matrix A with eigenvalues λ_i

$$\mathrm{tr}(A) = \sum_{i=1}^{n} \lambda_i(A) \tag{30}$$

$$\det(A) = \prod_{i=1}^{n} \lambda_i(A) \tag{31}$$

Thus for a 2x2 matrix A

$$\det(\lambda I - A) = (\lambda-\lambda_1)(\lambda-\lambda_2) = \lambda^2 - (\lambda_1+\lambda_2)\lambda + \lambda_1\lambda_2$$

$$= \lambda^2 - \mathrm{tr}(A)\lambda + \det A \tag{32}$$

and the eigenvalues of A are given by

$$\lambda_i(A) = \left[\frac{\mathrm{tr}(A)}{2}\right] \pm \sqrt{\left[\frac{\mathrm{tr}(A)}{2}\right]^2 - \det A} \quad . \tag{33}$$

Thus for a hermitian 2x2 matrix we have that

$$||A||_2 = \left| \frac{\mathrm{tr}(A)}{2} \right| + \sqrt{\left[\frac{\mathrm{tr}(A)}{2}\right]^2 - \det A} \quad . \tag{34}$$

When A is not hermitian, but still 2x2, we simply replace A by $A^H A$ in (34) and obtain

$$||A^H A||_2 = ||A||_2^2 = \frac{\mathrm{tr}(A^H A)}{2} + \sqrt{\frac{\mathrm{tr}(A^H A)}{2}^2 - \det(A^H A)} \tag{35}$$

or

$$||A||_2^2 = \frac{1}{2}||A||_E^2 + \sqrt{\left[\frac{1}{2}||A||_E^2\right]^2 - |\det A|^2} \quad . \tag{36}$$

2.3 Singular Values and the Singular Value Decomposition [19,38,39,40,44,53,54]

The singular values of a complex nxm matrix A, denoted $\sigma_i(A)$, are the k largest nonnegative square roots of the eigenvalues of $A^H A$ where $k = \min(n,m)$, that is

$$\sigma_i(A) = \lambda_i^{1/2}(A^H A) \qquad i = 1,2,\ldots, k \tag{37}$$

where we assume that σ_i are ordered such that $\sigma_i \geq \sigma_{i+1}$. The maximum

and minimum singular values may alternatively be defined by

$$\sigma_{max}(A) = \max_{\underline{x}\neq 0} \frac{||A\underline{x}||_2}{||\underline{x}||_2} = ||A||_2 \tag{38}$$

$$\sigma_{min}(A) = \min_{\underline{x}\neq 0} \frac{||A\underline{x}||_2}{||\underline{x}||_2} = ||A^{-1}||^{-1} \text{ if } A^{-1} \text{ exists} \tag{39}$$

The smallest singular value $\sigma_{min}(A)$ measures how near the matrix A is to being singular or rank deficient (a matrix is rank deficient if <u>both</u> its rows <u>and</u> columns are linearly dependent). To see this consider finding a matrix E of minimum spectral norm that makes A+E rank deficient. Since A+E must be rank deficient there exists a nonzero vector $\underline{x}$ such that $||\underline{x}||_2 = 1$ and $(A+E)\underline{x} = 0$ thus by (38) and (39)

$$\sigma_{min}(A) \leq ||A\underline{x}||_2 = ||E\underline{x}||_2 \leq ||E||_2 = \sigma_{max}(E) \ . \tag{40}$$

Therefore, E must have spectral norm of at least $\sigma_{min}(A)$ otherwise A+E cannot be rank deficient. The property that

$$\sigma_{min}(A) > \sigma_{max}(E) \tag{41}$$

implies that A+E is nonsingular (assuming square matrices) will be a basic inequality used in the formulation of various robustness tests. The inequality (41) implies that

$$A^H A > E^H E \tag{42}$$

which is a useful inequality for algebraic manipulation. However (42) does <u>not</u> imply (41) except when $A^H A$ and $E^H E$ share the same eigenvector

for their minimum and maximum eigenvalues respectively.

A convenient way of representing a matrix that exposes its internal structure is known as the singular value decomposition (SVD). For an nxm matrix A, the SVD of A is given by

$$A = U\Sigma V^H = \sum_{i=1}^{k} \sigma_i(A)\underline{u}_i\underline{v}_i^H \tag{43}$$

where U and V are unitary matrices with column vectors denoted by

$$U = [\underline{u}_1, \underline{u}_2, \ldots, \underline{u}_n] \tag{44a}$$

$$V = [\underline{v}_1, \underline{v}_2, \ldots, \underline{v}_m] \tag{44b}$$

and Σ contains a diagonal nonnegative definite matrix Σ_1 of singular values arranged in descending order as in

$$\Sigma = \begin{cases} \left[\begin{array}{c} \Sigma_1 \\ \hline 0 \end{array}\right], & n \geq m \\ \left[\Sigma_1 \quad 0\right], & n \leq m \end{cases} \tag{45}$$

and

$$\Sigma_1 = \text{diag}[\sigma_1, \sigma_2, \ldots, \sigma_k] \quad ; \quad k = \min(m,n) \; . \tag{46}$$

The columns of V and U are unit eigenvectors of A^HA and AA^H respectively and are known as <u>right and left singular vectors</u> of the matrix A.

Any unitary matrices, such as the U and V produced by computing the SVD of a matrix, can be used to generate an orthonormal basis in which to express an arbitrary matrix E. Let U and V be nxn unitary matrices with columns as in (44) and express E as

$$E = \sum_{i=1}^{n} \sum_{j=1}^{n} \langle \underline{u}_i \underline{v}_j^H, E \rangle \underline{u}_i \underline{v}_j^H \tag{47}$$

where the innerproduct for matrices is defined by

$$\langle A,B \rangle \triangleq \text{tr}(A^H B) \tag{48}$$

for complex matrices A and B. Note that with this innerproduct the n^2 rank one matrices $\underline{u}_i \underline{v}_j^H$ are orthogonal to each other and have unit spectral and Euclidean norms and thus form an orthonormal basis. The matrix $\langle \underline{u}_i \underline{v}_j, E \rangle \underline{u}_i \underline{v}_j^H$ is simply the projection of the matrix E onto the one-dimensional subspace spanned by $\underline{u}_i \underline{v}_j^H$. If the elements of $\underline{u}_i \underline{v}_j^H$ are formed into a n^2 length vector $\underline{x}$ by stacking the n rows of $\underline{u}_i \underline{v}_j^H$ and the same procedure is used to reduce the matrix E to a vector $\underline{y}$ then $\langle \underline{u}_i \underline{v}_j^H, E \rangle$ is equal to the usual $\underline{x}^H \underline{y}$ innerproduct between these n^2 length vectors. This makes it clear that $\langle \underline{u}_i \underline{v}_j^H, E \rangle \underline{u}_i \underline{v}_j^H$ can be rearranged into a vector $(\underline{x}^H \underline{y})\underline{x}$ which is just the projection of $\underline{y}$ in the direction of the vector $\underline{x}$. Also, if all the matrices $\underline{u}_i \underline{v}_j^H$ are formed into vectors, they will all be orthogonal to each other and have unit Euclidean length. We will thus think of the n^2 rank one matrices as representing n^2 orthogonal directions and refer to $\langle \underline{u}_i \underline{v}_j^H, E \rangle$ as the projection of E along the direction $\underline{u}_i \underline{v}_j^H$. This type of perspective is useful in studying the structure of the error matrix $E = \tilde{A} - A$.

2.4 Error Matrix Structure

In this section we will use the tools developed in earlier sections to solve the problem of finding a singular matrix $\tilde{A}$ nearest to a given matrix. This can be formulated more precisely as a mathematical

optimization problem:

Problem A:

$$\min_{E} \; ||E||_2$$

$$\text{s.t.} \quad \det(A+E) = 0 \tag{49}$$

In this formulation the matrix $\tilde{A}$ is simply A+E, where we refer to E as the error matrix. This is the simplest problem to solve since E is unconstrained. In what follows we make the following technical assumption.

Assumption 1: The matrix A is nxn nonsingular and has distinct singular values.

The assumption of nonsingularity of A assures us of a nontrivial problem otherwise E is identically zero when A is singular. The assumption of distinct singular values is a technical one which allows us to avoid some combinatoric problems associated with multiple solutions. Once this section's material has been understood by the reader it is not difficult to remove this assumption.

Solution to Problem A:

Suppose that A has the SVD given by

$$A = U\Sigma V^H \tag{50}$$

where

$$\Sigma = \text{diag}[\sigma_1, \sigma_2, \ldots, \sigma_n] \; ; \quad \sigma_k > \sigma_{k+1} \tag{51}$$

$$U = [\underline{u}_1, \underline{u}_2, \ldots, \underline{u}_n] \tag{52}$$

$$V = [\underline{v}_1, \underline{v}_2, \ldots, \underline{v}_n] \; . \tag{53}$$

Now since A+E must be singular there exists a unit vector $\underline{x}$ such that

$$(A+E)\underline{x} = 0 \tag{54}$$

and thus from (38) and (39) or (11) we have that

$$\sigma_{min}(A) \leq ||A\underline{x}||_2 = ||E\underline{x}||_2 \leq ||E||_2 \ . \tag{55}$$

For a minimum $||E||_2$ equal to $\sigma_{min}(A)$ it is necessary that for some arbitrary θ that

$$\underline{x} = e^{j\theta}\underline{v}_n \tag{56}$$

otherwise

$$||A\underline{x}|| > \sigma_{min}(A) \ . \tag{57}$$

This can be seen by considering

$$||A\underline{x}||_2 = ||U\Sigma V^H\underline{x}||_2 = ||\Sigma(V^H\underline{x})||_2 \tag{58}$$

and defining a unit vector $\underline{z}$ as

$$\underline{z} \triangleq V^H\underline{x} \tag{59}$$

and thus

$$||A\underline{x}||_2 = ||\Sigma\ \underline{z}||_2 = \left(\sum_{i=1} \sigma_i^2|z_i|^2\right)^{1/2} > \sigma_n \tag{60}$$

unless

$$\underline{z}^T = [0,\ 0,\ \ldots,0,1]e^{j\theta}, \quad \theta \text{ arbitrary} \ . \tag{61}$$

Therefore, $A\underline{x}$ is given by

$$\underline{A}\underline{x} = A\underline{v}_n e^{j\theta} = \sigma_n \underline{u}_n e^{j\theta} = -E\underline{v}_n e^{j\theta} \tag{62}$$

and hence

$$E\underline{v}_n = -\sigma_n \underline{u}_n \quad . \tag{63}$$

By similar arguments involving the equation

$$\underline{x}^H (A+E) = 0 \tag{64}$$

one can show that

$$\underline{u}_n^H E = -\sigma_n \underline{v}_n^H \quad . \tag{65}$$

From equations (64) and (65) we can characterize the form that all solutions to Problem A must have, namely

$$E = U \begin{bmatrix} P_s & \underline{0} \\ \underline{0}^T & -\sigma_n \end{bmatrix} V^H \tag{66}$$

where P_s is $(n-1) \times (n-1)$ and

$$||P_s||_2 \leq \sigma_n = ||E||_2 \tag{67}$$

but is otherwise arbitrary.

Recall from equation (47) the interpretation of $\langle \underline{u}_n \underline{v}_n^H, E \rangle \underline{u}_n \underline{v}_n^H$ as the projection of E onto the direction $\underline{u}_n \underline{v}_n^H$. From (66) we see that all solutions to Problem A have the same projection in the direction $\underline{u}_n \underline{v}_n^H$ which we shall call <u>the most sensitive direction</u> since this is the direction it is "easiest" to make A singular by changing its elements the "least". Note also the additional conditions that for any two

solutions to Problem A say E_1 and E_2 that

$$< \underline{u}_n \underline{v}_j^H, E_1 > = < \underline{u}_n \underline{v}_j^H, E_2 > = 0, \qquad j \neq n \tag{68}$$

and

$$< \underline{u}_j \underline{v}_n^H, E_1 > = < \underline{u}_j \underline{v}_n^H, E_2 > = 0, \qquad j \neq n \tag{69}$$

requiring the projections of E_1 and E_2 to be equal along any direction $\underline{u}_j \underline{v}_n^H$ and $\underline{u}_n \underline{v}_j^H$ where $j = 1,2,\ldots,n$. In fact, the matrix P given by

$$P = U^H E V \tag{70}$$

is just the matrix of projections onto each of the n^2 directions $\underline{u}_i \underline{v}_j^H$ (slightly abusing the notion of projection to mean $< \underline{u}_i \underline{v}_j^H, E >$ instead of $< \underline{u}_i \underline{v}_j^H, E > \underline{u}_i \underline{v}_j^H$) that is,

$$P_{ij} = < \underline{u}_i \underline{v}_j^H, E > \quad . \tag{71}$$

Now suppose that we construct a constraint set for E so that E cannot have a projection of magnitude σ_n in the most sensitive direction $\underline{u}_n \underline{v}_n^H$. This means that the matrix A+E cannot become singular along the direction $\underline{u}_n \underline{v}_n^H$ and thus $||E||_2$ must increase if A+E is to be singular. To find out just how much larger $||E||_2$ must become we formulate the constrained optimization problem:

Problem B:

$$\begin{aligned} &\min_E \ ||E||_2 \\ &\text{s.t. } \det(A+E) = 0 \\ &\qquad |< \underline{u}_n \underline{v}_n^H, E >| \leq \phi < \sigma_n \end{aligned} \tag{72}$$

Solution to Problem B:

The error matrix E is given by

$$E = U \left[\begin{array}{c|cc} P_s & 0 & \\ \hline & \phi & \gamma \\ 0 & \gamma^* & -\phi \end{array}\right] V^H \tag{73}$$

where P_s arbitary and

$$||P_s|| \leq \sqrt{\sigma_n \sigma_{n-1} + \phi(\sigma_n - \sigma_{n-1})} = ||E||_2, \tag{74}$$

where γ is given by

$$\gamma = \sqrt{(\phi + \sigma_{n-1})(\phi - \sigma_n)}\, e^{j\theta}, \quad \theta \text{ arbitrary} \tag{75}$$

and A has the SVD

$$A = U \begin{bmatrix} \sigma_1 & & & \\ & \sigma_2 & & \\ & & \ddots & \\ & & & \sigma_n \end{bmatrix} V^H, \quad \sigma_i > \sigma_{i+1} \quad . \tag{76}$$

The proof of the solution to Problem B is somewhat involved and will be broken into several steps. However, a geometric interpretation of a simplified version of Problem B will be given at the end of this section (this is how I actually first worked the problem). Nevertheless, there is a need to understand the 2x2 analytical proof of the problem as well as the next simple Lemma in order to understand the geometric interpretation.

Lemma 1: If the SVD of A is given by

$$A = U\Sigma V^H \tag{77}$$

then A+E is singular if and only if $\Sigma+P$ is singular where

$$P = U^H E V \tag{78}$$

and furthermore $||P||_2 = ||E||_2$.

Proof:

$$A+E = U(\Sigma+P)V^H \tag{79}$$

and thus

$$|\det(A+E)| = |\det(\Sigma+P)| \tag{80}$$

since $|\det U| = |\det V| = 1$ because unitary matrices have only eigenvalues of the form $e^{j\theta}$ (Property 2). Therefore A+E is singular if and only if $\Sigma+P$ is. To show $||E||_2 = ||P||_2$ write

$$E = UPV^H \tag{81}$$

then from (10), (78) and Property 5 we have

$$||P||_2 \leq ||U^H||_2 \, ||E||_2 ||V||_2 = ||E||_2 \tag{82}$$

and from (81) that

$$||E||_2 \leq ||P||_2 \tag{83}$$

and thus

$$||E||_2 = ||P||_2 \, . \tag{84}$$

The significance of Lemma 1 is that we need only consider the case where A is the diagonal matrix of singular values Σ, for once this problem is solved for P, all we need do is use equation (81). Therefore, from this

point on we make the following assumption.

Assumption 2: The matrix A is diagonal.

At this point we describe the steps in the solution to Problem B. The first step is modify Problem B in accordance with Assumption 2. The next step is to show that for the modified Problem B, if a nonhermitian E solves the modified Problem B, then a hermitian solution E_H also exists. We proceed by finding all hermitian solutions to the 2x2 case and then show that in the 2x2 case the solution is unique. The final step is to show that the 2x2 case can be extended to the nxn case.

We now give the modified version of Problem B.

Modified Problem B (MPB):

$$\min_{E} \; ||E||_2$$

$$\text{s.t. } \det(A+E) = 0, \quad A \text{ diagonal and } A>0$$

$$|e_{nn}| \leq \phi < \sigma_n$$

This form of the last constraint occurs since U and V in the SVD of a positive definite diagonal A are both simply the identity matrix.

We proceed to the next step in Lemma 2.

Lemma 2: If a nonhermitian E solves MPB then there exists a hermitian solution E_H to MPB where

$$E_H = \frac{1}{2}(E+E^H) \tag{85}$$

and

$$||E_H||_2 = ||E||_2 \quad . \tag{86}$$

Proof: Since A+E must be singular there exists a unit vector $\underline{x}$ such that

$$(A+E)\underline{x} = 0 \tag{87}$$

and

$$\underline{x}^H(A+E^H) = 0 \tag{88}$$

since $A = A^H$ and thus

$$\underline{x}^H(A+E)\underline{x} = 0 \tag{89}$$

and

$$\underline{x}^H(A+E^H)\underline{x} = 0 \quad . \tag{90}$$

Adding (89) and (90) and dividing by 2 we obtain

$$\underline{x}^H(A+E_H)\underline{x} = 0 \quad . \tag{91}$$

Now since $A+E_H$ is hermitian, we know from Rayleigh's Principle [55] that

$$0 = \underline{x}^H(A+E_H)\underline{x} \geq \lambda_{min}(A+E_H) \tag{92}$$

where $\lambda_{min}(A+E_H)$ is strictly real (Property 1). If $\lambda_{min}(A+E_H) < 0$, then since $A > 0$ there exists a positive scalar $\alpha < 1$ such that

$$\lambda_{min}(A+\alpha E_H) = 0 \tag{93}$$

because the eigenvalues of a matrix are continuous functions of their elements. However,

$$||\alpha E_H||_2 \leq (\alpha/2)\,[||E||_2 + ||E^H||_2] = \alpha||E||_2 < ||E||_2 \tag{94}$$

which means that $||E||_2$ could not be a minimum if

$$|e_{H_{n,n}}| \leq \phi < \sigma_n \tag{95}$$

which is satisfied since

$$|e_{H_{n,n}}| = |\mathrm{Re}(e_{nn})| \leq |e_{nn}| \leq \phi < \sigma_n \tag{96}$$

and thus it must be true that

$$\lambda_{min}(A+E_H) = 0 \ . \tag{97}$$

Therefore, since $||E||_2$ is minimum, from (94) with $\alpha = 1$ we conclude that

$$||E_H||_2 = ||E||_2 \ . \tag{98}$$

The significance of Lemma 2 is that any solution E which is not hermitian has a hermitian part (i.e., $E_H = 1/2(E+E^H)$) which is also a solution to MPB. Thus by finding hermitian solutions to MPB we need only determine if $E_H + E_{SH}$, where E_{SH} is skew hermitian, can be a solution to MPB.

Continuing our proof, we now find all hermitian solution to MPB for the 2x2 case. In this MPB may be restated as

MPb; 2x2 Hermitian Case:

$$\begin{aligned} &\min_E ||E||_2 \\ &\text{s.t. } \det(A+E) = 0 \\ &\qquad |d| \leq \phi < \sigma \end{aligned} \tag{99}$$

where

$$A = \begin{bmatrix} \sigma_1 & 0 \\ 0 & \sigma_2 \end{bmatrix} \tag{100}$$

$$E^H = E = \begin{bmatrix} a & b \\ b^* & d \end{bmatrix}, \quad a,d \text{ real} \tag{101}$$

Solution:

$$E = \begin{bmatrix} \phi & \gamma \\ \gamma^* & -\phi \end{bmatrix} \tag{102}$$

where

$$\gamma = \sqrt{(\sigma_1+\phi)(\sigma_2-\phi)}\, e^{j\theta}, \quad \theta \text{ arbitrary} \tag{103}$$

Proof: Calculating $||E||_2$ via equation (34) we have

$$||E||_2 = \left|\frac{a+d}{2}\right| + \sqrt{\left(\frac{a+d}{2}\right)^2 - ad + |b|^2} \tag{104}$$

or

$$||E||_2 = \left|\frac{a+d}{2}\right| + \sqrt{\left(\frac{a-d}{2}\right)^2 + |b|^2} \quad . \tag{105}$$

From the singularity constraint on A+E we can determine $|b|^2$ as

$$|b|^2 = (\sigma_1+a)(\sigma_2+d) \tag{106}$$

and then substitute for $|b|^2$ in (105) and obtain

$$||E||_2 = \left|\frac{a+d}{2}\right| + \sqrt{\left(\frac{a-d}{2}\right)^2 + (\sigma_1+a)(\sigma_2+d)} \quad . \tag{107}$$

Note from (106), and the bound on $|d|$ in (99), that

$$-\sigma_1 \leq a \tag{108}$$

since $|b|^2 \geq 0$. Next we calculate the partial of $||E||_2$ with respect to a and d to locate a minimum. This results in

$$\frac{\partial ||E||_2}{\partial a} = \frac{1}{2}\left[\operatorname{sgn}(a+d) + \frac{\left(\frac{a+d}{2}\right) + \sigma_2}{\sqrt{\left(\frac{a-d}{2}\right)^2 + (\sigma_1+a)(\sigma_2+d)}}\right] \tag{109}$$

and

$$\frac{\partial ||E||_2}{\partial d} = \frac{1}{2}\left[\operatorname{sgn}(a+d) + \frac{\left(\frac{a+d}{2}\right) + \sigma_1}{\sqrt{\left(\frac{a-d}{2}\right)^2 + (\sigma_1+a)(\sigma_2+d)}}\right] \tag{110}$$

where sgn(·) is the sign function defined by

$$\operatorname{sgn}(x) = \begin{cases} 1 & , \quad x>0 \\ \text{undefined}, & x=0 \\ -1 & , \quad x<0 \end{cases} . \tag{111}$$

Note that the partial in (109) and (110) do not exist at a = -d because there is a jump discontinuity in their values at that point. It also happens that $\partial ||E||_2 / \partial a$ is never zero but changes sign at a = -d in a way to indicate a minimum at a = -d. To see this consider the ratio z given by

$$z = \frac{\left(\frac{a+d}{2}\right) + \sigma_2}{\sqrt{\left(\frac{a-d}{2}\right)^2 + (\sigma_1+a)(\sigma_2+d)}} \tag{112}$$

which can be shown to have magnitude less than unity by the following computations

$$\sigma_2 < \sigma_1 \tag{113}$$

$$(\sigma_2+d)\sigma_2 < \sigma_1(\sigma_2+d) \tag{114}$$

since by (99) σ_2+d is positive and thus

$$ad + a\sigma_2 + (\sigma_2+d)\sigma_2 < ad + a\sigma_2 + \sigma_1(\sigma_2+d) \tag{115}$$

$$\left(\frac{a+d}{2}\right)^2 - \left(\frac{a-d}{2}\right)^2 + a_2 + (\sigma_2+d)\sigma_2 < ad + a\sigma_2 + \sigma_1(\sigma_2+d) \tag{116}$$

$$\left(\frac{a+d}{2}\right)^2 + \sigma_2(a+d) + \sigma_2^2 < \left(\frac{a-d}{2}\right)^2 + (\sigma_1+a)(\sigma_2+d) \tag{117}$$

$$\left|\left(\frac{a+d}{2}\right) + \sigma_2\right|^2 < \left|\left(\frac{a-d}{2}\right)^2 + (\sigma_1+a)(\sigma_2+d)\right| \tag{118}$$

or

$$z^2 < 1 \tag{119}$$

Now $\partial||E||_2/\partial a$ can be written as

$$\frac{\partial||E||_2}{\partial a} = \frac{1}{2}[\text{sgn}(a+d) + z] = \frac{1}{2}[\pm 1+z] \tag{120}$$

and thus $a+d$ and $\partial||E||_2/\partial a$ have the same sign which indicates that a global minimum occurs at $a = -d$ and implies that $|a| = |d| \leq \phi < \sigma_2$.

By similar simple arguments, it can be shown that $\partial||E||_2/\partial d$ is strictly positive for all $|a| = |d| \leq \phi$ indicating that the optimum value for d occurs on the boundary $d = -\phi$. Thus using (106) the value of b may by calculated as

$$b = \sqrt{(\sigma_1+\phi)(\sigma_2-\phi)}\ e^{j\theta} \tag{121}$$

since

$$a = -d = \phi \tag{122}$$

and thus

$$||E||_2 = \sqrt{\phi^2+(\sigma_1+\phi)(\sigma_2-\phi)} \tag{123}$$

and specify E as

$$E = \begin{bmatrix} \phi & b \\ b^* & -\phi \end{bmatrix} \tag{124}$$

with b given by (121).

The next step is to show that the only solution to the 2x2 case of MPB is hermitian. To do this we use (36) to express $||E||_2$ as

$$||E||_2^2 = \frac{1}{2}||E||_E^2 + \sqrt{(\frac{1}{2}||E||_E^2)^2 - |\det E|^2} \tag{125}$$

which is only valid in the 2x2 case. Now suppose that E is nonhermitian and is decomposed into

$$E = E_H + E_{SH} \tag{126}$$

where E_H is of the form given in (124) and E_{SH} is a nonzero skew hermitian matrix. From (124) and (125) we note that

$$||E_H||_2^2 = 1/2\ ||E_H||_E^2 \tag{127}$$

and that from (126) and (26) we have

$$||E||_E^2 = ||E_H||_E^2 + ||E_{SH}||_E^2 \tag{128}$$

Now using (127) and (128), $||E||_2^2$ in (125) may be written as

$$||E||_2^2 = \frac{1}{2}||E_H + E_{SH}||_E^2 + c^2 \tag{129}$$

$$||E||_2^2 = \frac{1}{2}||E_H||_E^2 + \frac{1}{2}||E_{SH}||_E^2 + c^2 > ||E_H||_2^2 \tag{130}$$

where c is some real scalar, the inequality in (130) follows because E_{SH} is not identically zero. Thus, any nonhermitian matrix E with hermitian part E_H that makes A+E singular must have a spectral norm strictly greater than $||E_H||_2$.

Continuing our proof, we must extend the 2x2 case to the nxn case. This is done by considering two special cases of the case where A is nx2

and reformulating MPB to the case in which A+E must be rank definient. When A is of the form

$$A = \begin{bmatrix} \sigma_1 & 0 \\ 0 & \sigma_2 \\ \hline & 0 \end{bmatrix} = \begin{bmatrix} A_1 \\ \hline 0 \end{bmatrix} \tag{131}$$

and E is conformably partitioned with A and given by

$$E = \begin{bmatrix} E_1 \\ \hline E_2 \end{bmatrix} \tag{132}$$

it is clear that for A+E to rank deficient it is necessary that $A_1 + E_1$ is singular and thus E_1 must be of the form given by (124). Also since

$$||E||_E^2 = ||E_1||_E^2 + ||E_2||_E^2 \tag{133}$$

we can conclude by the same argument used in (125) through (130), that E_2 is identically zero. This can be generalized to the case where A is composed of two orthogonal vectors $\underline{x}$ and $\underline{y}$ so that the SVD of A is given by

$$A = \begin{bmatrix} \underline{x} , \underline{y} \\ \end{bmatrix} = U\Sigma V^H \tag{134}$$

where

$$\Sigma = \begin{bmatrix} ||\underline{x}||_2 & 0 \\ 0 & ||\underline{y}||_2 \\ \hline & 0 \end{bmatrix} . \tag{135}$$

Since Σ is of the form of A in (131) we have just considered, we need

only solve for the E_0 that makes $\Sigma + E_0$ rank deficient with minimum $||E_0||_2$ and use the unitary matrices U and V of (134) to calculate the E that makes A+E rank deficient with minimum $||E||_2$. This is of course given by

$$E = UE_0V^H \tag{136}$$

We are now finally ready to calculate the nxn solution to MPB. In the general nxn case when A+E is singular there exists a vector $\underline{x}$ such that

$$(A+E)\underline{x} = 0 \tag{137}$$

with

$$x = [\underline{x}_1^T, x_n] \tag{138}$$

where $\underline{x}_1$ is an n-1 dimensional vector, with $||\underline{x}_1||_2 = 1$, and x_{n-1}, the last element in $\underline{x}$, is strictly real and nonnegative. Note that $\underline{x}$ could never be such that $\underline{x}_1$ would be zero since that would require the last column of A+E to be identically zero which is inconsistent with the bounds in (99). By defining a special matrix Z we may rewrite (137) as

$$(AZ + EZ)\begin{bmatrix} 1 \\ x_n \end{bmatrix} = 0 \tag{139}$$

where

$$Z = \left[\begin{array}{c|c} \underline{x}_1 & 0 \\ \hline 0 & 1 \end{array}\right] . \tag{140}$$

Now note that AZ + EZ must be rank deficient and that

$$||EZ||_2 \leq ||E||_2 \, ||Z||_2 = ||E||_2 \tag{141}$$

and also that AZ has the form (134) and is given by

$$AZ = \left[\begin{array}{c|c} \underline{w} & \underline{0} \\ \hline \underline{0}^T & \sigma_n \end{array}\right] \tag{142}$$

where

$$\underline{w}^T = [\sigma_1 x_1, \sigma_2 x_2, \ldots, \sigma_{n-1} x_{n-1}] \tag{143}$$

Since $||\underline{x}_1||_2 = 1$ and x_{n-1} is real and nonnegative we have that

$$||\underline{w}||_2 \geq \sigma_{n-1} \tag{144}$$

with equality holding if and only if

$$\underline{x}_1^T = [0,0,\ldots,1] \tag{145}$$

Using (124), (142) and (144) we conclude that

$$||EZ||_2 \geq \sqrt{\phi^2 + (\sigma_{n-1}+\phi)(\sigma_n-\phi)} \tag{146}$$

with equality holding if and only if (145) holds. As will be shown later $||E||_2 = ||EZ||_2$ so the bound in (141) is achieved and thus it is necessary that $||EZ|_2$ is minimized requiring (145) to hold which implies that

$$Z = \left[\begin{array}{c|c} & 0 \\ \hline 1 & 0 \\ 0 & 1 \end{array}\right] \tag{147}$$

Thus since EZ is known the last two columns of E are determineed. Using analogous arguments it can be shown that the last two rows of E are also

completely determined and thus E, the solution to MPB, has the form

$$E = \left[\begin{array}{c|cc} P_s & 0 & \\ \hline & \phi & \gamma \\ 0 & \gamma^* & -\phi \end{array}\right] \tag{148}$$

where

$$\gamma = e^{j\theta}\sqrt{(\sigma_1+\phi)(\sigma_2-\phi)}, \quad \theta \text{ arbitrary} \tag{149}$$

$$||P_s||_2 \leq \sqrt{\phi^2+(\sigma_1+\phi)(\sigma_2-\phi)} \tag{150}$$

but otherwise P_s is arbitrary so that

$$||E||_2 = \sqrt{\phi^2 + (\sigma_1+\phi)(\sigma_2-\phi)} = ||EZ||_2 \quad . \tag{151}$$

Using Lemma 1 with these results gives the desired solution of Problem B given in (73) to (75).

At this point we will give a geometric interpretation of a special case of MPB and possible extensions of constraint set for E.

2.5 Geometric Interpretation

A special case of MPB with $\phi = 0$ has a nice geometric interpretation using vectors. With $\phi = 0$ we require that E must have no projection in the direction $\underset{n\times 1}{u}\,\underset{n\times 1}{v}^H$. If we think of the columns of the matrix A, where

$$A = \begin{bmatrix} \sigma_1 & & 0 \\ & \sigma_2 & \\ & & \ddots \\ 0 & & \sigma_n \end{bmatrix} , \tag{152}$$

as orthogonal vectors then in the 3x3 case the A matrix could be displayed as in Fig. 1.

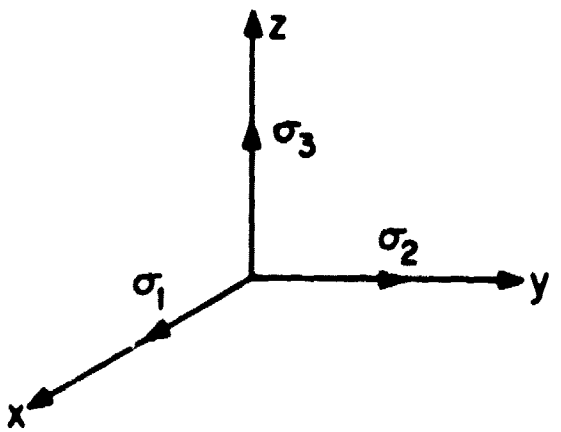

Fig. 1: Column Vectors of A Matrix

In the 2x2 case, MPB simply poses the problem of making two vectors parallel with minimum "effort" with the proviso that the original component in the x-direction of the shortest vector must remain unchanged. This is illustrated in Fig. 2 where $\tilde{\sigma}_1$ and $\tilde{\sigma}_2$ are the resultant vectors when σ_1 and σ_2 are changed minimally in order to align them. If there was no ϕ bound as in the case in Problem A the optimal change would be to shrink the σ_2 vector to zero. Note that for MPB when ϕ is zero that the magnitude of the change (i.e., $||E||_2$ is simply the geometric mean of the two smallest (in this case the only) singular values which is computed from (103) with ϕ=0. If we now

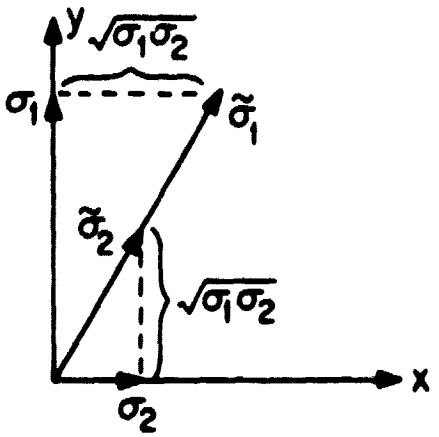

Fig. 2: Column Vectors of $\tilde{A} = A+E$

proceed to the 3x3 case of Fig. 1 MPB poses the problem of making the shortest vector parallel to some linear unitary combination of the other two vectors without changing the original x-component of the σ_3 vector. The term linear unitary combination of vectors is nonstandard. It means that in a weighted sum of vectors, the weights themselves form a vector of unit length. The solution to this problem is the same as in Fig. 2 and the fact that there is an additional orthogonal vector makes no difference. The solution is depicted in Fig. 3 where only the two shortest vectors are changed. The x vector is a unitary linear combination of the σ_2 and σ_1 vectors and its tip sweeps out an elipse in the y-z plane as the particular unitary combination changes. The "effort" required to

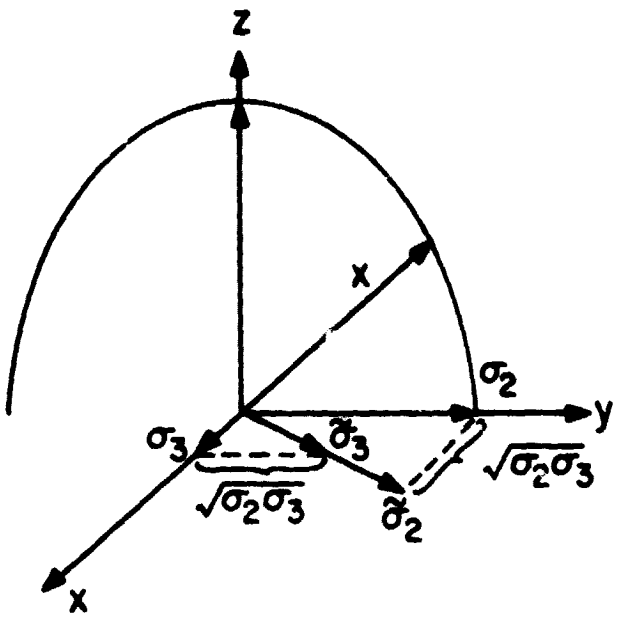

Fig. 3: Solution to MPB with ϕ=0

align σ_3 and x is the geometric mean of their lengths. Thus since the σ_2 vector always is shorter than x, it is the best vector in the set of vectors generated by unitary linear combinations of σ_1 and σ_2 to align with the σ_3 vector.

The observations allow us to generalize Problem B by accomodating a much larger constraint set for the E matrix. This is suggested naturally by supposing that in addition to the constraint

$$\langle \underline{u}\, \underline{v}^H, F \rangle = 0 \qquad (153)$$

in Problem B we also have the constraint

$$\langle \underline{u}_n \underline{v}_{n-1}^H, E \rangle \langle \underline{u}_{n-1} \underline{v}_n^H, E \rangle = 0 \tag{154}$$

which rules out a solution of the form given by (73) to (75) with $\phi=0$. Thus we have ruled out what we will call "the worst perturbation" (i.e., an E on the form of (66)) as well as the "next worst perturbation", that is an error matrix E of the form given by (73) to (75). We use the adjective worst because in our robustness work the singularity of A+E is associated with control system instability and thus the smallest error matrix that makes A+E singular is considered as the worst possible type of perturbation that is possible. The term "next worst" arises because in Problem B with $\phi=0$ we eliminate the worst type of perturbation from consideration. Now we could continue this process and eliminate the next worst perturbation by imposing (154) and ask what is the "next next worst perturbation" and so on. If we do this a nice structure of the "successively worst perturbations" emerges and can be formalized in the following optimization problem.

Problem C:

$$\begin{aligned} &\min_E \|E\|_2 \\ &\text{s.t. } \det(A+E) = 0 \\ &\langle \underline{u}_i \underline{v}_j^H, E \rangle \langle \underline{u}_j \underline{v}_i^H, E \rangle = 0 \quad \text{for all } (i,j) \in \Omega \end{aligned} \tag{155}$$

where A has the usual SVD given by

$$A = U\Sigma V^H = \sum_{i=1}^{n} \sigma_i(A) \underline{u}_i \underline{v}_i^H \tag{156}$$

Solution:

Let

$$\sqrt{\sigma_k \sigma_\ell} = \min_{(i,j)\in\Omega} \sqrt{\sigma_i \sigma_j} \tag{157}$$

$$E_1 = \sqrt{\sigma_k \sigma_\ell}\ [\underline{u}_k \underline{v}_\ell^H e^{j\theta} + \underline{u}_\ell \underline{v}_k^H e^{-j\theta}] \tag{158}$$

where

$$\theta = \begin{cases} 120°, & \text{if } k=\ell \\ \text{arbitrary}, & \text{if } k\neq\ell \end{cases} \tag{159}$$

then

$$E = E_1 + E_0 \tag{160}$$

where

$$||E_0||_2 \leq \sqrt{\sigma_k \sigma_\ell} = ||E||_2 \tag{161}$$

and satisfies the projection constraint in (155) and also

$$\langle \underline{u}_j \underline{v}_i^H, E_0 \rangle = \langle \underline{u}_i \underline{v}_j^H, E_0 \rangle = 0, \quad \begin{matrix} j = 1,2,\ldots, n \\ i = k \text{ or } \ell \end{matrix} \tag{162}$$

but E_0 is otherwise arbitrary.

What the solution to Problem C formalizes is the procedure of finding the minimum effort required in aligning any two column vectors in the Σ matrix or shrinking any of its column vectors and then determining which of these is possible given the constraints or how each of the vectors may or may not be changed or perturbed.

To make this clearer we will illustrate the solutions to the problem of finding the matrices E of minimum spectral norm that make A+E singular under various constraints on the E matrix.

Example:

Let A be given by

$$A = \begin{bmatrix} 9 & 0 & 0 \\ 0 & 4 & 0 \\ 0 & 0 & 1 \end{bmatrix} \tag{163}$$

and consider the various constraints on E.

Unconstrained Case:

$$E = \left[\begin{array}{cc:c} & & 0 \\ & E_s & 0 \\ \hdashline 0 & 0 & -1 \end{array}\right] \tag{164}$$

where $||E_s||_2 \leq 1$ but otherwise E_s is arbitrary.

$e_{33} = 0$ Case:

$$E = \begin{bmatrix} e_{11} & 0 & 0 \\ 0 & 0 & 2e^{j\theta} \\ 0 & 2e^{-j\theta} & 0 \end{bmatrix} \tag{165}$$

where $|e_{11}| \leq 2$ and otherwise e_{11} and θ are arbitrary.

$e_{23} = e_{33} = 0$ Case:

$$E = \begin{bmatrix} 0 & 0 & 3e^{j\theta} \\ 0 & e_{22} & 0 \\ 3e^{-j\theta} & 0 & 0 \end{bmatrix} \tag{166}$$

where $|e_{22}| \leq 3$ and otherwise e_{22} and θ are arbitrary.

$e_{13} = e_{23} = e_{33} = 0$ Case:

$$E = \begin{bmatrix} e_{11} & 0 & 0 \\ 0 & -4 & 0 \\ e_{31} & 0 & 0 \end{bmatrix} \tag{167}$$

where

$$\sqrt{|e_{11}|^2 + |e_{31}|^2} \leq 4 = ||E||_2 \tag{168}$$

but otherwise e_{11} and e_{31} are arbitrary.

$|e_{33}| \leq 1/2$ Case:

$$E = \begin{bmatrix} e_{11} & 0 & 0 \\ 0 & 1/2 & 3/2\ e^{j\theta} \\ 0 & 3/2\ e^{-j\theta} & -1/2 \end{bmatrix} \tag{169}$$

where

$$|e_{11}| \leq ||E||_2 = \frac{\sqrt{10}}{2} \approx 1.58 \tag{170}$$

and e_{11} and θ are otherwise arbitrary.

It is important to point out that we have limited ourselves to constraints on E of a very special form and in general arbitrary constraints on the form of E lead to a mathematical nonlinear programming problem that does not in general have a closed form solution. However, it turns out that the special form of constraints on E will be useful in obtaining robustness results of Chapter IV. Next, however, we turn to the basic robustness problem formulation of the next chapter.

2.6 Concluding Remarks

This chapter has briefly introduced singular values and the singular value decomposition of a matrix and shown their use in finding the nearest singular matrix $\tilde{A}$ to a given nonsingular matrix A. The main results are the solutions to Problems B and C which give the structure of the error matrix $E = \tilde{A} - A$ when E is constrained to belong to a certain set. The norm of the matrix E is given by the geometric mean of the two smallest singular values of the matrix A, when E has no projection in the subspace spanned by $\underline{u}_n \underline{v}_n^H$, where $\underline{u}_n$ and $\underline{v}_n$ are the left and right singular vectors associated with σ_n, the smallest singular value of A.

These results were collected in this chapter in order not to entangle the algebraic aspects of this problem with the robustness issues of feedback control systems discussed in later chapters, which utilize these results in the frequency domain via Nyquist's stability criterion.

3. ROBUSTNESS ANALYSIS FOR LINEAR SYSTEMS WITH UNSTRUCTURED MODEL ERROR

3.1 Introduction

The purpose of this chapter is to give a very simple explanation of how to measure the stability robustness of multivariable feedback control systems using singular values of certain frequency response matrices. The difference between multiple-input-multiple-output (MIMO), multivariable and single-input-single-output (SISO) feedback control systems with respect to the robustness problem is illustrated by a worked example and some of the shortcomings of treating a multi-loop system as a series of single-loop systems are exposed. In this chapter, we assume that the only information we possess about the model uncertainty or model error is described by a single frequency dependent number which measures the size or magnitude of the model error. Results that use only error magnitude information are called unstructured. Those that use more than just error magnitude information are called structured. The unstructured robustness results of this chapter are first presented in the SISO case in section 3.2 for additive and multiplicative types of modelling errors to clearly illustrate the ideas that are later generalized in the MIMO case.

In section 3.3 a multivariable version of Nyquist's theorem is given and the worked example is given to show that although the stability of a MIMO system may be determined from the multivariable Nyquist diagram the stability margins for the MIMO feedback system cannot be determined from the multivariable Nyquist diagram. This is in contrast to the SISO case where the stability margins can be determined by inspection

of the Nyquist diagram. In fact, in the SISO case, this is the main reason for the value of the Nyquist diagram; it determines the stability of a whole class of systems near the nominal system and not just the stability of the nominal system.

In order to efficiently generalize the SISO results of section 3.1, a very general robustness theorem is derived in section 3.4 that forms the basis of the derivation of all subsequent robustness theorems in this chapter. This theorem is based on the idea of deforming the Nyquist diagram of the nominal feedback system into a Nyquist diagram of the actual system without changing the number of encirclements of the critical point required for stability in the multivariable Nyquist theorem.

In section 3.5, different kinds of modelling errors are defined and it is shown that if the magnitude of these errors are bounded appropriately then the feedback system will remain stable despite these modelling errors. It is then shown, in section 3.6, how these errors can be interpreted from a block diagram of the perturbed or actual system that incorporates these model errors and a comparison of the different theorems guarding against different types of errors is made.

From bounds on the modelling errors it is shown in section 3.7.1 how guaranteed multivariable gain and phase margins may be defined and determined. Section 3.7.2 introduces a new type of margin which places bounds on the allowable amount of crossfeed from one feedback channel to another. This crossfeed margin is also derived from bounds on the modelling error obtained in the theorems of section 3.5. Using these robustness results the example of section 3.3 is reworked in section 3.8,

the stability margins are calculated, and the near instability of the feedback system that was undetected by single-loop methods is detected by the methods of this chapter.

In the section 3.9 additional robustness theorems are derived and related to separating functions. These additional theorems include versions of the well-known small gain and passivity theorems [12]. The separating functions are used to show the basic similarity of the various robustness criteria to the small gain theorem. Section 3.10 gives some simple extensions of the theorems for linear systems to the nonlinear case. Concluding remarks about the relationships and use of the various theorems is given in section 3.11.

The major new results of this chapter are contained in Theorems 2, 5 and 6. Theorem 2 is the general robustness theorem from which all subsequent theorems are derived. Theorems 5 and 6 concern robustness results for modelling errors not previously considered in the literature. Versions of Theorems 3, 4, 7, 8 and 9 have previously appeared in the literature [12, 13, 14, 19, 47, 48, 49] and are presented herein so as to place in perspective the newly obtained results and support the explicit interpretation of the robustness criteria as bounds on the allowable modelling errors.

3.2 Robustness and the SISO Nyquist Criterion

The robustness of a SISO feedback system is determined by the distance that its Nyquist diagram avoids the critical (-1, 0) point in the complex plane. Suppose that we have the SISO control system of Fig. 1

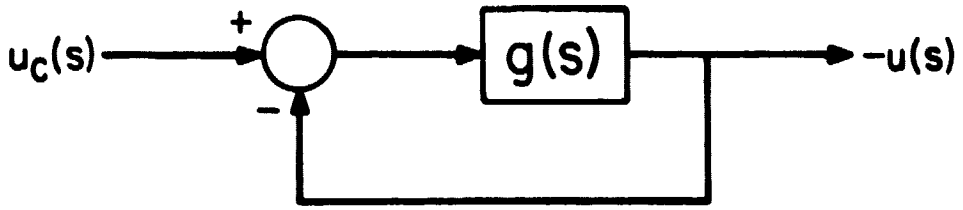

Fig. 1: SISO System under consideration

where g(s) represents the nominal open-loop plant transfer function together with any other compensation that has been introduced. Now due to modelling errors the actual compensated plant is better represented by the transfer function $\tilde{g}(s)$, a perturbed g(s). Therefore, we would like to know if the closed-loop system will remain stable when $\tilde{g}(s)$ is replaced by g(s). This question is answered by drawing the Nyquist diagram of $\tilde{g}(s)$ and determining if the Nyquist diagram of $\tilde{g}(s)$ encircles the (-1, 0) point the same number of times as the Nyquist diagram of g(s) does, (this assumes g(s) and $\tilde{g}(s)$ have the same number of unstable poles). Suppose the Nyquist diagrams of g(s) and $\tilde{g}(s)$ are those illustrated in Fig. 2.

From Fig. 2 one would conclude that the perturbed closed-loop system is stable since the number encirclements of (-1, 0) is unchanged. If $d(\omega)$ denotes the distance to the critical point (-1, 0) and $p(\omega)$

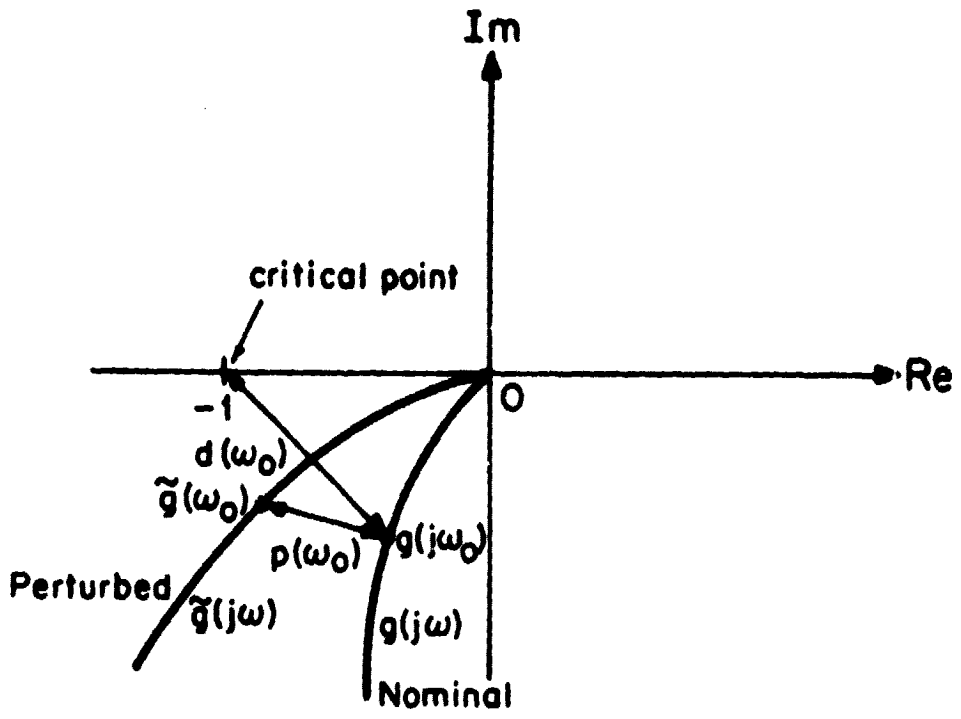

Fig. 2: Nyquist diagrams of nominal and perturbed systems

denotes the distance between $\tilde{g}(j\omega)$ and $g(j\omega)$, then it is apparent, from Fig. 2, that the closed-loop system will remain stable if $d(\omega) > p(\omega)$ for all ω. That is we could draw a graph, as in Fig. 3, denoting the distance to the critical point (-1, 0) for all ω and guarantee the stability of the perturbed closed-loop system if the $p(\omega)$ curve lay below the $d(\omega)$ curve.

There are several ways to define $d(\omega)$ and $p(\omega)$ but the most natural seems to be

$$d(\omega) = |1+g(j\omega)| \tag{1}$$

$$p(\omega) = |\tilde{g}(j\omega) - g(j\omega)| \tag{2}$$

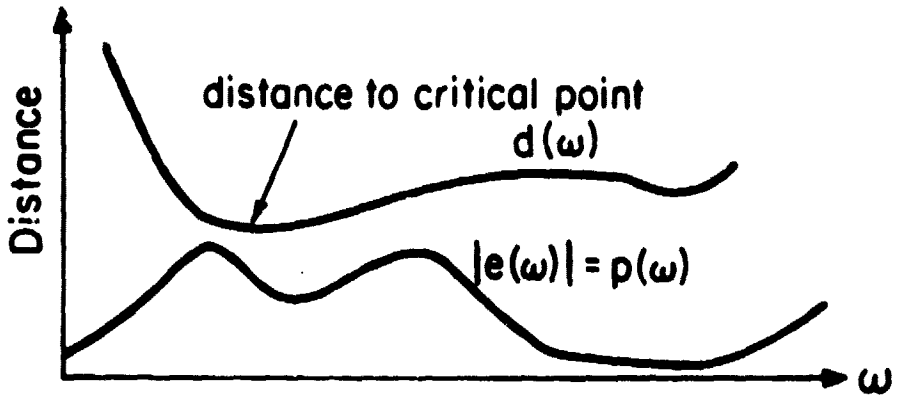

Fig. 3: Graph of $d(\omega)$ and $p(\omega)$ as a function of frequency, ω .

This corresponds to an additive model of the error shown in Fig. 4 where $e(s) = \tilde{g}(s) - g(s)$ and $p(\omega) = |e(j\omega)|$.

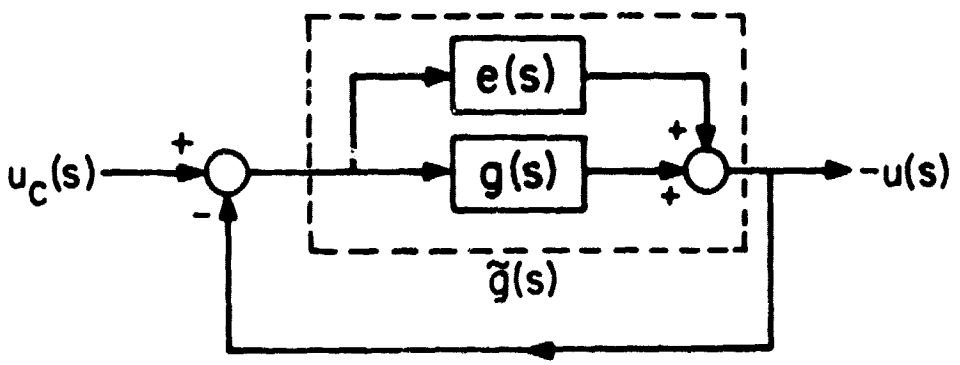

Fig. 4: Additive Model error e(s).

For a multiplicative model of the error between g(s) and $\tilde{g}(s)$ we define e(s) as

$$e(s) = \frac{\tilde{g}(s) - g(s)}{g(s)} \qquad (3)$$

With this definition of model error the block diagram of the perturbed closed-loop system is shown in Fig. 5

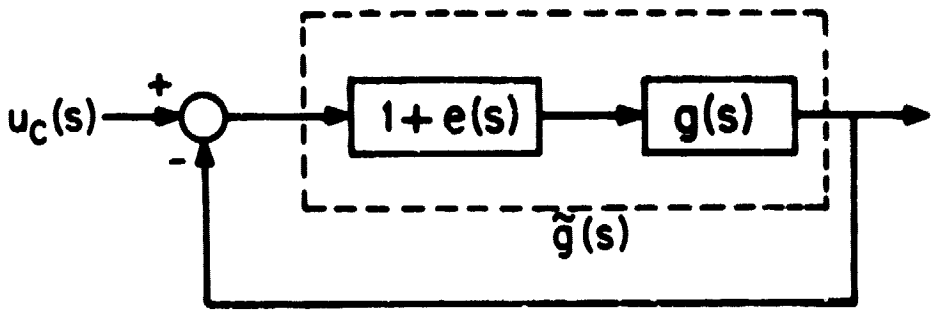

Fig. 5: Multiplicative model error e(s).

Also, with this type of model error, the measures of distances, $d(\omega)$ and $p(\omega)$, become

$$d(\omega) = |1+g^{-1}(j\omega)| \tag{4}$$

and

$$p(\omega) = |e(j\omega)| = \left|\frac{\tilde{g}(j\omega) - g(j\omega)}{g(j\omega)}\right| . \tag{5}$$

Equation (4) is simply obtained by letting $\tilde{g}(j\omega) = -1$ in (5) or by using the additive error robustness criterion that

$$|\tilde{g}(j\omega)-g(j\omega)| < |1+g(j\omega)| \tag{6}$$

then dividing by $|g(j\omega)|$ to obtain the multiplicative error robustness criterion that

$$p(\omega) = |e(j\omega)| = \left|\frac{\tilde{g}(j\omega) - g(j\omega)}{g(j\omega)}\right| < |1+g^{-1}(j\omega)| = d(\omega) \tag{7}$$

and identifying the quantity $d(\omega) = |1+g^{-1}(j\omega)|$ as that which bounds the magnitude of the modelling error.

In the MIMO case, the multivariable analogs of the criteria of (6) and (7) will be developed using singular values as well as robustness tests involving other types of modelling errors. The basic test is to upper bound the magnitude of some type of model error (i.e., the distance between the nominal and perturbed systems) by a generalization of the distance to the critical point. The key problem in the MIMO case is that these distances can no longer be measured off of a multivariable Nyquist diagram or a series of single-loop Nyquist diagrams.

3.2.1 Gain and Phase Margins

Classically, in the SISO case, a measure of the nearness of the Nyquist diagram to the critical point is given by the gain and phase margins. These margins are defined with respect to Fig. 6

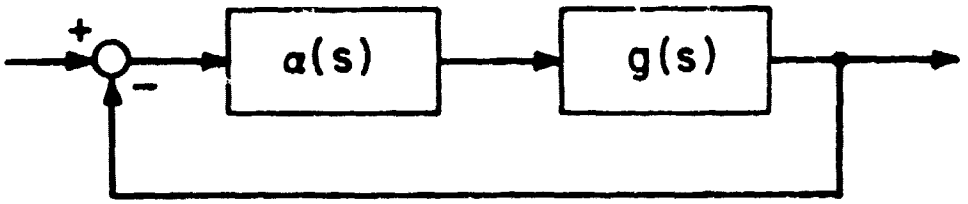

Fig. 6: System for definition of SISO gain and phase margins

The gain margin, denoted GM, is the largest interval (c_1, c_2) such that if $\alpha(s) = k$, k a real constant, then the system of Fig. 6 is stable for

all $k \in (c_1, c_2)$. The number c_1 is the downward gain margin and the number c_2 is the upward gain margin. The phase margin, denoted PM, is the largest interval $(-c_1, c_1)$ such that if $\alpha(j\omega) = e^{j\theta(\omega)}$, $\theta(\omega)$ real, then the system of Fig. 6 is stable for all $\theta \in (-c_1, c_1)$. These margins are depicted in the Nyquist diagram of g(s) in Fig. 7.

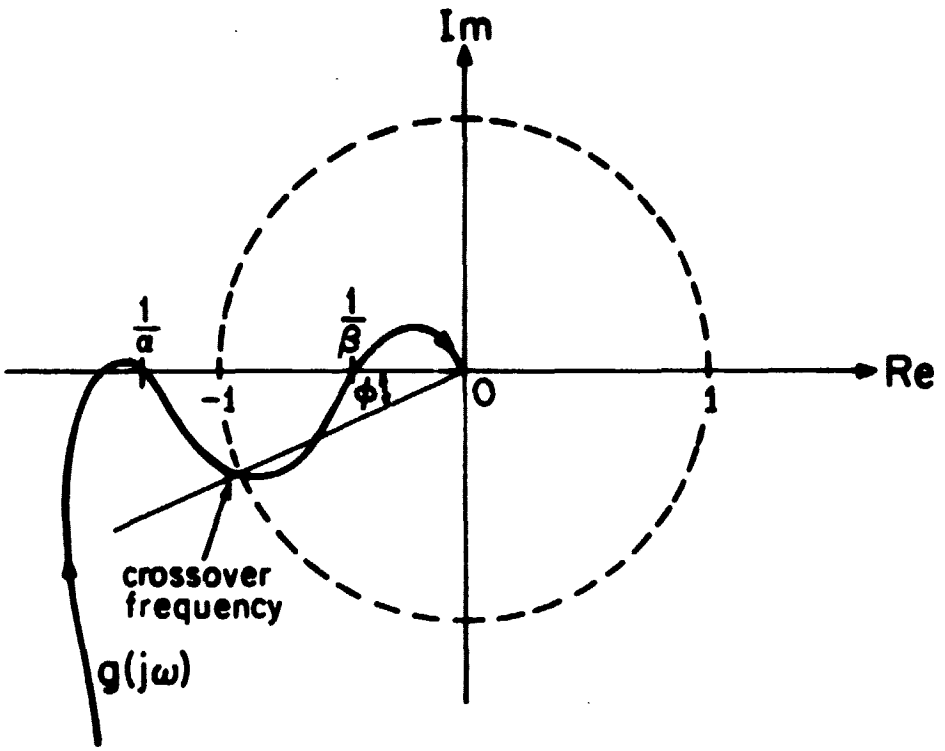

Fig. 7: Nyquist diagram with GM = (α,β) and PM = $(-\phi,\phi)$.

The largest value of ω such that $|g(j\omega)| = 1$ is known as the crossover frequency and is used to indicate the bandwidth of a control system feedback loop.

From Fig. 7 it is apparent that the gain and phase margins measure the distance of the Nyquist diagram to the critical point (-1, 0) at some particular values of ω. They are generally good indicators of the

nearness of a system to instability but may not be accurate indicators of robustness in pathological cases such as the one shown in Fig. 8.

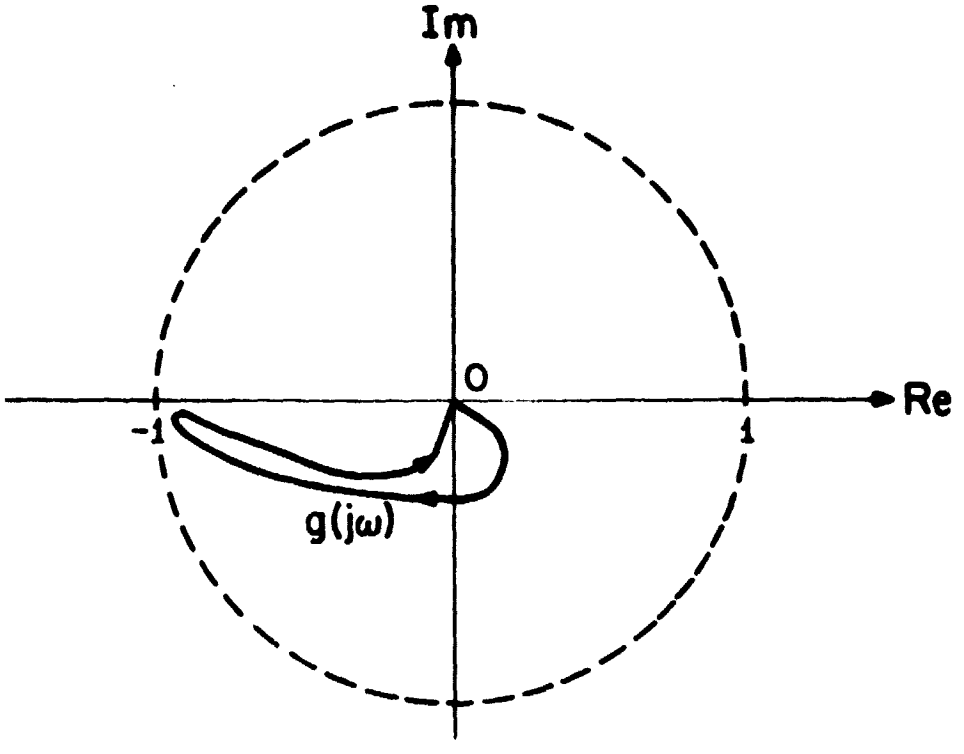

Fig. 8: Nyquist diagram with GM = $(-\infty,\infty)$ and PM = [-180°, 180°]

In the MIMO case it is also possible to define multiloop gain and phase margins which also provide an indication of system robustness but do not rule out the type of situation shown in Fig. 8 appropriately generalized to the MIMO setting. This will be done in section 3.7.1 but first we turn to the development of multivariable generalizations of the robustness tests of (6) and (7).

3.3 Robustness and the Multivariable Nyquist Theorem

In this section we discuss a version of the multivariable Nyquist theorem [1] and work a simple illustrative example that shows single-loop

type of stability analysis is inadequate when applied to MIMO systems. The feedback system to be discussed is depicted in Fig. 9 where the loop transfer matrix G(s) is assumed to incorporate both the open-loop plant dynamics and any compensation employed.

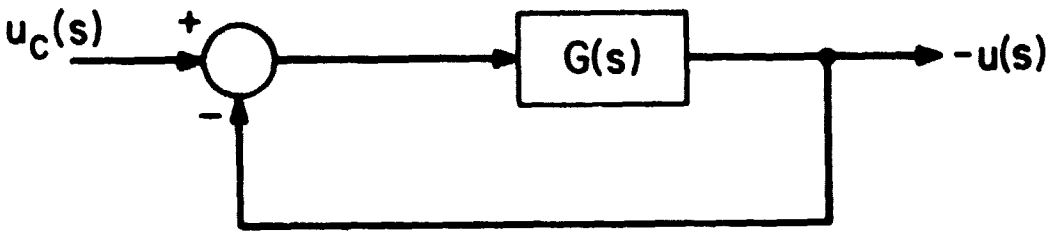

Fig. 9: Feedback system where G(s) represents the open-loop plant plus a compensator

In addition, G(s) is assumed to be derived from a state space realization so that $\underline{y}(s) = G(s)\ \underline{u}(s)$ is given in the time domain by

$$\dot{\underline{x}} = A\underline{x} + B\underline{u} \tag{8}$$

$$\underline{y} = C\underline{x} \tag{9}$$

and thus

$$G(s) = C(Is-A)^{-1}B \quad . \tag{10}$$

The basic issue of concern is to characterize the robustness of the feedback system, i.e., the extent to which the elements of the loop transfer function matrix G(s) can vary from their nominal design values without compromising the stability of the closed-loop system of Fig. 9. The analysis is based on the multivariable Nyquist theorem which is derived from the following relationship

$$\det[I+G(s)] = \frac{\phi_{CL}(s)}{\phi_{OL}(s)} \tag{11}$$

where

$$\phi_{OL}(s) = \det(sI-A): \text{ open-loop characteristic polynominal} \tag{12}$$

$$\phi_{CL}(s) = \det(sI-A+BC): \text{ closed-loop characteristic polynominal} \tag{13}$$

and from the Principle of the Argument of complex variable theory.

Definition (Number of encirclements): Let $N(\Omega, f(s), C)$ denote the number of clockwise encirclements of the point Ω by the locus of $f(s)$ as s traverses the closed contour C in the complex plane in clockwise sense.

A simple version of the multivariable Nyquist theorem can now be stated in the following form.

Theorem 1 (Multivariable Nyquist Theorem): The system of Fig. 9 is closed-loop stable (in the sense that $\phi_{CL}(s)$ has no closed-right-half-plane (CRHP) zeros) if and only if for all R sufficiently large

$$N(0, \det[I+G(s)], D_R) = -P \tag{14}$$

or equivalently

$$N(-1, -1+\det[I+G(s)], D_R) = -P \tag{15}$$

where D_R is the contour[1] of Fig. 10 which encloses all P CHRP zeros

[1]The indentations on the imaginary axis are made to include open-loop $j\omega$-axis poles which will be considered as unstable.

of $\phi_{OL}(s)$ and where $N(\Omega, f(s), C)$ is indeterminate if $f(s_0) = \Omega$ for some $s_0 \in C$.

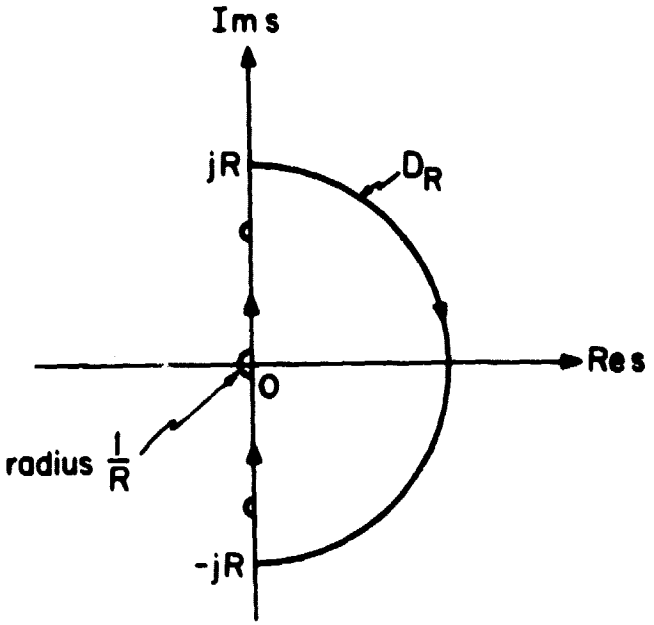

Fig. 10: Nyquist Contour D_R which encloses all zeros of $\phi_{OL}(s)$ in the CRHP, avoiding zeros on the imaginary axis by identations of radius 1/R.

Notice that no controllability or observability assumptions have been made. If [A,B,C,] is a nonminimal realization [50], pole-zero cancellations will occur when G(s) is formed, eliminating uncontrollable or unobservable modes. Nevertheless, it is important to count these modes in the Nyquist criterion since infinitesimal changes in the matrices A,B, and C may make them controllable and observable even though it is not possible to detect the instability of these modes in terms of G(s). However, by using the zeros of $\phi_{OL}(s)$ instead of the poles of the loop transfer matrix G(s), this version of the Nyquist theorem allows one to test for the internal stability of the closed-loop system. For other multivariable versions of Nyquist theorem refer to [1-6].

Remark: When compared with the classical Nyquist theorem for the SISO case, the multivariable Nyquist theorem is much more difficult to use, for two reasons.

First, the dependence of det[I+G(s)] on the compensation implicit in G(s) is complicated, and cannot easily depicted with a Nyquist, Bode or related plot. This fact has motivated a considerable amount of research on synthesis methods, e.g., [1] - [6]. These will not be discussed at length since the main thrust of this thesis is primarily analysis.

Second, and this is the key observation, one cannot get a satisfactory notion of the robustness of a feedback system directly from the multivariable Nyquist diagram. The following extremely simple example illustrates this fact.

Example 1:

Consider the linear system [1] specified by

$$\begin{bmatrix} \dot{x}_1 \\ \dot{x}_2 \end{bmatrix} = \begin{bmatrix} -1 & 0 \\ 0 & -1 \end{bmatrix} \begin{bmatrix} x_1 \\ x_2 \end{bmatrix} + \begin{bmatrix} 1 & b_{12} \\ 0 & 1 \end{bmatrix} \begin{bmatrix} u_1 \\ u_2 \end{bmatrix} \tag{16}$$

$$\begin{bmatrix} y_1 \\ y_2 \end{bmatrix} = \begin{bmatrix} x_1 \\ x_2 \end{bmatrix} \tag{17}$$

which is illustrated in Fig. 11.

[1] This example is a modified version of one found in [58].

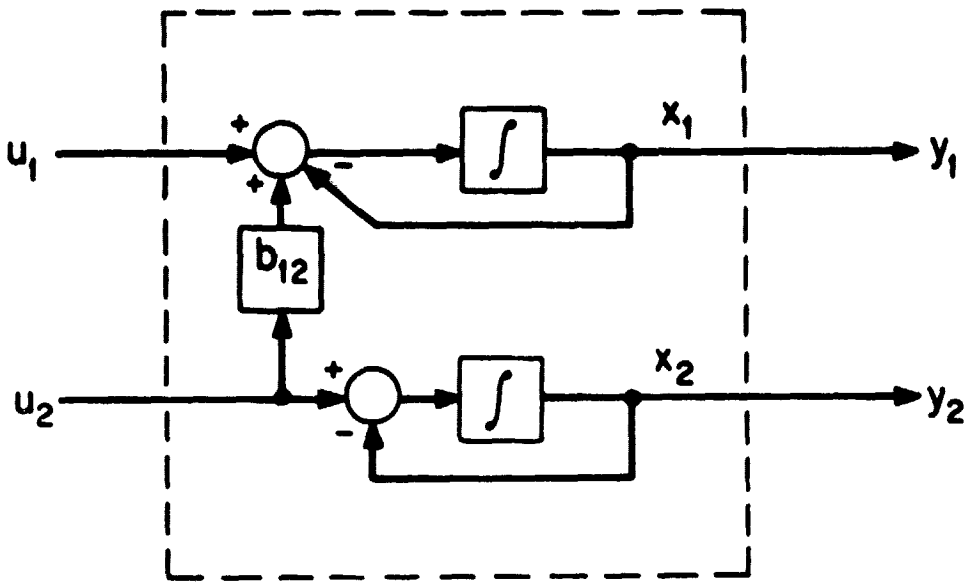

Fig. 11: Internal Structure of Example 1

If the feedback compensation

$$\begin{bmatrix} u_1 \\ u_2 \end{bmatrix} = - \begin{bmatrix} x_1 \\ x_2 \end{bmatrix} + \begin{bmatrix} u_{c1} \\ u_{c2} \end{bmatrix} \tag{18}$$

is used the closed-loop system is given by

$$\begin{bmatrix} \dot{x}_1 \\ \dot{x}_2 \end{bmatrix} = \begin{bmatrix} -2 & -b_{12} \\ 0 & -2 \end{bmatrix} \begin{bmatrix} x_1 \\ x_2 \end{bmatrix} + \begin{bmatrix} 1 & b_{22} \\ 0 & 1 \end{bmatrix} \begin{bmatrix} u_{c1} \\ u_{c2} \end{bmatrix} \tag{19}$$

The eigenvalues of this closed-loop system matrix are obviously -2, -2 indicating a stable system. The <u>return difference matrix</u>, I+G(s), is

given by

$$I+G(s) = \begin{bmatrix} \frac{s+2}{s+1} & \frac{b_{12}}{s+1} \\ 0 & \frac{s+2}{s+1} \end{bmatrix} \tag{20}$$

and thus

$$\det[I+G(s)] - 1 = \frac{2s+3}{(s+1)^2} \quad . \tag{21}$$

The multivariable Nyquist diagram for this system is just the usual Nyquist diagram of $\frac{2s+3}{(s+1)^2}$ shown in Fig. 12 where we count encirclements of the (-1, 0) point to determine closed-loop stability.

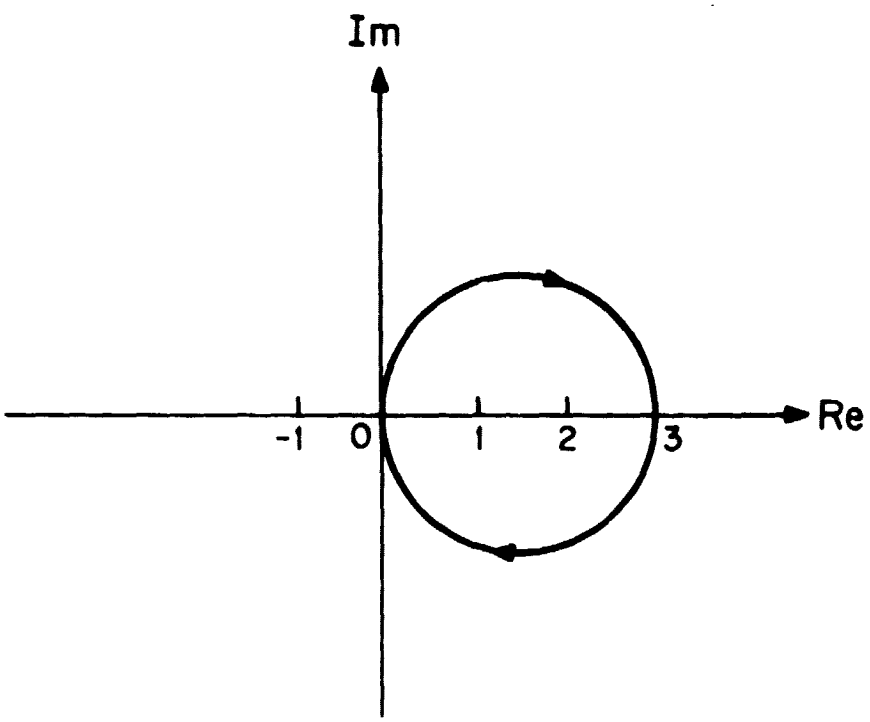

Fig. 12: Nyquist diagram of $\frac{2s+3}{(s+1)^2}$

Since the system (16) is open-loop stable we also can conclude from Fig. 12 that the closed-loop system is stable since the Nyquist diagram does

not encircle the (-1,0) point[1].

Suppose now that we attempt to interpret this multivariable Nyquist diagram as a SISO Nyquist diagram and read off the gain and phase margins.

We find that a SISO system with this Nyquist diagram has an infinite upward gain margin, a gain reduction margin of -1/3 and a phase margin in the neighborhood of $\pm 106°$. These margins are usually indicative of a highly robust system. For example, it is typically assumed that a ± 6 dB gain margin (i.e., GM = [1/2, 2]) and a 30° to 45° phase margin is adequate insurance against model uncertainty within a limited bandwidth in which the model is accurate and 20 dB upward gain margin and $\pm$ 180° phase margin above the frequency range for which the model is valid.

In practice, stability margins for multiloop systems are often calculated for each feedback loop separately by opening one feedback loop at a time while keeping the remaining loops closed and determining the gain and phase margins for the resulting SISO systems. To make this clear, consider Fig. 13 where $\alpha(s)$ has been inserted in one of the feedback channels.

By determining the allowable values of $\alpha(s)$ for $\alpha(s)$ a real constant or of the form $e^{j\phi}$ a gain and phase margin for the feedback channel with $\alpha(s)$ in it may be determined. Moving the $\alpha(s)$ to different channels, a gain and phase margin may be associated with each feedback loop.

---

[1] Note that the mere determination of stability is accomplished more simply in the time domain by calculating eigenvalues of A-BC.

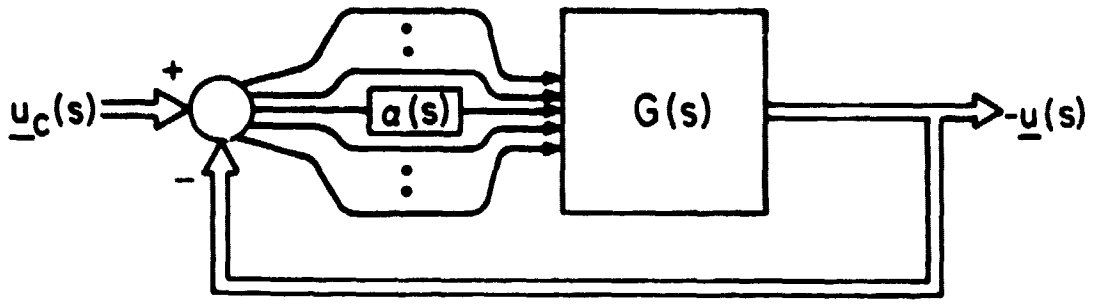

Fig. 13: MIMO Feedback system used to measure gain and phase margins in each feedback channel.

This is illustrated in Fig. 14 for our current example with the first loop open and the second loop closed.

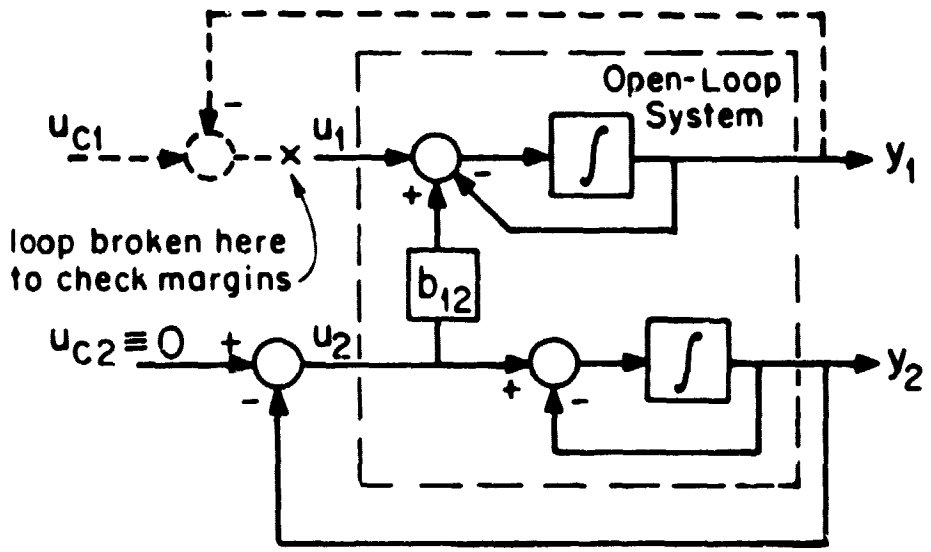

Fig. 14: System with Loop 1 opened and Loop 2 closed - used to check stability margins for SISO system with input u_1 and output y_1.

Carrying this procedure out on our example we obtain (setting $u_{c1} = u_{c2} = 0$)

Loop 1 open; loop 2 closed:

$$y_1(s) = \frac{1}{s+1} u_1(s) \tag{22}$$

Loop 2 open; loop 1 closed:

$$y_2(s) = \frac{1}{s+1} u_2(s) \tag{23}$$

The Nyquist diagram for $\frac{1}{s+1}$ is given in Fig. 15.

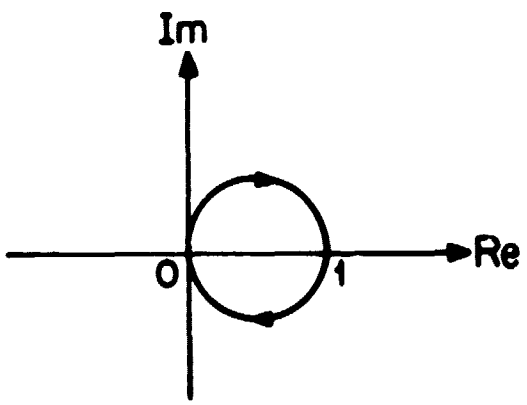

Fig. 15: Nyquist diagram of $\frac{1}{s+1}$

Thus we see that in each feedback loop with the other held at its nominal value we have the following stability margins

$$GM = (-1, \infty) \tag{24}$$

$$PM = (-180°, 180°) \tag{25}$$

Again the system would seem to be highly robust (using the previously mentioned typical margin requirements). In fact, if two different $\alpha_i(s)$ are inserted simultaneously (instead of one at a time as in Fig. 13) in the two feedback channels, the closed-loop system will remain stable if both $\alpha_i(s)$ are such that $\alpha_i(s) \in (-1, \infty)$ for $\alpha_i(s)$ real and constant and $\theta_i \in (-180°, 180°)$ for $\alpha_i(s) = e^{j\theta_i}$. That is, (24) and (25) hold simultaneously in both feedback loops[1].

Note, however, that the Nyquist diagrams of Figs. 12 and 15 do not depend on the value of the parameter b_{12} and that as b_{12} becomes large the closed-loop system is close to instability in the following sense. If the open-loop system of Fig. 11 is perturbed slightly to obtain the system of Fig. 16, the closed-loop system obtained by negative identity feedback (i.e., $\underline{u} = -\underline{y}$) is unstable and has closed-loop poles at $(1\pm\sqrt{5})/2$. This situation cannot be detected by inspection of the multivariable Nyquist-diagram or a series of single-loop Nyquist diagrams. It also cannot be detected by characteristic loci plots [4,5] which are merely polar plots of the eigenvalues of G(s) for $s \in D_R$ which in our case are both given by $1/(s+1)$ plotted in Fig. 15. Clearly, these eigenvalues do not depend upon the value of b_{12}, and hence are unable, to detect the near instability problem just described. An example is given in reference [43] which shows also that Rosenbrock's synthesis procedure [1] based on diagonal dominance has similar deficiencies. This deficiency can be interpreted as a failure to account

[1] This is not true in general and is one of the deficiencies of the loop-at-a-time method of determining stability margins; one cannot expect model uncertainty to only affect one loop at a time!

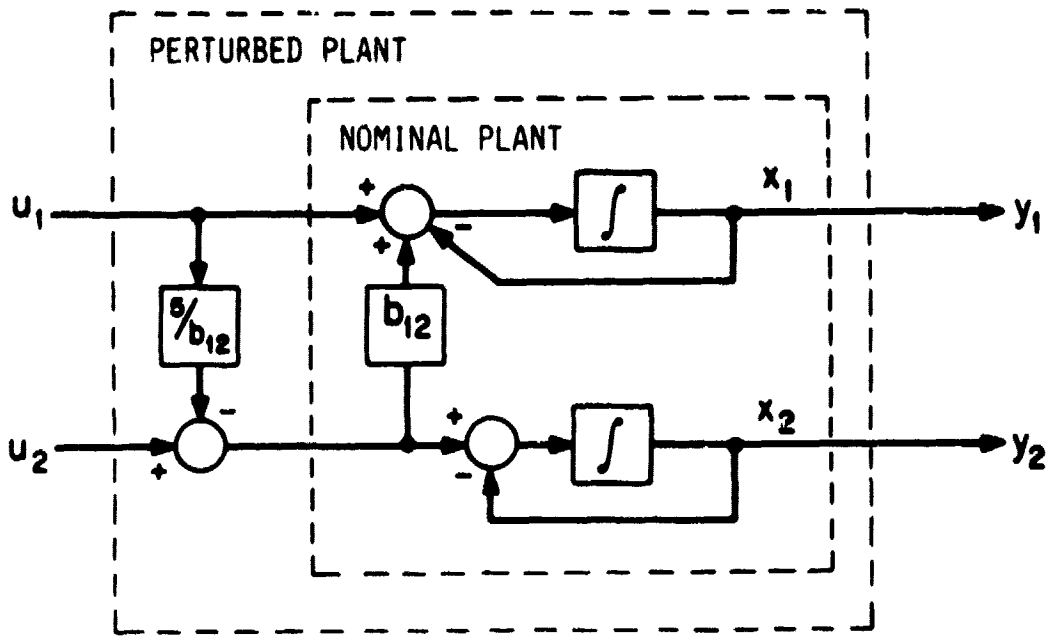

Fig. 16: Perturbation in Nominal Open-Loop Plant that makes closed-loop system unstable

for certain types of modelling error.

The difficulty we have uncovered can be explained in the following way. A multivariable system will not be robust with respect to modelling errors if its return difference transfer function matrix $I+G(j\omega)$ is nearly singular at some frequency ω_0, since then a small change in $G(j\omega_0)$ will make $I+G(j\omega_0)$ exactly singular. When this happens, $\det[(I+G(j\omega_0)] = 0$ and the number of encirclements of the origin counted in the multivariable Nyquist criterion changes.

In this example, a small change in $I+G(j\omega_0)$ produces a large change in $\det[I+G(j\omega_0)]$ showing that the near singularity of a matrix cannot be detected in terms of its determinant. Instead, tests such

as those developed in the following sections must be employed which utilize the minimum singular value to measure the near singularity of matrices (see equations (2.70) and (2.41)).

3.4 Fundamental Robustness Characterization

From the example of the previous section, we can see that the problem of determining the robustness of a multivariable feedback system, (i.e., its distance from instability), is of fundamental importance. Some recent work in this area is due to Safonov [7,18], who generalized an approach of Zames [10, 11]. Safonov's work heavily utilizes concepts of functional analysis, as is standard in the modern input-output formulation of stability theory[1]. However, in the finite dimensional linear-time-invariant case, a powerful robustness characterization can be derived more simply in terms of the multivariable Nyquist theorem.

In order to present the basic robustness theory from which all the other robustness results that work with specific model error criteria may be derived, we need the following notation.

Definition: Let $\check{G}(s)$ denote the perturbed loop transfer function matrix, which represents the actual system and differs from the nominal transfer function matrix $G(s)$ because of the uncertainty in the open-loop plant model. We will assume that $\check{G}(s)$ has the state space realization $(\tilde{A},\tilde{B},\check{C})$ and open- and closed-loop characteristic polynomials

---

[1] See, e.g., [12] or [13].

given by

$$\tilde{\phi}_{OL}(s) = \det(sI-\tilde{A}) \tag{26}$$

and

$$\tilde{\phi}_{CL}(s) = \det(sI-\hat{A}+\tilde{B}\tilde{C}) \tag{27}$$

respectively. Furthermore, we define $G(s,\theta)$ as a matrix of rational transfer functions with real coefficients which are continuous functions of θ for all θ such that $0 \leq \theta \leq 1$ and for all $s \in D_R$, which satisfies the following two conditions

$$G(s,0) = G(s) \tag{28}$$

and

$$G(s,1) = \tilde{G}(s) \tag{29}$$

With these definitions we may state the fundamental robustness theorem of this chapter. This theorem does not adopt a specific model error criteria but works directly with a perturbed $\tilde{G}(s)$ from which any particular model error may be computed.

Theorem 2 (Fundamental Robustness Theorem): The polynomial $\tilde{\phi}_{CL}(s)$ has no CRHP zeros and hence the perturbed feedback system is stable if the following conditions hold:

1. (a) $\phi_{OL}(s)$ and $\tilde{\phi}_{OL}(s)$ have the same number of CRHP zeros

   (b) if $\tilde{\phi}_{OL}(j\omega_0) = 0$, then $\phi_{OL}(j\omega_0) = 0$

(c) $\phi_{CL}(s)$ has no CRHP zeros

2. $\det[I+G(s,\theta)] \neq 0$ for all $(s,\theta) \in D_R \times [0,1]$ for all R sufficiently large.

Proof: For any θ in [0,1] and for all R sufficiently large the contour D_R will enclosed all open-right-half-plane (ORHP) zeros of $\phi_{OL}(s)$ and $\tilde{\phi}_{OL}(s)$. By virtue of condition 1b and the identation construction of D_R, D_R will enclose all CRHP zeros of $\phi_{OL}(s)$ and $\tilde{\phi}_{OL}(s)$. Also, for R sufficiently large, D_R avoids all open-left-half-plane (OLHP) zeros of $\phi_{OL}(s)$, $\tilde{\phi}_{OL}(s)$ and $\phi_{CL}(s)$. From Theorem 1 (multivariable Nyquist theorem) and condition 1c we conclude that

$$N(0, \det[I+G(s,0)], D_R) = -P \tag{30}$$

where P is the number of CRHP zeros of $\phi_{OL}(s)$ and also of $\tilde{\phi}_{CL}(s)$ by condition 1a. Clearly, $\det[I+G(s,\theta)]$ is a continuous function of θ for all $s \in D_R$.

Now suppose that as θ is varied continuously from zero to unity that the number of encirclements given by $N(0, \det[I+G(s,\theta)], D_R)$ changes. Since $\det[I+G(s,\theta)]$ is continuous in (s,θ) in $D_R \times [0,1]$, its locus on D_R forms a closed bounded contour in the complex plane for any θ in [0,1]. The only way to change the number of encirclements of the critical point (0,0) is for the locus for some θ in [0,1] to pass through the critical point, that is for some θ_0 in [0,1]

$$\det[I+G(s,\theta_0)] = 0 \tag{31}$$

for some s in D_R.

Condition 2 eliminates the possibility that $\det[I+G(s,\theta_0)]$ equals zero. This contradicts the assumption that $N(0,\det[I+G(s,\theta)], D_R)$ changes as θ is varied from zero to unity, and thus it must be true that it remains constant at -P for all θ. However, this fact along with (20) imply that

$$N(0, \det[I+\tilde{G}(s)], D_R) = -P \tag{32}$$

and thus by condition 1a and Theorem 1 (Nyquist's theorem), $\tilde{\phi}_{CL}(s)$ has no CRHP zeros.

Q.E.D.

Remark: The basic idea behind this theorem is that of continuously deforming the Nyquist diagram for the nominal system G(s) into one corresponding to the Nyquist diagram of the perturbed or actual system $\tilde{G}(s)$ without changing the number of encirclements of the critical point. If this can be done and the number of encirclements of the critical point required for $\tilde{G}(s)$ and G(s) are the same, then no CRHP zeros of $\tilde{\phi}_{CL}(s)$ will result from this perturbation.

Imbedding arguments of this type have been previously used, implicitly by Rosenbrock [1] and explicitly by Doyle [14], in connection with linear systems and in the more general context of nonlinear and multidimensional systems by DeCarlo, Saeks and Murray [15] - [17], utilizing homotopy theory from algebraic topology.

Remark: The significance of Theorem 2 is that various multivariable robustness characterizations can be stated in terms of conditions that guarantee condition 2 is satisfied. In checking condition 2, it is unnecessary to consider all $s \in D_R$ if $||G(s,\theta)||_2 \to 0$ as $|s| \to \infty$.

This will be the case in what follows and it is related to the assumption that the state-space realizations of $G(s)$ and $\tilde{G}(s)$ have no direct feedthrough from input to output so that $||G(s)||_2$ and $||\tilde{G}(s)||_2$ approach zero as $|s| \to \infty$. It is therefore convenient to define the segment Ω_R as

$$\Omega_R = \{s | s \in D_R \text{ and } Re(s) \leq 0\} \tag{33}$$

which is the only part of the Nyquist contour D_R on which condition 2 need be verified.

3.5 Robustness Theorems and Unstructured Model Error

In this section, we develop theorems that guarantee the stability of the perturbed closed-loop system for different characterizations of model uncertainty (i.e., different types of model error). This is done via Theorem 2 by using a specific error criterion to construct a transfer matrix $G(s,\theta)$ continuous in θ on $D_R \times [0,1]$ that satisfies (28) and (29). Then a simple test bounding the magnitude of the error is devised which guarantees that condition 2 of Theorem 2 is satisfied. This procedure is carried out for four different types of errors. These tests use only the magnitude of the modelling error and do not exploit any other characteristics or structure of the model error and hence are based on the unstructured part of the model error. These different types of model errors will emphasize different aspects of the difference between the nominal $G(s)$ and $\tilde{G}(s)$ and thus under certain circumstances will give essentially different assessments of the robustness or margin of stability of the feedback control system.

Probably the most familiar types of errors are those of absolute and relative errors. Absolute errors are additive in nature whereas relative errors are multiplicative in nature. One can use both types of errors to derive robustness theorems. However, the familiar notions of gain and phase margins are associated only with relative type of error since these margins are multiplicative in nature.

If we let the matrix E(s) generically denote the particular modelling error under consideration, the absolute error is obviously given by

$$E(s) = \tilde{G}(s) - G(s) \tag{34}$$

and the relative error, in a matrix sense, by

$$E(s) = G^{-1}(s)[\tilde{G}(s)-G(s)] \ . \tag{35}$$

In (35) $G^{-1}(s)$ could post-multiply the absolute error and serve as an alternative definition of relative error in the matrix sense but all subsequent results will still hold with trivial modifications. Using these errors we will prove two robustness theorems. However, first $G(s,\epsilon)$ must be constructed.

Using (34) and (35) we can define $G(s,\epsilon)$ by replacing $\tilde{G}(s)$ in (34) and (35) by $G(s,\epsilon)$ and $E(s)$ by $\epsilon E(s)$ and solving for $G(s,\epsilon)$. If we do this we obtain

$$G(s,\epsilon) = G(s) + \epsilon E(s) \tag{36}$$

where E(s) is the absolute error given by (34) or

$$G(s,\epsilon) = G(s)[I+\epsilon E(s)] \tag{37}$$

where E(s) is the relative error given by (35). Both (36) and (37) imply the same G(s,e) although they employ different types of errors to arrive at G(s,e). In either (36) or (37) G(s,e) is simply given by

$$G(s,e) = (1-e)G(s) + e\check{G}(s) \tag{38}$$

showing that G(s,e) is continuous in e for e on [0,1] and for all s e D_R and that G(s,e) satisfies (28) and (29).

In deriving stability margins based on theorems using different error criteria, we will find it useful to define a multiplicative uncertainty matrix L(s) to account for modelling errors in the open-loop plant. The perturbed or actual system $\check{G}(s)$ in this case is given by

$$\check{G}(s) = G(s)L(s) \tag{39}$$

which implicitly defines L(s). Notice that for the relative error criteria that L(s) is very simply given by

$$L(s) = (I+E(s)) \tag{40}$$

where E(s) is given by (35). However, as will be shown later (40) is not the only description of L(s); there are other types of relative errors yet to be discussed in which the relationship between L(s) and the generic E(s) is not so simply given by (31). We will use both L(s) as defined implicitly in (30) and a variety of error matrices denoted by E(s) in stating the subsequent robustness theorems.

Two robustness theorems based on the preceedings definitions of absolute and relative errors in (34) and (35) respectively are the following.

Theorem 3 [48,49]: The polynomial $\tilde{\phi}_{CL}(s)$ has no CRHP zeros and hence the perturbed feedback system is stable if the following conditions hold:

1. condition 1 of Theorem 2 holds
2. $\sigma_{min}[I+G(s)] > \sigma_{max}[E(s)]$ for all $s \in \Omega_R$ where $E(s)$ is given by (34), and Ω_R was defined by (33).

Proof: From (36) we see that $I+G(s,\epsilon)$ is given by

$$I+G(s,\epsilon) = I+G(s) + \epsilon E(s) \quad .$$

From the properties of singular values (see (2.41)) we know that $I+G(s) + \epsilon E(s)$ will be nonsingular if

$$\sigma_{min}[I+G(s)] > \sigma_{max}[\epsilon E(s)] = \epsilon\, \sigma_{max}[E(s)] \qquad (41)$$

which is clearly guaranteed by condition 2 since ϵ is always between zero and unity and thus condition 2 of Theorem 2 holds.

Q.E.D.

Theorem 4 [14,48,49]: The polynomial $\tilde{\phi}_{CL}(s)$ has no CRHP zeros and hence the perturbed feedback system is stable if the following conditions hold:

1. condition 1 of Theorem 2 holds
2. $\sigma_{min}[I+G^{-1}(s)] > \sigma_{max}[E(s)]$ for all $s \in \Omega_R$ where $E(s)$ is given by (35).

Proof: From (37) we see that $I+G(s,\epsilon)$ is given by

$$I+G(s,\epsilon) = I+G(s)[I+\epsilon E(s)]$$

$$= G(s)[I+G^{-1}(s) + \epsilon E(s)] \quad . \tag{42}$$

Here by writing $G^{-1}(s)$ we assume it exists[1] so that $I+G(s,\epsilon)$ is singular if and only if $[I+G^{-1}(s) + \epsilon E(s)]$ is singular. As in the proof of Theorem 3, we know from (2.41) that condition 2 guarantees that $I+G^{-1}(s) + \epsilon E(s)$ is nonsingular, hence Theorem 2 is satisifed.

Q.E.D.

Theorem 4 was first proved by Doyle [14] using singular values and Nyquist's theorem but under the slightly stronger condition that E(s) be stable. An operator version of Theorem 3 is due to Sandell [48] who was the first to consider additive perturbations. Laub [49] provides further numerical insights to the relationship of Theorems 3 and 4.

Before we give some discussion of these theorems and some possible corollaries, we will develop some additional robustness theorems which are complementary to Theorems 3 and 4 and are derived on the basis of alternate definitions of the error matrix E(s).

Suppose that instead of measuring the absolute relative errors

---

[1] The assumption that G^{-1} exists guarantees that any pertrubed system $\tilde{G}$ can be represented as $\tilde{G} = G(I+E)$. However, if G is singular but $\tilde{G}$ is in the range space of G then E may be implicitly defined as a bounded solution of $GE = \tilde{G}-G$. In this case Theorem 4 still holds if $\sigma_{min}(I+G^{-1})$ is replaced by its equivalent for all G, $\sigma^{-1}_{max}[G(I+G)^{-1}]$, which is bounded by condition 1 if $G \neq 0$. If $\tilde{G}$ is not in the range of G then $\tilde{G}$ cannot be represented as $\tilde{G} = G(I+E)$.

between $\tilde{G}(s)$ and $G(s)$, we measure the absolute and relative errors between $\tilde{G}^{-1}(s)$ and $G^{-1}(s)$. In the SISO case, this would correspond to measuring the absolute and relative errors between the nominal and perturbed systems on an <u>inverse</u> Nyquist diagram in which the inverse loop transfer functions $g^{-1}(s)$ and $\tilde{g}^{-1}(s)$ are plotted. (The inverse Nyquist diagram can also be used to determine stability by counting encirclements of the critical points (0,0) and (-1,0) in the complex plane.)[1] Therefore, it would be natural to define the absolute and relative errors between the nominal and perturbed systems as

$$E(s) = \tilde{G}^{-1}(s) - G^{-1}(s) \tag{43}$$

for the absolute error and

$$E(s) = [\tilde{G}^{-1}(s) - G^{-1}(s)]G(s) \tag{44}$$

for the relative error. Using (43) and (44) we may define a $G(s,\epsilon)$, again by replacing $\tilde{G}(s)$ by $G(s,\epsilon)$ and $E(s)$ by $\epsilon E(s)$ in (43) and (44), and then solving for $G(s,\epsilon)$. If this is done, we obtain

$$G(s,\epsilon) = [G^{-1}(s) + \epsilon E(s)]^{-1} \tag{45}$$

where $E(s)$ is given by (43) and

$$G(s,\epsilon) = G(s)[I+\epsilon E(s)]^{-1} \tag{46}$$

where $E(s)$ is given by (44). Both (45) and (46) give the same $G(s,\epsilon)$ which written in terms of $G(s)$ and $\tilde{G}(s)$ is

---

[1] It is not intended to give a discussion of the inverse Nyquist criterion [1] but only mention it to suggest that the use of $G^{-1}(s)$ is as reasonable as $G(s)$ in a definition of model error.

$$G(s,\theta) = [(1-\theta)G^{-1}(s) + \theta\tilde{G}^{-1}(s)]^{-1} \tag{47}$$

where now we see that θ enters <u>nonlinearly</u> and it is not clear that $G(s,\theta)$ is continuous in θ in [0,1] for all $s \in D_R$ but is is clear that it does satisfy (28) and (29). The type of $G(s,\theta)$ in (47) could be replaced by the one in (38) and theorems worked out in terms of the errors described by (43) and (44). This approach was taken by Lehtomaki, Sandell and Athans [51] and led to more restrictive and complicated conditions to check than the approach using (47).

Since (45), (46) and (47) are all equivalent in that they give rise to the same $G(s,\theta)$ we may work with any one of them to prove assertions about the continuity of $G(s,\theta)$ required by Theorem 2. If $\tilde{G}^{-1}(s)$ and $G^{-1}(s)$ exist, so that $E(s)$ in (44) is well-defined, then we can see that for $G(s,\theta)$ to be continuous in θ for $(s,\theta) \in D_R \times [0,1]$ all we need to guarantee is that $[I+\theta E(s)]$ is nonsingular . Notice that in this case $L(s)$ is simply

$$L(s) = [I+E(s)]^{-1} \tag{48}$$

and that $[I+\theta E(s)]$ is nonsingular for all θ in [0,1] if $L(s)$ defined by (39) has no strictly negative eigenvalues. This is true since if $L(s)$ has no zero or negative eigenvalues, neither does $I+E(s)$ and thus $E(s)$ cannot have eigenvalues in the interval $(-\infty, -1]$ so that $\theta E(s)$ never has eigenvalues of -1. Therefore with these restrictions $G(s,\theta)$ is continuous in θ on $D_R \times [0,1]$. We also see from (46) that if $E(s)$ is bounded (i.e., $\tilde{G}^{-1}(s)$ and $\tilde{G}^{-1}(s)$ exist) and $L(s)$ has no zero or negative eigenvalues that $||G(s,\theta)||_2 \to 0$ as $|s| \to \infty$ for any

θ in [0,1]. This allows us to check for the nonsingularity of $I+G(s,\theta)$ only on $\Omega_R \times [0,1]$ in Theorem 2. We may now state the theorems analogous to Theorems 3 and 4.

Theorem 5: The polynomial $\tilde{\phi}_{CL}(s)$ has no CRHP zeros and hence the perturbed feedback system is stable if the following conditions hold:

1. condition 1 of Theorem 2 holds
2. $L(s)$ of (39) has no zero or strictly negative real eigenvalues for any $s \in \Omega_R$
3. $\sigma_{min}[I+G^{-1}(s)] > \sigma_{max}[E(s)]$ for all $s \in \Omega_R$ where $E(s)$ is given by (43)

Proof: From (45) we have that

$$I+G(s,\theta) = I + [G^{-1}(s) + \theta E(s)]^{-1}$$

$$= [I+G^{-1}(s) + \theta E(s)][G^{-1}(s) + \theta E(s)]^{-1}$$

$$= [I+G^{-1}(s) + \theta E(s)]G(s,\theta) \qquad (49)$$

and since $G(s,\theta)$ is nonsingular[1], $I+G(s,\theta)$ is nonsingular if and only if $[I+G^{-1}(s) + \theta E(s)]$ is nonsingular which is true by condition 3. Condition 2 merely ensures that we have a $G(s,\theta)$ continuous in θ to work with as required to apply Theorem 2. Thus, Theorem 2 holds and $\tilde{\phi}_{CL}(s)$ has no CRHP zeros.

Q.E.D.

---

[1] In this proof essential use of the fact that $G(s)$ and $\tilde{G}(s)$ are both invertible on D_R is made. This is different from the case of the footnote of Theorem 4.

The next theorem works with the relative error between $\tilde{G}^{-1}(s)$ and $G^{-1}(s)$ and plays a fundamental role in establishing the properties of LQ (linear-quadratic) state feedback regulators which will be discussed in Chapter 5.

Theorem 6: The polynomial $\tilde{\phi}_{CL}(s)$ has no CRHP zeros and hence the perturbed feedback system is stable if the following conditions hold:

1. condition 1 of Theorem 2 holds
2. L(s) of (39) has no zero or strictly negative real eigenvalues
3. $\sigma_{min}[I+G(s)] > \sigma_{max}[E(s)]$ for all $s \in \Omega_R$
   where E(s) is given by (44)

Remark: If condition 3 is satisfied and $\sigma_{min}[I+G(s)] \leq 1$ then it can be easily shown via (48) that condition 2 is automatically satisfied.

Proof: From (46) we have that

$$I+G(s,\epsilon) = I + G(s)[I+\epsilon E(s)]^{-1} = [I+G(s) + \epsilon E(s)][I+\epsilon E(s)]^{-1} \quad (50)$$

and condition 2 not only ensures $G(s,\epsilon)$ is continuous[1] on $D_R x[0,1]$ but also that $I+\epsilon E(s)$ is nonsingular on the same set. Thus $I+G(s,\epsilon)$ is

[1] In this proof no essential use of the fact that $\tilde{G}^{-1}$ and G^{-1} exist is made. If E is implicitly defined by $G = \tilde{G}(I+E)$ rather than (34), then Theorem 6 still holds. However, if $\tilde{G}$ is not in the range space of G, and vice versa, it is not possible to represent $\tilde{G}$ as $\tilde{G} = G(I+E)^{-1}$. Thus, even if G^{-1} and $\tilde{G}^{-1}$ do not exist it may be that $G(s,\epsilon)$ is continuous on $D_R x[0,1]$ by using the implicit definition of E if $\tilde{G}$ can be so represented.

nonsingular if and only if [I+G(s) + $\Delta E(s)$] is nonsingular which is guaranteed by condition 3. Hence, again Theorem 2 is satisfied and therefore $\tilde{\phi}_{CL}(s)$ has no CRHP zeros.

Q.E.D.

Theorem 6 is an improved version of a theorem found in [51].

Observation: The condition that L(s) have no strictly real and negative eigenvalues or be singular can be interpreted in terms of a phase reversal of certain signals between the nominal and perturbed systems or as the introduction of transmission zeros by the modelling error. To make this precise, suppose that for some ω_0 that $L(j\omega_0)\underline{x} = \lambda\underline{x}$ for some complex nonzero vector $\underline{x}$ and some real $\lambda \leq 0$. Then there exists a vector $\underline{u}(t)$ of input sinusoids of various phasing and at frequency ω_0 which when applied to the nominal system produces an output $\underline{y}(t)$ and produces an output $\lambda\,\underline{y}(t)$ when applied to the perturbed system. This is depicted in Fig. 17.

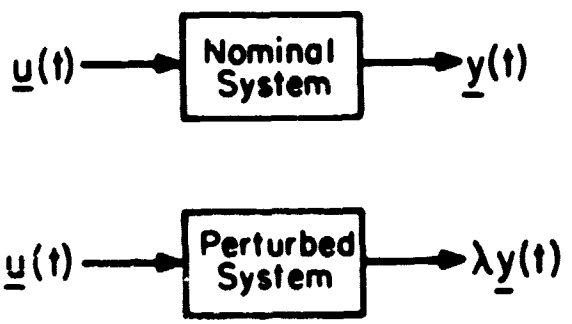

Fig. 17: Relationship between nominal and perturbed system for special input $\underline{u}(t)$ when $L(j\omega_0)$ has eigenvalue λ.

Thus when λ is negative the phase difference between the sinusoidal outputs of the nominal and perturbed systems is 180°. If $\lambda=0$ then the perturbed system has transmission zeros at $\pm j\omega_0$.

This fact is significant since Theorems 5 and 6 can never guarantee stability with respect to model uncertainty when the phase of the system outputs is completely uncertain above some frequency or with respect to sensor or actuator failures in the feedback channels.

Note that in general that condition 1 of Theorems 3 to 6 and the state-space description of the nominal and perturbed systems implicitly place other restrictions on L(s) (and also E(s)). These are simply that L(s) represent a finite dimensional linear time-invariant system that is possibly unstable and that L(s) has no purely imaginary poles. Similar conditions may be derived for each of the four forms of errors used in Theorems 3 to 6.

3.6 Interpretations of Robustness Theorems

Up to this point, it is probably unclear to the reader what the significance of the various error criteria are and how they are related. This can be partly clarified by an understanding of how each error enters into the structure of the perturbed system from a block diagram perspective. This is done in Fig. 18 where a very pleasing symmetry occurs that corresponds to the four basic arithmetic operations of addition, subtraction, multiplication and division. As can be seen from Fig. 18 the absolute type of errors correspond to addition and subtraction whereas the relative errors correspond to multiplication and division. Other types of errors can be represented as combinations

Block Diagram of Perturbed System	Error Criterion Perturbed Systems and Stability Test
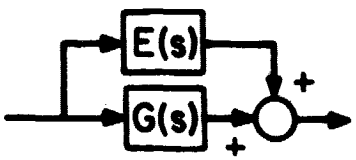 Feedforward (Addition)	$E(s) = \tilde{G}(s) - G(s)$ $\tilde{G}(s) = G(s) + E(s)$ $\sigma_{min}(I+G(s)) > \sigma_{max}(E(s))$
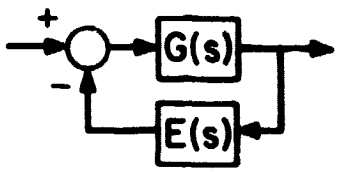 Feedback (subtraction)	$E(s) = \tilde{G}^{-1}(s) - G^{-1}(s)$ $\tilde{G}(s) = (G^{-1}(s) + E(s))^{-1}$ $\sigma_{min}(I+G^{-1}(s)) > \sigma_{max}(E(s))$
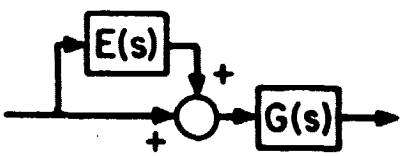 (Multiplication)	$E(s) = G^{-1}(s)[\tilde{G}(s)-G(s)]$ $\tilde{G}(s) = G(s)(I+E(s))$ $\sigma_{min}(I+G^{-1}(s)) > \sigma_{max}(E(s))$
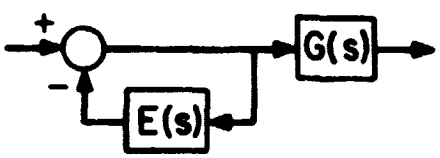 (Division)	$E(s) = [\tilde{G}^{-1}(s)-G^{-1}(s)]G(s)$ $\tilde{G}(s) = G(s)(I+E(s))^{-1}$ $\sigma_{min}(I+G(s)) > \sigma_{max}(E(s))$

Fig. 18: Physical Representation of Perturbed Models Corresponding to Various Error Criteria and Associated Stability Test.

C-2

of these basic types of errors.

For now however, we will defer that topic and discuss the interpretations of the robustness theorems that deal with relative errors and give some pictorial illustrations of why these theorems ensure that $I+G(s,\Theta)$ is nonsingular and how they are related.

We shall work mainly with the relative error type theorems since from them we may derive gain and phase margins for which design engineers have a more intuitive feel. In the theorems dealing with absolute type errors it is difficult to account for the effect of the compensator implicit in G(s) on the model error (i.e., the model error depends on the compensator used). This does not happen with the relative error criteria.

To begin with, recall that in Theorems 4 and 6 that L(s) is given respectively by

$$L(s) = I + E(s) \tag{51}$$

for E(s) given by (35) and

$$L(s) = (I+E(s))^{-1} \tag{52}$$

for E(s) given by (44). If we solve these last two equations for E(s) we obtain from (51)

$$E(s) = L(s) - I \tag{53}$$

and from (52)

$$E(s) = L^{-1}(s) - I \ . \tag{54}$$

Thus by making $||E(s)||_2$ small in (53) L(s) is kept close to the identity matrix whereas in (54) it is $L^{-1}(s)$ that is kept close to the identity matrix by making $||E(s)||_2$ small. This points out the difference in the types of errors since the same L(s) may make one error quite large while making the other only moderately large.

The basic inequalities in Theorems 4 and 6 written in terms of L(s) are given respectively by

$$\sigma_{min}[I+G^{-1}(s)] > \sigma_{max}[L(s)-I] \tag{55}$$

for Theorem 4 and by

$$\sigma_{min}[I+G(s)] > \sigma_{max}[L^{-1}(s) - I] \tag{56}$$

for Theorem 6. The inequality (55) is the MIMO generalization of the SISO inequality (7) of section 3.2 but written in terms of $\ell(s)$ rather than $\tilde{g}(s)$. Thus in (55) we see that $\sigma_{min}[I+G^{-1}(s)]$ is just the multivariable version of the distance to the critical point (0,0) and $\sigma_{max}[L(s)-I]$ is just the generalization of the distance between $\tilde{G}(s)$ and G(s). Similar interpretations of (56) can be made.

The SISO analogs of (55) and (56) are given by

$$|1+g^{-1}(s)| > \alpha > |\ell(s) - 1| \tag{57}$$

and

$$|1+g(s)| > \alpha > |\ell^{-1}(s)-1| \tag{58}$$

respectively. In the form using $\ell(s)$ rather $\tilde{g}(s)$, the inequalities (57) and (58) provide a geometric insight to the relationship of g(s)

and $\ell(s)$. The admissable region of the complex plane for $-g^{-1}(s)$ and $\ell(s)$ satisfying (57) is depicted in Fig. 19. Fig. 20 gives the analogous regions for $g(s)$ and $-\ell^{-1}(s)$ satisfying (58). From Fig. 19 it is clear that

$$-g^{-1}(s) \neq \ell(s) \tag{59}$$

and from Fig. 20 that

$$-\ell^{-1}(s) \neq g(s) \tag{60}$$

which simply ensure that $1+g(s)\ell(s) = 1+\tilde{g}(s) \neq 0$ or that $\tilde{g}(s)$ does not pass through $(-1,0)$. Recall that in Theorem 2 not only must $1+\tilde{g}(s) \neq 0$ but we must be able to construct a $g(s,\theta)$ such that $1+g(s,\theta) \neq 0$ for θ in $[0,1]$. However, due to the way that $g(s,\theta)$ was constructed this merely results in the requirement that

$$|1+g^{-1}(s)| > \theta|\ell(s)-1| \tag{61}$$

in the case of Theorem 4, and

$$|1+g(s)| > \theta\ |\ell^{-1}(s) - 1| \tag{62}$$

for Theorem 6. These inequalities are obviously guaranteed by (59) and (60) since θ is between zero and unity.

The main point of this discussion was to show the use of circles to divide the complex plane into disjoint regions, one in which $\ell(s)$ (or $\ell^{-1}(s)$) lies and its complement in which $-g^{-1}(s)$ (or $g(s)$) must lie. The fact that the radii of the circles can be interpreted as the magnitude of an error or the distance to the critical point is not crucial. Later on in this chapter we will use the idea of separating the complex plane into two disjoint regions to derive additional robustness theorems

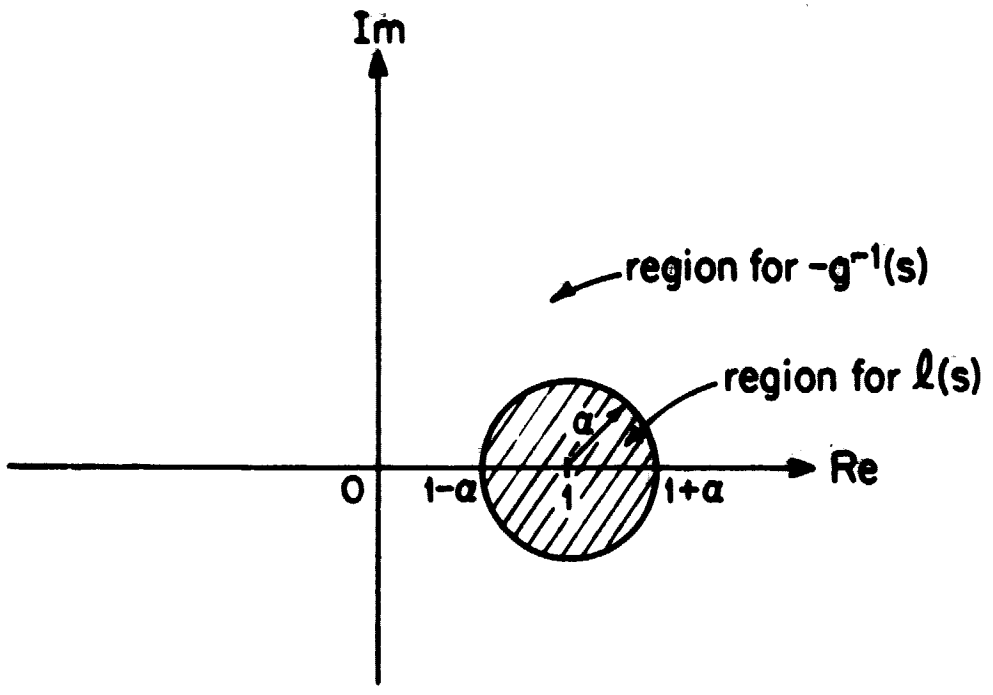

Fig. 19: Admissable regions for $g > (s)$ and $\ell(s)$ satisfying $|1+g^{-1}(s)| > \alpha > |\ell(s)-1|$

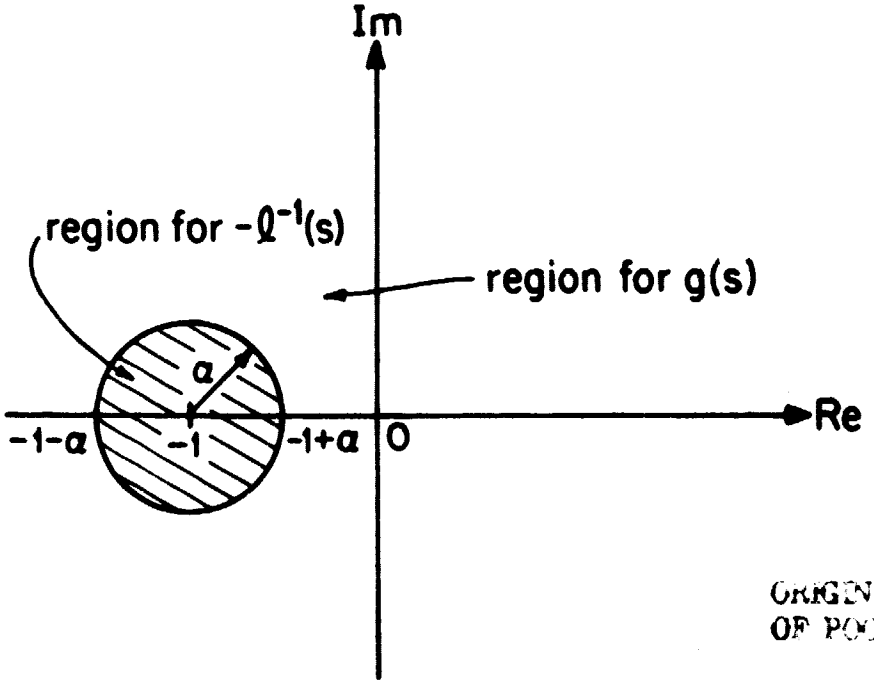

Fig. 20: Admissable regions for $g(s)$ and $-\ell^{-1}(s)$ satisfying $|1+g(s)| > \alpha > |\ell^{-1}(s)-1|$

and clarify their relationships to the well-known small gain theorem [12].

To continue the discussion on the relationship of Theorems 4 and 6, we make the following observation that in (55) and (56) as $\sigma_{min}(I+G)$ and $\sigma_{min}(I+G^{-1})$ increases the bounds on L(s) and the error becomes less stringent. Therefore, to tolerate both kinds of modelling errors, one would like to make both $\sigma_{min}(I+G)$ and $\sigma_{min}(I+G^{-1})$ as large as possible. However, these two quantities are related algebraically so that we cannot make them both independently large. Their algebraic relationship can be derived trivially from the matrix identity [49]

$$(I+G)^{-1} + (I+G^{-1})^{-1} \equiv I \tag{63}$$

using the triangle inequality and the simple relationship $\sigma_{min}(A) = \sigma^{-1}_{max}(A^{-1})$. There are three inequalities relating $\sigma_{min}(I+G)$ to $\sigma_{min}(I+G^{-1})$ which are given by

$$\sigma^{-1}_{min}(I+G) + \sigma^{-1}_{min}(I+G^{-1}) \geq 1 \tag{64}$$

$$\sigma^{-1}_{min}(I+G) + 1 \geq \sigma^{-1}_{min}(I+G^{-1}) \tag{65}$$

$$\sigma^{-1}_{min}(I+G^{-1}) + 1 \geq \sigma^{-1}_{min}(I+G) \tag{66}$$

Two other inequalities relating $\sigma_{min}(G)$ and $\sigma_{max}(G)$ to $\sigma_{min}(I+G)$ and $\sigma_{min}(I+G^{-1})$ are given by

$$\sigma_{max}(G) \geq \frac{\sigma_{min}(I+G)}{\sigma_{min}(I+G^{-1})} \geq \sigma_{min}(G) \quad . \tag{67}$$

These inequalities are illustrated in Fig. 21.

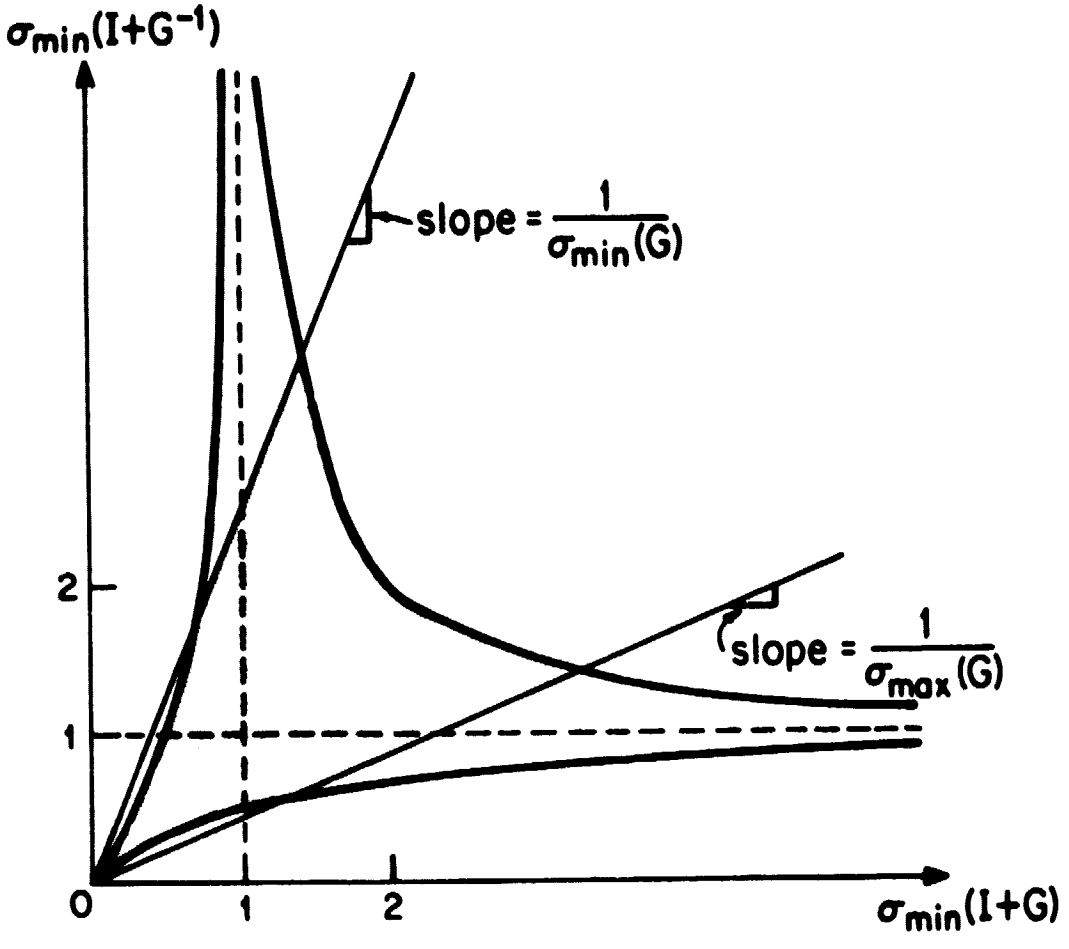

Fig. 21: Shaded Area Represents Allowable Values of $(\sigma_{min}[I+G], \sigma_{min}[I+G^{-1}])$ ordered pairs.

From Fig. 21 it is clear that when $\sigma_{min}(G)$ is large (i.e., large loop gain in every feedback loop) that $\sigma_{min}(I+G^{-1})$ is necessarily near one and $\sigma_{min}(I+G)$ is large. This indicates that Theorem 6 will give a better indication of control system robustness with respect to the model error criterion (44) in the typically high performance - low frequency region than will Theorem 4. Likewise when $\sigma_{max}(G)$ is small (i.e., all

feedback loops are rolled off) Theorem 4 gives a better indication of the robustness of the system with respect to the model error criterion (35) since $\sigma_{min}(I+G^{-1})$ is large and $\sigma_{min}(I+G)$ is near unity. The exact sense in which one theorem gives a better robustness indication depending on the nature of G(s) will be made precise in the corollaries of Theorems 4 and 6 that specify different types of stability margins discussed in the next section.

3.7 Multiloop Stability Margins

In this section we shall derive guaranteed minimum gain and phase margins for MIMO systems as functions of both $\sigma_{min}[I+G(s)]$ and $\sigma_{min}[I+G^{-1}(s)]$. We shall also introduce the notion of a crossfeed tolerance which again is specified by $\sigma_{min}[I+G(s)]$ or $\sigma_{min}[I+G^{-1}(s)]$. These stability margins are simply corollaries to Theorems 4 and 6 and are easily obtained by assuming specific forms for L(s).

3.7.1 Multiloop Gain and Phase Margins

In contrast to the SISO case, it is not clear what gain and phase margins are in a multiloop system since gain or phase changes in one loop may affect the calculation of the gain and phase margins in another loop. Therefore, to avoid this problem we shall define what we mean by multiloop gain and phase margins. This can be done with reference to Fig. 22 where L(s) is chosen to be a diagonal matrix.

Definition: The multiloop gain margin is the pair of real numbers c_1 and c_2 defining the largest interval[1] (c_1, c_2) such that when $\ell_i(s)$

[1] We could also use closed-intervals in the definition of these margins.

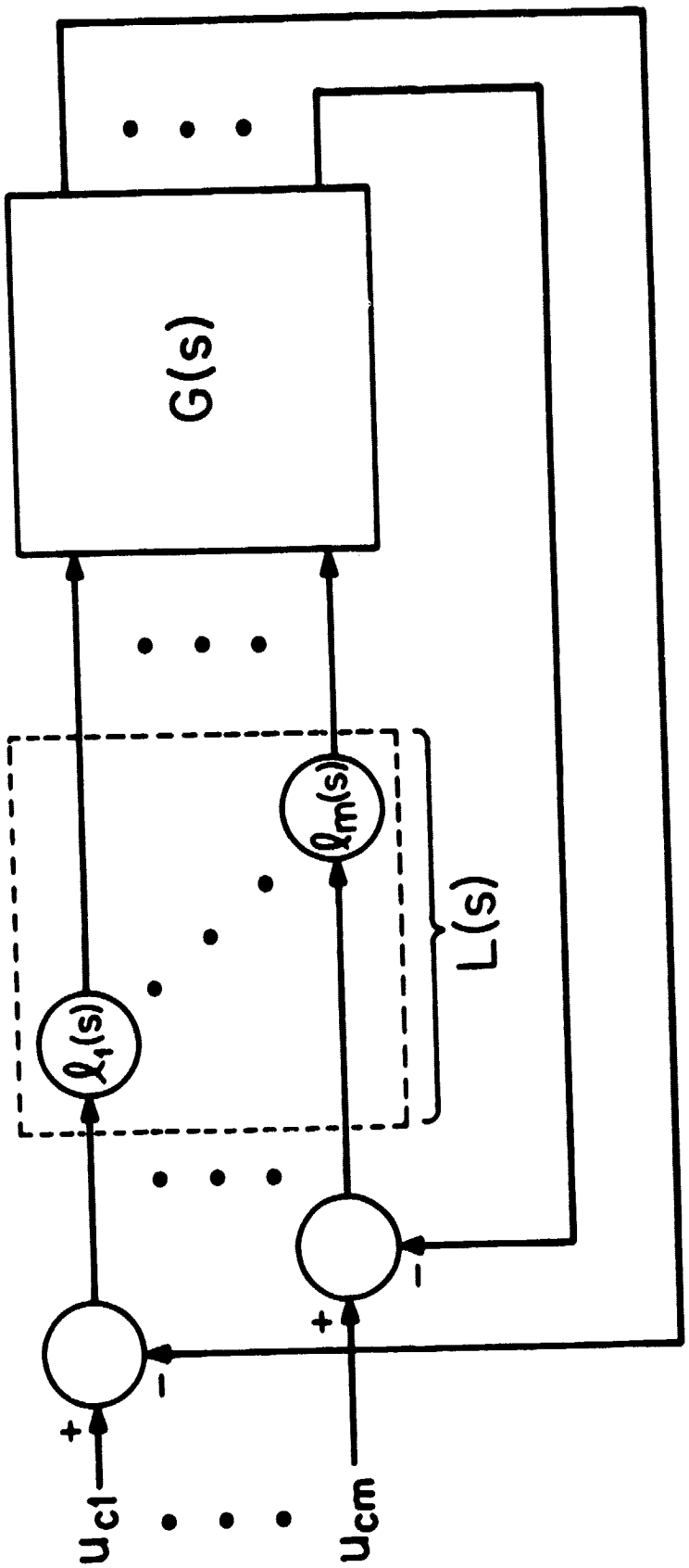

Fig. 22: Configuration for Multiloop Gain and Phase Margin Definition

$i = 1,2,\ldots,m$ in Fig. 22 are all real constants ℓ_i and satisfy the inequalities

$$c_1 < \ell_i < c_2 \quad , \quad i = 1,2,\ldots,m \tag{68}$$

the closed-loop system remains stable.

Definition: The multiloop phase margin is pair of real numbers c_1 and $-c_1$ defining the largest interval $(-c_1,c_1)$ such that when $\ell_i(j\omega)$, $i = 1,2,\ldots,m$ in Fig. 22 are of the form[1] $e^{j\phi_i(\omega)}$ where $\phi_i(\omega)$ are real and satisfy the inequality

$$-c_1 < \phi_i(\omega) < c_1 \quad , \quad i = 1,2,\ldots,m \tag{69}$$

and the closed-loop system remains stable.

We will denote the multiloop gain margin of (68) by

$$GM = (c_1, c_2) \tag{70}$$

and similiarly we denote the multiloop phase margin of (69) by

$$PM = (-c_1, c_1) \ . \tag{71}$$

Note that in the SISO case (refer to Fig. 7) that these multiloop stability margins reduce to the usual single stability margins but that in the MIMO case they differ from the stability margins obtainable a single loop at a time since these stability margins apply in all loops simultaneously. Of course, the word "simultaneously" does not mean that we can apply gain and phase changes simultaneously in the same feedback

[1] We assume also that $e^{j\phi_i(\omega)}$ has a state space representation in order to ensure that $\tilde{G}(s)$ has a state space representation.

loop but that only strict gain changes or only strict phases changes may occur in separate feedback channels simultaneously within the prescribed limits of the multiloop stability margins. We emphasize that these types of multiloop margins consider only a small class of modelling errors describable by a diagonal L(s). With these preliminaries we are ready to present the following corollaries to Theorems 4 and 6 respectively.

Corollary 1: If $\phi_{CL}(s)$ has no CRHP zeros and

$$\sigma_{min}(I+G^{-1}(s)) > \alpha \tag{72}$$

for all $s \in \Omega_R$ then the multiloop gain and phase margins are bounded[1] in the following manner

$$GM \supset [1-\alpha,\ 1+\alpha] \tag{73}$$

and

$$PM \supset [-2\sin^{-1}\frac{\alpha}{2},\ \ 2\sin^{-1}\frac{\alpha}{2}]. \tag{74}$$

Proof: From Theorem 4 and (51) we know that $\tilde{\phi}_{CL}(s)$ has no CRHP zeros if for all $s \in \Omega_R$

$$\sigma_{max}(L(s)-I) < \sigma_{min}(I+G^{-1}(s)) \tag{75}$$

and thus also if

---

[1] The symbol $\supset$ refers to set inclusion. Thus $A \supset B$ means that B is contained in A. Thus (73) means that the upward gain margin is at least as big as $1+\alpha$ and that the gain reduction margin is at least as small as $1-\alpha$. Similar statements apply to (74).

$$\sigma_{max}(L(s)-I) \leq \alpha \tag{76}$$

for all $s \in \Omega_R$. Now if L(s) is given by

$$L(s) = \text{diag}[\ell_1(s), \ell_2(s), \ldots, \ell_m(s)] \tag{77}$$

then (76) implies that for all i

$$|\ell_i(s)-1| \leq \alpha \quad . \tag{78}$$

If $\ell_i(s)$ is real and is denoted by ℓ_i then

$$1-\alpha \leq \ell_i \leq 1+\alpha \tag{79}$$

and if $\ell_i(j\omega)$ is of the form $e^{j\phi_i(\omega)}$ with $\phi_i(\omega)$ being real, then

$$|e^{j\phi_i(\omega)} - 1| \leq \alpha \tag{80}$$

$$\left| e^{j\frac{\phi_i(\omega)}{2}} - e^{j\frac{\phi_i(\omega)}{2}} \right| \leq \alpha \tag{81}$$

$$-\alpha \leq 2 \sin \frac{\phi_i(\omega)}{2} \leq \alpha \tag{82}$$

or

$$|\phi_i(\omega)| \leq 2 \sin^{-1} \left(\frac{\alpha}{2}\right) \quad . \tag{83}$$

The bounds on the multiloop stability margins follow from (79) and (83).

Q.E.D.

Corollary 2: If $\phi_{CL}(s)$ has no CRHP zeros and

$$\sigma_{min}(I+G(s)) > \alpha \tag{84}$$

for all $s \in \Omega_R$ and $\alpha \leq 1$ then the multiloop gain and phase margins are bounded in the following manner

$$GM \supset \left[\frac{1}{1-\alpha}, \frac{1}{1+\alpha}\right] \tag{85}$$

and

$$PM \supset [-2 \sin^{-1}\frac{\alpha}{2}, 2 \sin^{-1}\frac{\alpha}{2}] . \tag{86}$$

Proof: Following the proof of Corollary 1 we similarly deduce that the corresponding analog to equation (78) is

$$|\ell_i^{-1}(s) - 1| \leq \alpha \tag{87}$$

and thus for real $\ell_i(s)$ denoted ℓ_i we must have that

$$\frac{1}{1+\alpha} \leq \ell_i \leq \frac{1}{1-\alpha} \tag{88}$$

and for $\ell_i(j\omega)$ of the form $e^{j\phi_i(\omega)}$, $\phi_i(\omega)$ real, we have

$$|e^{-j\phi_i(\omega)} - 1| \leq \alpha \tag{89}$$

which implies

$$|\phi_i(\omega)| \leq 2 \sin^{-1}(\alpha/2) . \tag{90}$$

Q.E.D.

It must be emphasized that corollaries 1 and 2 provide worst case analysis bounds on what the actual stability margins are. This can be illustrated in the SISO case by Fig. 23 where $|1+g(s)| \geq \alpha$ for

all $s \in D_R$ so that Corollary 2 is applicable[1].

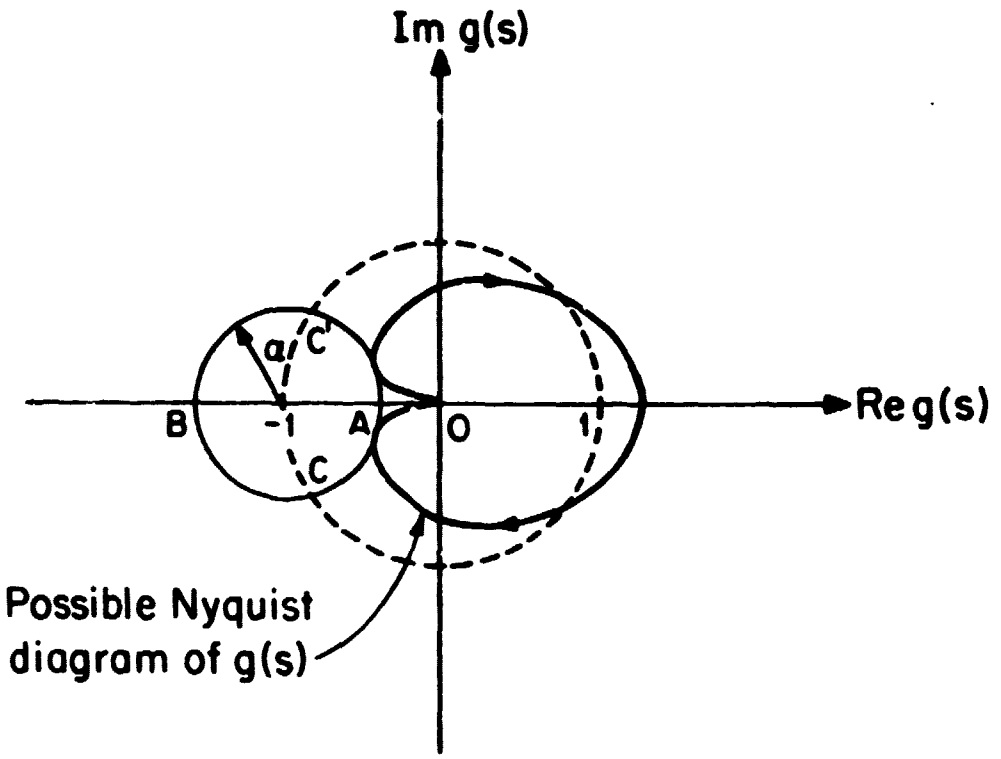

Fig. 23: Nyquist Diagram Illustrating Bounds of Corollary 2.

Since the only information about the system g(s) is contained in the single parameter α, the only information utilized by Corollary 2 is that g(s) touches the circle of radius α centered at -1 but that the Nyquist locus of g(s) never penetrates the interior of the circle. Thus to derive the worst case upward gain margin the corollary assumes that

---

[1] We have used $|1+g(s)| \geq \alpha$ rather than $|1+g(s)| > \alpha$ for convenience. The only modification of Corollary 2 is to make the bounds in (85) and (86) open sets.

g(s) passes through point A. Similarly, the worst case gain reduction margin and worst case phase margin are obtained by assuming that g(s) passes through points B and C (or C') respectively. These worst case margins are then useful bounds on the actual gain and phase margins. We refer to these bounds as guaranteed minimum gain or phase margins.

3.7.2 Crossfeed Tolerance

The previous stability margins have assumed that I(s) is diagonal. If this is not true then there are cross couplings from one feedback channel to another as in the example considered in section 3.3. The ability to tolerate crossfeed type of perturbations is also determined by the two quantities $\sigma_{min}[I+G^{-1}(s)]$ and $\sigma_{min}[I+G(s)]$ as in the following two corollaries to theorems 4 and 6 respectively.

Corollary 3: The polynomial $\tilde{\phi}_{CL}(s)$ has no CRHP zeros and hence the perturbed feedback system is stable if the following conditions hold:

1. condition 1 of Theorem 2 holds

2 $\sigma_{max}[X(s)] < \sigma_{min}(I+G^{-1}(s))$

and

$\sigma_{max}[Y(s)] < \sigma_{min}(I+G^{-1}(s))$

for all $s \in \Omega_R$ and where L(s) is given by

$$L(s) = \begin{bmatrix} I & X(s) \\ Y(s) & I \end{bmatrix} \qquad (91)$$

Proof: Immediate from the form of L(s) in (81) and Theorem 4.

In this corollary L(s) of (91) represents a bilateral crossfeed perturbation where X(s) is the fraction of the control signals of the second group of feedback channels fed into the first group of feedback channels and Y(s) is the fraction of the control signals of the first group of feedback channels fed into the second. If either X(s) or Y(s) is identically zero, then L(s) of (91) represents a unilateral crossfeed from one group of feedback channels to another. This is the particular form of crossfeed considered in Corollary 4.

Corollary 4: The polynomial $\tilde{\phi}_{CL}(s)$ has no CRHP zeros and hence the perturbed feedback system is stable if the following conditions hold:

1. condition 1 of theorem 2 holds
2. $\sigma_{max}[X(s)] < \sigma_{min}[I+G(s)]$

   for all $s \in \Omega_R$ and where L(s) is given by

$$L(s) = \begin{bmatrix} I & X(s) \\ 0 & I \end{bmatrix} \quad \text{or} \quad \begin{bmatrix} I & 0 \\ X(s) & I \end{bmatrix}. \tag{92}$$

Proof: Again immediate from Theorem 6 and the form of L(s) in (92).

3.8 Example of Section 3.3 Continued

If was shown that the system of Fig. 11 under the feedback $\underline{u} = -\underline{y}$ is nearly unstable if the value of b_{12} is very large. This nearness to instability is easily detected using Theorems 3, 4, 5 or 6 because

$\sigma_{min}[I+G^{-1}(s)]$ or $\sigma_{min}[I+G(s)]$ become very small at frequencies below 1 rad/sec. Fig. 24 shows a plot of $\sigma_{min}[I+G(j\omega)]$ as a function of ω with $b_{12} = 50$.

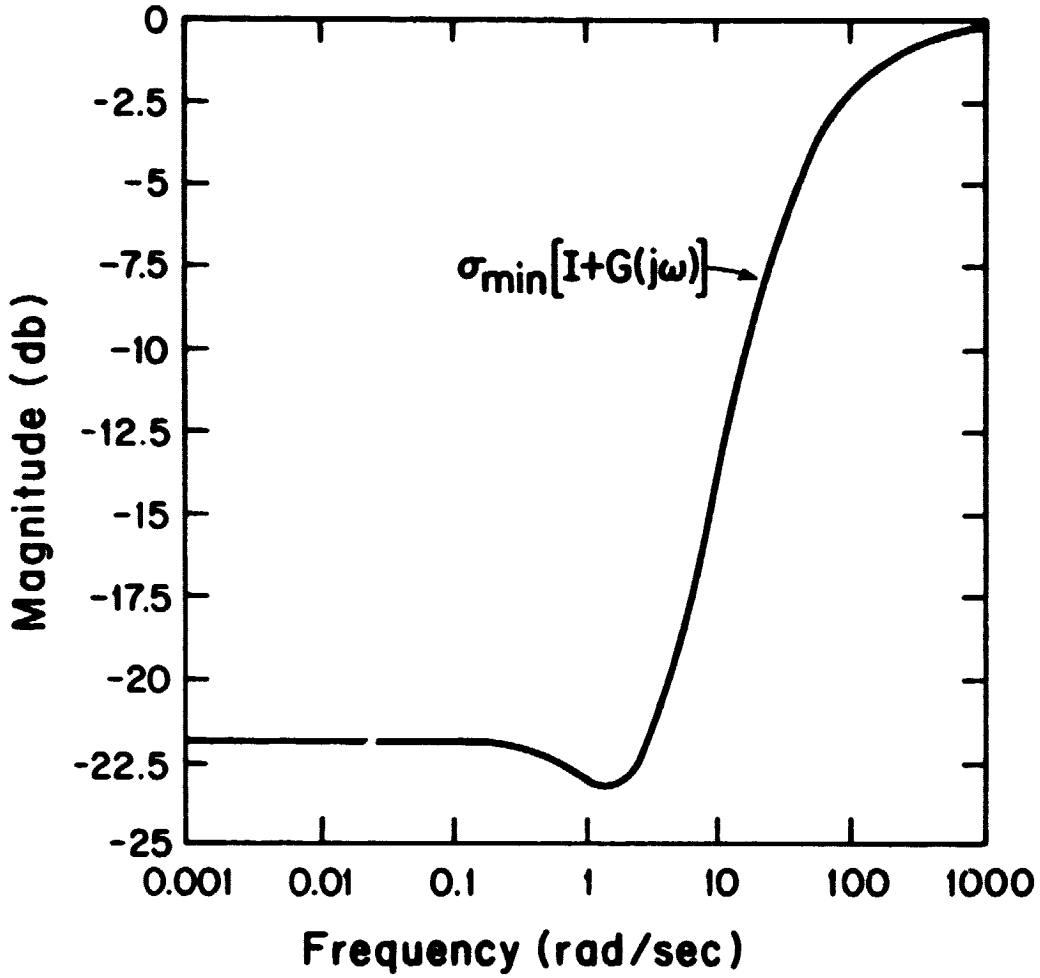

Fig. 24: Plot of $\sigma_{min}(I+G(j\omega))$ for Example of Section 3.3 (b_{12}=50), see Fig. 3.16.

If we use Corollary 2 we obtain the following bounds on the multiloop gain and phase margins

$$GM \supset (.93, 1.08) \tag{93}$$

$$PM \supset (-4.1°, 4.1°) \tag{94}$$

which are very conservative estimates of the multiloop gain and phase margins. Nevertheless, they indicate a robustness problem which is exhibited by the very small crossfeed tolerance of Corollary 4 which gives

$$\sigma_{max}[X(j1)] < \sigma_{min}[I+G(j1)] \cong 0.071 = -23\,dB. \tag{95}$$

This again is a worst-case bound on the allowable amount of crossfeed at $\omega=1$ but in this case it turns out that the magnitude of the error (i.e., $E(s) = [\tilde{G}^{-1}(s)-G^{-1}(s)]G(s)$) induced by the crossfeed perturbation of Fig. 16 is -20dB, nearly the smallest necessary to destabilize the closed-loop system.

3.9 Separating Functions and Additional Robustness Theorems

At this point after having given several different robustness theorems, whose method of proof depended upon the ability to ensure that $I+G(s,\theta)$ was nonsingular on $D_R \times [0,1]$, we shall consider a more general framework that allows us to generate stability theorems not necessarily derived from any particular error criterion as Theorems 4 to 6 were. After these additional theorems are generated we shall look for a possible associated natural definition of model error which if bounded in magnitude can not induce instability .

In this section, we will define $G(s,\theta)$ of Theorem 2 in terms of an $L(s,\theta)$ giving

$$G(s,\theta) = G(s)L(s,\theta) \tag{96}$$

where $L(s,\theta)$ is now continuous on $D_R \times [0,1]$ and such that (28) and (29) hold and find conditions on $G(s)$ and $L(s,\theta)$ to guarantee closed-loop stability. Recall from section 3.6, that the explanation of why Theorems 4 and 6 worked is that they ensured (in the SISO case) that

$$1+g(s,\theta) = 1+g(s)\ell(s,\theta) \neq 0 \tag{97}$$

on $D_R \times [0,1]$. That is they divided the complex plane into two disjoint regions by using a circle and then ensured that $-g^{-1}(s)$ was in one region and $\ell(s,\theta)$ in its complement. The different theorems used different circles and thus give different allowable regions where $\ell(s,\theta)$ may be located. It thus seems natural to generate other theorems by choosing different circles to separate the values of $\ell(s,\theta)$ and $-g^{-1}(s)$.

A simple way to specify a circle or line in the complex plane is to use a function $f(\cdot)$ known as a bilinear fractional transformation [52] given by

$$f(z) = \frac{az+b}{cz+d} \tag{98}$$

where $ad-bc \neq 0$ and z is a complex variable as are a,b,c and d. A circle or line can be specified by the equation

$$|f(z)| = \text{constant} \tag{99}$$

where different values of a,b,c,d and the constant may give different lines or circles (refer to Fig. 25 for an example). The function $f(\cdot)$ has the property that it always maps circles and lines into circles and

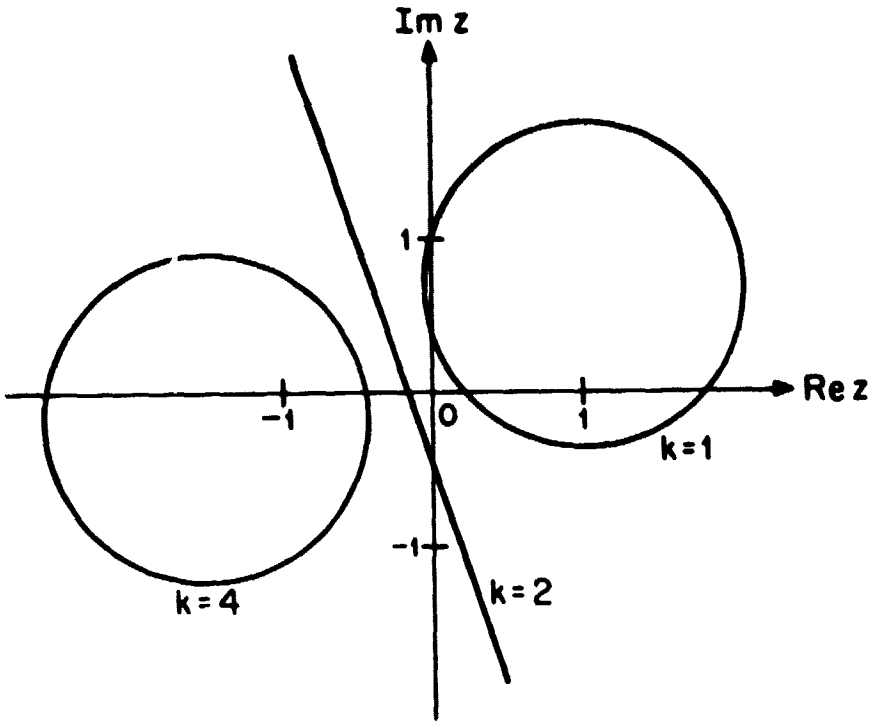

Fig. 25: Example $f(z) = \left|\frac{2z-(1+j)}{z+1}\right| = k$.

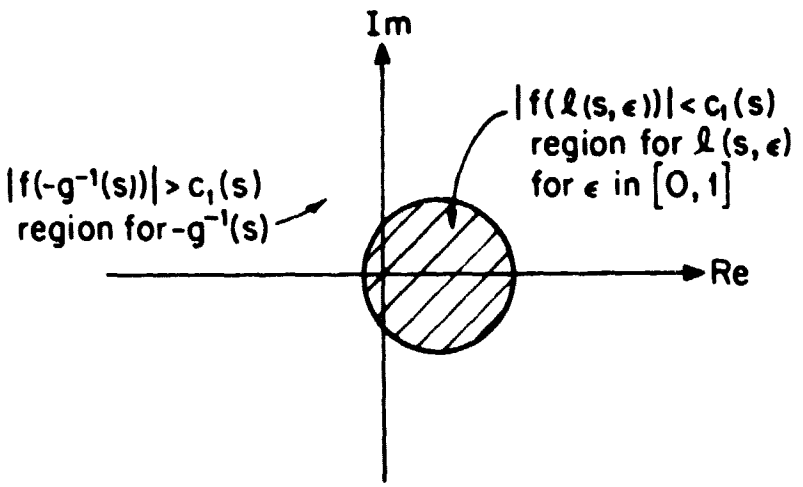

Fig. 26: Illustration of separating function in SISO case.

lines. The inverse function of $f(\cdot)$ denoted $f^{-1}(\cdot)$ also is a bilinear fractional transformation and thus shares these properties.

Now if we put $-g^{-1}(s)$ on the outside of a circle and $\ell(s,\theta)$ on the inside of a circle to separate them (Fig. 26) then we have a pair of inequalities of the form

$$|f(-g^{-1}(s))| > c_1(s) > |f(\ell(s,\theta))| \tag{100}$$

on $D_R x[0,1]$ where $c_1(s)$ is a positive scalar. It may be that in (100) $-g^{-1}(s)$ is on the inside of the circle and $\ell(s,\theta)$ on the outside depending on how $f(\cdot)$ is chosen but the key point is that $f(\cdot)$ in (100) separates $-g^{-1}(s)$ and $\ell(s,\theta)$ and thus will be called a <u>separating function</u>.

In order to develop a test that does not depend explicitly on θ as in (100), we may define $\ell(s,\theta)$

$$\ell(s,\theta) \triangleq f^{-1}[(1-\theta)f(1) + \theta f(\ell(s)] \tag{101}$$

so that

$$f(\ell(s,\theta)) = (1-\theta)f(1) + \theta f(\ell(s)) \quad . \tag{102}$$

Now since (100) must hold for $\ell(s,0) = 1$ and also for $\ell(s,1) = \ell(s)$, (102) implies that

$$|f(\ell(s,\theta))| \leq (1-\theta)|f(1)| + \theta|f(\ell(s))| \tag{103}$$

or

$$|f(\ell(s,\theta))| \leq \max\{|f(1)|, |f(\ell(s))|\} \tag{104}$$

and so we need only verify (100) at $\theta=0$ and $\theta=1$. Now if

$$|f(-g^{-1}(s))| > c_1(s) > |f(\ell(s))| \tag{105}$$

we are assured that (100) holds for all θ in [0,1] since $f(\cdot)$ must be picked to separate $-g^{-1}(s)$ from 1 or $g(s)$ from -1 and thus

$$|f(-g^{-1}(s))| > |f(1)| \tag{106}$$

Of course, the definition of $\ell(s,\theta)$ in (101) may place restrictions on $\ell(s)$ in order that $\ell(s,\theta)$ be continuous on $D_R x[0,1]$ that may need to be checked in addition to (105).

The preceeding discussion of the scalar case can be directly extended to the matrix case except that the circles become hyperspheres and the absolute value signs in the inequalities are replaced by $\sigma_{min}(\cdot)$ or $\sigma_{max}(\cdot)$. The objective now becomes to make sure that $I+G(s)L(s,\theta)$ is nonsingular or equivalently (assuming $G^{-1}(s)$ exists) that $L(s,\theta) - [-G^{-1}(s)]$ is nonsingular on $D_R x[0,1]$.

Now suppose that we can find a function $f(\cdot)$ mapping $\mathbb{C}^{nxn}$ to $\mathbb{C}^{nxn}$ such that $f(A) - f(B)$ is nonsingular if and only if $A-B$ is nonsingular for all A and B in $\mathbb{C}^{nxn}$ for which $f(A)$ and $f(B)$ are defined. This means that the nonsingularity of $L(s,\theta) - [-G^{-1}(s)]$ can be checked in terms of the nonsingularity of $f(L(s,\theta)) - f(-G^{-1}(s))$. A simple sufficient condition that guarantees the nonsingularity of $f(L(s,\theta)) - f(-G^{-1}(s))$ is the singular value inequality (see (2.41)) given by

$$\sigma_{min}[f(-G^{-1}(s))] > \sigma_{max}[f(L(s,\theta))] \ . \tag{107}$$

We again call $f(\cdot)$ a separating function since through (107) $f(\cdot)$ "separates" $-G^{-1}(s)$ and $L(s,\theta)$ (i.e., $L(s,\theta) + G^{-1}(s)$ is nonsingular).

In (107) $L(s,\theta)$ may be defined by

$$L(s,\theta) = f^{-1}[(1-\theta)f(I) + \theta f(L(s))] \tag{108}$$

which is analogous to (101). In (107) it is assumed again that

$$\sigma_{min}[f(-G^{-1}(s))] > \sigma_{max}[f(I)] \tag{109}$$

since with $L(s,0) = I$ the nominal system must satisfy (107) if $f(\cdot)$ is to be an appropriate separating function. Therefore (107) can be guaranteed for all θ in $[0,1]$ if

$$\sigma_{min}[f(-G^{-1}(s))] > \sigma_{max}[f(L(s))] \tag{110}$$

for all s in D_R.

In the matrix case, the separating functions $f(\cdot)$ may also be given by the matrix bilinear fractional transformation

$$f(X) = (AX+B)(CX+D)^{-1} \tag{111}$$

where A,B,C,D and X are complex matrices. To verify that they are indeed separating functions we present the following lemma.

Lemma 1: If the matrices A, CX+D and CY+D are nonsingular then X-Y is nonsingular if and only if $(AX-B)(CX+D)^{-1} - (AY+B)(CY+D)^{-1}$ is nonsingular.

Proof: Suppose X-Y is singular. Then there exists a vector $\underline{z}$ such that

$$X\underline{z} = Y\underline{z} \tag{112}$$

and thus

$$(AX+B)\underline{z} = (AY+B)\underline{z} \tag{113}$$

and

$$(CX+D)\underline{z} = (CY+D)\underline{z} \quad . \tag{114}$$

Since CX+D and CY+D are nonsingular, let the nonzero vector $\underline{v}$ be given by

$$\underline{v} = (CX+D)z = (CY+D)z \tag{115}$$

or

$$\underline{z} = (CX+D)^{-1}\underline{v} = (CY+D)^{-1}\underline{v} \quad . \tag{116}$$

Now substituting in (113) for $\underline{z}$ given by (116) we obtain

$$(AX+B)(CX+D)^{-1}\underline{v} = (AY+B)(CY+D)^{-1}\underline{v} \tag{117}$$

that is $(AX+B)(CX+D)^{-1} - (AY+B)(CY+D)^{-1}$ is singular. To show the converse, assume that (117) holds for some nonzero $\underline{v}$ and define a nonzero $\underline{z}$ as in (116), then (113) holds and implies that

$$A(X-Y)\underline{z} = 0 \quad . \tag{118}$$

Since A is nonsingular it must be that X-Y is singular.

Q.E.D.

One problem that occurs with the use of separating functions which are not defined over all of $\mathbb{C}^{nxn}$, as when CX+D is singular in (111), is that the matrices X for which f(X) is not defined must be examined for their effect on the continuity of L(s,θ) defined by (108) as well as its effect on $\sigma_{min}[f(-G^{-1}(s))]$ in (110) which may alternatively defined as

$||\{f(-G^{-1}(s))\}^{-1}||_2^{-1}$ (see 2.39) which may be well defined even though $\sigma_{min}[f(-G^{-1}(s))]$ is not because (AX+B) in (111) may be invertible.

Although in Lemma 1 and (111) the A,B,C and D coefficients are matrices we will only use scalars a,b,c and d in the presentation of several additional theorems. The first of these theorems is a somewhat unusual version of the well-known small gain theorem [12]. This theorem is obtained by choosing f(X) = X, using origin centered circles.

Theorem 7 (Small Gain Theorem): The polynomial $\tilde{\phi}_{CL}(s)$ has no CRHP zeros and hence the perturbed feedback system is stable if the following conditions hold:

1. condition 1 Theorem 2 holds
2. $\sigma_{min}^{-1}(-G^{-1}(s)) = ||G(s)||_2 < 1$
   for all $s \in \Omega_R$
3. $\sigma_{min}(-G^{-1}(s)) > \sigma_{max}(L(s))$
   or equivalently,
   $||G(s)||_2||L(s)||_2 < 1$
   for all $s \in \Omega_R$.

Proof: In this case L(s,e) is given by

$$L(s,e) = (1-e)I + eL(s) \tag{119}$$

and thus $||G(s)L(s,e)||_2$ is simply bounded by use of conditions 2 and 3 as

$$\begin{aligned} ||G(s)L(s,e)||_2 &= ||(I-e)G(s) + eG(s)L(s)||_2 \qquad (120)\\ &\leq (1-e)||G(s)||_2 + e||G(s)||_2||L(s)|| \\ &\leq (1-e) + e = 1 \quad . \end{aligned}$$

Clearly, from (120), $I+G(s)L(s,\theta) = I+G(s,\theta)$ is nonsingular and by Theorem 2 $\tilde{\phi}_{CL}(s)$ has no CRHP zeros.

Q.E.D.

Several remarks about this theoremm are in order. First the name small gain theorem arises from the fact that condition 3 requires the loop gain to be less than unity (small enough not to destabilize the closed-loop system). Furthermore this version of the theorem is rather unusual in that typically the conditions that $\phi_{CL}(s)$ have no CRHP zeros (condition 1c of Theorem 2) and that $||G(s)||_2 < 1$ are replaced by the simple conditions that G(s) and L(s) are open-loop stable. Note that $||G(s)||_2 < 1$ and $\phi_{CL}(s)$ having no CRHP zeros guarantees that G(s) is open-loop stable. Also L(s) need not be stable as long as G(s) and $\tilde{G}(s)$ have the same number of CRHP poles. Recall from section 3.4 the reason we require $\phi_{CL}(s)$ to have no CRHP zeros is that the nominal closed-loop system must be stable in order to determine its stability margins and determine if it is robustly stable. We are not merely determining the stability of some arbitrary system with loop transfer matrix G(s)L(s) where L(s) = I has no special significance. <u>This the main difference between robustness theorems and stability theorems</u>. In robustness theory we are trying to determine when stability will be preserved and in stability theory we are trying to determine useful conditions under which stability will occur without the benefit of knowing that with $L(s) \equiv I$ the feedback system (the nominal system) is stable. Note also that condition 2 is simply condition 3 with L(s) = I and that condition 2 is the condition given in (109).

Finally we point out that $G^{-1}(s)$ need not exist since by alternating formulating $\sigma_{min}[-G^{-1}(s)]$ as $||G(s)||_2^{-1}$ we completely avoid the problem. However, it is convenient to perform some formal manipulations with the $f(-G^{-1}(s))$ in order to gain insight on how to select certain useful circles and then go back and determine what assumptions are actually necessary.

It will now be shown how all robustness theorems using the $\tilde{G} = GL$ form can be understood as a small gain theorem on an equivalent feedback which is stable only if the original system is stable. For this purpose we introduce Fig. 27 where for convenience the matrix L(s) appears in the feedback loop instead of in series with G(s) and where we have suppressed the dependence of G(s) and L(s) on s. In Fig. 27-1 we have the original perturbed system which is transformed into Fig. 27-2 by use of a constant scalar multiplier a. Obviously, the systems in Figs. 27-1 and 27-2 are equivalent in terms of stability, that is, one is stable if and only if the other is stable. To go from the system of Fig. 27-2 to that of 27-3 we employ what is known as a loop shifting transformation. This simply adds a pair of feedback loops with feedback gains of $\pm bI$ around the system $\frac{1}{a}G$ that cancel each other out because they have opposite polarity. Then cleverly, the $+bI$ feedback loop around $\frac{1}{a}G$ is moved so that it becomes a feedforward loop around the aL system. Again it is obvious that the systems in Figs. 27-2 and 27-3 are equivalent in terms of stability. Next, in order to go from Fig. 27-3 to 27-4 we define the systems G_1 and L_1 shown by the dotted boxes in Fig. 27-3. Now we simply apply the same type of multiplier and

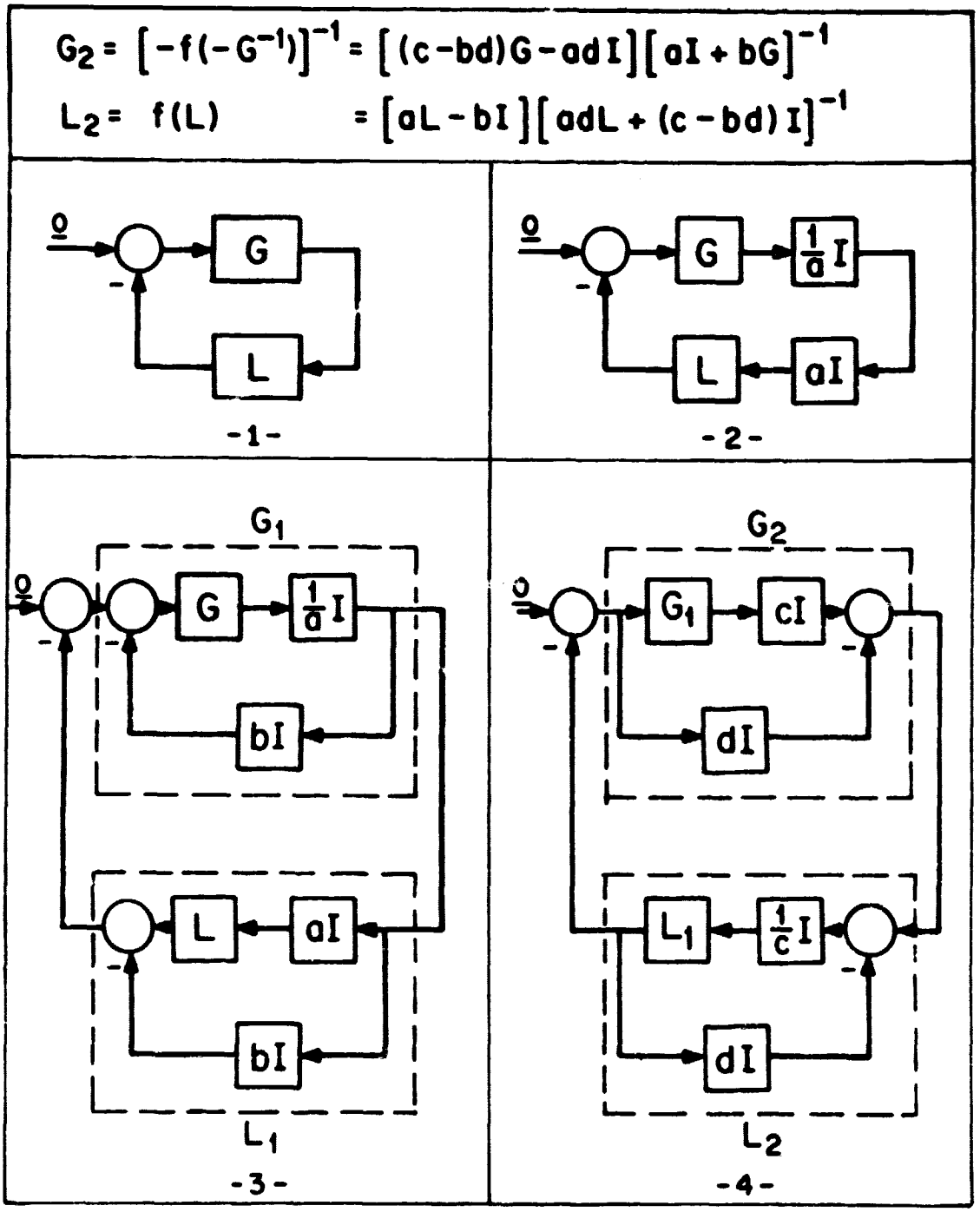

Fig. 27: Loop Transformations with Multipliers Ilustrating the Relationship between the Small Gain Theorem and the use of the Bilinear Fractional Transformation f(·).

and loop shifting transformation in one step to the system composed of G_1 and H_1 to obtain Fig. 27-4. Now, however, we have in the loop shifting transformation involving cG_1 started out by adding two feedforward loops of opposite polarity around cG_1 and then moved the +dI feedforward term around the $\frac{1}{c} L_1$ system so that it becomes a feedback loop. Again, we claim that the system in Fig. 27-4 is stability equivalent to the system of Fig. 27-3 and thus stability equivalent to the original system in Fig. 27-1.

The next thing to notice is that the systems G_2 and L_2 defined by the dotted boxes in Fig. 27-4 can be associated with a bilinear fractional transformation f(·) by the following equations

$$G_2 = [-f(-G^{-1})]^{-1} = [(c-bd)G - adI][aI + bG]^{-1} \tag{121}$$

and

$$L_2 = f(L) = [aL-bI][adL - (c-bd)I]^{-1} \quad . \tag{122}$$

Suppose now that we may prove the stability of the G_2, L_2 system of Fig. 27-4 by means of the small gain theorem which has the basic inequality

$$||G_2||_2||L_2||_2 < 1. \tag{123}$$

This last condition, however, is equivalent to the condition

$$\sigma_{min}[f(-G^{-1})] > \sigma_{max}[f(L)] \tag{124}$$

where in both (123) and (124) the dependence on s has been suppressed and must hold on D_R. This shows that any particular robustness test as

in (124) involving bilinear fractional transformation may be formulated as a small gain test on an equivalent system. Also, though it was not done here, the parameters a,b,c and d of the function f(·) can in general be stable minimum phase rational transfer functions instead of constant scalars.

Two final theorems which use a different separating function f(·) will be discussed. They are the well-known passivity theorem [12] and its generalization due to Barrett [47]. The passivity theorem we shall state has the same unorthodox assumption that closed-loop system is stable rather than the usual assumption that the open-loop system is stable. This again happens because we are using the theorem for determining robustness of a nominal system under modelling errors rather then to ascertain the stability of an arbitrary system.

Theorem 8 (Passivity Theorem): The polynomial $\tilde{\phi}_{CL}(s)$ has no CRHP zeros and hence the perturbed feedback system is stable if the following conditions hold:

1. condition 1 of Theorem 2 holds
2. $G(s) + G^H(s) \geq 0, \quad s \in \Omega_R$
3. $L(s) + L^H(s) > 0, \quad s \in \Omega_R$

Proof: This proof is accomplished most simply without resorting to explicit use of separating functions and, therefore, they will not be used. Let I+G(s,e) by given by

$$I+G(s,e) = I+G(s)[(1-e)I + eL(s)] = I+G(s)L(s,e) \qquad (125)$$

and notice that $L(s,\theta)$ is such that

$$L^H(s,\theta) + L(s,\theta) > 0 \tag{126}$$

on $D_R \times [0,1]$. Now suppose that $I+G(s,\theta)$ is singular for some (s,θ) in $D_R \times [0,1]$; then, there exists a nonzero vector $\underline{x}$ such that $[I+G(s)L(s,\theta)]\underline{x} = 0$ and hence

$$\underline{x} = -G(s)L(s,\theta)\underline{x} \quad . \tag{127}$$

Defining $\underline{z} = L(s,\theta)\underline{x}$, we note that $\underline{z}$ is nonzero else $\underline{x}$ in (127) is zero and thus

$$\underline{z} = -L(s,\theta)G(s)\underline{z} \quad . \tag{128}$$

Condition 2 and (128) imply that

$$\underline{z}^H G(s)z + \underline{z}^H G^H(s)\underline{z} = -\underline{z}^H G^H(s)[L(s,\theta) + L^H(s,\theta)]G(s)\underline{z} \geq 0 \tag{129}$$

and since $G(s)\underline{z} \neq 0$ a contradiction to condition 3 is obtained and thus $I+G(s,\theta)$ is nonsingular on $D_R \times [0,1]$. Theorem 2 again holds and the desired result follows. Q.E.D.

Remark: In conditions 2 and 3 the strictness of the inequalities can be reversed and Theorem 8 still holds.

Specializing to the SISO case illustrates the types of $G(s)$ and $L(s)$ that are required in Theorem 8. Conditions 2 and 3 keeps $g(s)$ and $\ell(s)$ from entering the OLHP and show (see Fig. 28) that since $g(s)$ cannot encircle the -1 point, it must be open-loop stable in order to apply the

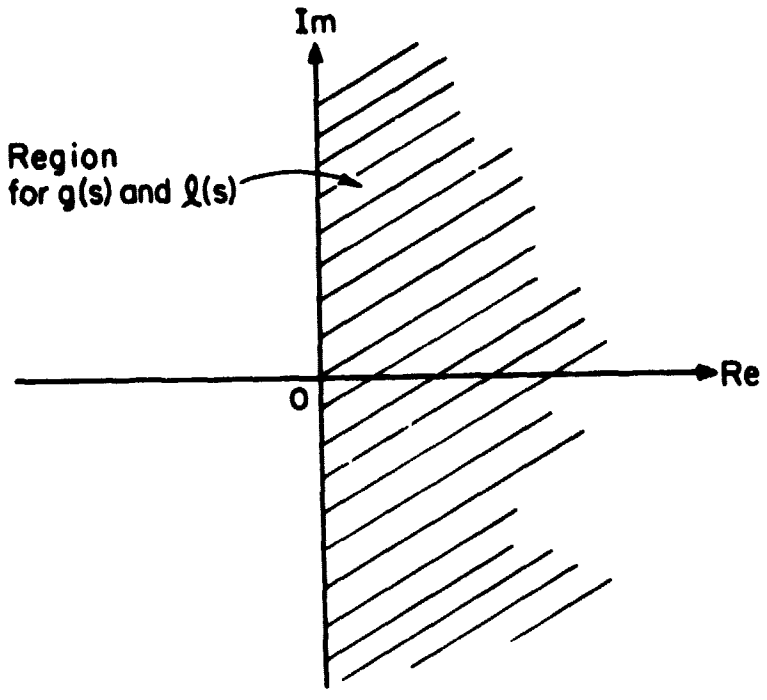

Fig. 28: Admissable Region for g(s) and ℓ(s) in Theorem 8 (shaded).

theorem. It is fairly obvious that the phase of $g(s)\ell(s)$ is strictly less than 180° and thus $g(s)\ell(s) \neq -1$. We can interpret conditions 2 and 3 as separating $-g^{-1}(s)$ and $\ell(s)$ by the $j\omega$-axis since $-g^{-1}(s)$ lies in the CLHP and $\ell(s)$ in the ORHP. The $j\omega$-axis can be viewed as a degenerate circle of infinite radius and we will use this notion to relate the passivity theorem to the next theorem which generalizes it.

To derive the generalization of Theorem 8 we perform some algebraic manipulations on condition 2 (and also condition 3) to relate these conditions to equivalent singular value conditions. First, note

that from condition 2 we can deduce that

$$2(G^H+G) = (I+G)^H(I+G) - (I-G)^H(I-G) \geq 0 \tag{130}$$

and hence

$$(I+G)^H(I+G) \geq (I-G)^H(I-G) \quad . \tag{131}$$

This last inequality can be rewritten as

$$[(I+G)(I-G)^{-1}]^H[(I+G)(I-G)^{-1}] \geq I \tag{132}$$

or

$$\sigma_{min}[(I+G)(I-G)^{-1}] \geq 1 \quad . \tag{133}$$

Similarly we can deduce from condition 3 that

$$\sigma_{max}[(I-L)(I+L)^{-1}] < 1 \tag{134}$$

which when combined with (133) results in

$$\sigma_{min}[(I+G)(I-G)^{-1}] \geq 1 > \sigma_{max}[(I-L)(I+L)^{-1}] \quad . \tag{135}$$

In this last inequality, one wonders whether the 1 in the middle of (135) is really necessary and that if we use an inequality of the form

$$\sigma_{min}[(I+G(s))(I-G(s))^{-1}] > \sigma_{max}[(I-L(s))(I+L(s))^{-1}] \tag{136}$$

if it will guarantee closed-loop stability when (136) holds on D_R. The answer to this question is <u>yes</u>, provided that we impose some additional restrictions on L(s). The next theorem formalizes this.

<u>Theorem 9</u> [47]: The polynomial $\tilde{\phi}_{CL}(s)$ has no CRHP zeros and hence the perturbed feedback system is stable if the following conditions hold:

1. condition 1 of Theorem 2 holds

2. $L(s)$ has no real eigenvalues less than or equal to -1 for all $s \in \Omega_R$

3. $\sigma_{min}[(I+G(s))(I-G(s))^{-1}] > \sigma_{max}[(I-L(s))(I+L(s))^{-1}]$ for all $s \in \Omega_R$

Remark: If condition 3 is satisfied and $\sigma_{min}[(I+G(s))(I-G(s))^{-1}] \leq 1$ in condition 3 then it can be easily shown that condition 2 is automatically for all $s \in \Omega_R$ for which this inequality holds.

Proof: $L(s,\theta)$ is given by

$$L(s,\theta) = f^{-1}[\theta\, f(L(s))] \tag{137}$$

since $f(I) = 0$ where

$$f(X) = (I-X)(I+X)^{-1} = f^{-1}(X) \tag{138}$$

and thus

$$L(s,\theta) = [I - \theta(I-L(s))(I+L(s))^{-1}][I+\theta(I-L(s))(I+L(s))^{-1}]^{-1} \tag{139}$$

and is continuous on $D_R \times [0,1]$ because of condition 2. Since $f(\cdot)$ is a separating function, condition 3 implies that $I+G(s)L(s,\theta)$ is nonsingular on $D_R \times [0,1]$ and hence Theorem 2 holds.

Q.E.D.

Note that in condition 3, the invertibility of $I-G(s)$ is not essential as long as $G(s) \neq I$ for all $s \in D_R$ since

$$\sigma_{min}[(I+G(s))(I-G(s))^{-1}] = ||(I-G(s))(I+G(s))^{-1}||_2^{-1} \qquad (140)$$

and $(I+G(s))^{-1}$ must exist because $\phi_{CL}(s)$ has no CRHP zeros and thus $||(I-G(s))(I+G(s))^{-1}||_2$ is not zero unless $G(s) = I$. Utilizing condition 3 of Theorem 9 we may derive some corollaries on the stability margins of the feedback system.

Corollary 5: If $\phi_{CL}(s)$ has no CRHP zeros and

$$\sigma_{min}[(I+G(s))(I-G(s))^{-1}] > \alpha \qquad (141)$$

for all $s \in \Omega_R$ and $\alpha \leq 1$ then the multiloop gain and phase margins are bounded in the following manner

$$GM \supset \left[\frac{1-\alpha}{1+\alpha}, \frac{1+\alpha}{1-\alpha}\right] \qquad (142)$$

and

$$PM \supset [-2\tan^{-1}\alpha, 2\tan^{-1}\alpha] \qquad (143)$$

Proof: Analogous to the proofs of corollaries 1 and 2.

Note that in the case $\alpha=1$ we obtain the bounds on the multiloop gain and phase margins associated with the passivity theorem which are given by

$$GM \supset [0,\infty) \qquad (144)$$

and

$$PM \supset [-90°, 90°] \quad . \qquad (145)$$

Also, as for Theorems 4 and 6 we may derive a corollary involving the tolerance to crossfeed for systems that satisfy condition 3 of Theorem 9 but this will not be done here because it merely repeats the essential natures of corollaries 3 and 4.

The similarity between the theorems of section 3.5 and the theorems of this section is incomplete because it is not clear what type of modelling error is being bounded in Theorems 7,8 and 9. It happens that Theorem 7 cannot be interpreted in terms of bounding the magnitude of any type of modelling error and Theorem 8 always bounds the magnitude of the model error by unity. This can be seen by identifying $\sigma_{max}[f(L(s))]$ as the magnitude of the model error which is true in the case of Theorems 4,6,8 and 9. In Theorem 7, $\sigma_{max}[L(s)] \neq 0$ when $L(s) = I$ and thus when $\tilde{G}(s) = G(s)$ (no model error) the magnitude of the "error" (i.e., $\sigma_{max}[L(s)]$) is not zero. Therefore $\sigma_{max}[L(s)]$ does not correspond to the magnitude of a modelling error. Another manifestation of the lack of similarity between Theorems 4 and 6, and Theorems 7 and 8 is the fact that Theorems 7 and 8 cannot be applied to all G(s) and $\tilde{G}(s)$ that satisfy condition 1. of Theorem 2 whereas Theorems 4, 6 and 9 can. Theorems 7 and 8 place additional conditions on the allowed G(s) (i.e., in the SISO case g(s) must lie inside of the unit disk in the complex plane for Theorem 7 (Fig. 29) and the CRHP (Fig. 28) for Theorem 8). In Theorems 4, 6 and 9 (again in the SISO case) the Nyquist diagram of g(s) may approach the critical point (-1,0) from any direction. This is not true for Theorems 7 and 8.

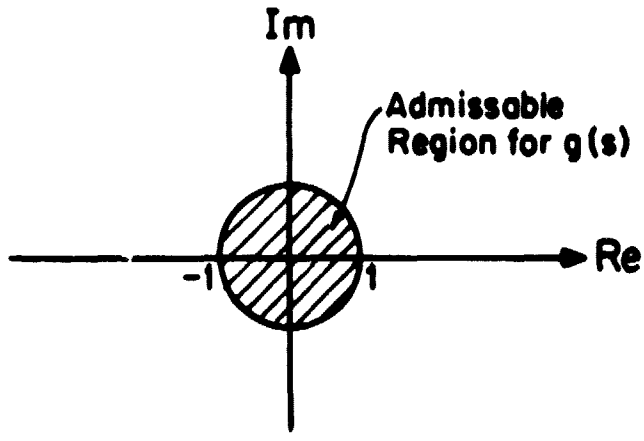

Fig. 29: Admissable Region for g(s) in Theorem 7

To discover the underlying error criteria associated with Theorems 8 and 9 make the following identification between L(s) and E(s) given by

$$E(s) = -f(L(s)) \tag{146}$$

since in Theorems 4 and 6 it is $f(-G^{-1}(s)) + E(s)$ that is tested for singularity. Thus, in the case of Theorems 8 and 9 we have that

$$E(s) = (L(s)+I)^{-1}(L(s)-I) \tag{147}$$

or since $\tilde{G}(s) = G(s)L(s)$

$$E(s) = (G^{-1}(s)\tilde{G}(s)+I)^{-1}(G^{-1}(s)\tilde{G}(s)-I) \tag{148}$$

and thus

$$E(s) = [\tilde{G}(s)+G(s)]^{-1}[\tilde{G}(s)-G(s)] \quad . \tag{149}$$

Now note that we can write 2E(s) in the two following forms (dropping the s dependence)

$$2E = \left[\frac{(\tilde{G}+G)}{2}\right]^{-1} [\tilde{G}-G] \tag{150}$$

or

$$2E = [\tfrac{1}{2} E_1^{-1} + \tfrac{1}{2} E_2^{-1}]^{-1} \tag{151}$$

where

$$E_1 = G^{-1}(\tilde{G}-G) \tag{152}$$

and

$$E_2 = -[\tilde{G}^{-1} - G^{-1}]G \quad . \tag{153}$$

From (150) 2E(s) can be interpreted as a relative error between $\tilde{G}$ and G where the base value is taken as the arithemetic average of $\tilde{G}$ and G. Another interpretation that is suggested by (151) is that 2E can be compared to a resistance as can the errors E_1 and E_2. Then $(2E)^{-1}$ is like a conductance that is merely the average of the conductances E_1^{-1} and E_2^{-1}. We note that E_1 is merely the usual relative error between $\tilde{G}$ and G and that E_2 is the negative of the relative error between $\tilde{G}^{-1}$ and G^{-1}. In a sense the error criteria for Theorem 9 is a compromise between the error criteria of Theorems 4 and 6. Note that as E_1 (or E_2) become small that 2E approaches E_1 (E_2), that is 2E picks out the smaller of the two types of errors and uses that as a measure of the error. Fig. 30 illustrates the nature of this error in a block diagram where by (147) L(s) is simply $[I-E(s)][I+E(s)]^{-1}$.

This type of error criterion is pleasing in that it leads to the symmetric (in a logarithmic scale) gain and phase margins of corollary 5 and correlates well with classical single-loop simultaneous design requirements on gain and phase margin [47]. To put all the various theorems presented here in perspective, the Table 1 describes the

THEOREM	MAIN RESULT H	$L(H)$	REP. FUNCTION $f(H)$	USED
3	$G \prec \tilde{G}$	——	——	$\sigma_{min}(I+G) > \sigma_{max}(H)$
4	$G^{-1}(\tilde{G}-G)$	$I+H$	$I-H$	$\sigma_{min}(I+G^{-1}) > \sigma_{max}(H)$
5	$\tilde{G}^{-1}-G^{-1}$	——	——	$\sigma_{min}(I+G^{-1}) > \sigma_{max}(H)$
6	$[\tilde{G}^{-1}-G^{-1}]G$	$(I+H)^{-1}$	$I-H^{-1}$	$\sigma_{min}(I+G) > \sigma_{max}(H)$
7	[illegible]	——	H	$\sigma_{min}(G^{-1}) > \sigma_{max}(L)$
8	$[\tilde{G}+G]^{-1}[\tilde{G}-G]$	$(I-H)(I+H)^{-1}$	$(I+H)(I-H)^{-1}$	$\sigma_{min}[(I+G)(\tilde{I}-G)^{-1}] \geq 1$ $\sigma_{max}[(L-I)(L+I)^{-1}] < 1$
9	$[\tilde{G}+G]^{-1}[\tilde{G}-G]$	$(I+H)(I+H)^{-1}$	$(I+H)(I-H)^{-1}$	$\sigma_{min}[(I+G)(I-G)^{-1}] > \sigma_{max}$[illegible]

TABLE 1: RELATIONSHIPS OF GENERATED THEOREMS

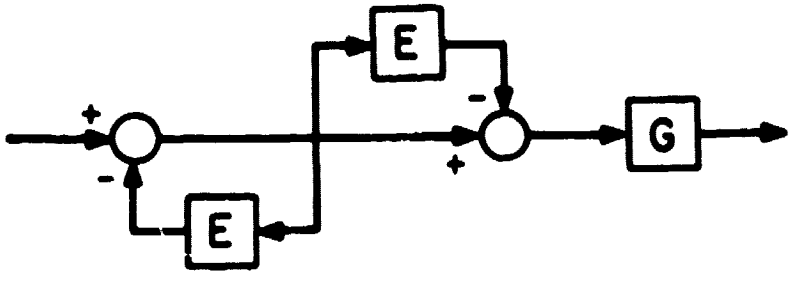

Fig. 30: Physical Representation of Perturbed Model in Theorem 9

separating functions, error criteria and the multiplicative L(s) factor corresponding to each the robustness test.

In the next chapter, robustness tests will be formulated that utilize the structure of the modelling errors that were discussed in this chapter. This means that having an understanding of how errors enter into the system models will be important if any judgement about their structure is to be made.

3.10 Extensions to Nonlinear Systems

The preceeding sections have dealt solely with the stability/robustness properties of linear time-invariant systems. The purpose of this section is to demonstrate that some of the theorems of the previous sections have corresponding nonlinear counterparts. These theorems may be proved by use of the well-known circle Theorem [10,11] formulated by Zames and

later generalized by Savonov [7, 18]. However, these theorems will not be proved here due to the lengthy discussion of extended function Banach spaces and other necessary mathematical development required. The key observation to be recognized is that the guaranteed gain margin for Theorems 4, 6 and 9 remain exactly the same when the multiplicative type of perturbation represented by the matrix L(s) is replaced by a nonlinear memoryless operator denoted as N (see Fig. 31). This means the gain of each feedback loop may be changed as nonlinear function of the output signal of the plant provided the effective linear gain change is within the bounds specified by the guaranteed gain margin. This notation of a gain margin for nonlinear systems is made more precise in the theorems of section 3.10.1.

3.10.1 Guaranteed Gain Margins for Nonlinear Systems

One of the first problems encountered in determining the stability of nonlinear systems is to clarify what is meant by the notion of stability. Various authors define stability differently but the basic concept is that of boundedness. Thus, stability must be defined before discussing the generalizations of Theorems 4, 6 and 9. For the purpose of this section we define stability in the following manner.

Definition (Stability): A causal system with an arbitrary input $\underline{u}(t)$ and corresponding output $\underline{y}(t)$ is stable if there exists a nonnegative scalar k such that

$$||y(t)||_2 \leq k\, ||\underline{u}(t)||_2 \tag{154}$$

where $||\cdot||_2$ is defined as

$$||\underline{z}(t)||_2 \triangleq \left[\int_0^\infty \underline{z}^T(t)\underline{z}(t)dt\right]^{1/2} . \qquad (155)$$

The norm in (155) is proportional to the energy in the time signal $\underline{z}(t)$.

Using this definition of stability[1] we will examine the stability of the feedback system shown in Fig. 3 where G is a linear time-invariant convolutional operator representing the nominal loop operator and $N(\cdot)$ is a memoryless nonlinear operator given by

$$N(\underline{x}(t)) = [n_1(x_1(t)), n_2(x_2(t)),\ldots,n_m(x_m(t))]^T \qquad (156)$$

where each $n_i(\cdot)$ is a memoryless time-invariant nonlinearity and $x_i(t)$ are the components of $\underline{x}(t)$.

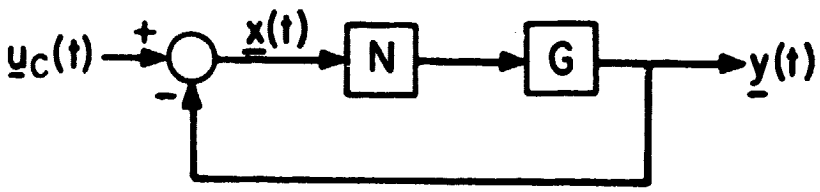

Fig. 31: Nonlinear System

[1] In the completely linear time-invariant case this definition of stability requires that a stable system have all its poles in the open-left-half-plane.

In Fig. 31 we assume that the nominal feedback system with $N(\underline{x}(t)) = \underline{x}(t)$ is stable and that the transfer function of the loop operator G is given by G(s). Here N is playing the role of L(s) in the completely linear case (i.e., the perturbed loop operator $\tilde{G}$ is given by GN).

A graph of the $n_i(x_i(t))$ components of $N(\underline{x}(t))$ in (156) might be a saturation type nonlinearity shown in Fig. 32.

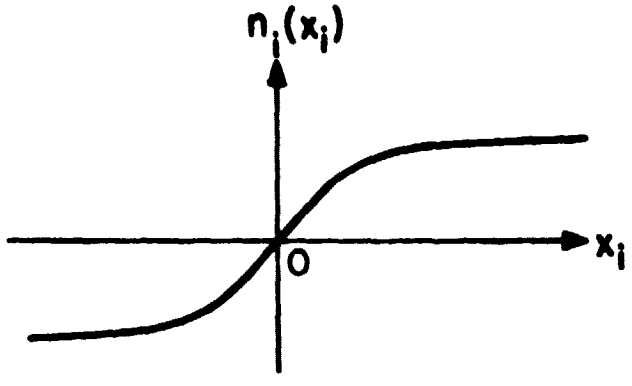

Fig. 32: Saturation nonlinearity $n_i(x_i)$

In the next two simplified theorems, it is shown that by bounding the graph of the $n_i(x_i)$ appropriately the stability of the closed-loop system is ensured and nonlinear guaranteed gain margins obtained.

Theorem 10: The closed-loop system of Fig. 31 is stable if:

1. it is stable with $N(\underline{x}) = \underline{x}$
2. $N(\underline{x})$ is memoryless and time-invariant and given by (156)
3. for $\alpha \triangleq \inf_{\omega \geq 0} \sigma_{min}(I+G^{-1}(j\omega))$ and for all scalar x

$$(1-\alpha)x < n_i(x) < (1+\alpha)x \qquad \text{for all } i$$

Remark: Here it is assumed for conveience that $\phi_{OL}(j\omega) \neq 0$ for all ω.

This theorem is the corresponding analogue to Theorem 4 and gives bounds on the slope of the graph of $n_i(x)$ as shown in Fig. 33. The bounds on a SISO case for the Nyquist locus of g(s) is shown in Fig. 34. This is a simple application of the celebrated Circle Theorem [10,11] as are the next two Theorems.

Theorem 11: The closed-loop system of Fig. 31 is stable if:

1. it is stable with $N(\underline{x}) = \underline{x}$
2. $N(\underline{x})$ is a memoryless, time-invariant nonlinearity given by (156)
3. for $\alpha \triangleq \inf_{\omega \geq 0} \sigma_{min}(I+G(j\omega)) \leq 1$ for all scalar x

$$\frac{1}{1+\alpha} x < n_i(x) < \frac{1}{1-\alpha} x \qquad \text{for all } i$$

Again we assume that $\phi_{OL}(j\omega) \neq 0$ for all ω and observe that the gain margin for Theorem 11 is the same as in the completely linear case of Theorem 6. A similar nonlinear extension for Theorem 9 is available.

Theorem 12: The closed-loop system of Fig. 31 is stable if:

1. it is stable with $N(\underline{x}) = \underline{x}$
2. $N(\underline{x})$ is a memoryless, time-invariant nonlinearity given by (156)
3. for $\alpha \triangleq \inf_{\omega \geq 0} \sigma_{min}[(I-G(j\omega))^{-1}(I+G(j\omega))] \leq 1$ and for all scalar x

$$\frac{1-\alpha}{1-\alpha} x < n_i(x) < \frac{1+\alpha}{1-\alpha} x \quad \text{for all } i.$$

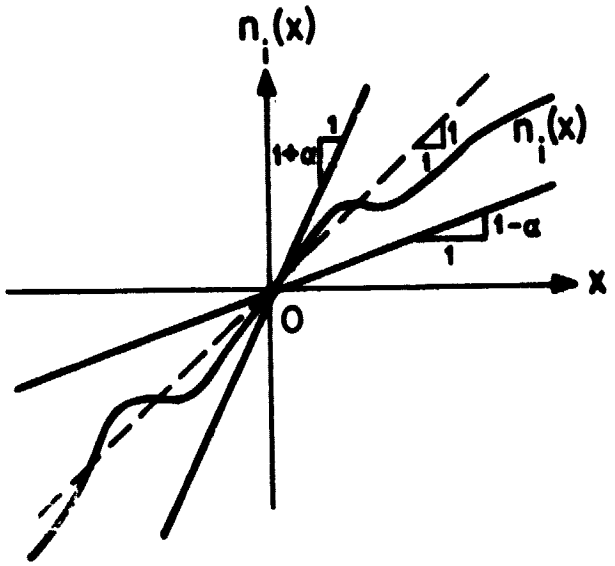

Fig. 33: Bounds of Theorem 10 on graph of $n_i(x)$

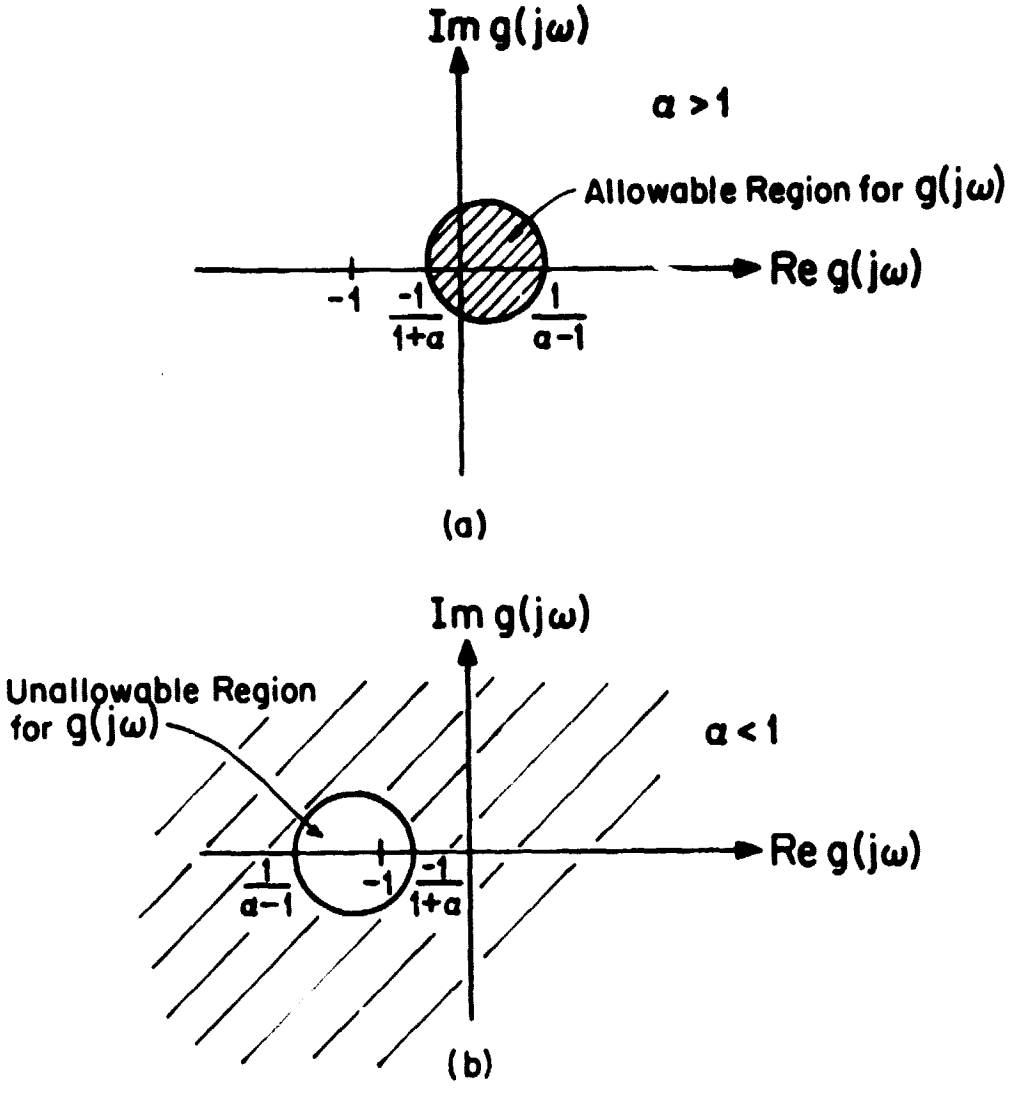

Fig. 34: Allowable region (shaded) for Nyquist locus of g(s) in Theorem 10

In these three theorems the quantity $n_i(x)/x$ is upper and lower bounded and can be considered as the effective linear gain for the $i^{\underline{th}}$ feedback channel when the component $x_i(t)$ of the vector $\underline{x}(t)$ takes on the numerical value x. Thus with this interpretation of $n_i(x)/x$ as an effective linear gain the guaranteed gain margins for the nonlinear system are the same as those for the linear case.

Notice that in the case of a saturation nonlinearity as in Fig. 32 that Theorem 11 cannot be applied since $\alpha \leq 1$ in condition 3 implies that $n_i(x) > 1/2x$ which cannot be satisfied for a saturation nonlinearity.

3.11 Concluding Remarks

This section will attempt to give a perspective on the usefulness and relationship of the robustness results of this chapter. This chapter has presented a variety of robustness results and one wonders if there is a best robustness theorem to use in determining the largest class of model errors that the feedback system will tolerate. Practically, the nswer to this question is no but theoretically Theorem 2 characterizes the largest[1] class of allowable perturbed loop transfer matrices $\{\tilde{G}(s)\}$, namely those whose multivariable Nyquist diagram is a deformed version of the multivariable Nyquist diagram for G(s) having the same number of encirclements of (0,0). However, the only practical way to determine if this is true is to use one of the robustness theoorems of sections 3.5 and 3.9. These theorems work with different types of model error

[1] Largest under the restriction G(s) and $\tilde{G}(s)$ have the same number of unstable poles.

and one can only say that one theorem is better than another if a particular characterization of the model uncertainty has been selected to be the sense in which better is meant.

For example, if one wanted to use the gain reduction margin as the criteria for the best theorem, that is, the best theorem would be the one that gave the smallest number for the gain reduction margin upper bound. Then of Theorems 4, 6, and 9 one would say that Theorem 4 is the best theorem to use since given any G(s), the upper bound on the gain reduction computed from $\sigma_{min}[I+G^{-1}(s)]$ is always less than or equal to the upper bounds on the gain reduction margin computed from $\sigma_{min}[I+G(s)]$ of Theorem 6 or from $\sigma_{min}[(I-G(s))^{-1}(I+G(s))]$ of Theorem 9.

Similarly, if one wanted the best indication of the upward gain margin, the lower bound computed from $\sigma_{min}[I+G(s)]$ of Theorem 6 is best. These observations can be easily deduced via the relationships of $\sigma_{min}[I+G]$ and $\sigma_{min}[I+G^{-1}]$ of Fig. 21 and similar relationships that may be derived for $\sigma_{min}[(I+G)(I-G)^{-1}]$ in relation to $\sigma_{min}[I+G]$ or $\sigma_{min}[I+G^{-1}]$. It seems likely that in some sense that Theorem 9 should prove best but at present it is not clear what the particular criteria might be.

Another way to compare Theorems 4, 6, and 9 in the SISO case is to compare the regions for allowable $\ell(s)$ given a nominal $g(s)$. This is illustrated in Fig. 35 where $g(j\omega_0) = 3/4$ for some ω_0. As can be seen from Fig. 35, Theorem 9 places the least restriction on $\ell(j\omega_0)$ in the sense that forbidden region for $\ell(j\omega_0)$ in the complex plane has the smallest area for any of the theorems. In general, these regions for $\ell(j\omega_0)$ may overlap but may not be contained in each other, so that each

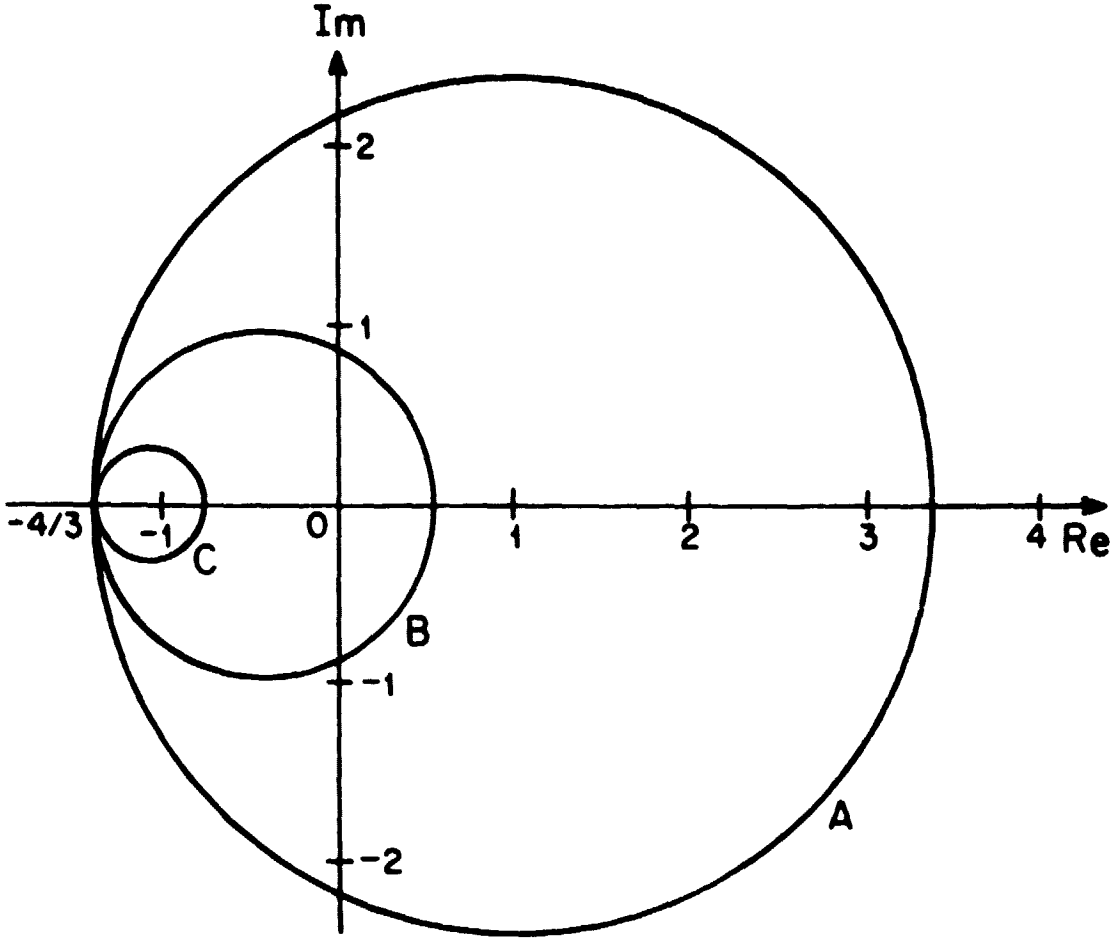

Fig. 35: Allowable Regions for $\ell(j\omega_0)$ if $g(j\omega_0) = 3/4$ using Theorems 4, 6, and 9.

Theorem 4: strictly inside circle A
Theorem 6: strictly outside* circle B
Theorem 9: strictly outside* circle C

*Except for 0 and the negative real axis

theorem may indicate a tolerance to a certain modelling error not guaranteed by either of the other two remaining theorems alone. Note that each of the circles in Fig. 35 pass through -4/3, the value for $\ell(j\omega_0)$ which makes $1+g(j\omega_0)\ell(j\omega_0) = 0$, and since $\ell(j\omega_0)$ cannot be on the circle's boundaries $1+g(j\omega_0)\ell(j\omega_0) \neq 0$ is ensured.

In the MIMO case, drawing appropriate circles cannot easily be done and comparison of the theorems must proceed by devising some other appropriate criteria that is easy to check.

The observations made so far, have been made on the basis of only the algebraic properties of the robustness inequalities of the theorems. However, using the typical frequency dependence of G(s) some additional typical comparisons may be made. In order to obtain a good response to command inputs, typically of low frequency content, the loop gain in SISO systems is large in the frequency band where good following of the inputs is desired. The MIMO generalization of the loop gain is given by $\sigma_{min}(G(s))$ and $\sigma_{max}(G(s))$ where the former represents the lower bound on the loop gain of the "slowest" loop of the feedback and the latter represents an upper bound on the loop gain "fastest" feedback loop. The crossover frequency of the SISO case becomes the frequency range where $\sigma_{min}(G(s)) \leq 1$ and $\sigma_{max}(G(s)) \geq 1$ in the MIMO case.

In the high performance (good command following) low frequency range $\sigma_{min}(G(s))$ is large and thus so is $\sigma_{min}[I+G(s)]$ (refer to Fig. 21) and in this region the tolerance to the modelling errors of Theorems 5 and 6 is generally good.

In the frequency region above crossover $\sigma_{max}(G(s))$ is small and thus $\sigma_{min}[I+G^{-1}(s)]$ is large and, therefore, the tolerance to the modelling

errors of Theorems 3 and 4 is generally good. This is the frequency region where it is important to have good tolerance to model error since in general modelling error increases as frequency does (because of unmodelled high frequency dynamics in nominal design model). This recommends that Theorem 4 always be used since Theorems 6 or 9 cannot be applied when the phase of the plant becomes completely uncertain as it surely will at high enough frequency. A similar discussion of this nature is given in [43].

As mentioned previously in this chapter, the theorems using a multiplicative model perturbation or relative error measure are generally favored over the ones that use the additive model perturbatiion or absolute error measure, because the compensation employed does not affect the measure of modelling error. To make this clear, let $G_p(s)$ denote the open-loop plant transfer matrix and $G_c(s)$ the compensation transfer matrix. Then for the relative error criteria of Theorems 4, 6 and 9 with $G(s) = G_c(s)G_p(s)$ we have that

Theorem 4: $$G^{-1}(s)[\tilde{G}(s) - G(s)] = G_p^{-1}(s)[\tilde{G}_p(s) - G_p(s)] \qquad (157)$$

Theorem 6: $$[\tilde{G}^{-1}(s) - G^{-1}(s)]G(s) = [\tilde{G}_p^{-1}(s) - G_p^{-1}(s)]G_p(s) \qquad (158)$$

Theorem 9: $$[\tilde{G}(s) + G(s)]^{-1}[\tilde{G}(s) - G(s)] = [\tilde{G}_p(s) + G_p(s)]^{-1}[\tilde{G}_p(s) - G_p(s)] \qquad (159)$$

where $\tilde{G}_p(s)$ is the perturbed open-loop plant model. Thus we see that the compensation $G_c(s)$ does not affect the error computation. This is not true for the additive or absolute error criteria.

4. ROBUSTNESS ANALYSIS FOR LINEAR SYSTEMS WITH STRUCTURED MODEL ERROR

4.1 Introduction

The robustness tests of chapter 3 used only the magnitude of the model error in their formulation. It was shown there that if the model error magnitude is bounded by a MIMO generalization of the "distance to the critical (-1,0) point" then the closed-loop stability of the perturbed feedback system is guaranteed. However, there are many model errors whose magnitude is greater than the MIMO generalization of "distance to the critical (-1,0) point" and yet the perturbed feedback system remains stable.

In this chapter, the robustness tests of chapter 3 are refined to distinguish between those model errors which do not destabilize the feedback system and those that do, but both of which have magnitudes larger than the MIMO generalization of the "distance to the critical (-1,0) point". To do this it is necessary to be able to distinguish between model errors that increase the margin of stability for the feedback system and those that decrease it. This cannot be done on the basis of the magnitude of the model error. Therefore, it must be done on the basis of the structure of the model error.

The structure of model error, in general terms, is simply the numerical relationship of the elements of the error matrix E(s),

representing the difference between the nominal and the perturbed loop transfer matrices. In other words, the structure of the model is specified by magnitude and phase relationships between the $e_{ij}(s)$ elements of $E(s)$. In this chapter the structure of $E(s)$ which is important to determine the stability of the perturbed feedback system is extracted using the results of chapter 2 and the singular value decomposition (SVD), to generate an orthonormal basis for the expansion of $E(s)$. It will be shown that the projections of $E(s)$ on only certain elements of the basis need be known precisely to extract the information relevant for stability analysis. Thus, only a partial characterization of the modelling error is necessary and its structure is constructively produced by the method of analysis used in chapter 2. Another recently proposed method, principal gain and phase analysis [57], which uses a somewhat different partial characterization of the model error to extend the robustness test in Theorem 3.4, is discussed in chapter 6.

In order to make a practical use of these results that utilize the structure of the model error, it is necessary to determine if the model error of minimum magnitude that will destabilize the feedback system can be guaranteed not to occur. This assessment must be made on the basis of engineering judgement about the type of model uncertainties that are reasonable for the nominal design model representing the physical system. For discussions on how to practically determine what constitutes a reasonable modelling error, the reader is referred to

[42] for a discussion of model errors in an automotive engine control system and [46] for a similar discussion with regard to power system models.

Some knowledge of what is a reasonable model error is absolutely essential since all models are uncertain in some frequency band. Model error always occurs when the frequency is sufficiently high and this uncertainty must be accounted for. In MIMO control systems, the maximum crossover frequency where the loop transfer matrix, $G(s)$, has a norm of unity (i.e. the maximum ω for which $||G(j\omega)||_2=1$) must occur in a frequency band where the model still adequately represents the physical system if stability is to be ensured. It is up to the designer to decide how and in what way the model is uncertain.

Having now briefly described the key role of the model error structure for the results of this chapter it is appropriate to outline the remaining sections of this chapter. In section 4.2, it is shown exactly how the structure of the modeling error can be used to obtained improved versions of the theorems in chapter 3.

Theorems 4.1 and 4.2 show that the necessary magnitude of the model error, at a particular frequency, that destabilizes the feedback system, but is essentially unlike in structure to the smallest possible destabilizing model error, may be much larger in magnitude than the magnitude of the smallest destabilizing model error. This means by differentiating the model errors on the basis of their

similarity to the structure of the smallest destabilizing error, the feedback system can guaranteed to tolerate a possibly much larger model error.

This is explained first for the SISO case and then generalised to the MIMO case. Section 4.3 interprets the nature of the modelling error of minimum magnitude, that destabilizes the feedback, via block diagram manipulations. Next in section 4.4, the example of chapter 3 (illustrating the deficiencies of the single-loop type of stability margins) is continued to show that the analysis of this chapter predicts the type of model perturbation used to demonstrated the near instability of the closed-loop system. Finally, in section 4.5, the possibility of combining different robustness tests as a way of extending their usefulness is discussed.

4.2 Robustness Tests Utilizing Model Error Structure

In the robustness theorems of chapter 3, the key conditions ensuring the stability of the perturbed closed-loop system were inequalities of the form

$$\sigma_{max}[E(s)] < \sigma_{min}[h(G(s))] \qquad (1)$$

where $h(\cdot)$ is some bilinear fractional transformation (i.e., $I+G$, $I+G^{-1}$, $(I-G)^{-1}(I+G)$) and where (1) must hold for all $s\in\Omega_R$. Recall from (3.33) that Ω_R is the portion of D_R in Fig. 3.10 for which $Re(s)\leq 0$. This condition assures that the model error

is sufficiently small so that a closed-loop system designed on the basis of G(s) will remain stable when it is replaced by $\tilde{G}(s)$. However, the approach used to develop these robustness theorems neglects the fact that there are perturbations or modelling errors for which (1) does not hold, i.e., the model error is not small, and yet the closed-loop system remains stable. These chapter 3 theorem are conservative if one restricts the allowable type of model error structure because they guard against absolutely all types of structure in linear model errors.

One way to reduce this conservatism is to obtain additional conditions that distinguish between modelling errors that do not destabilize the feedback system but violate the test of (1), and those that violate the test of (1) but also destabilize the feedback system. Or better yet, obtain some conditions that discriminate between modelling errors, that violate (1), between those, that increase and those that decrease the margin of stability of the feedback system.

The problem is illustrated in Fig. 1 for SISO systems where two different perturbed systems $\tilde{g}_1(s)$ and $\tilde{g}_2(s)$ produce exactly the same size of relative error on the Nyquist diagram. As can be seen from Fig. 1, the difference between the perturbed systems $\tilde{g}_1(s)$ and $\tilde{g}_2(s)$ cannot be determined from the magnitude of the error alone. Clearly, $\tilde{g}_2(s)$ has a smaller margin of stability than the nominal

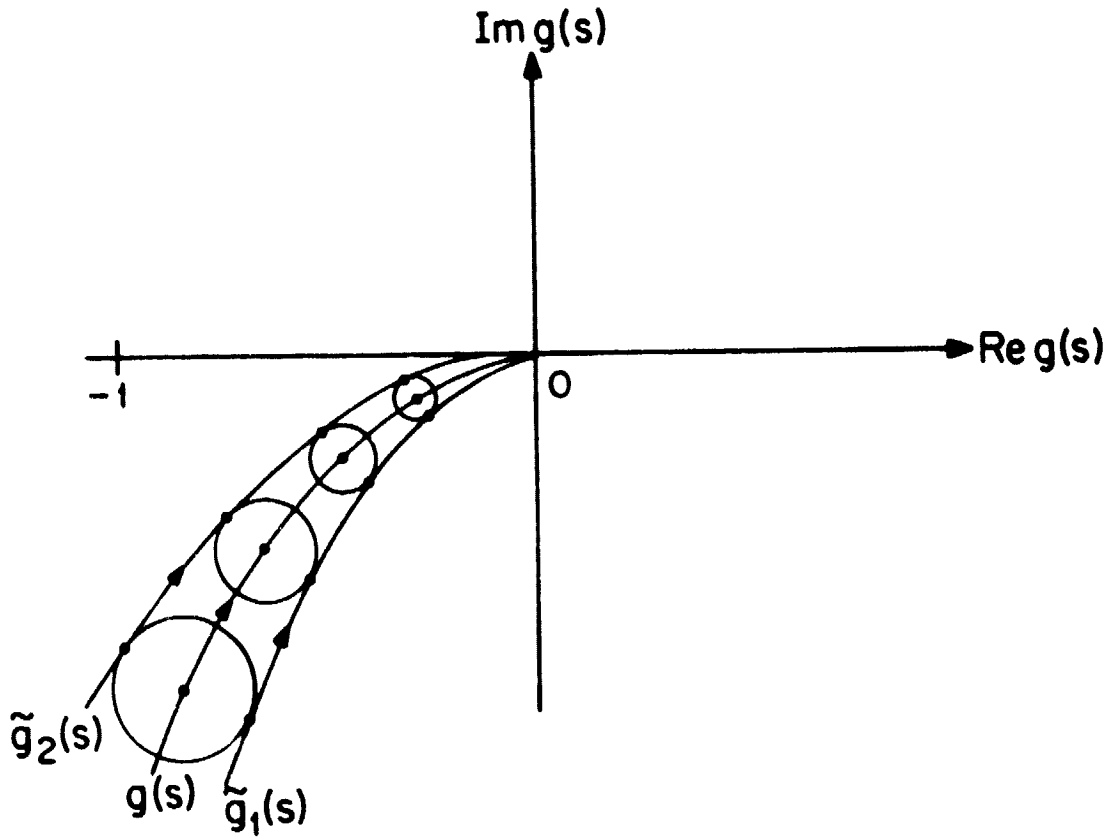

Fig. 1: Two Different Perturbed Models with the same Relative Error Magnitude on a SISO Nyquist Diagram.

system g(s), and $\tilde{g}_1(s)$ has a larger margin of stability than the nominal g(s). Since this is a scalar system the only additional information about the error needed to distinguish between $\tilde{g}_1(s)$ and $\tilde{g}_2(s)$ is the phase of the error. Thus, in the SISO case this gives us a complete characterization of the error.

In the MIMO case, the problem is not so simple because for an nxn system G(s) the error matrix E(s) has $2n^2$ degrees of freedom (two for each element of E(s) i.e., gain and phase or real and imaginary part). Thus, if a single degree of freedom is eliminated from E(s), by information in addition to the norm of E(s), there are still $2n^2-1$ degrees of freedom left. Therefore, it is important that exactly the right additional information about E(s) is obtained so that only a partial characterization of E(s) is necessary to distinguish between modellings errors that increase or decrease the margin of stability of the feedback system. In order to do this it is necessary to examine the structure of the smallest error that destabilizes the feedback loop. We will call this error the worst error.

In the SISO case, the worst error is illustrated in the Nyquist diagram of Fig. 2.

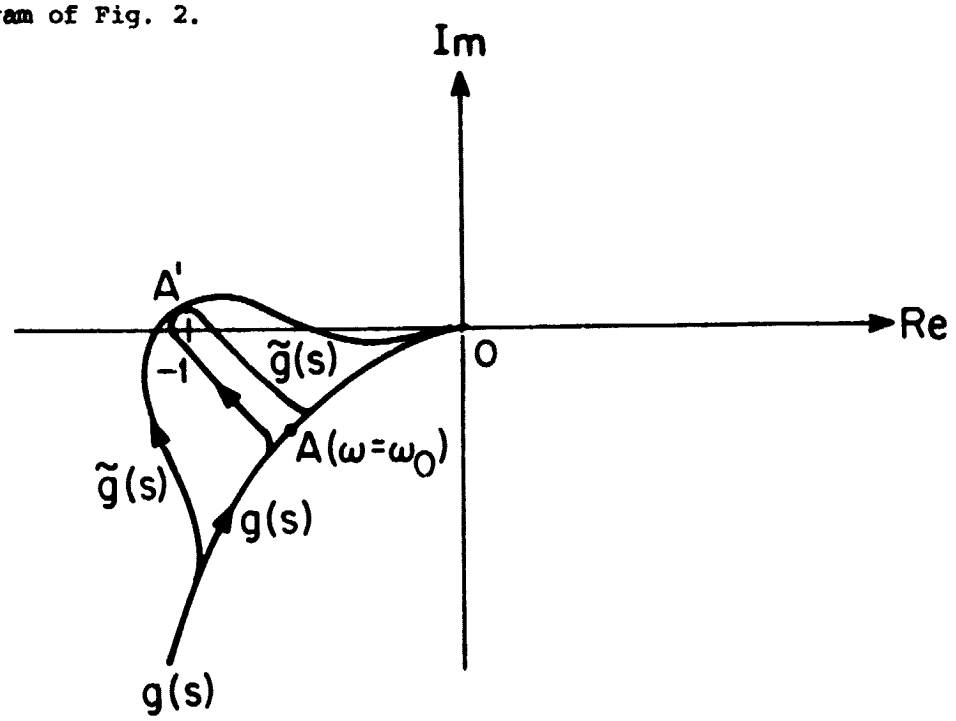

Fig. 2: Illustration of worst type of error in SISO case on a Nyquist diagram.

At point A, in Fig. 2, the Nyquist locus of g(s) is nearest the critical -1 point and thus the worst error simply moves point A to A' by "stretching" the Nyquist locus at that particular frequency to just pick up an extra encirclement of the -1 point (the point A' is infinitesimally close to -1). It is important to point out that this type of perturbation could be applied to g(s) in any frequency range but that it need happen only at one particular frequency, ω_0 near A, in order to induce instability. Thus we will speak of the worst error at a particular value of $s \in D_R$.

Notice also that there are any number of curves that we could pass through A' representing perturbations of the original Nyquist diagram of g(s) as depicted by $\tilde{g}_1(s)$ in Fig. 2, that induce instability and are identical to the worst error at the frequency of point A but differ at other frequencies. However, these curves will also be considered as worst errors since it is really their nature at a single frequency that is important in distinguishing them from other curves.

One other point must be emphasized. The system $\tilde{g}(s)$ may be constructed quite simply by finding a continuous stable $\ell(s) = \tilde{g}(s)/g(s)$ that meets as closely as desired the ideal specifications given by

$$\ell_{ideal}(s) = \begin{cases} -g^{-1}(j\omega_0), & s=j\omega_0 \\ 1, & s\neq j\omega_0 \end{cases} \qquad (2)$$

where ω_0 is the frequency corresponding to point A in Fig. 2. For example, one continuous, stable $\ell(s)$ that approximates $\ell_{ideal}(s)$ in (2) can be generated simply by taking $\ell(s)$ to be of the form

$$\ell(s) = 1 - q(s)\left|1 + g^{-1}(j\omega_0)\right| \tag{3}$$

where

$$q(s) = \frac{2\rho}{s^2+2\rho\omega_0 s+\omega_0^2}\left(\frac{s-\alpha}{s+\alpha}\right)c \ . \tag{4}$$

To approximate $\ell_{ideal}(s)$ closely, $\rho>0$ in (4) must be very small so that $|q(s)|$ is as small as desired whenever $|s-j\omega_0|>\epsilon$ for a given ϵ. The constants $\alpha\geq 0$ and $c=\pm 1$ in (4) are used to adjust the phase of $q(s)$ without affecting $|q(s)|$ so that

$$q(j\omega_0) = \exp[j\{\arg(1+g^{-1}(j\omega_0)\}] \ . \tag{5}$$

This selection of ρ, α and c in (4) makes $q(s)$ essentially zero everywhere except in a suitably small frequency range near ω_0 where it has the value given in (5). Thus $\ell(s)$ is as close as desired to the specifications in (2) but is still continuous in s and stable. The $\ell(s)$ determined by (3), (4) and (5) produces a $\tilde{g}(s)$ essentially like the one of Fig. 2.

Returning to the MIMO case, we can make all the analogous statements to those concerning Fig. 2, once we have specified the worst error. Then similarities between the SISO and MIMO cases can be easily demonstrated using the ideas of chapter 2 developed in

Problems A and B and by use of the SVD on the matrix h(G(s)) of (1). Suppose that the SVD of h(G(s)) is given by

$$h(G(s)) = U(s)\Sigma(s)V^H(s) \tag{6}$$

where

$$U(s) = [\underline{u}_1(s), \underline{u}_2(s), \ldots, \underline{u}_n(s)] \tag{7}$$

$$V(s) = [\underline{v}_1(s), \underline{v}_2(s), \ldots, \underline{v}_n(s)] \tag{8}$$

$$\Sigma(s) = \text{diag}[\sigma_1(s), \sigma_2(s), \ldots, \sigma_n(s)] \tag{9}$$

$$\sigma_i(s) \geq \sigma_{i+1}(s) \geq 0 \tag{10}$$

where the singular values $\sigma_1(s) = \sigma_{max}(s)$ and $\sigma_n(s) = \sigma_{min}(s)$. Recall from (2.66) that the error matrix E(s) of smallest norm that will make h(G(s)) + E(s) singular is given by

$$E(s) = U(s)\left[\begin{array}{c|c} E_0(s) & \underline{0} \\ \hline \underline{0}^T & -\sigma_n(s) \end{array}\right] V^H(s) \tag{11}$$

where $||E_0(s)|| \leq \sigma_n(s)$ but is otherwise arbitrary.[1] Provided the norm of the matrix $E_0(s)$ is bounded by $\sigma_n(s)$, its structure is completely unimportant information for the test determining the singularity or nonsingularity of h(G(s)) + $E_0(s)$. Therefore, $E_0(s)$ will be taken as identically zero in the following discussion and

[1] Of course it must also be such that $\tilde{G}(s)$ satisfies condition 1 of Theorem 3.2.

thus, E(s) given by (11) reduces to

$$E(s) = -\sigma_n(s)\underline{u}_n(s)\underline{v}_n^H(s) \quad . \tag{12}$$

The E(s) given by (12) will be called the <u>essential structure</u> of the more general form of E(s) given by (11) when $E_0(s) \neq 0$. The quantity $-\sigma_n(s)\underline{u}_n(s)\underline{v}_n^H(s)$ is the component of E(s) given by (11) that alone must be exactly known if it is to be ascertained whether or not the matrix h(G(s)) + E(s) is singular. Hence, the description of the E(s) given by (12) as the essential structure of E(s) given by (11) is justified.

<u>Remark</u>: The fact that E(s) in (12) is singular or that E(s) in (11) may be almost singular will be important in chapter 6 where a method that assumes that E(s) is nonsingular or not even close to being singular is discussed.

Again, as in the SISO case, the error given by (12) need only occur at one particular complex frequency s_0 to destabilize the feedback system. That is, we may construct a perturbed $\tilde{G}(s)$ having the same number of unstable poles as the nominal G(s) that has the property that $E(s_0)$ satisfies (11) arbitrarily closely and hence destabilizes the feedback system. The MIMO error matrix $E(s_0) = -\sigma_n(s_0)\underline{u}_n(s_0)\underline{v}_n^H(s_0)$ is the generalization of the model errors that produce the $\tilde{g}(s)$ and $\tilde{g}_1(s)$ of Fig. 2 passing through point A' just picking up an extra encirclement of the critical point (-1,0). From (12) we see that for an arbitrary error matrix E(s) that the

projection,[1] $\langle \underline{u}_n(s)\underline{v}_n^H(s), E(s)\rangle \underline{u}_n(s)\underline{v}_n^H(s)$, of E(s) onto the one dimensional subspace spanned by $\underline{u}_n(s)\underline{v}_n^H(s)$ can be used to determine if the component of modelling error in the most sensitive direction $\underline{u}_n(s)\underline{v}_n^H(s)$ will move the multivariable Nyquist diagram of the nominal system nearer or farther from the critical point (0,0) in the complex plane. The direction of this movement of the MIMO Nyquist diagram is simply ascertained by determining if $\langle \underline{u}_n(s)\underline{v}_n^H(s), E(s)\rangle$ is nearer or farther than a distance of $\sigma_n(s)$ from the point $(-\sigma_n(s),0)$ in the complex plane. However, the quantity $\langle \underline{u}_n(s)\underline{v}_n^H(s), E(s)\rangle$ merely determines the effect of one component of the model error and does not take into account the effect of the other components of the model error (i.e., the projections $\langle \underline{u}_i(s)\underline{v}_j^H(s), E(s)\rangle \underline{u}_i(s)\underline{v}_j^H(s)$) have on the multivariable Nyquist diagram. Therefore, some restrictions on these other model error components must be placed if their effect on the stability of the closed-loop system is to be easily predicted.

Suppose now that we restrict the component of modelling error in the most sensitive or worst direction $\underline{u}_n(s)\underline{v}_n^H(s)$ to be exactly zero (i.e., $\langle \underline{u}_n(s)\underline{v}_n^H(s), E(s)\rangle = 0$) so that it has no effect on the multivariable Nyquist diagram. Naturally, for this class of modelling errors, one expects that the magnitude of the error required to destabilize the feedback system should increase since the worst possible

---

[1] The innerproduct notation $\langle \cdot, \cdot \rangle$ was defined in (2.48) of chapter 2 where a discussion of projections on subspaces is also given.

type of error has been ruled out and indeed this is the case. The elimination of this type of error can only be done using engineering judgement about what type of error can occur in the physical system. The next theorem assumes that the worst model error can be ruled out and extends Theorems 3.4, 3.6 and 3.9, by allowing them to deal with errors of larger magnitudes than previously allowable.

Theorem 1: The polynomial $\tilde{\phi}_{CL}(s)$ has no CRHP zeros and hence the perturbed feedback system is stable if the following four conditions hold:

1. (a) $\phi_{0L}(s)$ and $\tilde{\phi}_{0L}(s)$ have the same number of CRHP zeros.

   (b) if $\tilde{\phi}_{0L}(j\omega_0)=0$, then $\phi_{0L}(j\omega_0)=0$

   (c) $\phi_{CL}(s)$ has no CRHP zeros

2. h(G(s)) is of the form:

   (a) $h(G(s)) = I+G(s)$, $\lambda(L(s)) \notin (-\infty,0]$ and

   $E(s) = [\tilde{G}^{-1}(s)-G^{-1}(s)]G(s)$ or

   $E(s) = \tilde{G}(s)-G(s)$ for all $s \in \Omega_R$

or (b) $h(G(s))=(I+G(s))(I-G(s))^{-1}$, $\lambda(L(s)) \notin (-\infty,-1]$

and $E(s) = [\tilde{G}(s)+G(s)]^{-1}[\tilde{G}(s)-G(s)]$ for all $s \in \Omega_R$

or

(c) $h(G(s)) = I+G^{-1}(s)$ and $E(s) = G^{-1}(s)[\tilde{G}(s)-G(s)]$ or

$E(s) = [\tilde{G}^{-1}(s)-G^{-1}(s)]$ and $\lambda(L(s)) \notin (-\infty,0]$ for all $s \in \Omega_R$.

3. $\sigma_{max}[E(s)] < [\sigma_n(s)\sigma_{n-1}(s)]^{1/2}$

for all $s \in \Omega_R$ where $\sigma_n(s)$ and $\sigma_{n-1}(s)$ are the two smallest singular values (assumed to be distinct) of $h(G(s))$

4. $\langle \underline{u}_n(s)\underline{v}_n^H(s), E(s) \rangle = 0$

for all $s \in \Omega_R$ where $\underline{u}_n(s)$ and $\underline{v}_n(s)$ are the left and right singular vectors of $h(G(s))$ associated with $\sigma_n(s)$.

Proof: Conditions 1 and 2 are the same conditions used in Theorems 3.3 to 3.6 and 3.9 to ensure that $G(s,\epsilon)$ is continuous in ϵ on $D_R \times [0,1]$ so that Theorem 3.2 can be applied. Therefore, we need only show that $h(G(s)) + E(s)$ is nonsingular. This, however, is guaranteed by conditions 3 and 4 using the solution to Problem B in chapter 2 (see (2.73) to (2.76)). Q.E.D.

Note that in Theorem 1, conditions 3 and 4 are required to hold for all $s \in \Omega_R$ even though they need only be used in the frequency range where the sufficient conditions (all given by (1) of this chapter) of Theorems 3.3 to 3.6 and 3.9 are violated.

The significance of Theorem 1 is that by requiring very little information (condition 4) in addition to the magnitude of the model error, the worst type of modelling error that could destabilize the feedback system (and whose exclusion might be justified on physical grounds) is effectively eliminated. Hence, the "size" of the error

necessary to destabilize the system may increase significantly if $\sigma_{n-1}(s) >> \sigma_n(s)$. Thus, the conservatism of the chapter 3 theorems for this class of modelling errors is reduced. The <u>essential structure</u> of the next worst error (i.e., next smallest error) that destabilizes the system in this restricted class of modelling errors is given by (from (2.73) with $\phi=0$ because $\langle \underline{u}_n(s)\underline{v}_n(s), E(s)\rangle = 0$)

$$E(s) = \sqrt{\sigma_n(s)\sigma_{n-1}(s)}\left[\underline{u}_n(s)\underline{v}_{n-1}^H(s)e^{j\theta(s)} + \underline{u}_{n-1}(s)\underline{v}_n^H(s)e^{-j\theta(s)}\right]. \tag{13}$$

where (a) $\theta(s)$ is real and arbitrary and (b) the vectors $\underline{u}_{n-1}(s), \underline{u}_n(s), \underline{v}_{n-1}(s)$ and $\underline{v}_n(s)$ are the left and right singular vectors of $h(G(s))$ corresponding to $\sigma_{n-1}(s)$ and $\sigma_n(s)$ respectively. The spectral norm of the matrix $E(s)$ in (13) is precisely $\sqrt{\sigma_n(s)\sigma_{n-1}(s)}$.

However, it must be pointed out, that it is extremely unlikely that condition 4 of Theorem 1 will hold exactly for a realistic modelling error since the model error in the particular direction $\underline{u}_n(s)\underline{v}_n^H(s)$ will rarely be exactly zero. A more likely expectation is that this component of the error not be exactly zero but sufficiently small in magnitude. By requiring only that the model error in the direction $\underline{u}_n(s)\underline{v}_n^H(s)$ be sufficiently small, Theorem 1 may be modified so that the essential nature of its results are still valid when the class of model errors considered is characterized by

$$\left|\langle \underline{u}_n(s)\underline{v}_n^H(s), E(s)\rangle\right| \leq c(s) < \sigma_n(s) = \sigma_{min}(s). \tag{14}$$

The positive scalar c(s) in (14) bounds the magnitude of the worst modelling error as a function of frequency to be less than $\sigma_{min}(s)$, the minimum magnitude of the smallest destabilizing error required to destabilize the feedback system. Therefore, the magnitude of the model error in the most sensitive or worst direction $\underline{u}_n(s)\underline{v}_n^H(s)$ is not large enough by itself to destabilize the feedback system. In order to destabilize the feedback system when the model errors satisfy (14), other model error components, besides the model error component in the worst direction, must contribute to the movement of the MIMO Nyquist diagram through the critical point (0,0). This is stated formally in the next theorem.

Theorem 2: The polynomial $\tilde{\phi}_{CL}(s)$ has no CRHP zeros and hence the perturbed feedback system is stable if the following conditions hold:

1. conditions 1 and 2 of Theorem 1 hold
2. $\sigma_{max}[E(s)] < [\sigma_n(s)\sigma_{n-1}(s) + c(s)[\sigma_n(s) - \sigma_{n-1}(s)]]^{1/2}$ for all $s \in \Omega_R$
3. $|\langle \underline{u}_n(s)\underline{v}_n^H(s), E(s)\rangle| \leq c(s) < \sigma_n(s)$ for all $s \in \Omega_R$.

Proof: Identical to proof of Theorem 1 except that now the general solution of Problem B ((2.73) to (2.76)) via conditions 2 and 3 guarantees that h(G(s)) + E(s) is nonsingular. Q.E.D.

The essential structure of the next worst perturbation that does not violate condition 3 but destabilizes the feedback system is given by (from 2.73)

$$E(s) = [c(s)\underline{u}_{n-1}(s)\underline{v}^H_{n-1}(s) - c(s)\underline{u}_n(s)\underline{v}^H_n(s) + \gamma(s)\underline{u}_{n-1}(s)\underline{v}^H_n(s) + \gamma^*(s)\underline{u}_n(s)\underline{v}^H_{n-1}(s)] \tag{15}$$

where

$$\gamma(s) = \left[[c(s) + \sigma_n(s)][c(s) - \sigma_{n-1}(s)]\right]^{1/2} e^{j\phi(s)} \tag{16}$$

with $\phi(s)$ being arbitrary but real. Note that as $c(s) \to 0$, in condition 3 and in (15) and (16), that we recover the results of Theorem 1. To make the meaning of the results of Theorem 2 clearer, the following example is given.

Example 1: Suppose that we wish to determine stability robustness of a 2x2 control system which actually has a loop transfer function matrix $\tilde{G}(s)$ but is represented by the nominal diagonal loop transfer matrix $G(s)$ given by

$$G(s) = \begin{bmatrix} g_{11}(s) & 0 \\ 0 & g_{22}(s) \end{bmatrix} = \begin{bmatrix} \frac{1}{s+7.5} & 0 \\ 0 & \frac{1}{s+0.5} \end{bmatrix} \tag{17}$$

so that the nominal closed-loop system has poles at -8.5 and -1.5. If we use the relative error criterion

$$E(s) = G^{-1}(s)[\tilde{G}(s) - G(s)] = \begin{bmatrix} \frac{\tilde{g}_{11}(s) - g_{11}(s)}{g_{11}(s)} & \frac{\tilde{g}_{12}(s)}{g_{11}(s)} \\ \frac{\tilde{g}_{21}(s)}{g_{22}(s)} & \frac{\tilde{g}_{22}(s) - g_{22}(s)}{g_{22}(s)} \end{bmatrix} \tag{18}$$

then the multiplicative uncertainty factor matrix L(s) is given by

$$L(s) = I+E(s) = \begin{bmatrix} \dfrac{\tilde{g}_{11}(s)}{g_{11}(s)} & \dfrac{\tilde{g}_{12}(s)}{g_{11}(s)} \\ \dfrac{\tilde{g}_{21}(s)}{g_{22}(s)} & \dfrac{\tilde{g}_{22}(s)}{g_{22}(s)} \end{bmatrix} . \tag{19}$$

First, we compute $\sigma_{min}(I+G^{-1}(j\omega))$ to determine the magnitude of the smallest destabilizing model error E(s). This is simply given by

$$\sigma_{min}(I+G^{-1}(j\omega)) = \left|1.5+j\omega\right| = \sqrt{(1.5)^2+\omega^2} \geq 1.5 \tag{20}$$

because

$$I+G^{-1}(s) = \begin{bmatrix} s+8.5 & 0 \\ 0 & s+1.5 \end{bmatrix} . \tag{21}$$

Now suppose that the error in the loop gain of each loop of the feedback system is known within $\pm 50\%$ of the nominal loop gain, that is

$$0.5 \leq \left| \frac{\tilde{g}_{11}(j\omega)}{g_{11}(j\omega)} \right| = \left| \ell_{11}(j\omega) \right| \leq 1.5 \tag{22}$$

and

$$0.5 \leq \left| \frac{\tilde{g}_{22}(j\omega)}{g_{22}(j\omega)} \right| = \left| \ell_{22}(j\omega) \right| \leq 1.5 . \tag{23}$$

Next, suppose that we are more uncertain about the channel crossfeeds in the sense that we can only assert that

$$|e_{12}(j\omega)| = |\ell_{12}(j\omega)| = \left| \frac{\tilde{g}_{12}(j\omega)}{g_{11}(j\omega)} \right| \leq 2 \tag{24}$$

and that

$$|e_{21}(j\omega)| = |\ell_{21}(j\omega)| = \left| \frac{\tilde{g}_{21}(j\omega)}{g_{11}(j\omega)} \right| \leq 2 \ . \tag{25}$$

It follows from (22) and (23) that we can bound $|e_{11}(j\omega)|$ and $|e_{22}(j\omega)|$ by 1/2 and thus, by (24) and (25), we can only conclude that

$$||E(j\omega)||_2 = \sigma_{max}[E(j\omega)] \leq 2.5 \ . \tag{26}$$

From (26) and (20) it is clearly possible to have

$$\sigma_{max}[E(j\omega)] > \sigma_{min}[I+G^{-1}(j\omega)] \ . \tag{27}$$

Therefore, Theorem 3.4 of chapter 3 does not apply. However, we can use Theorem 2 to ensure the stability of the perturbed feedback system. To see this, note that the SVD of $I+G^{-1}(j\omega)$ is given by

$$I+G^{-1}(j\omega) = \begin{bmatrix} e^{j\theta_1(\omega)} & 0 \\ 0 & e^{j\theta_2(\omega)} \end{bmatrix} \begin{bmatrix} |j\omega+8.5| & 0 \\ 0 & |j\omega+1.5| \end{bmatrix} \begin{bmatrix} 1 & 0 \\ 0 & 1 \end{bmatrix}$$

$$= U(j\omega)\Sigma(j\omega)V^H(j\omega) \tag{28}$$

where

$$\theta_1(\omega) = \arg[j\omega+8.5] \tag{29}$$

and

$$\theta_2(\omega) = \arg[j\omega+1.5] \ . \tag{30}$$

Note that condition 3 of Theorem 2 can be satisfied with $c(j\omega)=1/2$ since from (28) defining $\underline{u}_2(j\omega)$ and $\underline{v}_2(j\omega)$ and from (23) bounding $\ell_{22}(j\omega)$ and thus $e_{22}(j\omega)$ we have that for all ω

$$|<\underline{u}_2(j\omega)\underline{v}_2^H(j\omega),E(j\omega)>|=|\underline{u}_2^H(j\omega)E(j\omega)\underline{v}_2(j\omega)|=|e_{22}(j\omega)|\leq 1/2 \ . \qquad (31)$$

Thus, by (31) and (20) we have

$$\sigma_2(j\omega)\geq 1.5 > 1/2 \geq |<\underline{u}_2(j\omega)\underline{v}_2^H(j\omega),E(j\omega)>|. \qquad (32)$$

Next, we calculate the right-hand-side of condition 2 of Theorem 2 and a lower bound as follows

$$\left[\sigma_1(j\omega)\sigma_2(j\omega)+c(j\omega)[\sigma_2(j\omega)-\sigma_1(j\omega)]\right]^{1/2} = \left[|j\omega+8.5||j\omega+1.5|\right.$$
$$\left. + 1/2[|j\omega+1.5|-|j\omega+8.5|]\right]^{1/2} \geq (8.5)(1.5)+\left(\frac{-7}{2}\right) \geq 3. \qquad (33)$$

Therefore, using (26) we have that

$$\sigma_{max}[E(j\omega)]\leq 2.5 < 3 \leq \left[\sigma_1(j\omega)\sigma_2(j\omega)+c(j\omega)[\sigma_2(j\omega)-\sigma_1(j\omega)]\right]^{1/2} \qquad (34)$$

and so condition 2 of Theorem 2 holds. Assuming condition 1 of Theorem 2 holds we have shown that the perturbed feedback system is stable. The next smallest destabilizing error can be calculated from (15) and (16) with $\phi(j\omega)=0$ and $\omega=0$

since $\sigma_{min}(I+G^{-1}(j\omega)) \geq \sigma_{min}(I+G^{-1}(0)) = 1.5$ and is given by

$$E(0) = \begin{bmatrix} 1/2 & 3 \\ 3 & -1/2 \end{bmatrix} \tag{35}$$

which means that L(s) may be taken as the constant matrix L given by

$$L = \begin{bmatrix} 3/2 & 3 \\ 3 & 1/2 \end{bmatrix} \tag{36}$$

Thus, we see that (refer to Figs. 3 and 4) crossfeed gain errors of magnitude 3 and loop gain changes of $\pm 50\%$ are required to destabilize the feedback system if we insist that (22) and (23) must hold.

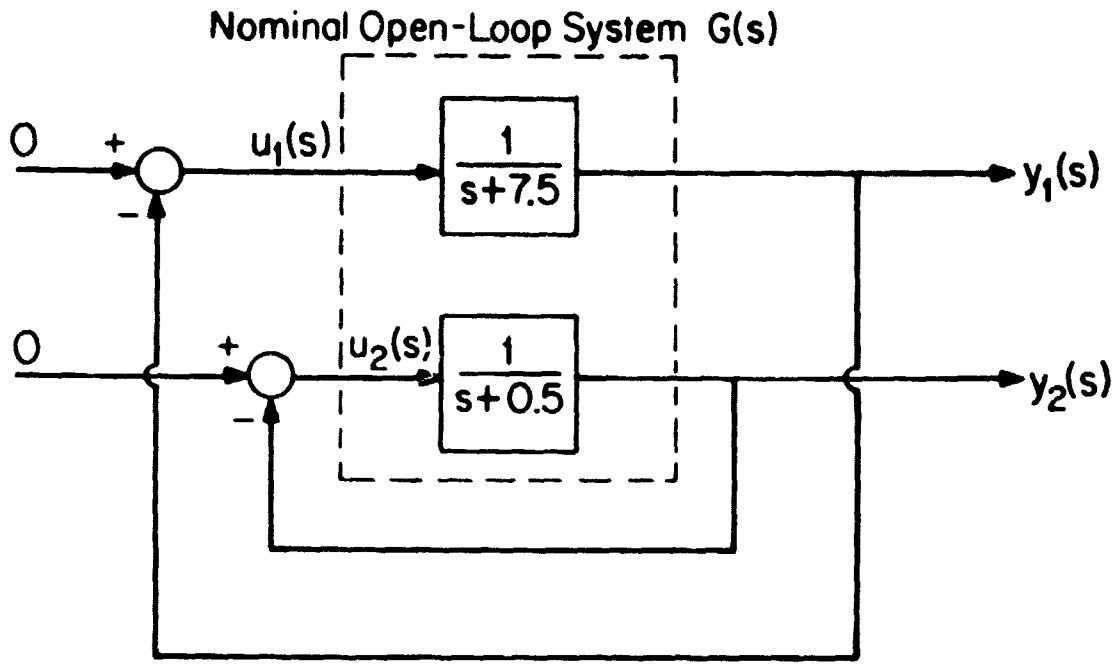

Fig. 3: Nominal Feedback System (Stable).

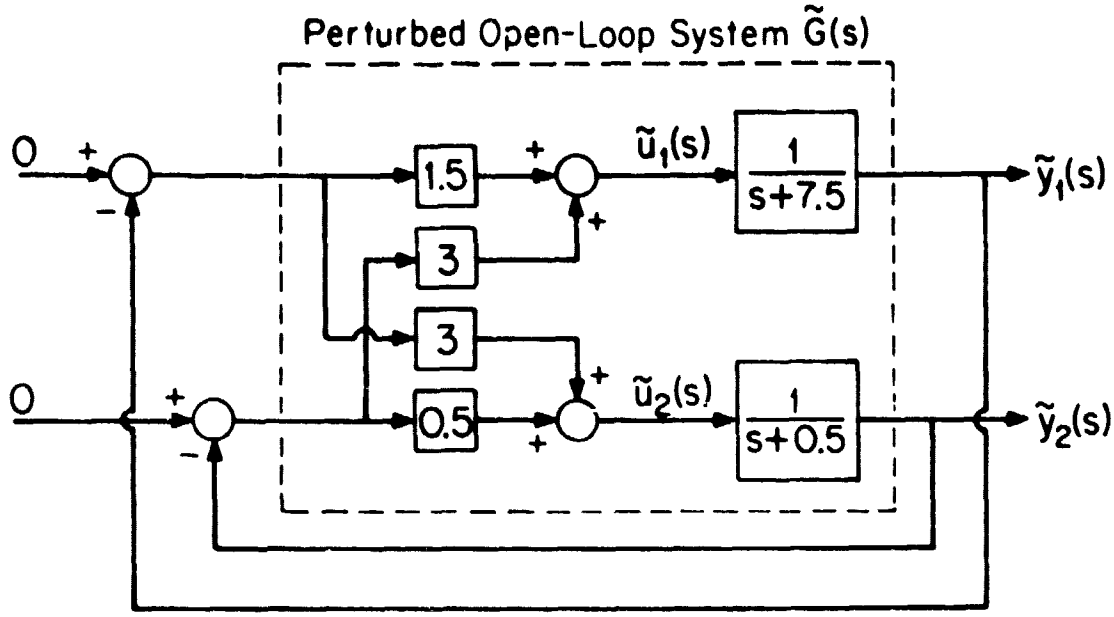

Fig. 4: Perturbed Feedback System (Unstable)

Remark: One possible exception, to the form of E(s) given in (13) or (15) occurs when E(s) is such that at least, one of the eigenvalues of L(s) is real and negative. In Theorem 1 and 2, condition 2 places restrictions on the eigenvalues of L(s) which may be violated when at least one of the eigenvalues of L(s) is real and negative. In this case, Theorems 1 and 2 do not apply and there may exist a smaller error that destabilizes the feedback system but yet conditions 4 and 3, of Theorems 1 and 2 respectively, still hold. However, when

the matrices U(s) and V(s) of the SVD of h(G(s)) are complex it is very unlikely that L(s) determined by the E(s) given in (13) or (15) will even have real eigenvalues.

We can now consider placing additional constraints on the modelling and further restrict the class of allowable modelling errors in the manner of Problem C in chapter 2 and derive the next theorem.

Theorem 3: The polynomial $\tilde{\phi}_{CL}(s)$ has no CRHP zeros and hence the perturbed feedback system is stable if the following conditions hold:

1. Conditions 1 and 2 of Theorem 1 hold.
2. E(s) is of the form

$$E(s) = U(s)\left[\begin{array}{c|c} E_1(s) & \underline{e}_2(s) \\ \hline \underline{e}_3^T & 0 \end{array}\right] V^H(s) \qquad (37)$$

where $\underline{e}_2(s)$ and $\underline{e}_3(s)$ are vectors whose last component is identically zero and where U(s) and V(s) are defined in (6).

3. $\sigma_{max}(E(S)) < \sqrt{\sigma_k(s)\sigma_\ell(s)}$

where $$\sigma_k(s)\sigma_\ell(s) = \min_{(i,j)\in M} \sigma_i(s)\sigma_j(s) \qquad (38)$$

and $$M \triangleq \{(n,n),(n-1,n),(n,n-1)\} \qquad (39)$$

Proof: Direct application of Problem C of chapter 2 and Theorem 3.2 as in Theorems 1 and 2.

Theorem 3 allows us to determine the next larger magnitude of the "next, next worst model error" required to produce instability when the smallest destabilizing model error and the next smallest destabilizing model error considered in Theorem 1 and given by (13) are completely eliminated from consideration. Theorem 3 eliminates these type of errors by requiring zero model error projections in the worst direction $\underline{u}_n(s)\underline{v}_n^H(s)$ and the next worst pair of directions $\underline{u}_n(s)\underline{v}_{n-1}^H(s)$ and $\underline{u}_{n-1}(s)\underline{v}_n^H(s)$. The process of eliminating each "successively worst direction" could obviously be continued and larger magnitudes of these classes of errors would then be necessary to destabilize the feedback system.

4.3 Block Diagram Interpretations of Worst Model Error

In this section, interpretations of the smallest destabilizing model error will be given using block diagrams revealing the role of the SVD of the matrices of $I+G(j\omega)$ and $I+G^{-1}(j\omega)$ in the input-output properties of the feedback system. The types of model error considered are those of Theorems 3.4 and 3.6 involving the relative errors between $G(j\omega)$ and $\tilde{G}(j\omega)$ or $G^{-1}(j\omega)$ and $\tilde{G}^{-1}(j\omega)$.

At some particular frequency ω_0, let the SVD of $I+G^{-1}(j\omega_0)$ be given by

$$I+G^{-1}(j\omega_0) = U(j\omega_0)\Sigma(j\omega_0)V^H(j\omega_0) \tag{40}$$

so that the closed-loop transfer matrix at ω_0, $G_{CL}(j\omega_0)$ is given by

$$G_{CL}(j\omega_0) = (I+G^{-1}(j\omega_0)^{-1} = V(j\omega_0)\Sigma^{-1}(j\omega_0)U^H(j\omega_0) = \sum_{i=1}^{n} \frac{1}{\sigma_i(j\omega_0)} \underline{v}_i(j\omega_0)\underline{u}_i^H(j\omega_0) \tag{41}$$

and thus

$$\underline{v}_i^H(j\omega_0)G_{CL}(j\omega_0)\underline{u}_i(j\omega_0) = \frac{1}{\sigma_i(j\omega_0)} \quad . \tag{42}$$

A block diagram of a closed-loop stable system representing equation (42) is given in Fig. 5.

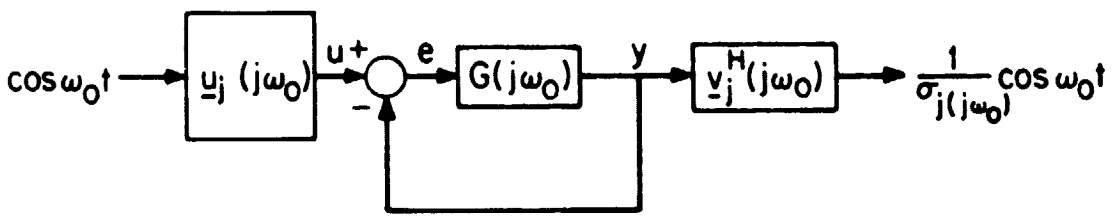

Fig. 5: Block Diagram Interpretation of SVD of $I+G^{-1}(j\omega_0)$.

This Figure illustrates that the left and right singular vectors $\underline{u}_j(j\omega_0)$ and $\underline{v}_j(j\omega_0)$ collapse the MIMO closed-loop system into a SISO system through which the signal $\cos\omega_0 t$ passes with a change of amplitude by a factor of $1/\sigma_j(j\omega_0)$ determined by the singular values. These vectors can be interpreted as input and output "directions" where for each different value of the index j input/output direction pair produces a different SISO system and represents a different route through the MIMO system for the signal $\cos\omega_0 t$. Therefore, from Fig. 5 with j=n, we see that if $\sigma_n(j\omega_0) = \sigma_{min}(j\omega_0)$ is near zero, then the system will amplify a sinusoidal signal by a large factor of $1/\sigma_n(j\omega_0)$ in the input/output directions of $\underline{u}_n(j\omega_0)$ and $\underline{v}_n(j\omega_0)$. As $\sigma_n(j\omega_0)$ approaches zero the amplification factor approaches infinity until at $\sigma_n(j\omega_0)=0$ the system with a bounded input produces an unbounded output, that is, the system becomes unstable. This is all rather obvious since if $\sigma_n(j\omega_0)=0$, the matrix $(I+G^{-1}(j\omega_0))^{-1}$ does not exist and therefore there must be closed-loop poles on the $j\omega$-axis at $\pm j\omega_0$.

As in the case of $I+G^{-1}(j\omega_0)$ a similar interpretation of the SVD of $I+G(j\omega_0)$ can be made. If the SVD of $I+G(j\omega_0)$ is given by $I+G(j\omega_0) = U(j\omega_0)\Sigma(j\omega_0)V^H(j\omega_0)$ making the SVD of $[I+G(j\omega_0)]^{-1}$

$$[I+G(j\omega_0)]^{-1} = V(j\omega_0)\Sigma^{-1}(j\omega_0)U^H(j\omega_0) = \sum_{i=1}^{n} \frac{1}{\sigma_i(j\omega_0)} \underline{v}_i(j\omega_0)\underline{u}_i^H(j\omega_0) \quad (43)$$

then Fig. 6 gives the block diagram analogous to Fig. 5. Figure 6 shows that the only change from the previous case shown in Fig. 5 is that the output is generated from the error signal e instead of the system output signal y.

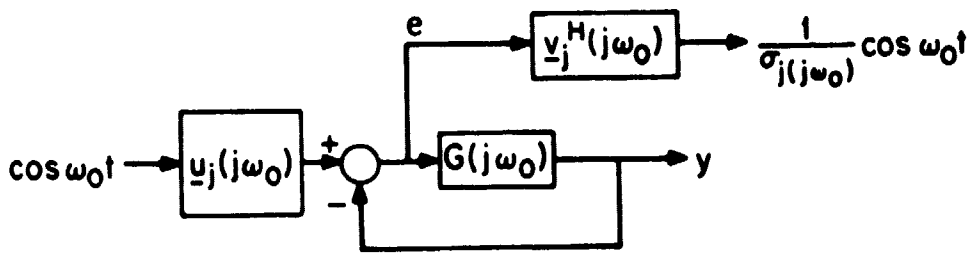

Fig. 6: Block Diagram Interpretation of SVD of $I+G(j\omega_0)$.

Notice that in (41) and (43) the vectors $\underline{u}_i(j\omega_0)$ and $\underline{v}_i(j\omega_0)$ depend on the particular frequency ω_0 that is selected when the SVD is accomplished. Thus the input-output relationship of Figs. 5 and 6 are only valid at the frequency ω_0. Note also that the unit vectors

$\underline{u}_j(j\omega_0)$ and $\underline{v}_j(j\omega_0)$ are in general complex but may be realized by passive attenuating filters that give the appropriate phase shift or time delay at frequency ω_0.

In the SISO case when $G(j\omega)$ is a scalar the vectors $\underline{u}_j$ and $\underline{v}_j$ become the complex scalars u and v which have unit magnitude. Since the input-output relationship in these figures is simply the positive gain of $1/\sigma_j(j\omega_0)$, it must be that at $\omega=\omega_0$ the phase of the product $u(j\omega_0)v^*(j\omega_0)$ is simply the negative of the phase of $[1+g^{-1}(j\omega_0)]^{-1}$ or $[1+g(j\omega_0)]^{-1}$.

Using Figs. 5 and 6 we may interpret the directional nature of the smallest (according to a particular error criterion) model error in $G(j\omega_0)$ that destabilizes the closed loop system. The gain from input to output in Fig. 5, as mentioned before, is simply $1/\sigma_j(j\omega_0)$. If the input-output directions $\underline{u}_n(j\omega_0)$ and $\underline{v}_n(j\omega_0)$ are used and if $\sigma_n(j\omega_0)$ is small, then a small amount of positive feedback around the system of Fig. 5 will destabilize the system. This is shown in Fig. 6 where the output of the system of Fig. 5 is fedback to the input with a gain of α. Notice in Fig. 7 that if $\alpha=\sigma_n(j\omega_0)$ the system becomes unstable because the system amplifies the input by $[\sigma_n(j\omega_0)-\alpha]^{-1}$. This additional feedback could be interpreted as a perturbation to the system of Fig. 5. However, by block diagram manipulations it is not difficult to see that this perturbed system is equivalent to those of Figs. 8, 9 and 10.

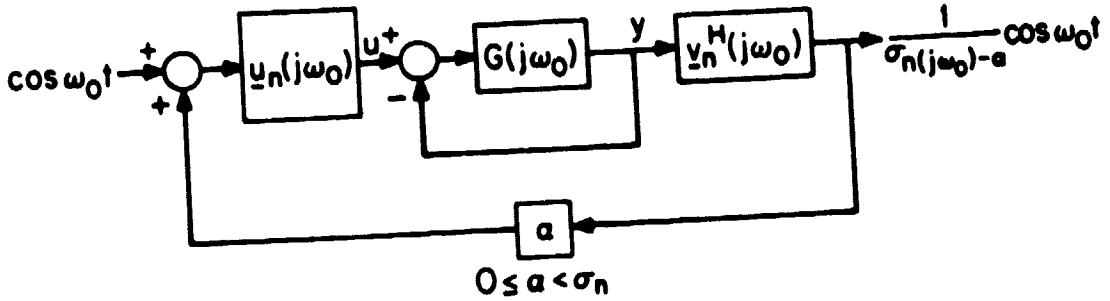

Fig. 7: Destabilizing Feedback in Most Sensitive Direction $\underline{u}_n(j\omega_0)\underline{v}_n^H(j\omega_0)$ for Error Criterion $E = G^{-1}[\tilde{G}-G]$.

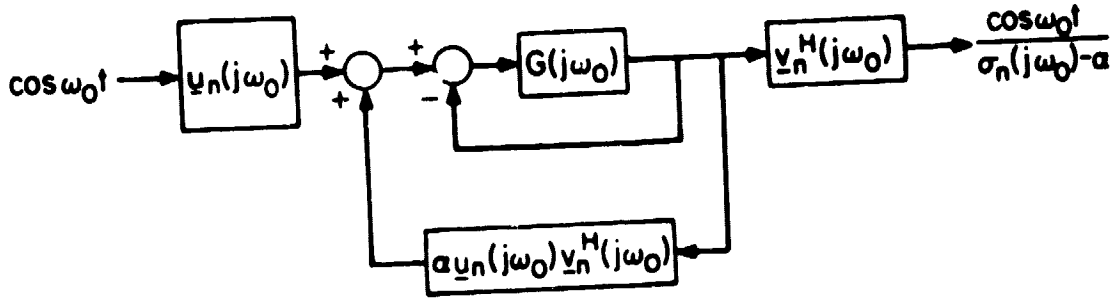

Fig. 8: Equivalent to Fig. 7.

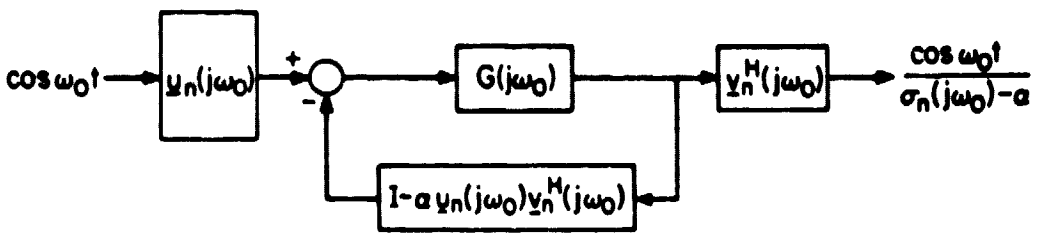

Fig. 9: Equivalent to Fig. 8.

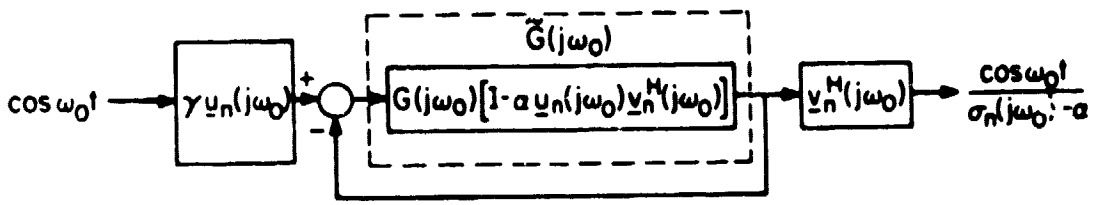

Fig. 10: Equivalent to Fig. 9 where $\gamma = [1-\alpha \underline{v}_n^H(j\omega_0)\underline{u}_n(j\omega_0)]^{-1}$.

In Fig. 10 an explicit inversion of $[I-\alpha \underline{u}_n(j\omega_0)\underline{v}_n^H(j\omega_0)\underline{v}_n^H(j\omega_0)]$ has been performed to simplify the block diagram.

From Figs. 9 or 10 it is clear that the stability of these equivalent perturbed closed-loop systems is completely characterized by the behavior of the loop transfer function matrix $\tilde{G}(j\omega)$ which at $\omega=\omega_0$ is given by

$$\tilde{G}(j\omega_0) = G(j\omega_0)L(j\omega_0) = G(j\omega_0)[I-\alpha \underline{u}_n(j\omega_0)\underline{v}_n^H(j\omega_0)] \tag{44}$$

Thus, in the error criterion $E(s) = G^{-1}(s)[\tilde{G}(s)-G(s)]$ given in (3.35) we have that $E(j\omega_0)$ is given by

$$E(j\omega_0) = -\alpha \underline{u}_n(j\omega_0)\underline{v}_n^H(j\omega_0) \tag{45}$$

This means that the perturbation matrix $L(j\omega_0)$ that perturbs the inputs to the open-loop $G(j\omega_0)$ has the same effect as applying additional positive feedback in the most sensitive direction $\underline{u}_n(j\omega_0)\underline{v}_n^H(j\omega_0)$. Just as we have interpreted the worst error as additional positive feedback in the direction $\underline{u}_n(j\omega_0)\underline{v}_n^H(j\omega_0)$ using the SVD of $I+G^{-1}(j\omega_0)$, we obtain similar interpretations using the SVD of $I+G(j\omega_0)$. Using Fig. 6 we may again determine the smallest destabilizing feedback as given in Fig. 11 and its open-loop equivalent in Fig. 12.

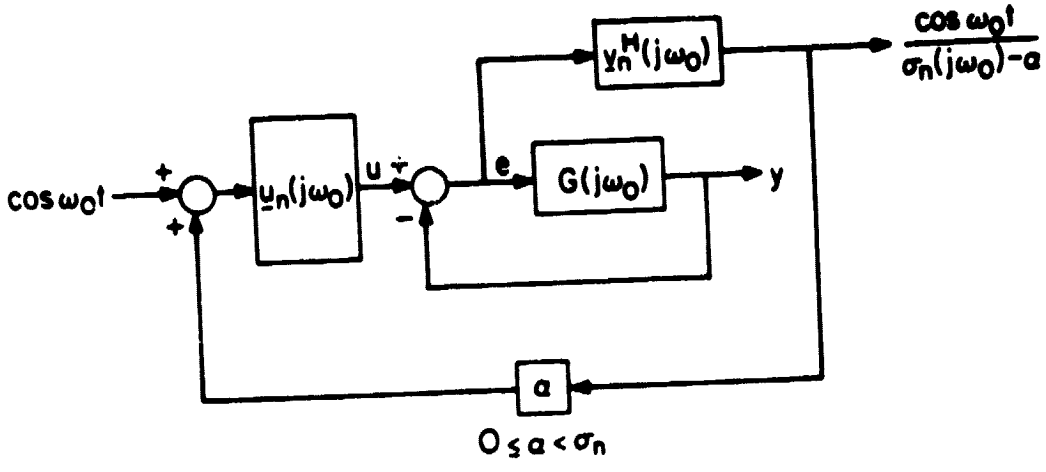

Fig. 11: Destabilizing Feedback in Most Sensitive Direction $\underline{u}_n(j\omega_0)\underline{v}_n^H(j\omega_0)$ for Error Criterion $E = [\tilde{G}^{-1}-G^{-1}]G$.

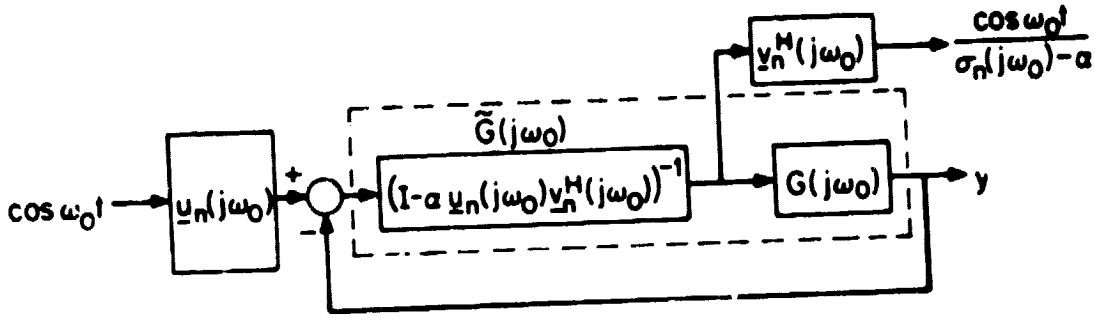

Fig. 12: Equivalent to Fig. 11.

Here again the model error criterion of (3.44) gives the model error as

$$E(j\omega_0) = -\alpha \underline{u}_n(j\omega_0)\underline{v}_n^H(j\omega_0) \tag{46}$$

and the perturbation $L(j\omega_0)$ as

$$L(j\omega_0) = (I-\alpha \underline{u}_n(j\omega_0)\underline{v}_n^H(j\omega_0))^{-1}. \tag{47}$$

Thus, by interpreting $\underline{u}_j(j\omega_0)$ and $\underline{v}_j(j\omega_0)$ as input-output directions, the model error in a certain direction can be viewed as the induced additional feedback in the directions specified by the input vectors $\underline{u}_j(j\omega_0)$ and the output vectors $\underline{v}_j(j\omega_0)$.

Thus to differentiate between those model errors that increase the margin of stability and those that decrease the margin of stability it is necessary to examine their contributions in certain input-output directions.

A model error will <u>decrease</u> the margin of stability of the feedback system if it can be interpreted as <u>additional positive feedback</u> in the input/output directions $\underline{u}_n(j\omega_0)$ and $\underline{v}_n(j\omega_0)$, which are equivalent to the most sensitive model error direction $\underline{u}_n(j\omega_0)\underline{v}_n^H(j\omega_0)$, <u>and</u> the contributions of the model error in the other input/output directions are negligible.

A model error will <u>increase</u> the margin of stability if it can be interpreted as <u>additional negative feedback</u> in the input/output directions $\underline{u}_n(j\omega_0)$ and $\underline{v}_n(j\omega_0)$ <u>and</u> the contributions of the model error in the other input/output directions are negligible.

The contributions of the model error in the other input/output directions are negligible, where the SVD of $I+G^{-1}(j\omega_0)$ is used, if for all i and j not both equal to n, $\underline{v}_i^H(j\omega_0)\tilde{G}_{CL}(j\omega_0)\underline{u}_j(j\omega_0)$ is sufficiently close to $\underline{v}_i^H(j\omega_0)G_{CL}(j\omega_0)\underline{u}_i(j\omega_0)$. If the SVD of $I+G(j\omega_0)$ is used, the perturbed closed-loop system $\tilde{G}_{CL}(j\omega_0)$ is replaced by $(I+\tilde{G}(j\omega_0))^{-1}$ and $G_{CL}(j\omega_0)$ is replaced by $[I+G(j\omega_0)]^{-1}$ in the previous sentence. The contributions of the model error in the other input/output directions must be negligible because they may potentially cancel out the effect or contribution of the model error in the input/output directions $\underline{u}_n(j\omega_0)$ and $\underline{v}_n(j\omega_0)$.

4.4 Example of Section 3.3 Continued

In this section, the example of section 3.3 is reconsidered and it is shown how the model error given in Fig. 3.16, that destabilizes the feedback system, can be predicted by computing the smallest destabilizing or worst model error by the methods of this chapter. Also, the class of modelling errors is restricted to completely exclude this type of worst or smallest destabilizing error, and the next worst or next smallest destabilizing error is computed. The size or norm of this error is given by Theorem 1 and its structure is given by (13).

These computations are displayed graphically for both the relative and inverse relative error criteria (i.e., $E=G^{-1}(\tilde{G}-G)$ and $E=(\tilde{G}^{-1}-G^{-1})G$). To make a comparison of the results with the different error criteria,

Bode-like plots of the elements of $L(j\omega)$, the matrix that makes $I+G(j\omega)L(j\omega)$ singular at <u>every</u> ω, are given. These $L(j\omega)$ matrices correspond to the minimum modelling errors of a specific criteria within an appropriately restricted class of modelling errors. As in the SISO case, illustrated in Fig. 2, the pertubed system $\tilde{G}(j\omega)$ needs only to correspond to $G(j\omega)L(j\omega)$ (for the $L(j\omega)$ that makes $I+G(j\omega)L(j\omega)$ singular at every ω) at a single frequency in order to destabilize the feedback system. The magnitude of these model error is given by the corresponding plots of the singular values of $I+G(j\omega)$ and $I+G^{-1}(j\omega)$.

In Fig. 13 the singular values of $I+G(j\omega)$, for our example, as well as their geometric mean are plotted in dB versus the frequency, ω.

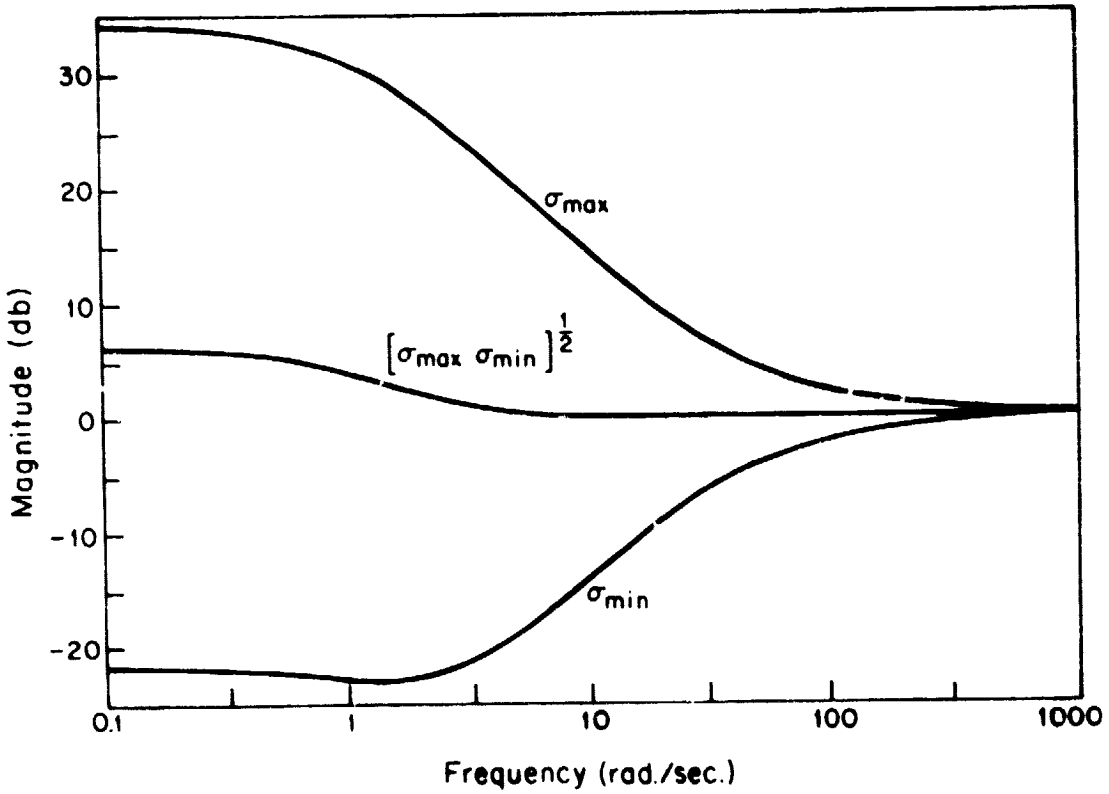

Fig. 13: Singular Value Quantities of $I+G(j\omega)$

These quantities determine the magnitude of the smallest and next smallest modelling error (when the class of errors is restricted by $\langle \underline{u}_n(s)\underline{v}_n^H(s), E(s)\rangle = 0$) that destabilize the system when $E = [\tilde{G}^{-1}G^{-1}]G$. The magnitude of the smallest or worst error is given by σ_{min} and the magnitude of the next smallest or next worst error is given by $[\sigma_{min}\sigma_{max}]^{1/2}$. The minimum of σ_{min} occurs near ω=1 rad/sec, ($\sigma_{min} \simeq$ -23dB); thus the required magnitude of the worst error is -23dB. However, at ω=0, $[\sigma_{min}\sigma_{max}]^{1/2} \simeq$ 4dB, indicating that the next worst modelling error occurring only in the frequencies about ω=0, is necessarily of a magnitude of 4dB in order to destabilize the feedback system. Since $[\sigma_{min}\sigma_{max}]^{1/2}$ approaches 0dB as $\omega \to \infty$, there exists a modelling error in the high frequency range of the next worst type that need only have a magnitude of 0dB that will destabilize the feedback system. Note, however that 0 dB is also the magnitude of the worst error if the error is restricted to the high frequency range, since $\sigma_{min} \simeq$ 0dB as $\omega \to \infty$.

The nature of the worst error corresponding to σ_{min} in Fig. 13, is obtained by plotting elements of

$$L(j\omega) = (I+E(j\omega))^{-1} \tag{48}$$

where

$$E(j\omega) = [\tilde{G}^{-1}(j\omega)-G^{-1}(j\omega)]G(j\omega) \tag{49}$$

is such that $I+\tilde{G}(j\omega)$ is singular at all ω. This is displayed in Figs. 14 and 15. Note that in Figs. 14 and 15 that the diagonal elements of $L(j\omega)$ near ω=1, (where $\sigma_{min} \simeq$ -23dB) are essentially unity

while $\ell_{12}(j)$ can be considered essentially zero ($\simeq$ -80dB in magnitude) and that $\ell_{21}(j)$ is essentially -.0708.

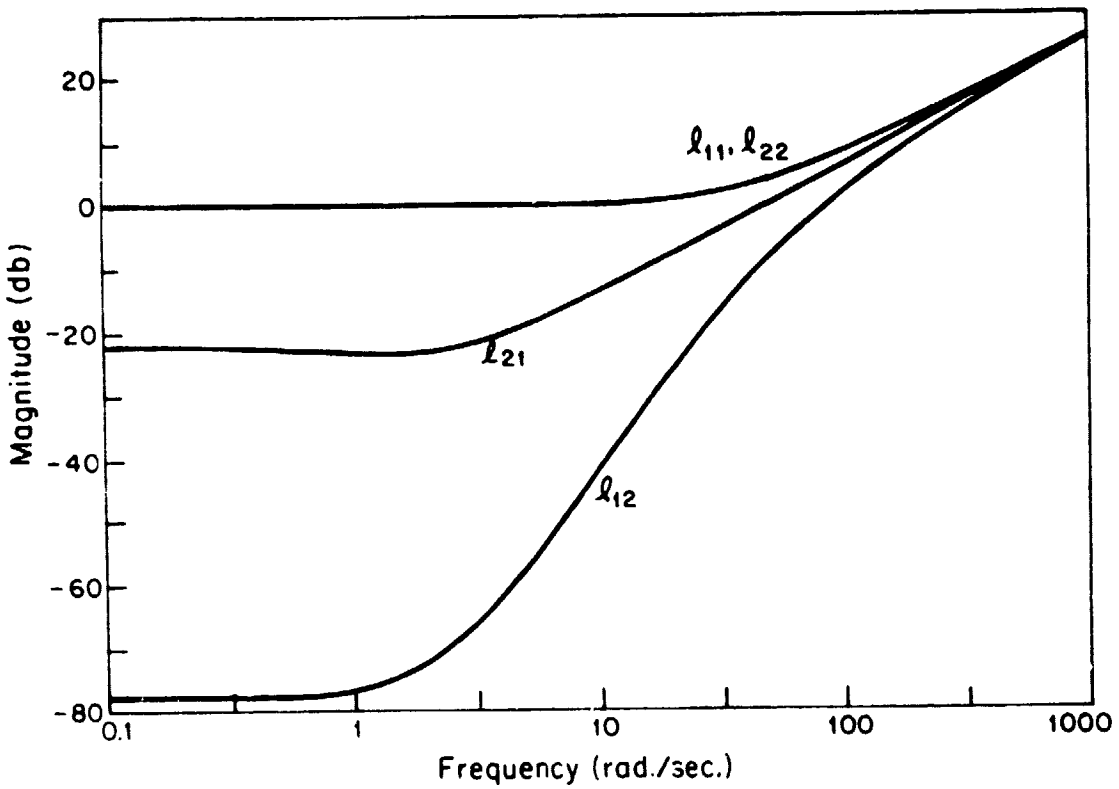

Fig, 14: Magnitude Bode-like plots of elements of $L(j\omega)$ for worst model error.

Thus at ω=1, L(j) is given approximately by

$$L(j) \simeq \begin{bmatrix} 1 & 0 \\ -.0708 & 1 \end{bmatrix} \tag{50}$$

and represents a crossfeed type of perturbation as in Fig. 3.16 which has a constant crossfeed perturbation L given by (with b_{12}=50)

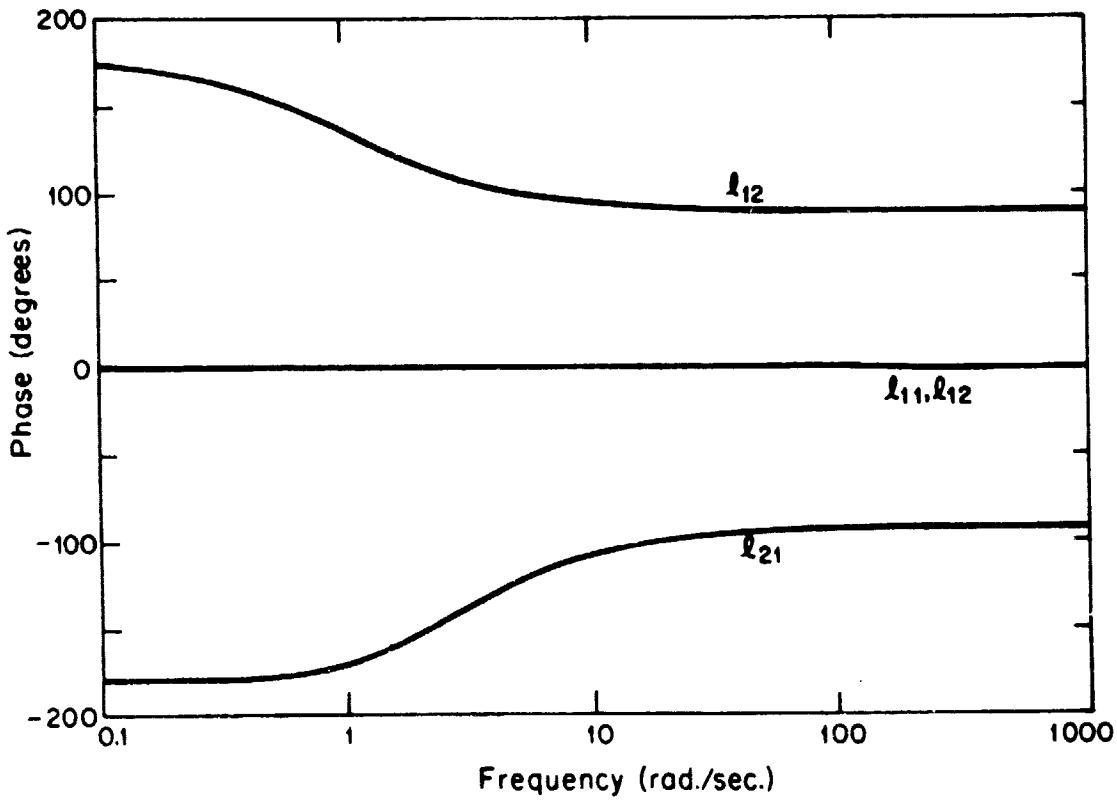

Fig. 15: Phase Bode-like plots of elements of L(jω) for worst model error

$$L = \begin{bmatrix} 1 & 0 \\ -.1 & 1 \end{bmatrix} \tag{51}$$

which gives a modelling error of -20dB. Therefore, we see that the essential nature of the crossfeed perturbation (51) is detected by the approach presented here as evidenced by L(0) in (50).

The above discussion points out that a control system designer can generate these plots and determine what type of gain changes or channel crossfeeds, that were neglected in his nominal design model, should be examined carefully; because if these gain and crossfeed errors occur the feedback system can become unstable. The control system designer does not need to worry ahead of time about <u>all</u> the different types of model uncertainties that might occur; the nature of these plots vs. frequency will provide him with guidance with what type of modelling errors and in what frequency range he should be most concerned with.

For comparison, the plots analogous to Figs. 13, 14 and 15 using the singular values of $I+G^{-1}(j\omega)$ rather than those of $I+G(j\omega)$ and the error criteria $E = G^{-1}[\tilde{G}-G] = L-I$ are shown in Figs. 16, 17 and 18 respectively. Note that, for $\omega \simeq 1$, Figs. 17 and 18 indicate nearly the same L(j) as in (50). However, as σ_{min} of $I+G(j\omega)$ or $I+G^{-1}(j\omega)$ both increase as ω increases, that from Figs. 14, 15, 17 and 18 that L(j1000)

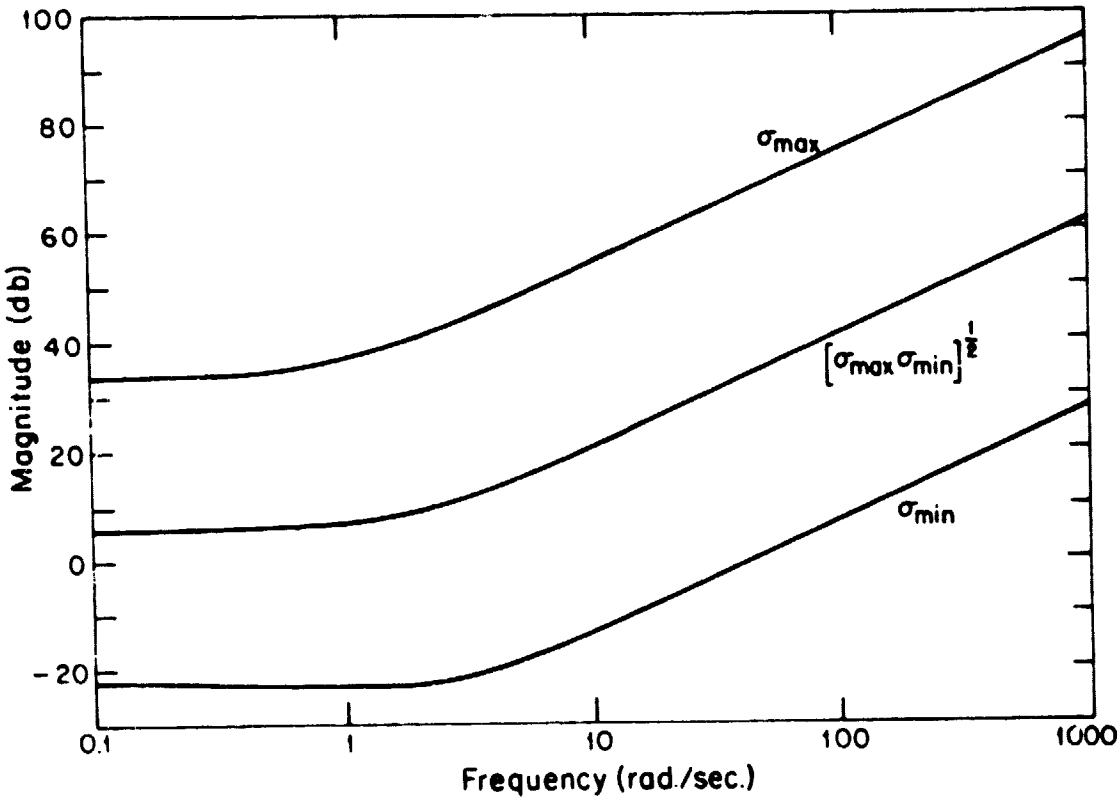

Fig. 16: Singular Value Quantities of $I+G^{-1}(j\omega)$.

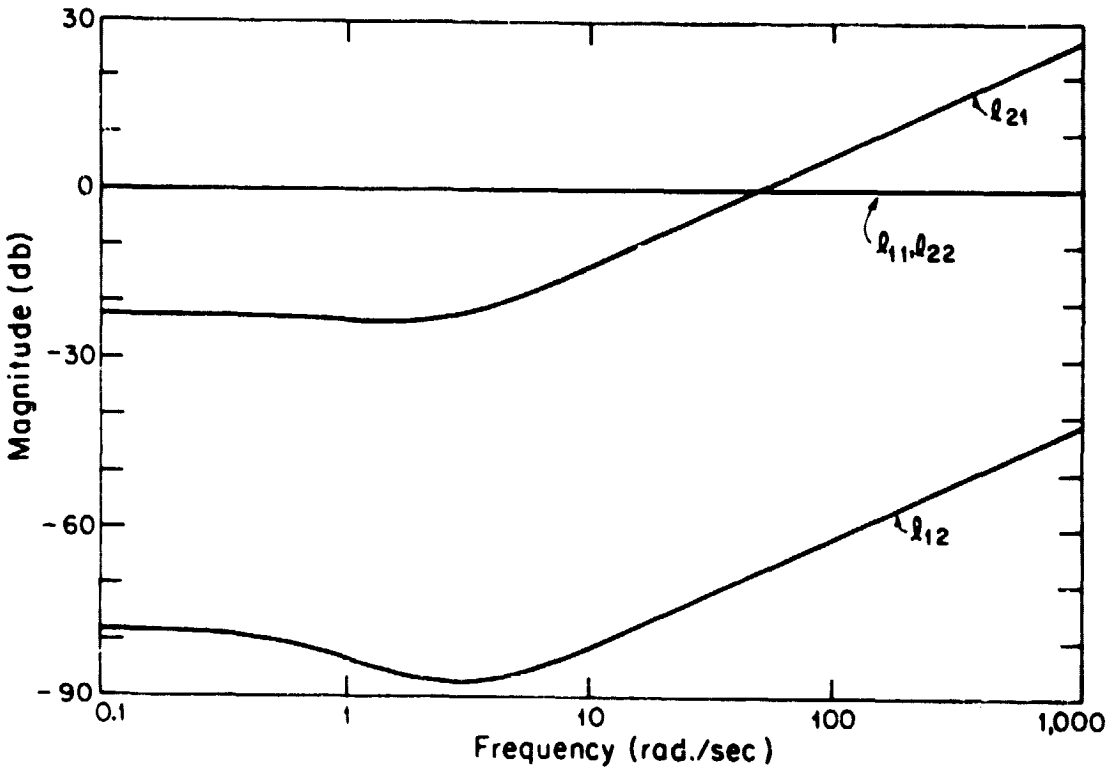

Fig. 17: Magnitude Bode-like plots of elements of $L(j\omega)$ for worst model error.

associated with $\sigma_{min}[I+G(j1000)]$ is approximately given by

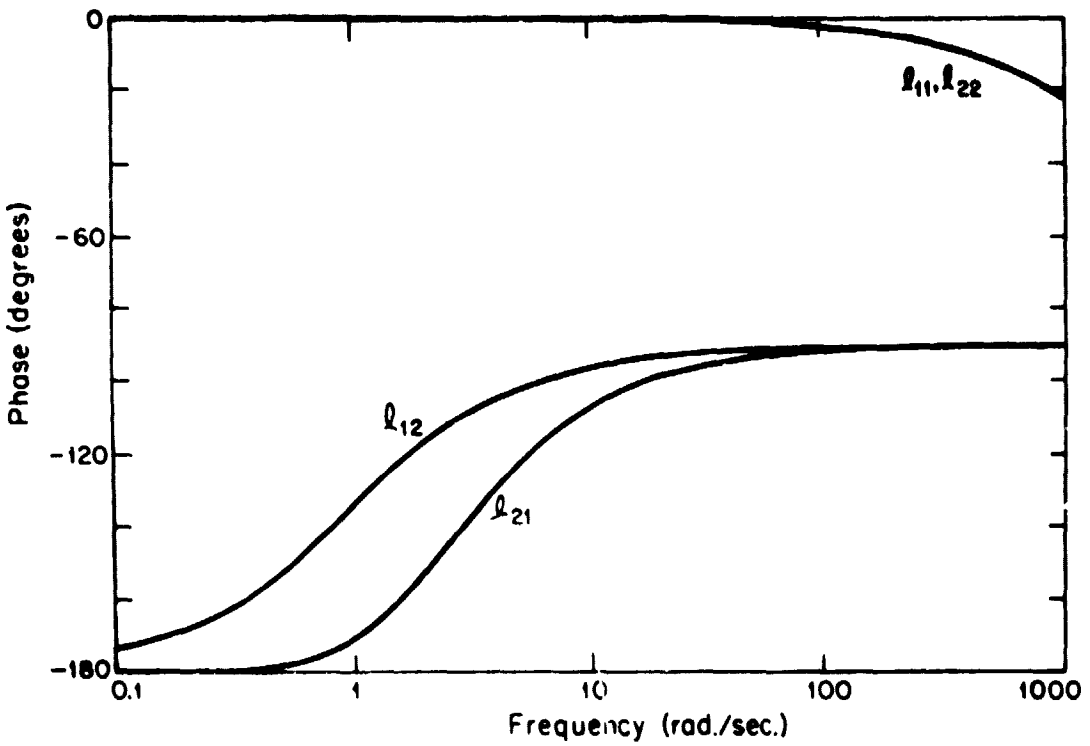

Fig. 18: Phase Bode-like plots of elements of $L(j\omega)$ for worst model error.

$$L(j1000) \simeq \begin{bmatrix} 30 & 30e^{j(100°)} \\ 30e^{-j(100°)} & 30 \end{bmatrix} \tag{52}$$

and $L(j1000)$ associated with $\sigma_{min}[I+G^{-1}(j1000)]$ is approximately given by

$$L(j1000) \simeq \begin{bmatrix} e^{-j(20°)} & 0.03e^{-j(90°)} \\ 30e^{-j(90°)} & e^{-j(20°)} \end{bmatrix}. \tag{53}$$

Thus, as the tolerable error becomes larger as $\sigma_{min}[I+G(j\omega)]$ and $\sigma_{min}[I+G^{-1}(j\omega)]$ become larger (as shown in Figs. 13 and 16 respectively), the type of errors that the different error criteria characterize may be rather different as (52) and (53) indicate. When both $\sigma_{min}[I+G(j\omega)]$ $\sigma_{min}[I+G^{-1}(j\omega)]$ are sufficiently small the different error criteria guard against the same type of model error or equivalently $L(j\omega)$ as shown by this example. This means that either test using $\sigma_{min}[I+G(j\omega)]$ or $\sigma_{min}[I+G^{-1}(j\omega)]$ will detect the near instability of a control system. However, they may give rather different estimates of gain and phase margin when the feedback system will tolerate a class of modelling errors of larger magnitude.

Now consider, the next worst model error for the two error criteria used in this chapter. Thus, the class of modelling errors now considered must exclude the worst model error type just discussed. The model errors now considered will have <u>zero</u> component in the most sensitive direction $\underline{u}_n(j\omega)\underline{v}_n^H(j\omega)$, (i.e., $\underline{u}_n^H(j\omega)E(j\omega)\underline{v}_n(j\omega)=0$).

For the $[\tilde{G}^{-1}-G^{-1}]G$ error criterion we may again draw Dode-like plots of $L(j\omega)$ that corresponds to the $[\sigma_{min}\sigma_{max}]^{1/2}$ error magnitude in Fig. 13. This is shown in Figs. 19 and 20 where the off-diagonal elements of $L(j\ )$ are not plotted because their magnitudes are insignificant.

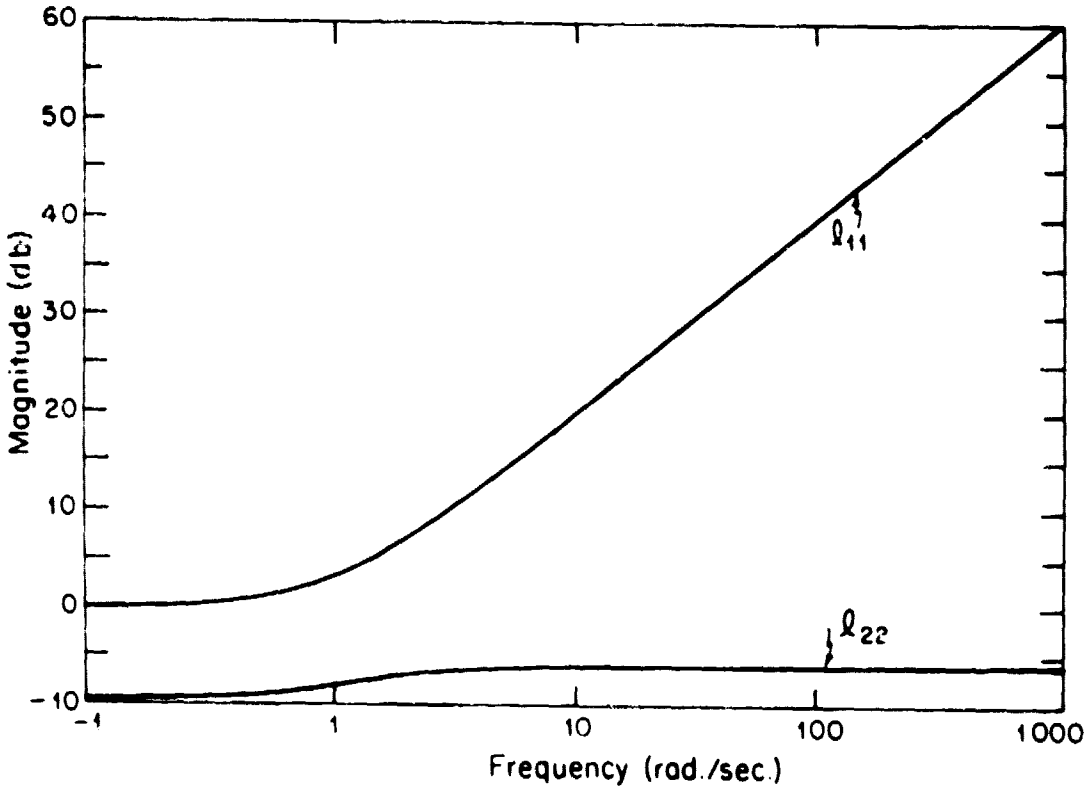

Fig. 19: Magnitude Bode-like plot of elements of $L(j\omega)$ for next worst error.

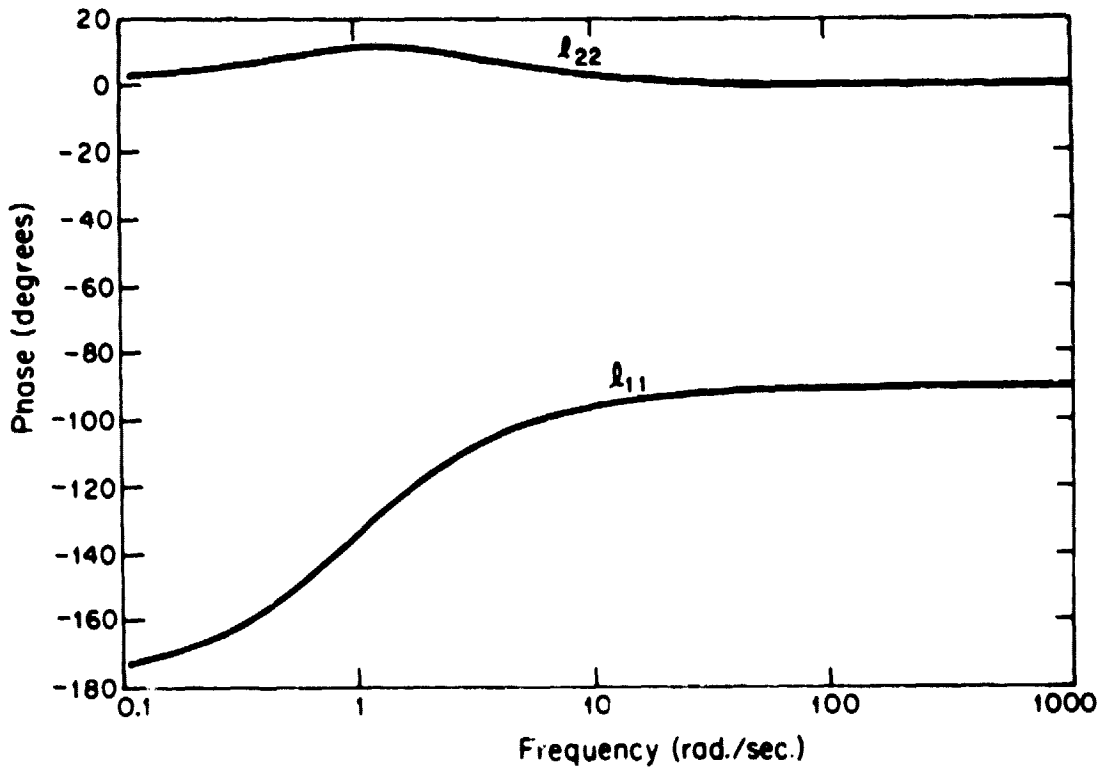

Fig. 20: Phase Bode-like plots of elements of $L(j\omega)$ for next worst error.

Recall that the error matrix $E(j\omega)$ for the next worst error is specified by (13) where $\theta(j\omega)$ is arbitrary but real. In Figs. 19 and 20, $\theta(j\omega)$ has been set to zero in order to calculate a single $L(j\omega)$. From Figs. 19 and 20, it is clear that the next worst type of error is to

simply reduce the gain in one feedback channel and increase it in the other while changing the phase of both channels. Here crossfeeds between the feedback channels play no essential role. The plots analogous to Figs. 19 and 20 are given in Figs. 21 and 22 for the error criterion $E=G^{-1}[\tilde{G}-G]=L-I$ where again the off-diagonal elements of $L(j\omega)$ are insignificant.

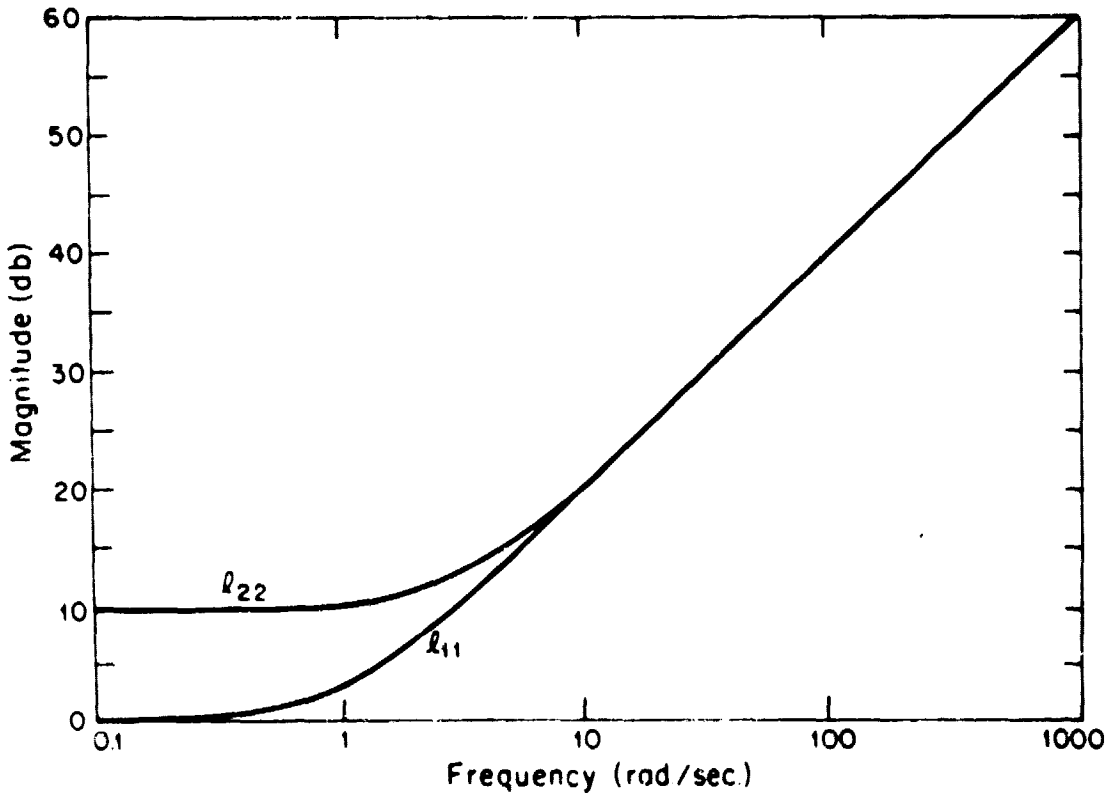

Fig. 21: Magnitude Bode-like plots of elements of $L(j\omega)$ for next worst error.

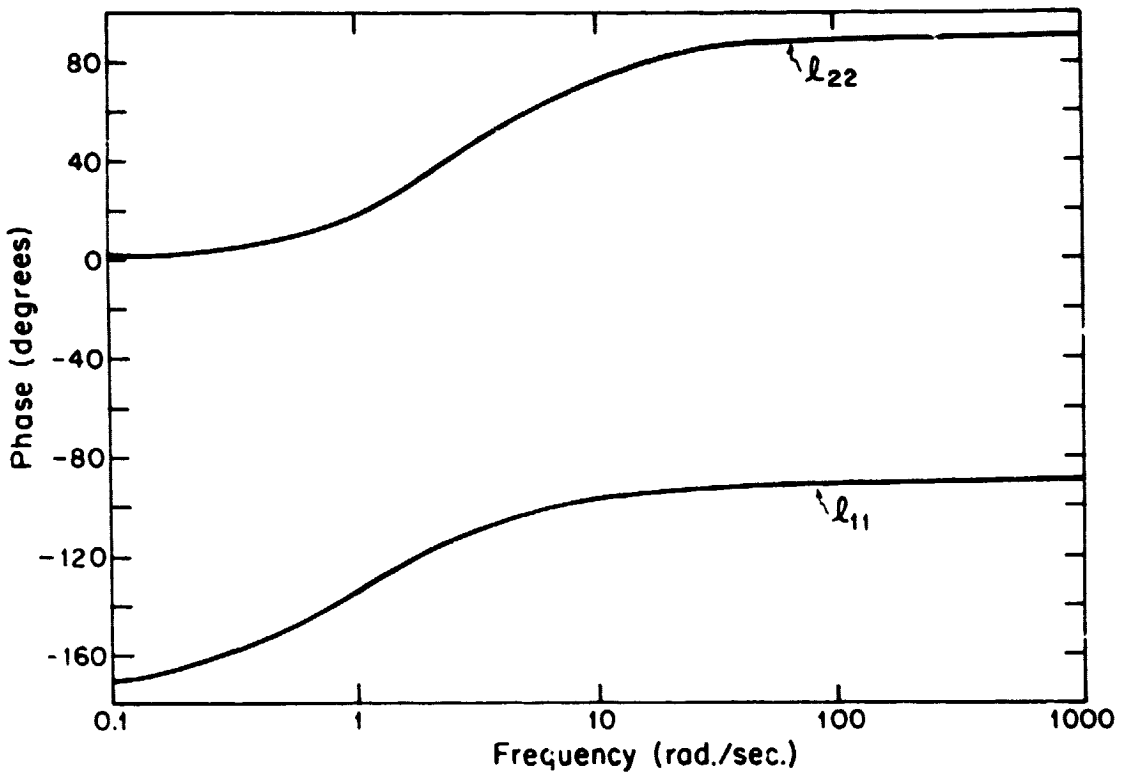

Fig. 22: Phase Bode-like plots of elements of $L(j\omega)$ for next worst error.

Note that in this case, $L(j\omega)$ increases the gain in both feedback channels while changing the phase of both channels. Thus, once more, we see from Figs. 19-22 that the model error, or $L(j\omega)$, the criteria guard against are essentially different.

C-3

4.5 Improving Robustness Tests by Combining Tests

It has been demonstrated in this chapter that the usefulness of the various robustness tests of chapter 3 can be extended by restricting the class of allowable model errors so that the error structure is exploited. In this section, it is shown that the usefulness of the robustness tests can be extended by a combination of two tests forming a single hybrid test. This effectively enlarges the class of allowable model errors and, therefore, in certain circumstances the stability of the feedback system may be confirmed when either test alone would fail to be conclusive.

The basic idea is to use tests that employ the same $G(s,\theta)$ in their proof via Theorem 3.2; one uses one test for a certain subset of frequencies and uses the other test for the remaining frequencies. The reason that this procedure works is that both tests guarantee exactly the same thing, that $I+G(s,\theta)$ is nonsingular for all θ in $[0,1]$ for any s in their respective subsets. Let D_R, the Nyquist contour of Fig. 3.10, be decomposed into two subsets D_{1R} and D_{2R} whose union is D_R and let TEST1 and TEST2 denote any of the tests bounding the model error magnitude in the theorems of chapters 3 and 4 that employ the same $G(s,\theta)$ in their proof. Then the following theorem may be stated.

Theorem 4: The polynomial $\tilde{\phi}_{CL}(s)$ has no CRHP zeros and hence the perturbed feedback system is stable if the following conditions hold:

1. Condition 1 of Theorem 3.2 holds
2. $D_R = D_{1R} \cup D_{2R}$
3. TEST1 implies $I+G(s,\epsilon)$ is nonsingular on $D_{1R} x [0,1]$
4. TEST2 implies $I+G(s,\epsilon)$ is nonsingular on $D_{2R} x [0,1]$

Proof: Condition 2, 3 and 4 guarantee condition 2 of Theorem 3.2 and therefore by Theorem 3.2, $\tilde{\phi}_{CL}(s)$ has no CRHP zeros. Q.E.D.

Theorem 4 allows us to combine tests that employ both absolute and relative error measures as well as tests that utilize model error structure and those that do not, provided they can work with the same $I+G(s,\epsilon)$. Even in the case where the tests were originally derived by use of different $G(s,\epsilon)$ matrices it is sometimes possible to find a single $G(s,\epsilon)$ from which versions of the original tests may be derived via Theorem 3.2. For example, a version of Theorem 3.6 is derived in [51] by use of the $G(s,\epsilon) = (1-\epsilon)G(s) + \epsilon\tilde{G}(s)$ which is used in the derivation of Theorem 3.4.

This version of Theorem 3.6 requires more complicated conditions on the allowable L(s) than the eigenvalue restrictions on L(s) in the present Theorem 3.6. However, these more complicated conditions are

automatically satisfied provided $\sigma_{max}(L^{-1}(s)-I) \leq 1$. Therefore, under this restriction on L(s), Theorem 3.4 may be used on D_{1R} and Theorem 3.6 on D_{2R} to prove the stability of the feedback system under variations in the system model G(s).

Example 2: To show how tests may be combined reconsider the example of section 4.2 where G(s) is given by

$$G(s) = \begin{bmatrix} \frac{1}{s+7.5} & 0 \\ 0 & \frac{1}{s+0.5} \end{bmatrix} \tag{54}$$

and where we use the same constraints on the model given in (22), (23),(24) and (25). Notice from (26) that

$$\sigma_{max}(E(j\omega)) \leq 2.5 \tag{55}$$

and that from (20) for all $\omega \geq 1$

$$\sigma_{min}(I+G^{-1}(j\omega)) = |1.5+j\omega| > 2.5 \geq \sigma_{max}(E(j\omega)). \tag{56}$$

Therefore we could use Theorem 2 for all $\omega \leq 1$ and Theorem 3.4 which employs the test in (56) for all $\omega > 1$ to ensure the stability of the feedback system.

Obviously, the division of the frequency axis could be carried out for n different tests which divide the frequency axis into the n subsets whose union is the whole frequency axis. In fact, as n becomes large this suggests that a single test that depends continuously on s could be devised. This was mentioned before in the context

of separating functions whose coefficients themselves could be transfer functions of s (see section 3.9).

4.6 Computational Considerations [19,49,53]

In this section, we discuss a few key relationships between the nominal closed-loop system, denoted by $G_{CL}(s)$, and the quantities involved in computing bounds on the allowable model error and the most significant error structures considered in this chapter.

We first make the simple observation that if the SVD of a square matrix A is given by

$$A = U\Sigma V^H \tag{57}$$

then the SVD of A^{-1} (assuming it exists) is given by

$$A^{-1} = V\,\Sigma^{-1}\,U^H \quad . \tag{58}$$

This relationship between the SVD's of A and A^{-1} is useful when the quantities $\sigma_{min}(I+G)$, $\sigma_{min}(I+G^{-1})$ and $\sigma_{min}[(I+G)(I-G)^{-1}]$, used in Theorems 3.4, 3.6 and 3.9, are required. The relationship between these quantities can be determined from the following equations:

$$G_{CL}^{-1} = (I+G^{-1}) \tag{59}$$

$$(G_{CL}-1/2I)^{-1} = -2(I+G)(I-G)^{-1} \tag{60}$$

$$(G_{CL}-I)^{-1} = -(I+G) \tag{61}$$

where the nominal closed-loop system G_{CL} is given by

$$G_{CL} = G(I+G)^{-1} \quad . \tag{62}$$

Thus by calculating the SVD's of $G_{CL}-\alpha I$ for $\alpha=0$, $\alpha=1/2$ and $\alpha=1$ one can easily obtain via (59), (60) and (61) the SVD's of $I+G$, $I+G^{-1}$ and $(I-G)^{-1}(I+G)$. This is significant since G_{CL} need only be calculated once for the three SVD's; also, no explicit inversion of G or I-G is needed since if

$$G(s) = C(Is-A)^{-1}B \tag{63}$$

then $G_{CL}(s)$ is given by

$$G_{CL}(s) = C(Is-A+BC)^{-1}B \tag{64}$$

Another computational saving can be realized if only approximations to the minimum and maximum singular values of a matrix and not its full SVD are required. Recall from (2.38) and (2.39) that $\sigma_{min}(A)$ and $\sigma_{max}(A)$ are given by

$$\sigma_{min}(A) = ||A^{-1}||_2^{-1} \tag{65}$$

and

$$\sigma_{max}(A) = ||A||_2 \quad . \tag{66}$$

Using matrix linear algebra, it can be shown that

$$\frac{1}{\sqrt{n}} ||A||_1 \leq ||A||_2 \leq \sqrt{n}\, ||A||_1 \tag{67}$$

and

$$\frac{1}{\sqrt{n}} ||A||_\infty \leq ||A||_2 \leq \sqrt{n}\, ||A||_\infty \tag{68}$$

if A is an nxn matrix. Since the matrix norms $||A||_1$ and $||A||_\infty$ are much cheaper to compute than $||A||_2$, the singular value quantities $\sigma_{min}(I+G)$, $\sigma_{min}(I+G^{-1})$ and $\sigma_{min}[(I+G)(I-G)^{-1}]$ may be approximated by

$$\sigma_{min}(I+G) = ||G_{CL}-I||_2^{-1} \simeq ||G_{CL}-I||_i^{-1} \tag{69}$$

$$\sigma_{min}(I+G^{-1}) = ||G_{CL}||_2^{-1} \simeq ||G_{CL}||_i^{-1} \tag{70}$$

$$\sigma_{min}[(I-G)^{-1}(I+G)] = \frac{1}{2} ||G_{CL}-1/2I||_2^{-1} \simeq \frac{1}{2} ||G_{CL}-1/2I||_i^{-1} \tag{71}$$

within the bounds given by (67) and (68) when i=1 or ∞, for computational savings. Note that as n increases these approximations may be poor. However, all the robustness theorems of chapter 3 can be formulated using the 1 or ∞ norms rather than the 2-norm (singular values) and approximations need not be used at all. Nevertheless, the results on the structure of model errors are only applicable in the case of the spectral or 2-norm.

4.7 Concluding Remarks

In this chapter we have shown how the structure of the model error may be used to improve the theorems of chapter 3. The nature of the worst model error was explored through the use of block diagrams showing that it is equivalent to additional positive feedback

in the input/output directions $\underline{u}_n(j\omega_0)$ and $\underline{v}_n(j\omega_0)$. The example of section 3.3 was used to illustrate that the nature of the smallest destabilizing error can be obtained from Bode-like plots of $L(j\omega)$. Also improving robustness tests by combining different robustness test over different frequency ranges was discussed as well as computational considerations for the efficient computation of quantities required by the robustness tests of this chapter and those of chapter 3.

To place these results in perspective, a design/analysis procedure is suggested. This procedure assumes that some particular synthesis procedure, such as the LQG methodology, is used to obtain specific controller designs. An outline of the procedure is the following sequence of steps:

1. Obtain an initial controller design that meets basic performance requirements but does not produce a controller with a bandwidth larger than the upper frequency limit for which the model is valid.

2. Obtain an estimate on the allowable model error magnitude as a function of frequency and compare with the values of σ_{min} of $I+G$ or $I+G^{-1}$.

2.1. If the model error magnitude is less than σ_{min} of $I+G$ or $I+G^{-1}$, stop.

2.2. If the model error magnitude is larger than σ_{min} of $I+G$ or $I+G^{-1}$ then go to step 2.2.1.

2.2.1. Calculate the worst model error and check to see if this error could possibly occur. If not go to step 2.2.1.1 otherwise go to step 2.2.1.2.

2.2.1.1 Calculate the magnitude of the next worst error. If the model error magnitude in step 2 is less than this, stop. If not, compute the magnitude of the "next worst error" and continue with a step similar to 2.2.1 etc. (this gets rather tedious!).

2.2.1.2 Try to improve model to reduce model error or change controller design. Return to step 1.

Exactly how to change the model to reduce model error based on the analysis methods of this chapter is an open research question. Also, it is not always clear how changes in controller design may affect the quantities $\sigma_{min}(I+G)$ and $\sigma_{min}(I+G^{-1})$. This is also an open research problem. However, in spite of these difficulties (which in the author's opinion may eventually be adequately circumvented) the key to making practical use of the results of this chapter depends on the engineer's ability to determine whether the model error magnitude in the most sensitive direction, i.e., the projection magnitude $|\langle \underline{u}_n(j\omega)\underline{v}_n^H(j\omega), \Sigma(j\omega)\rangle|$, can be bounded. Clearly, engineering judgement is necesarry; however, this engineering judgement may not easily translate into this type of bound. Thus, practical experience in

obtaining these type of bounds is necessary in order to further improve the type of robustness tests that are appropriate for the kinds of knowledge about model uncertainty that the designer has at his disposal.

5. ROBUSTNESS AND LQG CONTROL SYSTEMS

5.1 Introduction

The previous two chapters dealt with a loop transfer matrix G(s) that contained compensation as well as open-loop plant dynamics. The robustness results of these chapters hold independent of the MIMO design methodology used to determine the compensation required.

This chapter will be concerned with deriving robustness result for feedback control systems designed using the linear-quadratic-gaussian (LQG) design methodology [41]. This includes results for the linear-quadratic (LQ) state feedback regulator and some of its variations as well as the LQG regulator. The multivariable version of Kalman's inequality and Theorem 3.6 form the basis for the derivation of these results.

In section 5.2, the LQ and LQG control problems are stated for completeness and the definition of the loop-transfer matrices for the feedback systems is given. Section 5.3 continues with a discussion of the multivariable Kalman inequality derived from the Riccati equation. The stability margins for LQ regulators is then discussed in section 5.4 where it is shown that these regulators have guaranteed minimum stability margins which makes them attractive and that the control weighting R matrix determines the coordinate system in which these stability margins hold. Stability margins for the state feedback regulator, whose feedback gain is determined by a Lyapunov or a nonstandard parameterized Riccati equation, are also given. Section 5.5 concludes with a discussion of the stability margins for LQG regulators. It is shown that stability margins for LQG regulators are the same as those for LQ state feedback regulators but

only at a point inside the LQG compensator. These margins cannot be automatically guaranteed at the physical input or output of the plant unless the Kalman filter of the LQG compensator has an exact model of the perturbed open-loop plant, a very restrictive assumption. However, robustness recovery procedures [35, 36] are discussed that allow a properly designed LQG control system to asymptotically recover the LQ state feedback stability margins at the input or output to the physical plant provided that the plant is minimum phase. The significance of having margins at various points in the feedback loop is also discussed with reference to modelling error characterization.

Some of the results of this chapter have appeared previously in the literature. Based upon the preliminary gain margin results in Wong and Athans [27], Safonov and Athans [25] gave the definitive treatment of guaranteed minimum multiloop stability margins for the LQ state-feedback regulator allowing for nonlinear perturbations in the feedback loop. It was later shown by Doyle [33] that there are no guaranteed minimum stability margins for LQG regulators. Kwakernaak [36], and Doyle and Stein [35] have outlined procedures whereby the LQG regulators may asymptotically recover the LQ regulator guaranteed margins.

The contributions of this chapter are mainly the simplified derivation and characterization of LQ regulator stability margins. The structure (diagonal vs. nondiagonal) of the control weighting R matrix is shown to have important impact on the stability margins. If R is nondiagonal the LQ regulator may have arbitrarily small gain margins If R is not a multiple of the identity matrix it is shown that ability to tolerate

crossfeed perturbations is drastically reduced. Those results also apply to the variations of the LQ regulators discussed in Section 5.4. Also, in section 5.5 an inequality is derived that ensures that stability margins will apply at both the input and output of the physical plant.

5.2 The LQ and LQG Regulators

For the sake of completeness, the LQ and LQG regulator problems and their solution will be given for the linear-time-invariant, infinite time horizon case [41].

5.2.1 LQ Regulator Problem

For the open-loop plant given by

$$\dot{\underline{x}}(t) = A\underline{x}(t) + B\underline{u}(t) \tag{1}$$

find the optimal control $\underline{u}^*(t)$ that minimizes the quadratic cost functional $J(\underline{u})$ given by

$$J(\underline{u}) = \int_0^\infty [\underline{x}^T(t)Q\underline{x}(t) + \underline{u}^T(t)R\underline{u}(t)]dt \tag{2}$$

where $Q \geq 0$, $R > 0$, $[A,B]$ is stabilizable and $[A, Q^{1/2}]$ is detectable. The optimal control $\underline{u}^*(t)$ is given by

$$\underline{u}^*(t) = -R^{-1}B^T K\, \underline{x}(t) \tag{3}$$

where $K \geq 0$ satisfies the algebraic Riccati equation

$$A^T K + KA + Q - KBR^{-1}B^T K = 0. \tag{4}$$

The block diagram of this regulator control system is shown in Fig. 1.

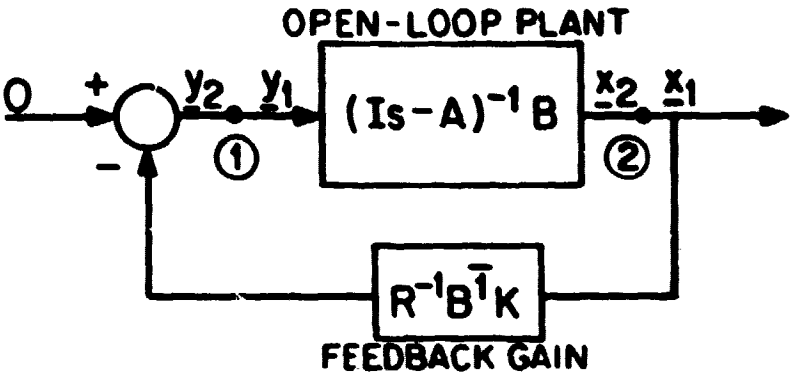

Fig. 1: LQ Regulator

To calculate the loop transfer matrix G(s) at the input to the plant, we break the loop at point (1) in Fig. 1 so that now $\underline{u}_1$ and $\underline{u}_2$ are no longer equal. Next we calculate the transfer function matrix from $\underline{u}_1$ to $-\underline{u}_2$. This is G(s), the loop transfer matrix at the plant input and is given by

$$G(s) = R^{-1}B^TK(Is-A)^{-1}B \tag{5}$$

To calculate the loop transfer matrix at the output of the plant (at point (2) of Fig. 1) we follow an analogous procedure. We break the loop at point (2) of Fig. 1 and calculate the transfer function matrix from $\underline{x}_1$ to $-\underline{x}_2$ which is given by

$$-\underline{x}_2(s) = (Is-A)^{-1}B\ R^{-1}B^TK\ \underline{x}_1(s) \quad . \tag{6}$$

Thus $(Is-A)^{-1}BR^{-1}B^{T}K$ is the loop transfer matrix at the output of the plant.

In general, if $G_p(s)$ denotes an open-loop plant with input $\underline{u}(s)$ and output $\underline{y}(s)$ and $\underline{u}(s) = -G_c(s)\underline{y}(s)$ where $G_c(s)$ represents the transfer matrix of a compensator, we call $G_c(s)G_p(s)$ the loop transfer matrix at the input and $G_p(s)G_c(s)$ the loop transfer matrix at the output.

5.2.2 LQG Regulator Problem

Let the stabilizable, detectable open-loop plant be given by

$$\dot{\underline{x}}(t) = A\underline{x}(t) + B\underline{u}(t) + \underline{\xi}(t) \tag{7}$$

$$\underline{y}(t) = C\underline{x}(t) + \underline{\theta}(t) \tag{8}$$

where the noises $\underline{\xi}(t)$ and $\underline{\theta}(t)$ are both Gaussian, white, zero mean, mutually independent and stationary with

$$E[\underline{\xi}(t)\underline{\xi}^{T}(\tau)] = \Xi\,\delta(t-\tau);\quad \Xi \geq 0 \tag{9}$$

$$E[\underline{\theta}(t)\theta^{T}(\tau)] = \Theta\,\delta(t-\tau);\quad \Theta > 0\quad . \tag{10}$$

Find the optimal feedback control $\underline{u}^*(t)$ depending causally on $\underline{y}(t)$ that minimizes the quadratic cost functional $J(\underline{u})$ given by

$$J(\underline{u}) = \lim_{T\to\infty} \frac{1}{T} \int_0^T [\underline{x}^{T}(t)Qx(t) + \underline{u}^{T}(t)R\underline{u}(t)]dt \tag{11}$$

where $Q \geq 0$ and $R > 0$. The optimal control $\underline{u}^*(t)$ is given by

$$\underline{u}^*(t) = -G_r\hat{\underline{x}}(t) \tag{12}$$

where $\hat{\underline{x}}(t)$ the state estimate is generated by the Kalman filter

$$\dot{\hat{\underline{x}}}(t) = A\hat{\underline{x}}(t) + B\underline{u}^*(t) + G_e[\underline{y}(t) - C\hat{\underline{x}}(t)] \tag{13}$$

or equivalently

$$\dot{\underline{\hat{x}}}(t) = [A - BG_r - G_f C]\underline{\hat{x}}(t) + G_f \underline{y}(t) \tag{14}$$

with G_r and G_f being given by

$$G_r = R^{-1}B^T K \tag{15}$$

$$G_f = \Sigma C^T \Theta^{-1} \tag{16}$$

with $[A, Q^{1/2}]$ detectable, $[A, \Xi^{1/2}]$ stabilizable, $K \geq 0$ satisfying

$$A^T K + KA + Q - KBR^{-1}B^T K = 0 \tag{17}$$

and $\Sigma \geq 0$ satisfying

$$A\Sigma + \Sigma A^T + \Xi - \Sigma C^T \Theta^{-1} C \Sigma = 0 \ . \tag{18}$$

From (12) and (14) we see that the transfer function matrix from $\underline{y}(s)$ to $\underline{u}(s)$ is given by

$$\underline{u}^*(s) = -[G_r(Is - A + BG_r + G_f C)^{-1} G_f]\underline{y}(s) \tag{19}$$

and thus the block diagram of the LQG regulator is given by Fig. 2.

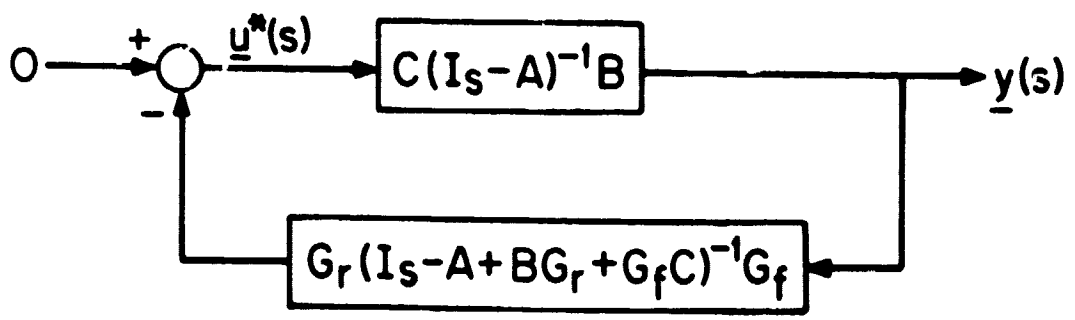

Fig. 2: LQG Regulator

From Fig. 2, we see that the loop transfer matrix at the input, G(s), is given by

$$G(s) = G_c(Is-A + BG_r + G_fC)^{-1}G_fC(Is - A)^{-1}B \ . \qquad (20)$$

5.3 Multivariable Kalman Inequality

The subject of qualitative feedback properties of LQ control systems is not a new one. An early and fundamental paper by Kalman [21] detailed properties shared by all LQ regulators in the single-input case. Kalman showed that the scalar return difference transfer function of a single-input LQ state feedback regulator satisfies the inequality

$$|1+g(j\omega)| \geq 1 \ ; \qquad \text{for all } \omega \ . \qquad (21)$$

This is both a classical condition for the reduction of sensitivity at the feedback input to the system (see, e.g., [19]) as well as necessary and sufficient for a (stable) state feedback regulator to be optimal with respect to some quadratic cost index. By inspection of the Nyquist diagram corresponding to (21), (Fig. 3 with β=1), it is straightforward to observe [22, pp. 70-76] that a SISO LQ state feedback regulator has a guaranteed infinite upward gain margin, at least a 50% gain reduction margin and also a guaranteed minimum phase margin of $\pm$ 60°. (These margins were defined in Section 3.7).

Anderson [23] developed a multivariable version of condition (21) as a property of LQ state-feedback regulators; a similar generalized condition arises in sensitivity theory[1] (see, e.g., Cruz and Perkins [24]). In this

[1] Sensitivity refers to the variation in system responses due to infinitesimal changes in the nominal system parameters. Robustness refers to the delineation of finite regions of allowable variation in nominal system parameters that preserve stability.

chapter we will exploit the multivariable form of (21) together with the results of Chapter 3 to establish the stability margin properties of LQ and LQG optimal regulators.

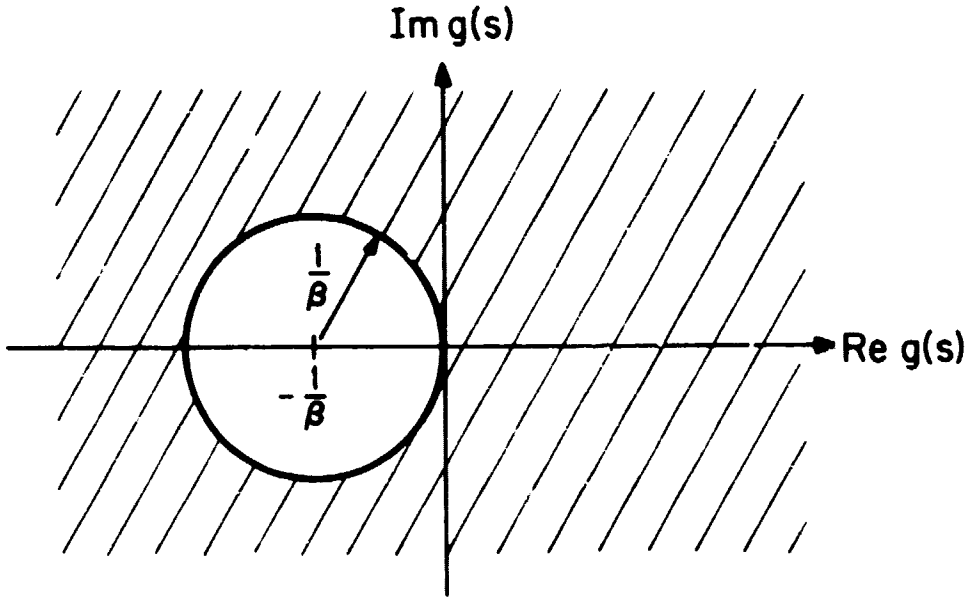

Fig. 3: Set (cross-hatched region) of allowable values of g(s) when $|1+\beta g(s)| > 1$.

We will need a precise statement of the multivariable LQ version of condition (21) in the sequel, and this is provided by the following theorem. The proof is by straightforward manipulation of the algebraic Riccati equation is included, for completeness.

For convenience we will assume that in all remaining theorems and corollaries that the Nyquist contour D_R of Fig. 3.10 is chosen with R sufficiently large so that the theorems of Chapter 3 may be applied.

Theorem 1 (LQ Kalman Inequality): If the matrix K satisfies the matrix algebraic Riccati equation

$$A^T K + KA + Q - KBR^{-1}B^T K = 0 \tag{22}$$

with $R > 0$ and $Q \geq 0$ then

$$(I+G(s))^H R(I+G(s)) = R + H(s) \tag{23}$$

where

$$G(s) = R^{-1}B^T K(Is-A)^{-1}B \tag{24}$$

$$H(s) = [(Is-A)^{-1}B]^H (Q + 2Re(s)K)[(Is-A)^{-1}B] \quad . \tag{25}$$

Furthermore, If $Q > 0$, B has full rank and $K \geq 0$ then (23) implies that

$$(I+G(s))^H R(I+G(s)) > R, \qquad s \in D_R \tag{26}$$

Alternatively, if $\det(j\omega I-A) \neq 0$, for all ω, and $K \geq 0$ then (23) implies that

$$(I+G(s))^H R(I+G(s)) \geq R, \qquad s \in D_R \quad . \tag{27}$$

Proof: Direct manipulation of (22) gives

$$(s^*I-A^T)K + K(sI-A) + KBR^{-1}B^T K = (Q + 2Re(s)K) \tag{28}$$

where s^* denotes the complex conjugate of s. Premultiplying and post-mulitplying (28) by $[(sI-A)^{-1}B]^H$ and $[(sI-A)^{-1}B]$ respectively we obtain

$$RG(s) + G^H(s)R + G^H(s)RG(s) = H(s) \tag{29}$$

Adding R to both sides of (29) gives (23). Now $Q + 2Re(s)K$ will be positive semidefinite for $s \in D_R$ if $Q > 0$ and the indentations of Ω_R are sufficiently small or if $Re(s) \geq 0$, $s \in D_R$ which happens if $\det(j\omega I - A) \neq 0$ for all ω. Thus under these conditions $H(s) > 0$ or $H(s) \geq 0$ respectively for all $s \in D_R$.

Q.E.D.

It is important to point out that this theorem uses $G^H(s)$ rather than $G^T(-s)$ as in [23]. These two quantities are the same when $s = j\omega$, but are different when $Re(s) \neq 0$. This is the case when s is evaluated along the Nyquist D_R contour and this contour is indented along the imaginary axis (Fig. 3.10). It is necessary to use $G^H(s)$ in order to apply the theorems of Chapter 3. Note, however, that when $\det(j\omega I - A) \neq 0$, for all ω, (i.e., when the open-loop system has no poles on the $j\omega$-axis), that Ω_R is just the imaginary axis from -jR to jR. In this case (27) could be written as

$$(I+G(j\omega))^H R(I+G(j\omega)) \geq R; \qquad \text{for all } \omega, \tag{30}$$

which is the previously mentioned multivariable generalization of condition (21).

5.4 Stability Margins of LQ Regulators

We can now employ Theorem 1 in conjunction with the results of Theorem 3.6 to establish the robustness properties of multivariable LQ regulators. Recall from Theorem 3.6 that one of the key quantities for multivariable robustness analysis is the minimum singular value $\sigma_{min}(I+G(s))$,

where G(s) is the loop transfer matrix. Unfortunately, the inequalities (26) and (27) of Theorem 1 do <u>not</u> provide a bound on $\sigma_{min}(I+G(s))$, where G(s) is the LQ regulator loop transfer matrix defined by (24). However, if we define

$$\hat{G}(s) = R^{\frac{1}{2}}G(s)R^{-\frac{1}{2}} \tag{31}$$

then (27) (for example) can be rewritten in the form

$$(I+\hat{G}(s))^{H}(I+\hat{G}(s)) \geq I, \qquad s \in D_R . \tag{32}$$

Equation (32) provides the bound

$$\sigma_{min}(I+\hat{G}(s)) \geq 1, \qquad s \in R_R \tag{33}$$

on the minimum singular value of $I+\hat{G}(s)$.

To work with $\hat{G}(s)$ instead of G(s), it is necessary to manipulate the system of Fig. 4 into the equivalent (for stability analysis) form depicted in Fig. 5. Then using (26) and (27) together with Theorem 3.6 leads directly to the following result. (Recall from (3.27) that $\tilde{\phi}_{CL}(s) = \det(sI-\tilde{A}+\tilde{B}\tilde{C})$ where $\tilde{G}(s) = \tilde{C}(Is-\tilde{A})^{-1}\tilde{B}$, was used in Theorem 3.2 to determine the stability of the perturbed closed-loop system.)

<u>Theorem 2:</u> The polynomial $\tilde{\phi}_{CL}(s)$ has no CRHP zeroes provided the following conditions are satisfied:

1. (a) $\phi_{CL}(s)$ and $\tilde{\phi}_{0L}(s)$ have the same number of CRHP zeros

   (b) if $\tilde{\phi}_{0L}(j\omega_0) = 0$ the $\phi_{0L}(j\omega_0) = 0$

   (c) $\phi_{CL}(s)$ has no CRHP zeros

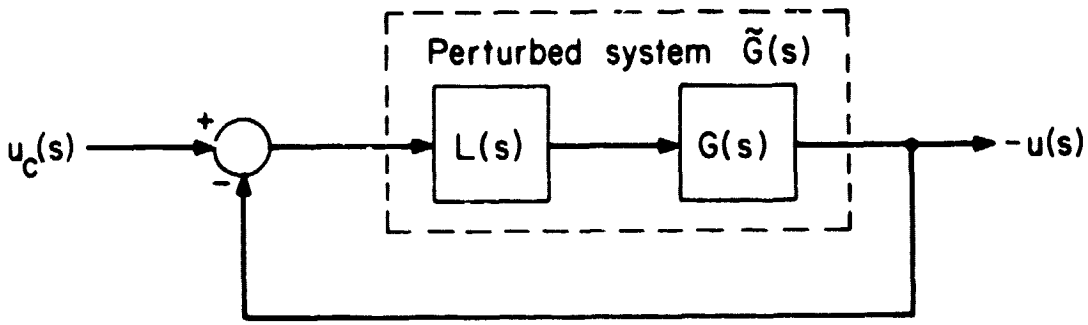

Fig. 4: Feedback system with multiplicative representation of uncertainty in G(s).

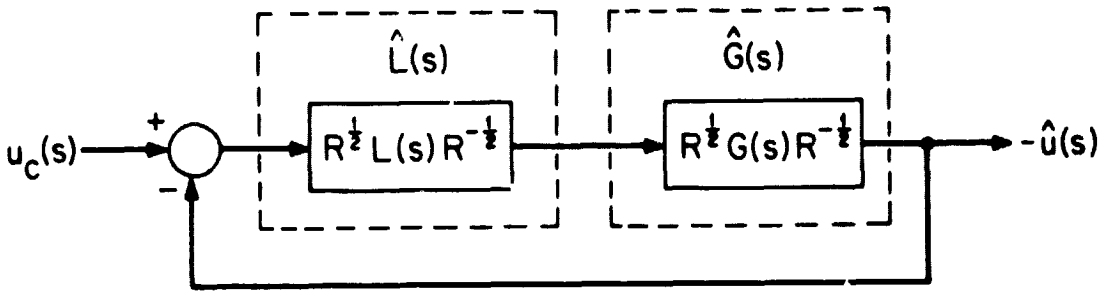

Fig. 5: Feedback system for stability margin derivation (compare Fig. 4).

2. G(s) is specified by (4) where K>0 satisfies (2) and [A,B] is stabilizable, $[A, Q^{\frac{1}{2}}]$ is detectable and B has full rank.

3. With $\gamma(s) \triangleq \sigma_{max}[R^{\frac{1}{2}}L^{-1}(s)R^{-\frac{1}{2}}-I]$ either of the following hold:

   (a) $Q>0$ and $\gamma(s) \leq 1, \quad s \in \Omega_R$

   (b) $\phi_{OL}(j\omega) \neq 0$ for all ω and $\gamma(s) < 1, \quad s \in \Omega_R$.

Proof: It is well-known that condition 2 ensures that $\phi_{CL}(s)$ has no CRHP zeros. Defining $\hat{G}(s) \triangleq R^{\frac{1}{2}}G(s)R^{-\frac{1}{2}}$, we see that G(s) has a state-space realization $[A, BR^{-\frac{1}{2}}, R^{-\frac{1}{2}}B^TK]$ and thus its open- and closed-loop characteristic polynomials $\hat{\phi}_{OL}(s)$ and $\hat{\phi}_{CL}(s)$ are identical to those of $(A,B,R^{-1}B^TK)$. Thus any assumptions about $\phi_{OL}(s)$ and $\phi_{CL}(s)$ obviously apply to $\hat{\phi}_{OL}(s)$ and $\hat{\phi}_{CL}(s)$. Similarly, by defining $\hat{L}(s) \triangleq R^{\frac{1}{2}}L(s)R^{-\frac{1}{2}}$, we may work with $\hat{G}(s)$ and $\hat{L}(s)$ instead of G(s) and L(s). The conditions (26) and (27) of Theorem 1 are equivalent to $\sigma_{min}[1+\hat{G}(s)] > 1$ and $\sigma_{min}(I+\hat{G}(s)) \geq 1$ respectively. The condition 3a and Theorem 1 require that

$$\sigma_{max}(\hat{L}^{-1}(s)-I) \leq 1 < \sigma_{min}(I+\hat{G}(s)), \qquad s \in \Omega_R \tag{34}$$

and by Theorem 3.6 we conclude that $\tilde{\phi}_{CL}(s)$ has no CRHP zeros. Alternatively condition 3b and Theorem 1 require that

$$\sigma_{max}(\hat{L}^{-1}(s)-I) < 1 \leq \sigma_{min}(I+\hat{G}(s)) \tag{35}$$

which again by Theorem 3.6 means $\tilde{\phi}_{CL}(s)$ has no CRHP zeros.

Q.E.D.

Note that the condition $\sigma_{max}(R^{\frac{1}{2}}L^{-1}(s)R^{-\frac{1}{2}}-I) \leq 1$ in condition 3a can be rewritten as

$$RL(s) + L^H(s)R - R \geq 0, \qquad s \in \Omega_R \tag{36}$$

or with $s = j\omega$

$$L(j\omega)R^{-1} + R^{-1}L^H(j\omega) - R^{-1} \geq 0; \quad \text{for all } \omega. \tag{37}$$

The inequality (37) was used by Safonov and Athans [25] to prove the LQ state feedback guaranteed gain and phase margins although their method, of proof is quite different. They implicity assume that $L(j\omega)$ is stable, something which we do not require.

Theorem 2 can now be employed to establish the guaranteed minimum multivariable gain and phase margins associated with LQ regulators.

Important Remark: We emphasize that these margins are guaranteed only if the control weighting matrix R is chosen to be a diagonal matrix; we will subsequently present an example showing that the margins can be made arbitrarily small for an appropriately chosen non-diagonal R matrix.

Corollary 1: The LQ regulator with loop transfer matrix $G(s)$ satisfying (16) with a diagonal $R>0$ has simultaneously in each feedback loop a guaranteed minimum gain and phase margins given by

$$GM \supset [\tfrac{1}{2}, \infty) \tag{38}$$

$$PM \supset [-60°, 60°] \tag{39}$$

if $Q>0$ and

$$GM \supset (\tfrac{1}{2}, \infty) \tag{40}$$

$$PM \supset (-60°, 60°) \tag{41}$$

if $Q \geq 0$ and $\phi_{OL}(j\omega) \neq 0$ for all ω.

Proof: From Theorems 1 and 2 we know if $Q > 0$ then

$$\sigma_{max}(R^{\frac{1}{2}}L^{-1}(s)R^{-\frac{1}{2}}-I) = \sigma_{max}(L^{-1}(s)-I) \leq 1, \qquad s \in \Omega_R \tag{42}$$

satisfying condition 3a when L(s) and R are diagonal. If $\phi_{CL}(j\omega) \neq 0$ for all ω then

$$\sigma_{max}(L^{-1}(s)-I) < 1, \qquad s \in \Omega_R \tag{43}$$

satisfying condition 3b when L(s) and R are diagonal. The remainder of the proof is completely analogous to Corollary 3.2.

Q.E.D.

Note that the margins of Corollary 1 are based on the inequality (42). This inequality will not hold for all $s \in \Omega_R$ for "real world" modelling uncertainties. In the SISO case, this is clearly demonstrated by the physical fact that the phase of $\tilde{g}(j\omega)$ is completely uncertain at high enough frequencies. This means that for some ω_0, $\ell(j\omega_0)$ is real and negative -- that is, there is a 180° phase difference between $g(j\omega_0)$ and $\tilde{g}(j\omega_0)$. If $\ell(j\omega_0)$ is real and negative, then $|\ell^{-1}(j\omega_0) - 1| > 1$ and (42) is violated. This means that a physical system cannot actually have an infinite upward gain margin because its Nyquist diagram always will cross the negative real axis at some sufficiently large frequency.

Results related to Corollary 1 have been derived by various authors [26] - [29]; but the definitive treatment including the multivariable phase margin result is due to Safonov and Athans [25]. The approach of this thesis, based on relatively simple frequency domain arguments, is new.

If R is not diagonal then the guarantees of Corollary 1 do not apply. The following example illustrates that the gain margins may become arbitrarily small.

Example 1:

Consider the LQ regulator specified of Fig. 1 with

$$(A,B,Q^{\frac{1}{2}}) = \left(I_2, \begin{bmatrix} 1 & \beta \\ 0 & 1 \end{bmatrix}, I_2\right) \tag{44}$$

where I_2 is the 2x2 identity matrix and $R > 0$ is a nondiagonal control-weighting matrix given by

$$R = B^T[K^{-2}+2K^{-1}]^{-1}B \ , \tag{45}$$

where $K>0$ is arbitrary. By section of R in (45), K satisfies (2). Now let the muliplicative perturbation $L(s)$ be given by the constant matrix L where

$$L = \begin{bmatrix} 1 & 0 \\ 0 & 1+\epsilon \end{bmatrix} \tag{46}$$

and $\epsilon \neq 0$ is arbitrary. The zeros of $\tilde{\phi}_{CL}(s)$ are the eigenvalues of the perturbed closed-loop system matrix $\tilde{A}_{CL}$ where

$$\tilde{A}_{CL} = A-BLB^{-1}(2I+K^{-1}) \tag{47}$$

or

$$\tilde{A}_{CL} = -\begin{bmatrix} (p_1+2) + \beta\,\epsilon\, p_2 - 1 & p_2 + \beta\,\epsilon\,(p_3+2) \\ (1+\epsilon)p_2 & (1+\epsilon)(p_3+2) - 1 \end{bmatrix} \tag{48}$$

where we have let K^{-1} be denoted by

$$K^{-1} = \begin{bmatrix} p_1 & p_2 \\ p_2 & p_3 \end{bmatrix} \tag{49}$$

For $\tilde{A}_{CL}$ to have no CRHP eigenvalues it is necessary for tr $\tilde{A}_{CL} < 0$. However, by inspection of (48), if $p_2 \neq 0$ then for any $\epsilon \neq 0$ there exists a β that will make tr $\tilde{A}_{CL} > 0$ and therefore for arbitrarily small ϵ, the perturbed closed-loop system will be unstable. Thus an LQ design can have an arbitrarily small gain margin.

The basic problem explosed this example is that the margins are really guaranteed at a different point in the loop than where we would like. This is illustrated in Fig. 6 where the perturbation $\hat{L}(s)$ is inserted at point (1). When $\hat{L}(s)$ is diagonal, as when calculating gain and phase margins, and R is also diagonal then $R^{-\frac{1}{2}}$ and $\hat{L}(s)$ commute and points (1) and (2) have identical guaranteed gain and phase margins. Point (2) is where it is important to have margins (i.e , at the input to the physical plant), not inside the compensator at point (1). If R is not diagonal and $||R^{-\frac{1}{2}}||_2||R^{\frac{1}{2}}||_2 >> 1$, a "small" perturbation at point (2) may look like a "large" perturbation at point (1) because of the amplifying effect of the nondiagonal R matrix scaling.

Returning to Example 3.1 of the Chapter 3 once more, an LQ feedback control law is given that has the same closed-loop poles as before,

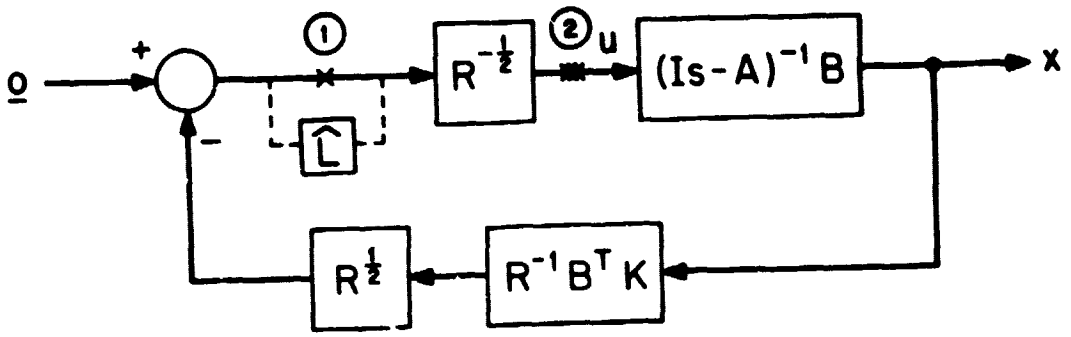

Fig. 6. LQ regulator with margins guaranteed at point ① for an R > 0 and at both ① and ② for diagonal R > 0.

but avoids the near instability associated with the negative identity feedback. This example shows that with R=I, $\sigma_{min}(I+G(j\omega))$, the upper bound on the allowable magnitude of modelling error of (3.44) given by $\sigma_{max}(L^{-1}(j\omega) - I)$, is automatically greater than or equal to unity.

Example 2:

With $b_{12} = 50$ in (3.20) as in the plot of $\sigma_{min}(I+G(j\omega))$ in Fig. 3.24, an LQ design using R=I and

$$Q = 3 \begin{bmatrix} 2501 & -50 \\ -50 & 1 \end{bmatrix} \tag{50}$$

gives a feedback gain of

$$R^{-1}B^{T}K = \begin{bmatrix} 1 & -50 \\ 0 & 1 \end{bmatrix} \tag{51}$$

and a closed-loop system matrix A_{CL} of

$$A_{CL} = A - BR^{-1}B^{T}K = -2I \quad . \tag{52}$$

This makes I+G(s)

$$I+G(s) = \begin{bmatrix} \frac{s+2}{s+1} & 0 \\ 0 & \frac{s+2}{s+1} \end{bmatrix} \tag{53}$$

and thus

$$\sigma_{min}(I+G(j\omega) = \left[\frac{\omega^2+4}{\omega^2+1}\right]^{\frac{1}{2}} \geq 1 \quad . \tag{54}$$

As one might expect the ability of LQ regulators to tolerate crossfeed perturbations defined in Section 3.7.2 is also affected by the choice of the control weighting matrix R. This is made precise in the following corollary.

Corollary 2: The LQ regulator with loop transfer matrix G(s) satisfying condition 2 of Theorem 2 will tolerate (i.e., $\tilde{\phi}_{CL}(s)$ will have no CRHP zeroes) a crossfeed perturbation of the form

$$L(s) = \begin{bmatrix} I & X(s) \\ 0 & I \end{bmatrix} \text{ or } \begin{bmatrix} I & 0 \\ X(s) & I \end{bmatrix} \tag{55}$$

where

$$\sigma^2_{max}(X(s)) < \min\left\{\frac{\lambda_{min}(R_1)}{\lambda_{max}(R_2)}\ ,\ \frac{\lambda_{min}(R_2)}{\lambda_{max}(R_1)}\right\}\ ,\qquad s \in \Omega_R \tag{56}$$

provided condition 1 of Theorem 2 is satisfied and where R is given by

$$R = \begin{bmatrix} R_1 & 0 \\ 0 & R_2 \end{bmatrix} \tag{57}$$

and is conformably partitioned with L(s) and either $Q > 0$ or $\phi_{0L}(j\omega) \neq 0$ for all ω holds.

Proof: Only conditions 3a and 3b of Theorem 2 need to be verified for the L(s) of (55) the rest are satisifed by assumption. Note that for $s \in \Omega_R$

$$\sigma_{max}(R^{\frac{1}{2}}L^{-1}(s)R^{-\frac{1}{2}}-I) = \sigma_{max}\left(\begin{bmatrix} 0 & -R_1^{\frac{1}{2}}X(s)R_2^{-\frac{1}{2}} \\ 0 & 0 \end{bmatrix}\right) \quad \text{or}$$

$$\sigma_{max}\left(\begin{bmatrix} 0 & 0 \\ -R_2^{\frac{1}{2}}X(s)R_1^{-\frac{1}{2}} & 0 \end{bmatrix}\right) \tag{58}$$

$$\leq \sigma_{max}(X(s))\ \max[\sigma_{max}(R_1^{\frac{1}{2}})\sigma_{max}(R_2^{-\frac{1}{2}}),\ \sigma_{max}(R_2^{\frac{1}{2}})\sigma_{max}(R_1^{-\frac{1}{2}})]$$

and hence if

$$\sigma_{max}(X(s))\ \max\left[\frac{\lambda^{\frac{1}{2}}_{max}(R_1)}{\lambda^{\frac{1}{2}}_{min}(R_2)}\ ,\ \frac{\lambda^{\frac{1}{2}}_{max}(R_2)}{\lambda^{\frac{1}{2}}_{min}(R_1)}\right] < 1 \tag{59}$$

then conditions (3a) and (3b) are both satisifed. However, (59) is

equivalent to (56).

Q.E.D.

Note that

$$\frac{\lambda \min(R)}{\lambda \max(R)} \leq \min\left\{\frac{\lambda\min(R_1)}{\lambda\max(R_2)}, \frac{\lambda\min(R_2)}{\lambda\max(R_1)}\right\} \leq \left[\frac{\lambda\min(R)}{\lambda\max(R)}\right]^{\frac{1}{2}} \qquad (60)$$

which indicates that if the ratio of $\lambda\min(R)/\lambda\max(R)$ is very small that the ability to tolerate crossfeed perturbations is drastically reduced. As illustrated in Fig. 6 the use of R scales the inputs and outputs such that the stability margins are obtained in the scaled system rather than the original system. This means that if our original model has the coordinate system in which we would like to guarantee margins, that R should be selected as $R = \rho I$ for some positive scalar ρ.

The effect of the R matrix on the tolerance of the closed-loop system to general modelling errors of the form of (3.44) can be accounted for by using the inequality

$$\sigma_{max}(R^{\frac{1}{2}}L^{-1}(s)R^{-\frac{1}{2}}-I) \leq ||R^{-\frac{1}{2}}||_2||R^{\frac{1}{2}}||_2\ \sigma_{max}(L^{-1}(s)-I) \quad . \qquad (61)$$

To guarantee stability via Theorem 2 we must have

$$\sigma_{max}(R^{\frac{1}{2}}L^{-1}(s)R^{-\frac{1}{2}}-I) \leq 1 \qquad (62)$$

which is ensured if

$$\sigma_{max}[L^{-1}(s)-I] \leq [||R^{\frac{1}{2}}||_2||R^{\frac{1}{2}}||_2]^{-1} = \left[\frac{\lambda\min(R)}{\lambda\max(R)}\right]^{\frac{1}{2}} , \qquad (63)$$

From (63), it is clear that the tolerance to model error may be reduced by a factor $\sqrt{\lambda\min(R)/\lambda\max(R)}$ from the case where $R = \rho I$ for a positive

scalar ρ when equality holds in (61).

5.4.1 Variations of LQ Designs

Since LQ designs have inherently good margins provided R is selected appropriately, it is natural to search for variations of this method. One such variation, proposed by Wong and Athans [27], is to solve a Lyapunov rather than a Riccati equation to compute K used in (3).

The Lyapunov equation with $Q \geq 0$ given by

$$A^T K + KA + Q = 0 \tag{64}$$

guarantees that the eigenvalues of A lie in the OLHP if $K \geq 0$ and $[A, Q^{\frac{1}{2}}]$ is detectable. The corresponding Kalman type inequality for loop transfer matrices G(s) specified by (24) where $K \geq 0$ satisfies (64) is given by

$$RG(j\omega) + G^H(j\omega)R \geq 0; \qquad \text{for all } \omega \tag{65}$$

and is the fundamental inequality used to derive stability margins. When $Q > 0$ the inequality (65) becomes strict. The stability margins for this type of feedback are given in the next theorem and its corollaries.

Theorem 3: For G(s) of the form of (24), $\tilde{\phi}_{CL}(s)$ has no CRHP zeros if the following conditions hold:

1. $\tilde{\phi}_{OL}(s)$ has no CRHP zeros
2. $K \geq 0$ satisfies (64) with $Q \geq 0$, $R > 0$ and $[A, Q^{\frac{1}{2}}]$ detectable, and B has full rank
3. either of the following holds
   (a) $Q > 0$ and $RL(s) + L^H(s)R \geq 0, \quad s \in \Omega_R$
   (b) $RL(s) + L^H(s)R > 0, \quad s \in \Omega_R$.

Proof: Conditions 1 and 2 and the Lyapunov stability criterion guarantee that condition 1 of Theorem 2 is satisfied. As in the proof of Theorem 2 we may work with $\hat{G}(s) = R^{\frac{1}{2}}G(s)R^{-\frac{1}{2}}$ and $\hat{L}(s) = R^{\frac{1}{2}}L(s)R^{-\frac{1}{2}}$ instead of G(s) and L(s). Condition (65) is simply condition 2 of Theorem 3.8 with $\hat{G}(s)$ replacing G(s), and $\hat{L}(s)$ replacing L(s) in its condition 3 is simply condition 3b. Thus by Theorem 3.8 the theorem is proved when condition 3b holds. When $Q > 0$ and condition 3a is satisfied, the strictness of the inequality of condition 3 of Theorem 3.8 may be changed to $\geq$ and the $\geq$ of its condition 2 to $>$ and Theorem 3.8 remains valid. Thus when condition 3a holds the theorem is proved.

Q.E.D.

Corollary 3: For G(s) as in Theorem 3 with R diagonal the guaranteed gain and phase margins are given by

$$GM \supset [0, \infty) \tag{66}$$

$$PM \supset [-90°, 90°] \tag{67}$$

if condition 3a of Theorem 3 holds and

$$GM \supset (0,\infty) \tag{68}$$

$$PM \supset (-90°, 90°) \tag{69}$$

if condition 3b of Theorem 3 holds.

Proof: Similar to Corollary 3.5.

The importance of Corollary 3 is that the standard LQ guaranteed gain reduction margin of $\frac{1}{2}$ can be reduced to 0 by using K satisfying the Lyapunov equation (43) with $Q > 0$ rather than the Riccati equation (2).

Of course, it is possible to have a zero gain reduction margin only for open-loop stable systems. However, standard LQ state feedback does not guarantee a zero gain reduction margin even in the open-loop stable case, and has been criticized on these grounds [20]. Having a zero or small gain reduction margin is important in situations where actuators may fail or saturate, respectively, and there is no opportunity to reconfigure the control system. In fact, the motivation for the thesis [26] (which in turn lead to most of the robustness developments reported in this chapter) was a study supporting the design of the automatic depth-keeping controller for the Trident submarine, in which saturation of one of the two hydrodynamic control surfaces produced an unstable closed-loop system.

Corollary 4: For G(s) as in Theorem 3 the crossfeed tolerance is given by

$$\sigma^2_{max}(X(s)) < 4 \min \left[\frac{\lambda min(R_1)}{\lambda max(R_2)} , \frac{\lambda min(R_2)}{\lambda max(R_1)} \right] , \quad s \in \Omega_R \qquad (70)$$

where L(s) is given by (55), $R > 0$ is given by (57) and $\tilde{\phi}_{OL}(s)$ has no CRHP zeros.

Proof: Analogous to Corollary 2.

The significance of Corollary 4 is that using the Lyapunov equation (64) to design the state feedback the tolerance to crossfeed perturbations has doubled over the crossfeed tolerance of the LQ state feedback regulator in Corollary 2. However, (64) can only be used on open-loop stable systems and thus even though the guaranteed stability margins for the Lyapunov

state feedback regulator are better than for the LQ regulator its use is limited. What is necessary is a compromise between these design approaches that is applicable to unstable open-loop systems.

Another way to modify the LQ design procedure that is a compromise between Theorem 2 and Theorem 3 applicable to unstable open-loop systems involves the use of a parameterized Riccati equation given by

$$A^TK + KA + Q - \beta KBR^{-1}B^TK = 0 \tag{71}$$

where β is an adjustable parameter and $0 < \beta < 2$. The feedback law is still given by (3) and G(s) is still given by (24) with $K \geq 0$. Since the β in (71) may be lumped together with the R matrix, (71) is just a standard Riccati equation and therefore has a unique solution $K \geq 0$ under the appropriate assumptions (condition 2 of Theorem 2). The standard LQ optimal feedback law associated with (71) is given by

$$\underline{u}(t) = -\beta R^{-1}B^TK\underline{x}(t) \ . \tag{72}$$

Instead of (72) we will use $\underline{u}(t) = -R^{-1}B^TK\underline{x}(t)$ as in (3). Thus depending on whether $\beta > 1$ or $\beta < 1$ we are merely decreasing or increasing, respectively, the optimal feedback gain by a scalar factor of $1/\beta$. Also with G(s) given by (24) the standard LQ loop transfer matrix is simply $\beta G(s)$. From Theorem 1 we know that if $Q > 0$

$$[1+\beta G(s)]^H \frac{1}{\beta} R[1+\beta G(s)) > \frac{1}{\beta} R \ , \qquad s \in \Omega_R \tag{73}$$

which in the SISO case becomes

$$\left| \frac{1}{\beta} + g(s) \right| > \frac{1}{\beta} \ , \qquad s \in \Omega_R \tag{74}$$

and is illustrated in Fig. 3. To obtain bounds on L(s) to ensure stability

we merely work with $\frac{1}{\beta} L(s)$ and $\beta G(s)$ and apply Theorem 2 for the standard LQ regulator problem. Doing this we obtain, in the SISO case, the inequality

$$|\beta \ell^{-1}(s)-1| < 1, \qquad s \in \Omega_R \tag{75}$$

illustrated in Fig. 7. Note that from that the critical (-1, 0) point is no longer contained inside the circle of Fig. 3 corresponding to (74) if $\beta \geq 2$ and thus there are no guaranteed margins. If $\beta \to 0$ the guaranteed minimum margins approach those of the Lyapunov feedback case given Corollaries 3 and 4. In general, for the multivariable case the

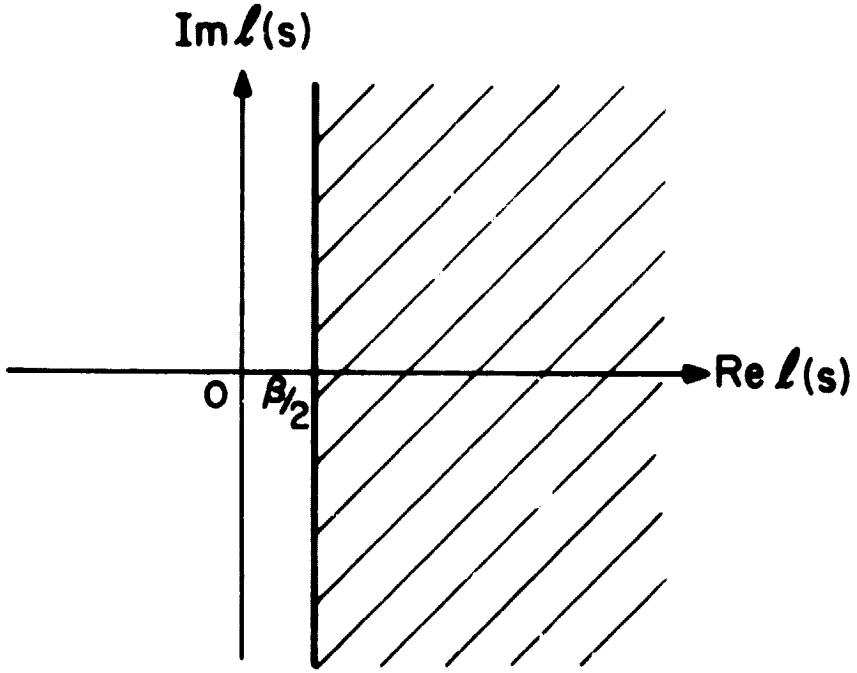

Fig. 7. Set of allowable values of $\ell(s)$ when $|\beta \ell^{-1}(s)-1| < 1$ and $0 < \beta < 2$.

guaranteed minimum margins, again if R is diagonal and Q is positive definite, are given by

$$GM \supset [\beta/2, \infty), \quad 0 < \beta < 2 \tag{76}$$

and

$$PM \supset [-\cos^{-1}\frac{\beta}{2}, \cos^{-1}\frac{\beta}{2}], \quad 0 < \beta < 2. \tag{77}$$

These guaranteed margins (when $\beta \leq 1$) can also be obtained by similar but distinctly different procedures reported in [30] and [31] which utilize standard LQ regulators with vanishingly small control weights. Recently [45] it has also been shown how to ensure preselected guaranteed minimum gain and phase margins by using a Riccati equation with an associated quadratic cost index, weighting the product of the state and the control.

5.5 Stability Margins of LQG Regulators

A basic limitation associated with the LQ guaranteed stability margins is that they are obtained only under the assumption of full state feedback. State feedback can never be exactly realized, and often it is impossible or too expensive to provide enough sensors to achieve even an approximate realization. Thus one is motivated to investigate what guaranteed stability margins might be associated with LQG controllers, in which a Kalman filter (KF) is used to provide state estimates for feedback.

Since the Kalman filter is the dual of the LQ regulator, dual robustness results are obtainable. They ensure a nondivergent Kalman filter under variations in the nominal model parameters of the plant whose state is to be estimated (see section 5.2 for the use of the Kalman filter in

the LQG regulator). To make precise the connection between the regulator and filter problems, consider the linear system

$$\dot{\underline{x}}(t) = A\underline{x}(t) + \underline{\xi}(t) \tag{78}$$

$$\underline{y}(t) = C\underline{x}(t) + \underline{\theta}(t) \tag{79}$$

where $\underline{\xi}(t)$ and $\underline{\theta}(t)$ are zero mean white noise sources with spectral intensity matrices Ξ and Θ respectively. We wish to estimate $\underline{x}(t)$ given $\underline{y}(\tau)$, $-\infty \leq \tau \leq t$, such that the mean square error is minimize. Under the assumption the [A,C] is detectable, it is well-known that the state estimate is specified by

$$\dot{\underline{\hat{x}}}(t) = A\underline{\hat{x}}(t) + \Sigma\, C^T\Theta^{-1}\underline{\nu}(t) \tag{80}$$

$$\underline{\nu}(t) = y(t) - C\hat{\underline{x}}(t) \tag{81}$$

where

$$A\Sigma + \Sigma A^T + \Xi - \Sigma C^T\Theta^{-1}C\Sigma = 0, \quad \Sigma \geq 0 \ . \tag{82}$$

If we calculate the transfer matrix from $\nu(s)$ to $\hat{\underline{y}}(s) - C\hat{\underline{x}}(s)$, we find that

$$\hat{\underline{y}}(s) = [C(Is-A)^{-1}\Sigma C^T\Theta^{-1}]\underline{\nu}(s) \triangleq F(s)\underline{\nu}(s). \tag{83}$$

Then, if $\Xi > 0$, $F(s)$ satisfies the dual of (26) given by

$$(I + F(s))\Theta\ (I+F(s))^H > \Theta, \qquad s \notin \Omega_R \tag{84}$$

which guarantees the stability of the error dynamics under a range of perturbations in $F(s)$. Thus, if $F(s)$ is perturbed to $\tilde{F}(s) = F(s)L(s)$,

where usual assumptions about G(s) are applied to F(s), the Kalman filter will remain nondivergent if

$$\sigma_{max}(\Theta^{-\frac{1}{2}} L^{-1}(s)\ \Theta^{\frac{1}{2}} - 1) \leq 1, \qquad s \notin \Omega_R \tag{85}$$

or equivalently,

$$\Theta L^H(s) + L(s)\Theta - \Theta \geq 0 \quad . \tag{86}$$

It is now readily apparent that F(s), the loop transfer matrix of the error dynamics loop of the Kalman filter, is the dual of G(s) in the LQ regulator and has the same guaranteed margins at its input, $\nu(s)$, for diagonal Θ.

Safonov and Athans [32] have developed these dual results for the nondivergence of the extended Kalman filter. Furthermore, they have considered the stability properties of a nonlinear LQG control system formed by the cascade of a constant gain extended Kalman filter and the LQ state feedback gain. The LQ state feedback gain and the constant gain of the extended Kalman filter are computed from the linearized model parameters. However, the extended Kalman filter must have the true nonlinear model of the plant. This violates the basic premise of robustness theory, that is, the controller has no knowledge or at most minimal knowledge of the model error. Nevertheless, the result emphasizes that model mismatch and not control or filter gains are responsible for a reduction in the margin of stability. We next examine these results in the completely linear case where the LQG stability margins are much easier to obtain.

The standard LQG control system block diagram is shown in Fig. 8. with various points of the loop marked. To determine the robustness of

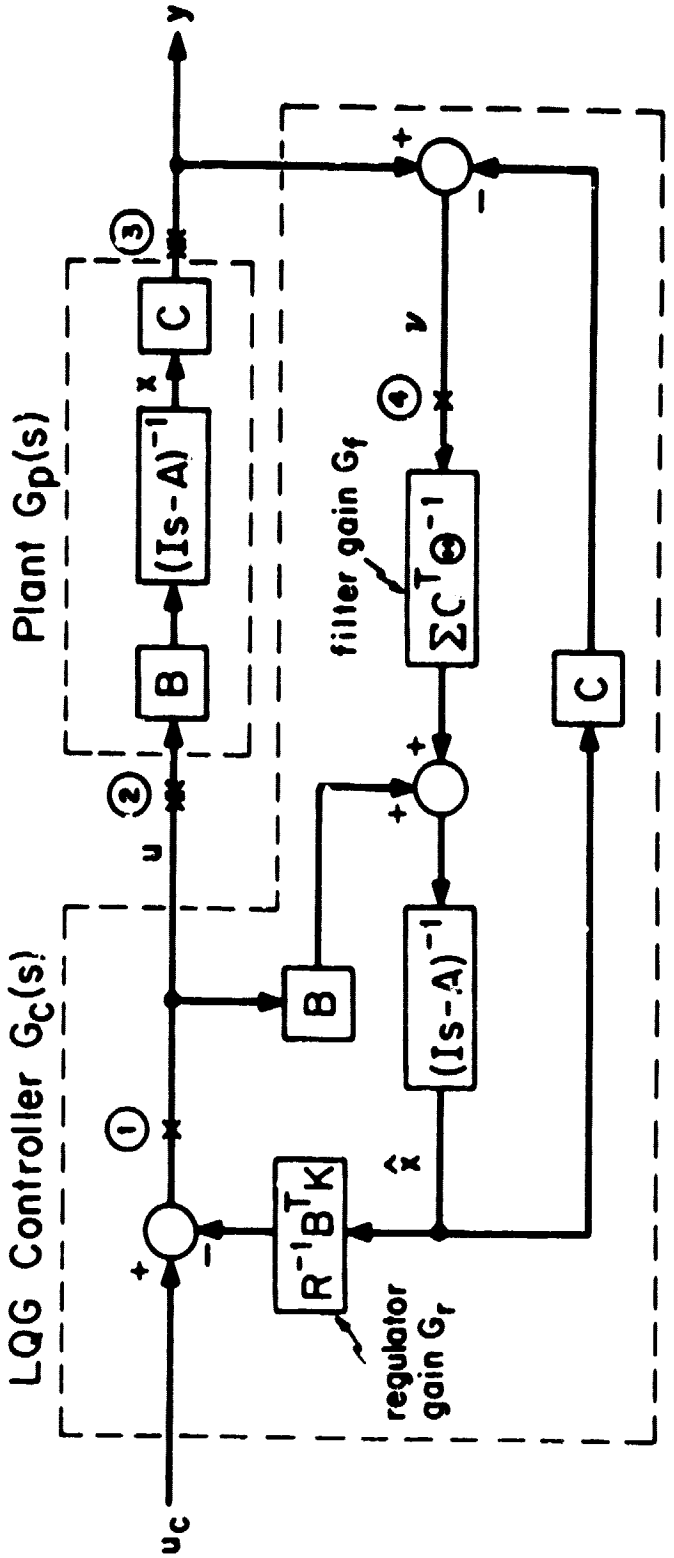

Fig. 8: LQG Control System.

the LQG control system we insert perturbations at points (2) and (3) (the input and output of the physical plant) and find out how large they can be made without destabilizing the closed-loop LQG system. It is therefore convenient to calculate the loop transfer matrices at points (1) to (4). The loop transfer matrix at point (K) will de noted by $T_K(s)$ and is calculated by breaking the loop at point (K) (see section 5.2) and using it as the input as well as the output. For the four points indicated in Fig. 8 we have

$$T_1(s) = G_r\phi(s)B \tag{87}$$

$$T_2(s) = C_r(\phi^{-1}(s) + BG_r + G_fC)^{-1}G_fC\phi(s)B \tag{88}$$

$$T_3(s) = C\phi(s)BG_r(\phi^{-1}(s) + BG_r + G_fC)^{-1}G_f \tag{89}$$

$$T_4(s) = C\phi(s)G_f \tag{90}$$

where

$$G_r \triangleq R^{-1}B^TK = \text{regulator gain} \tag{91}$$

$$G_f \triangleq \Sigma C^T\Theta^{-1} = \text{filter gain} \tag{92}$$

$$\phi(s) \triangleq (Is-A)^{-1} \tag{93}$$

Note that points at (1) and (4) we have the standard LQ regulator and Kalman filter loop transfer matrices respectively given previously in (20) and by F(s) in (83). Thus at points (1) and (4) (inside the LQG controller) the LQ and KF minimum guaranteed stability margins apply. The following theorem is a much simplified version of a theorem proved in [32] and gives LQG stability margins at points (2) and (3) (the

input and output of the physical plant), where we denote the open-loop plant as $G_p(s) \triangleq C(Is-A)^{-1}B$ and $G_c(s) \triangleq G_r(Is-A+BG_r+G_fC)^{-1}G_f$ as the compensator. We use N(s) to denote output perturbations in $G_p(s)$ at point (3) in Fig. 8.

Theorem 4: The LQG feedback control system of Fig. 8 is asymptotically stable under variations in the open-loop plant $G_p(s) \triangleq C(Is-A)^{-1}B$ if the following conditions hold:

(a) the perturbed open-loop plant $\tilde{G}_p(s) = \tilde{C}(Is-\tilde{A})^{-1}\tilde{B}$ is such that the $\det(sI-\tilde{A})$ and $\det(sI-A)$ have the same number of CRHP zeros and if $\det(j\omega_0 I-\tilde{A}) = 0$ then $\det(j\omega_0 I-A) = 0$. (94)

(b) [A,B] is stabilizable, $Q > 0$, $k > 0$ and $K \geq 0$ satisfies (22) and B has full rank. (95)

(c) $$\tilde{G}_p(s) = G_p(s)L(s) = N(s)G_p(s) \tag{96}$$

and either

$$\sigma_{max}(R^{\frac{1}{2}}L^{-1}(s)R^{-\frac{1}{2}}-I) \leq 1 \tag{97}$$

or

$$\sigma_{max}(\theta^{-\frac{1}{2}}N^{-1}(s)\theta^{\frac{1}{2}}-I) \leq 1 \tag{98}$$

hold for all $s \in \Omega_R$.

(d) the LQG controller transfer matrix $G_c(s)$ from the plant output to the plant input is given by

$$G_c(s) = G_r(Is-\tilde{A}+\tilde{B}G_r+G_f\tilde{C})^{-1}G_f \tag{99}$$

where G_r and G_f respectively satisfy (91) and (92).

Proof: Breaking the loop at point (1) of Fig. 8 we have a loop transfer function matrix of

$$G_r(sI-A+G_fC)^{-1}[G_fC(Is-A)^{-1}B + B] = G_r(sI-A)^{-1}B \triangleq G(s) \qquad (100)$$

so that

$$\phi_{0L}(s) = \det[sI-A + G_fC]\det[sI-A] \qquad (101)$$

and

$$\tilde{\phi}_{0L}(s) = \det[sI-A + G_fC]\ \det[sI-\tilde{A}] \qquad (102)$$

Since the Kalman filtering error dynamics are stable given (95) and since (94) holds, conditions 1a and 1b of Theorem 3.2 hold. Now by direct application of Theorem 2 we conclude that the system of Fig. 8 is stable if L(s) is inserted at point (1). However, this is not the location we desire to have the margins guaranteed. Nevertheless, by manipulation of the block diagram of Fig. 8 we may place L(s) at point (2) if we change B to $B\tilde{L}(s)$ inside the controller leaving $G_r = R^{-1}B^TK$ fixed (see Fig. 9). This, however, is equivalent to changing (A,B,C) to $(\tilde{A},\tilde{B},\tilde{C})$ inside the controller leaving G_f and G_r fixed. This also can be interpreted as giving the Kalman filter the correct dynamic model of the perturbed open-loop system without changing either the filter or regulator gains. The same result follows if we start with the perturbation N(s) at point (4) where the KF guarantees apply and move it to point (3) changing C to N(s)C (see Fig. 10.) Again the Kalman filter has the correct model of $\tilde{G}_p(s)$.

Q.E.D.

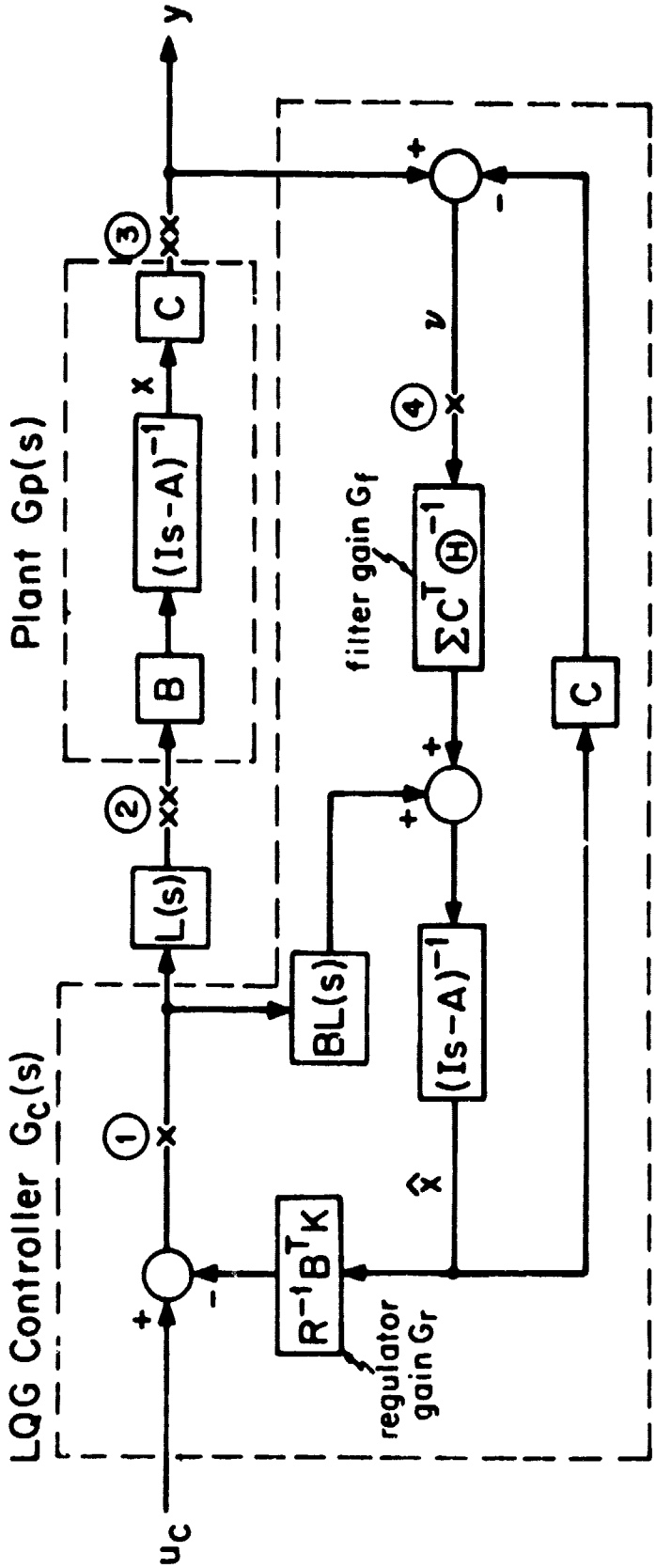

Fig. 9: LQG Control System used in proof of Theorem 4.

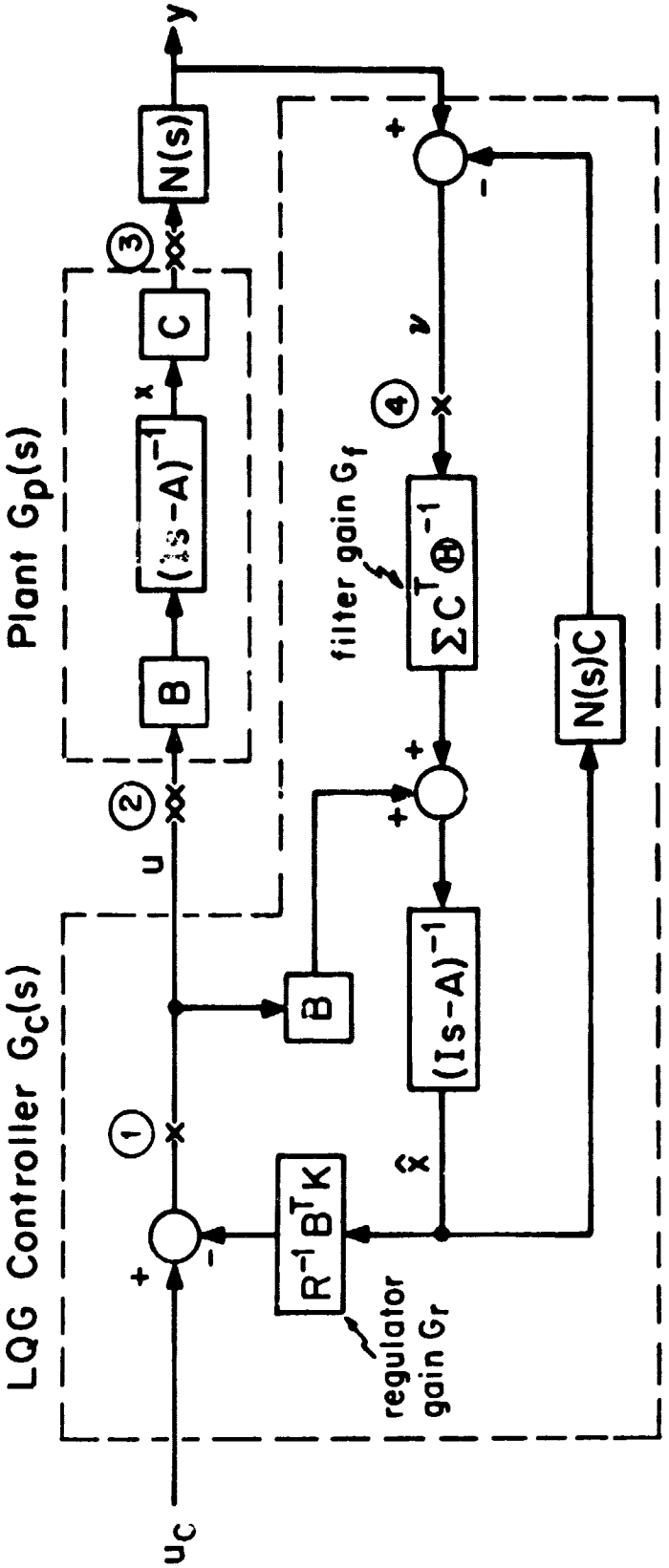

Fig. 10: LQG Control System and perturbation N(s).

Notice that in (96) L(s) represents the same perturbation in $G_p(s)$ at the input to the plant as N(s) represents at the output of the plant and that $\tilde{G}_p(s)$ is the same in both cases.

Thus the LQ and KF guaranteed stability margins will apply to LQG controllers at the input and output of the physical plant but under the restrictive assumption that the system model embedded within the Kalman filter is always the same as the true system (i.e., the perturbed system). For the more realistic case in which the internal model of the Kalman filter remains unchanged, there are unfortunately no guaranteed robustness properties[1], as Doyle has demonstrated with a simple counterexample [33]. This counterexample is extreme, but it is possible to obtain LQG controllers with inadequate stability margins that look quite reasonable in the time domain. Fig. 11 shows the Nyquist plot of a single-input design reported in the literature [34]; note that the phase margin is less than 10°.

5.5.1 Robustness Recovery

Fortunately, there are two dual procedures that do not require the Kalman filter to have the true system model and that still recover the LQ and KF guaranteed minimum margins. These procedures use the asymptotic properties of the Kalman filter and LQ regulator (see [43] and can be used only if the plant is minimum phase. If W is a nonsingular arbitrary matrix, then by selecting Ξ in (82) as ρBWW^TB^T and letting $\rho \to \infty$ the loop transfer matrix $T_2(s)$ in (88) approaches

[1] In other words, the robustness properties of LQG designs will depend on the actual values of A,B,C,Q,R,Ξ and Θ.

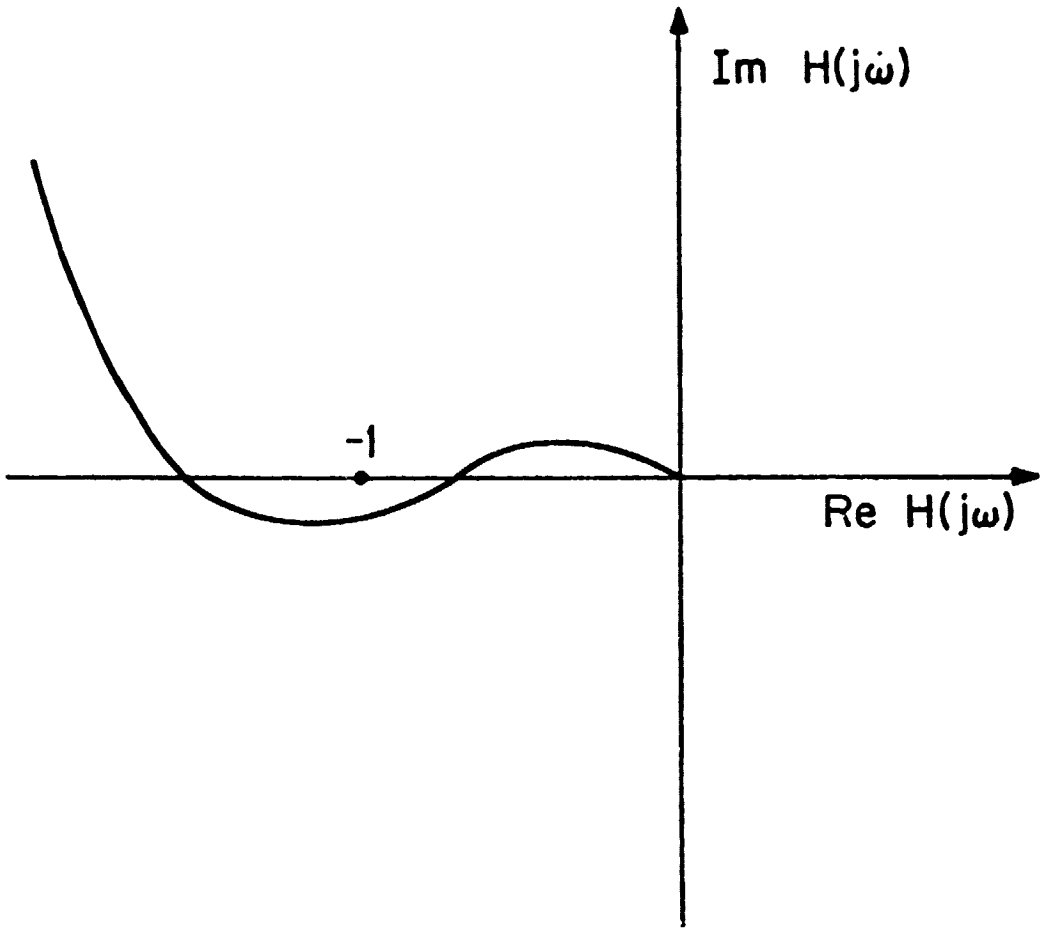

Fig. 11: Nyquist diagram for LQG design in [34]
($H(j\omega)$ = loop transfer function).

$T_1(s)$ of (87) if the minimum phase assumption holds [35]. Thus the LQ regulator guaranteed margins will be recovered at the input to the plant. Kwakernaak [36] proposeed the dual of the above procedure to obtain low sensitivity feedback systems. His procedure makes $T_3(s)$ of (89) approach $T_4(s)$ of (90) by selecting Q in (4) as $\rho\, C^T W^T W C$ and

letting $\rho \to \infty$ and thus the KF guaranteed minimum margins will be recovered at the output of the plant[1]. However, it is not always the case that an LQG controller needs to be robustified by these procedures since in some cases the LQG control system will have better stability margins than its full state feedback counterpart [42]. Also, in this case one must keep in mind that the stochastic error performance of the robustified LQG controller may be better (due to lower controller bandwidth) than the LQ state feedback regulator.

Even when these procedures are used, the guaranteed stability margins apply at the input or output of the physical plant but not necessarily at both input and output. It is desirable to have margins at both these locations since the perturbations in $G_p(s)$ are represented as either $G_p(s)L(s)$ or $N(s)G_p(s)$ and we would not like small perturbations in either input or output to destabilize the system. Margins at both input and output can be ensured if the inequalities

$$\sigma_{min}(I+G_c(s)G_p(s)) \geq 1 \tag{103}$$

and

$$\sigma_{min}(I+G_p(s)G_c(s)) \geq 1 \tag{104}$$

both hold. The relationship between these two quantities when $G_p(s)$ and $G_c(s)$ are square matrices is given by the following lemma.

---

[1] Dowdle [37] has adapted these procedures for use with minimal order observer based compensators and their duals.

Lemma 1: For arbitrary complex square matrices $G_p(s)$ and $G_c(s)$ it is true that

$$\frac{1}{k}\sigma_{min}(I+G_p(s)G_c(s)) \leq \sigma_{min}(I+G_c(s)G_p(s)) \leq k\sigma_{min}(I+G_p(s)G_c(s)) \tag{105}$$

where

$$k = \min\left[\frac{\sigma_{max}(G_p(s))}{\sigma_{min}(G_p(s))}, \frac{\sigma_{max}(G_c(s))}{\sigma_{min}(G_c(s))}\right] \geq 1. \tag{106}$$

Proof: Use the property of matrix norms that $||AB|| \leq ||A||\,||B||$ on the equation

$$[I + G_p(s)G_c(s)]^{-1} = G_p^{-1}(s)[I + G_c(s)G_p(s)]^{-1}G_p(s) \tag{107}$$

to obtain the left inequality of (105) with $k = \sigma_{max}[G_p(s)]/\sigma_{min}[G_p(s)]$. The right inequality in (105) is obtained by reversing the roles of $G_p(s)$ and $G_c(s)$ in (107).

Q.E.D.

The quantity k is the minimum of the condition numbers[1] of $G_p(s)$ and $G_c(s)$ with respect to inversion. From (105) we conclude that if k is close to unity then approximately the same robustness guarantees will apply at both input and output. Note that we have no control over $G_p(s)$ so that if $G_p(s)$ is nearly singular we must design our compensator so that $\sigma_{max}(G_c(s)) \cong \sigma_{max}(G_c(s))$. On the other hand, if our plant is well-conditioned with respect to inversion, our compensator $G_c(s)$ need not be so severaly constrained, allowing more flexibility in achieving

[1] In the numerical analysis of the linear equation $A\underline{x} = \underline{b}$, the condition number of A, given by $\sigma_{max}(A)/\sigma_{min}(A)$, bounds the error in the computed solution $\underline{x}$ in terms of an equivalent error in $\underline{b}$ [44].

performance objectives.

5.5.2 Characterization of Model Error

Note in (103) and (104) that ensuring that both $\sigma_{min}[I+G_p(s)G_c(s)]$ and $\sigma_{min}[I+G_c(s)G_p(s)]$ are greater than unity gives upper bounds on two different types of allowable modelling errors. These modelling errors differ in that one represents the perturbed open-loop model $\tilde{G}_p(s)$ as $G_p(s)L(s)$, an equivalent perturbation in the input to $G_p(s)$, and the other represents $\tilde{G}_p(s)$ as $N(s)G_p(s)$, an equivalent perturbation in the output of $G_p(s)$. These are both relative modelling errors between $\tilde{G}_p^{-1}(s)$ and $G_p^{-1}(s)$ and are given by

$$E_i(s) = L^{-1}(s)-I = [\tilde{G}_p^{-1}(s)-G_p^{-1}(s)]G_p(s) \tag{108}$$

$$E_0(s) = N^{-1}(s)-I = G_p(s)[\tilde{G}_p^{-1}(s)-G_p^{-1}(s)] \tag{109}$$

where $E_i(s)$ is the model error in $\tilde{G}_p(s)$ reflected to the input of $G_p(s)$ and $E_0(s)$ is the model error in $\tilde{G}_p(s)$ reflected to the output. The relationship between $E_i(s)$ and $E_0(s)$ is given very simply by (since they represent the same $\tilde{G}_p(s)$)

$$E_i(s) = G_p^{-1}(s)E_0(s)G_p(s) \tag{110}$$

and thus we conclude that

$$\frac{1}{k}\,\sigma_{max}(E_0(s)) \leq \sigma_{max}(E_i(s)) \leq k\,\sigma_{max}(E_0(s)) \tag{111}$$

where

$$k = \frac{\sigma_{max}[G_p(s)]}{\sigma_{min}[G_p(s)]} \quad . \tag{112}$$

If k is very large, (111) shows that what may look like an unreasonably large error at one point in the loop (either the input to $G_p(s)$ or its output) may look like a very reasonable size error at another point in the loop. The stability of the closed-loop system with respect to these errors is guaranteed under appropriate assumptions[1] if for all $s \in \Omega_R$

$$\sigma_{max}[E_i(s)] < \sigma_{min}[I+G_c(s)G_p(s)] \tag{113}$$

or

$$\sigma_{max}[E_0(s)] < \sigma_{min}[I+G_p(s)G_c(s)] \ . \tag{114}$$

Now suppose that $\sigma_{max}[E_i(s)]$, from our knowledge of the open-loop system physics, seems unreasonably large and condition (113) does not hold but will hold for all reasonable size errors. If the perturbed model $\tilde{G}_p(s)$ however is such that $\sigma_{max}[E_0(s)]$ seems reasonably small, that is an error of that magnitude could be justified (again by our knowledge of the open-loop system physics), then a sufficiently small value of $\sigma_{min}[I+G_p(s)G_c(s)]$ (small enough so that (114) does not hold) indicates that there is danger of the perturbed closed-loop becoming unstable. If we believe that having a reasonable size error, at the input of the open-loop system, completely characterizes the class of $\tilde{G}_p(s)$ that should be considered then we may rule out the possibility that the perturbed closed-loop system may become unstable as a result of the fact that (114) is violated for seemingly reasonably sized errors at

---

[1] Conditions 1 and 2 of Theorem 3.6 must be appropriately modified to also deal with N(s).

the output. However, our knowledge of what class of $\tilde{G}_p(s)$ should be considered may depend on what seem like reasonable errors at both input and output to the open-loop system. That is, our knowledge of what constitutes a reasonable class of $\tilde{G}_p(s)$ to consider is built up from our knowledge of what errors seem reasonable when reflected as equivalent perturbations at different points in the feedback loop. In this case, one could not rule out the small error at the output (i.e., $E_0(s)$) which violates (114). Thus it depends on how we decide what constitutes a reasonable class of $\tilde{G}_p(s)$ that determines if we need to check to make sure that both the values $\sigma_{min}[I+G_c(s)G_p(s)]$ and $\sigma_{min}[I+G_p(s)G_c(s)]$ are sufficiently large or that only one of them is sufficiently large.

In the author's opinion, it seems most likely that the class of $\tilde{G}_p(s)$ that should be considered is a composite class of the perturbed models that arise from reasonably sized errors reflected to both input and output of the open-loop system. Therefore, it would seem wise to check the size of both $\sigma_{min}[I+G_c(s)G_p(s)]$ and $\sigma_{min}[I+G_p(s)G_c(s)]$.

5.6 Concluding Remarks

This chapter has derived MIMO stability margins for LQ regulators and their variations including LQG regulators. This was accomplished using the MIMO version of Kalman's inequality and Theorem 3.6. The LQ regulator was shown to have at least a 50% gain reduction margin, an infinite upward gain margin and $\pm$ 60° phase margin provided the control weighting matrix R is diagonal. If R is not diagonal it was shown that the LQ regulator gain margin may be arbitrarily small. If R is not a

multiple of the identity the crossfeed tolerance is also reduced. The R matrix determines the coordinate system in which the stability margins hold. The margins in the R selected coordinate system may be much larger than the actual margins in the coordinate system specified by the inputs and outputs to the physical open-loop system. Similar comments may be made for the variations of LQ state feedback using the Lyapunov and modified Riccati equations.

The guaranteed margins for LQ regulators do not apply to LQG regulators except when the Kalman filter embedded in the LQG controller has a correct dynamic model of the perturbed system, a rather unrealistic assumption. However, when the open-loop plant model is minimum phase, there are two procedures that recover the guaranteed LQ margins asymptotically. These guaranteed margins may be recovered at either the input or the output of the open-loop plant but can only be guaranteed to be recovered at both input and output when either the open-loop plant transfer matrix or the compensator transfer matrix has a small condition number near unity for all frequencies. The necessity of input and output stability margins is shown to be dependent on the ability of the designer to characterize the set of reasonable perturbed models for which the perturbed closed-loop system stability must be preserved.

It is important to point out that the LQG methodology is inherently a multiloop design procedure which when coupled with the robustness recovery methods and used intelligently provides a systematic design procedure for robust multivariable compensators. This is in contrast to the characteristic loci [4, 5, 56] and inverse Nyquist array [1,2]

methods (discussed in the following chapter) which reduce multivariable controller design to a series of decoupled single loop designs. These methods obtain good stability margins in the coordinate system of the decoupled SISO systems but not in the coordinate system of the physical input and output of the open-loop multivariable system. Thus they may not produce robust controller designs and it is nontrivial, given the present state of the art to change these designs to obtain better robustness properties.

One word of caution is necessary when using the LQG approach to controller synthesis. It has been popular to reduce many more general control problems such as the tracking problem to a simple regulator problem by state augmentation. State augmentation has also been used to provide integral controllers or provide additional rolloff. When using augmented versions of control problems solved via the regulator problem one must be careful to determine exactly the point in the feedback loop where the guaranteed stability margins will apply. In many augmented regulator problems the point at which the guaranteed margins apply is not the input or output of the physical open-loop plant but a point associated with the addition of the augmented states.

6. ROBUSTNESS ANALYSIS WITH FREQUENCY DOMAIN METHODS

6.1 Introduction

The purpose of this chapter is to place in perspective current frequency domain techniques for controller synthesis and evaluation and their implications for the robustness characterization of feedback control systems. We shall not present a full tutorial description of these methods but only briefly describe their salient features with regard to their importance in robustness analysis, the main theme of this thesis.

In section 6.2 the characteristic loci (CL) [5,56] and inverse Nyquist array (INA) [1,2] methodologies are discussed. It is shown that these design methodologies ensure stability margins in a coordinate system based on the diagonalization of the open-loop plant transfer matrix rather than the coordinate system specified by the physical inputs and outputs of the nominal open-loop plant. In some cases, the CL and INA design methodologies will lead to acceptable stability margins at the physical input and output of the system; however, in other cases, the stability margins at the physical input and output of the system will be drastically reduced. The discussion of this section is not original but relies heavily on the work of Doyle and Stein [43] and Stein and Sandell [58].

In section 6.2, the principal gain and phase (PGP) analysis recently proposed in [57] is discussed. This method of analysis allows one to ensure stability of a feedback control system by taking into account the structure of the model in a somewhat different manner than that of

Chapter 4. The main shortcoming of the PGP approach is that it is not applicable to important classes of loop transfer matrices, G(s), and important classes of model errors. It is shown that the PGP method will fail for model error matrices E(s) that are singular or almost singular. Recall that in Chapter 4 (equation (4.13)) it was shown there exists a smallest destabilizing error matrix, E(s), that is singular and thus the PGP analysis is not applicable for this important class of model errors.

6.2 Characteristic Loci and Inverse Nyquist Array Methods

The CL and INA methodologies for the design of MIMO feedback control systems take advantage of the large body of well-developed tools for SISO control design by reducing the MIMO design problem to a sequence of independent SISO design problems. To make this precise, consider the feedback system shown in Fig. 1 where the nominal open-loop plant transfer matrix denoted by $G_p(s)$ and the compensator transfer matrix is denoted by $G_c(s)$ giving a loop transfer matrix G(s) as either $G_c(s)G_p(s)$ or $G_p(s)G_c(s)$ depending on whether the loop is broken at the input or the output respectively.

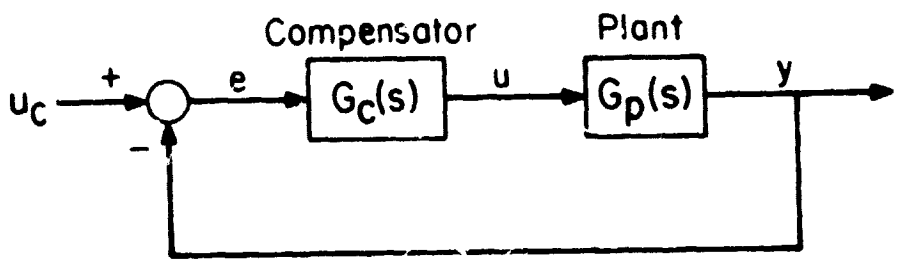

Fig. 1: Basic Feedback System

Both the CL and INA methods assume that $G_p(s)$ can be diagonalized either exactly or approximately for all $s \in D_R$. Therefore, assume that there exist matrices $W(s)$ and $V(s)$ composed of rational transfer functions such that $V(s)G_p(s)W(s)$ is bounded and either diagonal or diagonally dominant[1] for all $s \in D_R$ and is denoted by $\hat{G}_p(s)$, i.e.

$$\hat{G}_p(s) = V(s)G_p(s)W(s) . \tag{1}$$

If $G_p(s)$ is diagonally dominant then the diagonal matrix $\hat{G}_{pd}(s)$ given by

$$\hat{G}_{pd}(s) = \text{diag}[\hat{g}_{p11}(s), \hat{g}_{p22}(s),\ldots,\hat{g}_{pnn}(s)] \tag{2}$$

can be used as a good approximation to $\hat{G}_p(s)$ within bounds specified by the magnitude of the off diagonal elements of $\hat{G}_p(s)$. For the purposes of this chapter we will assume exact diagonalization of $G_p(s)$ by $V(s)$ and $W(s)$, since all the same observations to be made will apply if only diagonal dominance holds.

The form of the compensator proposed by the CL and INA methods is shown in Fig. 2 where $K(s)$ is a diagonal matrix given by

---

[1] An nxn complex matrix A is diagonally dominant if for i = 1,2,...,n

$$|a_{ii}| > \sum_{\substack{j=1 \\ j\neq i}}^{n} |a_{ij}|$$

or

$$|a_{ii}| > \sum_{\substack{j=1 \\ j\neq i}}^{n} |a_{ji}| \quad .$$

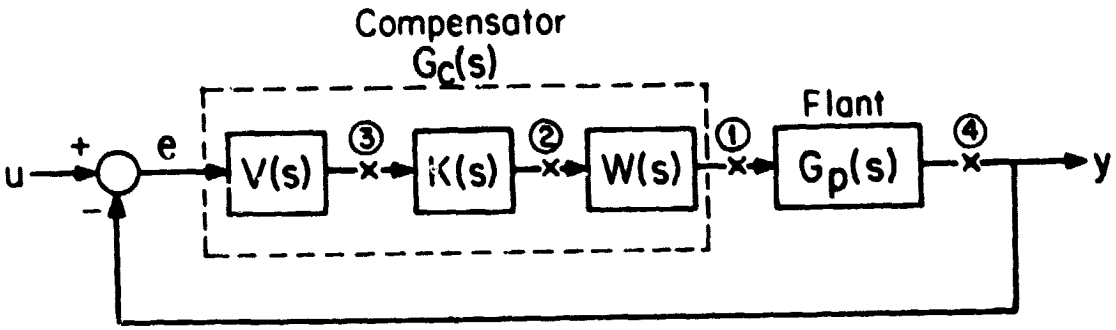

Fig. 2. Compensator used by INA and CL Methods

$$K(s) = \text{diag}[k_1(s), k_2(s), \ldots, k_n(s)] \quad . \tag{3}$$

If the loop transfer function calculated at point i, i=1,2,3,4, is denoted by $G_i(s)$, then

$$G_1(s) = (W(s)K(s)V(s))G_p(s) = G_c(s)G_p(s) \tag{4}$$

and

$$G_2(s) = K(s)(V(s)G_p(s)W(s)) = K(s)\hat{G}_p(s) \tag{5}$$

where we note that $G_2(s)$ is diagonal. The CL and INA methods use (5) to design the compensator $G_c(s)$, by selecting each $k_i(s)$ in K(s) as the appropriate robust compensator for each of the SISO systems represented by the diagonal elements of $\hat{G}_p(s)$, denoted $\hat{g}_{pii}(s)$. Thus, these

methods produce feedback control systems with good margins inside the compensator at point (2) in Fig. 2.

The key question is: when does this design methdology yield good margins at point (1), the input to the physical system? To determine the answer to this question, suppose that we insert the matrix $L_1(s)$ at point (1) to account for model uncertainty and determine the stability margins at the input to the physical system by placing bounds on the allowable $L_1(s)$. If we represent the equivalent model uncertainty at point (2) by $L_2(s)$ then the relationship between $L_1(s)$ and $L_2(s)$ is given by

$$L_2(s) = W^{-1}(s)L_1(s)W(s). \tag{6}$$

In chapter 3, the model error criterion (3.35) was used and is given in terms of both $L_i(s)$ or $\tilde{G}_i(s)$ and $G_i(s)$ by

$$E_i(s) = G_i^{-1}(s)[\tilde{G}_i(s) - G_i(s)] = L_i(s) - I \quad . \tag{7}$$

Thus, using (6) and (7), the tolerable model error at point (1) is related to that at point (2) by

$$E_2(s) = W^{-1}(s)E_1(s)W(s) \quad . \tag{8}$$

From (8) and the properties of singular values, we obtain

$$\sigma_{max}[E_2(s)] \leq c[W(s)]\sigma_{max}[E_1(s)] \tag{9}$$

where $c[W(s)]$ is the condition number[1] of $W(s)$ and is given by

[1] The condition number of a matrix is very large if the matrix is nearly rank deficient or almost singular.

$$c[W(s)] = \frac{\sigma_{max}[W(s)]}{\sigma_{min}[W(s)]} \geq 1 \quad . \tag{10}$$

Suppose that the model error $E_2(s)$ at point (2) of minimum magnitude $\sigma_{max}(E_2(s))$ that destabilizes the feedback system is such that equality holds in (9). Then the equivalent model error $E_1(s)$ at point (1) determined from (8) is of magnitude $\frac{1}{c[W(s)]}\sigma_{max}[E_2(s)]$ and also destabilizes the feedback system. Therefore, if the condition number $c[W(s)]$ is very large, the margins at point (1), i.e., at the input to the physical system, may be much smaller than those at point (2), inside the compensator.

The CL method selects $W(s)$ to be the matrix of eigenvectors of $G_p(s)$ and $V(s) = W^{-1}(s)$ when this possible choice for $W(s)$ is rational; otherwise, $W(s)$ is chosen to be as rational approximation of the matrix of eigenvectors of $G_p(s)$. Since, the designer has no control over $G_p(s)$, this choice of $W(s)$ does not guarantee that the condition number $c[W(s)]$ is near unity. Similary, the INA method seeks to find a rational $W(s)$ and $V(s)$ that diagonalize $G_p(s)$, (this is done numerically to obtain constant matrices $W(s)$ and $V(s)$) but there is no guarantee that $c[W(s)]$ is near unity. Similar conclusions may be drawn by breaking the feedback loop of Fig. 2 at points (3) and (4) and working with $V(s)$ rather than $W(s)$.

Therefore, these methods do not automatically produce robust controller designs. Indeed, in some cases they can lead to nearly unstable feedback systems (i.e., small stability margins at either input or output) if the diagonalizing matrices $W(s)$ and $V(s)$ have large condition

numbers at some frequency. They do produce good margins at a point inside the compensator but that is not the appropriate place to require good margins, from an engineering point of view. Doyle and Stein [43] give a simple example which exposes this deficiency.

6.3 The Principal Gain and Phase Analysis Method

This method [57] utilizes model error structure information to ensure stability of a perturbed feedback system. It uses the notions of principal gains, and principal phases of an nxn complex matrix A which are defined via its polar decomposition.

Definition (Polar Decomposition): Any nxn complex matrix A can be decomposed into a product given by

$$A = UH_R \tag{11}$$

or

$$A = H_L U \tag{12}$$

where U is a unitary matrix and, H_R and H_L are positive semidefinite hermitian matrices. The representation in (11) or (12) is called a polar decomposition of A.

Note that the polar decomposition in (11) and (12) are easily calculated from the singular value decomposition (SVD) of A as follows

$$A = (UV)(V^H \Sigma V) \tag{13}$$

and

$$A = (U\Sigma U^H)(UV) \tag{14}$$

where $A = U\Sigma V^H$ is the SVD of A.

Definition (Principal Gains and Phases): The principal gains of the matrix A in (11) (or (12)) are the eigenvalues of H_R (or H_L) which are identical to the singular values of A. The principal phases of A in (11) (or (12)) are the arguments of the eigenvalues of U in (11) and (12).

Since the eigenvalues of a unitary matrix are of the form $e^{j\theta_i}$, the identification of the θ_i as phases is obvious.

Definition (Spread of less than π): If the principal phases of a matrix, denoted ϕ_i, are such that the complex numbers $e^{j\phi_i}$ can all be contained strictly in a half-plane in the complex plane that has the origin of the complex plane on the boundary, then the principal phases are said to have a spread of less than π.

This is illustrated in Figs. 3 and 4.

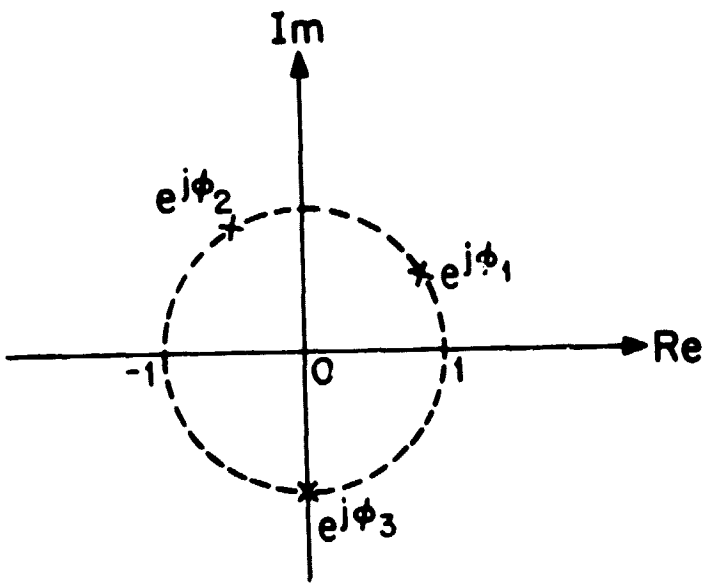

Fig. 3: Principal phases ϕ_i with a spread of more than π.

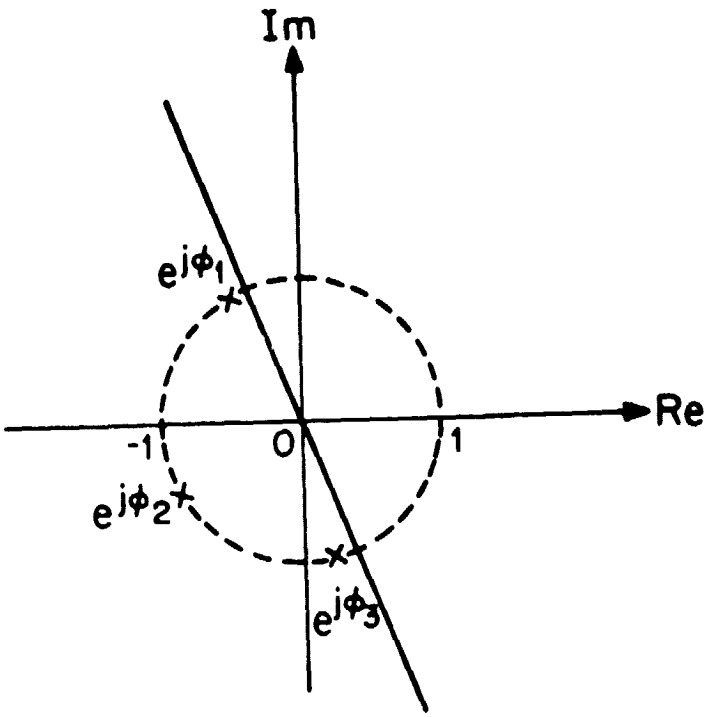

Fig. 4: Principal phases ϕ_i with a spread less than π

In the scalar case, the matrices H_R and H_L in (11) and (12) simply represent the magnitude of the scalar version of the matrix A and the matrix U becomes a scalar of the form $e^{j\theta}$ and thus the usual notion of the polar decomposition of a scalar is obtained.

The main theorem of PGP analysis will now be stated after some preliminary definitions. Using the usual notation that G(s) represents the mxm loop transfer matrix we define $G_{CL}(s)$ as the usual closed-loop transfer matrix obtained under unity feedback which is given by

$$G_{CL}(s) = (I+G(s))^{-1}G(s) \quad . \tag{15}$$

The model error criterion to be used is given by

$$E(s) \triangleq G^{-1}(s)[\tilde{G}(s) - G(s)] \tag{16}$$

where $\tilde{G}(s)$ as usual represents the perturbed-loop transfer matrix. Let the principal gains of $G_{CL}(j\omega)$ be denoted as $\alpha_i(\omega)$ where $0 \leq \alpha_i(\omega) \leq \alpha_{i+1}(\omega)$ and let the principal phases of $G_{CL}(j\omega)$ be denoted as $\theta_i(\omega)$ where $\theta_i(\omega) \leq \theta_{i+1}(\omega)$. Similarly let the principal gains of $E(j\omega)$ be denoted as $\delta_i(\omega)$ where $0 \leq \delta_i(\omega) \leq \delta_{i+1}(\omega)$ and let the principal phases of $E(j\omega)$ be denoted as $\varepsilon_i(\omega)$ where $\varepsilon_i(\omega) \leq \varepsilon_{i+1}(\omega)$.

Next, define the condition numbers $c_1(\omega)$ and $c_2(\omega)$ as

$$c_1(\omega) \triangleq \frac{\alpha_m(\omega)}{\alpha_1(\omega)} \geq 1 \tag{17}$$

where α_1 is the minimum singular value (or principal gain) and α_m is the maximum singular value (or principal gain) of G_{CL} and

$$c_2(\omega) = \frac{\delta_m(\omega)}{\delta_1(\omega)} \geq 1 \tag{18}$$

where δ_1 is the minimum singular value and δ_m is the maximum singular value of E. Also defined the quantity $\psi_m(\omega)$ as

$$\psi_m(\omega) = \tan^{-1}\left(\frac{[c_1(\omega) - 1]\, c_2(\omega)}{1 - [c_1(\omega)-1]c_2(\omega)}\right) \tag{19}$$

With these preliminary definitions the so-called Small Phase Theorem (SPT) of [57] may be stated.

Small Phase Theorem: The perturbed closed-loop system is stable if:

1. E(s) is stable.

2. $\{\theta_i(\omega)\}$ and $\{\theta_i(\omega) + \varepsilon_j(\omega)\}$ have a spread less than π for all ω and $i,j = 1,2,\ldots,m$

3. $[c_1(\omega) - 1]c_2(\omega) < 1$ for all ω

4. (a) $\theta_m(\omega) + \varepsilon_m(\omega) < \pi - \psi_m(\omega)$ for all ω

   and

   (b) $\theta_1(\omega) + \varepsilon_1(\omega) > \psi_m(\omega) - \pi$ for all ω

This theorem basically characterizes the tolerable model errors as those that do not introduce a significant amount of phase shift in the principal phases of $G_{CL}(j\omega)$ when perturbed by model error (condition 4). Conditions 2 and 3 place restrictions on the type of system and the type of model error that can be considered by the SPT. Condition 1 is simply a condition that automatically guarantees that the matrices G(s) and $\check{G}(s)$ have the same number of unstable poles. This theorem, as those presented in Chapter 4 of this thesis uses the structure of the error matrix $E(j\omega)$. However, the SPT does this by requiring restrictions on its principal phases $\varepsilon_j(\omega)$ in conditions 2 and 4, and, therefore is rather different from the characterization of model error in Theorems 4.1 and 4.2 in terms of the projection of the error matrix $E(j\omega)$ onto various one dimensional subspaces generated by the singular vectors of $I+G^{-1}(j\omega)$.

The main drawback of the SPT is that it cannot be applied in many cases of interest. This is illustrated by the restrictions condition 3 places on the system and the model error in the following two simple examples.

Example 1: The SPT does not apply when the closed-loop transfer matrix is given by

$$G_{CL}(s) = \text{diag}\left[\frac{10}{s+10} , \frac{1}{s+1}\right] \tag{20}$$

because the condition number $c_1(\omega)$ defined by (17) is

$$c_1(\omega) = \left[\frac{100(\omega^2+1)}{\omega^2+100}\right]^{\frac{1}{2}} > 2 \quad \text{for } \omega > 1.1 \tag{21}$$

and thus $[c_1(\omega) - 1]c_2(\omega) > 1$ for $\omega > 1.1$ since $c_2(\omega) \geq 1$ for any matrix $E(s)$. Hence, condition 3 of the SPT is violated. The loop transfer matrix $G(s)$ corresponding to $G_{CL}(s)$ in (20) is given by

$$G(s) = \text{diag}[\frac{1}{s+9} , \frac{1}{s}] \quad . \tag{22}$$

Example 1 demonstrates that closed-loop systems with input-output channels with widely differing bandwidths violate condition 3 of the SPT because $c_1(\omega) > 2$ for some frequency ω. In (20) the first input-output channel with transfer function $10/(s+10)$ has a bandwidth approximately 10 times as large as that of the second input-output channel with transfer function $1/(s+1)$. If $c_1(\omega)$ is to be less than 2 for all ω, it is necessary that all input-output channels of $G_{CL}(s)$ have roughly the same bandwidth or equivalently the same speed of response. This same restriction also applies to $G(s)$. Clearly, this restrictive condition eliminates many systems of interest from the point of view of robustness analysis via the SPT.

Example 2: Suppose $I+G^{-1}(j\omega)$ has the SVD given by

$$I+G^{-1}(j\omega) = U(j\omega)\Sigma(j\omega)V^H(j\omega) = \sum_{i=1}^{m} \sigma_i(j\omega)\underline{u}_i(j\omega)\underline{v}_i^H(j\omega) \tag{23}$$

where $\sigma_m(j\omega) = \sigma_{min}(j\omega)$. If the model error $E(j\omega)$ is such that for some ω_0, for which $\sigma_m(j\omega_0) \leq \sigma_m(j\omega)$ for all ω,

$$E(j\omega_0) = -\sigma_m(j\omega_0)\underline{u}_m(j\omega_0)\underline{v}_m^H(j\omega_0) \tag{24}$$

then from chapter 4 (equation 4.13) we know that the closed-loop feedback system is destabilized by the model error $E(s)$ but is stable for all model errors $E_0(j\omega)$ of magnitude $\sigma_{max}[E_0(j\omega)] < \sigma_{max}[E(j\omega_0)]$. That is, $E(j\omega_0)$ is the smallest destabilizing model error. However, condition 3 of SPT requires that

$$\frac{\sigma_{max}(E(j\omega))}{\sigma_{min}(E(j\omega))} = c_2(\omega) < \frac{1}{c_1(\omega)-1} \tag{25}$$

and thus since $E(j\omega_0)$ is singular $c_2(\omega_0) = +\infty$ and condition (25) is violated and thus also condition 3 of the SPT. Again, the SPT does not apply.

The results of the above example are significant because in a useful robustness analysis method it is very important to detect the <u>smallest</u> possible errors that may destabilize the feedback system and be able to distinguish them from model errors of equal magnitude that do not destabilize the feedback system. In many systems the smallest possible destabilizing errors may lead to a singular error matrix $E(j\omega)$ at some frequency. Note that even when $E(j\omega)$ is not singular, the inequality (25) is still <u>easily</u> violated if $c_1(\omega) \neq 1$ (i.e., all feedback loops do not have the same bandwidth as illustrated by Example 1).

These two examples have shown the SPT is a fairly restrictive theorem viewed from the robustness viewpoint. However, in certain cases, the SPT may be an easy way to most simply characterize a particular class of model errors.

6.4 Concluding Remarks

This chapter has briefly examined the characteristic loci (CL) and inverse Nyquist array (INA) control design procedures and shown that they do not guarantee good robustness properties of the resulting control system. The essential deficiency in these methods lies in the fact that they can only guarantee the desired stability margins at a point inside the compensator. The true stability margins at the interface between the physical plant and the compensator can be bounded in terms of the stability margins inside the compensator. This bound depends on the condition numbers of the matrices used to diagonalize the open-loop plant during the controller design procedure. If the condition numbers of these matrices are large, then the stability margins at the interface of the physical open-loop system and the compensator may be exceedingly small. When this happens, there is no presently known method to modify or correct the CL and/or INA designs based on information implicit in the diagonalizing matrices that have large condition numbers in order to obtain the desired robustness properties. Current research efforts[1] are being directed toward developing methods of diagonalizing $G_p(s)$ with rational transfer function matrices that are unitary for $s=j\omega$. This would guarantee that the margins that hold inside the compensator would also hold at the input or output to the physical system.

In contrast, to these aforementioned difficulties the LQG design procedure, utilizing the robustness recovery techniques discussed in

---

[1] Private communication with Professor Bernard Levy.

Chapter 5, does provide a systematic procedure to synthesize controllers that are robust or can be made robust if the nominal design model is minimum phase. Thus, if an LQG controller is evaluated for robustness and found lacking, there is a systematic way to restore the desired robustness properties and not merely trial and error in the redesign of the controller in an ad hoc manner. A drawback of LQG controllers is the large dimension of compensator states, often larger than necessary to meet performance and robustness objectives. However, in this era of microprocessor and VLSI implementation of control compensators the dimensionality of the compensator is not as crucial a problem, as was the case a few years ago. Current research [59] in the design of reduced order robust LQG controllers is progressing.

The other recently proposed principal gain and phase (PGP) frequency domain analysis discussed in this chapter ensures stability of a feedback system in the face of a special class of model uncertainty based on the model error matrix structure exhibited by its principal phases. It was shown however that this approach is not applicable to systems whose closed-loop speed of response in different input-output channels differ significantly. Furthermore, it was shown that PGP analysis requires a nonsingular error matrix. However, in Chapter 4 it was shown the smallest destabilizing model error matrix may be taken to be singular. Thus PGP analysis, cannot be applied to determine if a singular model error matrix is stabilizing or destabilizing. However, it must be said that it offers the potential in the case of model errors known to be of a small principal phase nature, to provide a relatively uncomplicated test for feedback system stability.

7. SUMMARY, CONCLUSIONS AND SUGGESTIONS FOR FUTURE RESEARCH

7.1 Summary

This thesis has addressed the following problem. Given a finite-dimensional linear-time invariant feedback control system designed using an inaccurate nominal model of the open-loop plant, how much and what kind of model error can the feedback system tolerate without becoming unstable? Thus, this thesis deals primarily with the evaluation of the robustness of stability of a feedback control system. This robustness evaluation is absolutely essential since all models of physical processes are only approximations to the actual relationship between the system inputs and outputs. In the single-input, single-output (SISO) case, this evaluation is readily accomplished using frequency domain plots, (e.g. using a Bode diagram) to display the behavior and characteristics of the feedback system. However, in the multiple-input, multiple-output (MIMO) case, many generalizations of the SISO methods have proved inadequate because they have not dealt with the MIMO system as a whole but as a sequence of SISO systems.

This thesis has avoided this deficiency by utilizing standard matrix theory concepts and methods appropriate for dealing with the MIMO case, namely the singular value decomposition (SVD) and properties of special types of matrices. These were discussed in Chapter 2, where the main problem solved was the determination of the nearest singular matrix, $\tilde{A}$, to a given nonsingular matrix, A, under certain constraints on $\tilde{A}$ - A. The solution to this problem (given in Problems A, B and C)

is fundamental to the control system robustness results of Chapters 3 and 4.

The basic formulation of the control system robustness problem was considered in Chapter 3 via a multivariable version of Nyquist's stability theorem. There, a fundamental robustness theorem (Theorem 3.2) was derived that implicitly characterized the class of perturbed models that would not destabilize the control system, in terms of the nonsingularity of the return difference matrix. Various robustness tests (Theorems 3.3 to 3.9), were then derived which can be used to test the nonsingularity of the return difference matrix for several types of model error criteria. These results were then related to the small gain theorem and some simple extensions for nonlinear feedback control system were presented that demonstrate that the basic robustness results of Chapter 3 are valid even when certain types of nonlinearities are introduced.

Chapter 4 heavily utilizes the results of chapter 2 in determining what types of model error will destablize a given feedback system. Model errors that tend to destabilize the feedback system are distinguished from those that tend to stabilize the feedback system by examining their structure as well as their magnitude. The key results, contained in Theorems 4.1, 4.2 and 4.3, show that the magnitude of the model error necessary to destabilize the feedback system may greatly increase if the class of model errors that can plausibly occur does not include model errors that are essentially alike in structure to the model error of minimum size that will destabilize the feedback system. This provides

an important characterization of the model errors that are important in feedback design. These types of model errors were then interpreted via block diagrams of the feedback system.

In Chapter 5, the robustness properties of control system designed using the linear-quadratic-gaussian (LQG) methodology were presented. Multiloop guaranteed gain, phase and crossfeed margins were obtained using the robustness theory of Chapter 3. The key results of Chapter 5 are contained in Theorems 5.2, 5.3 and 5.4 and their corollaries. These theorems showed that the guaranteed LQ robustness properties hold in a coordinate frame defined by the control weighting matrix (R) in the quadratic performance index. It was also shown that LQG control systems cannot automatically guarantee the same stability margins as the LQ state feedback regulator unless the internal model of the system embedded in the compensator Kalman filter is correct. This is a very restrictive condition and therefore robustness recovery procedures were outlined that do not require the compensator to have exact knowledge of the correct dynamic model of the system. These procedures allow LQG controllers to recover the robustness properties of LQ state-feedback controllers if the nominal open-loop plant is minimum phase.

Chapter 6 contrasts the frequency domain techniques for MIMO analysis and design (characteristic loci (CL), inverse-Nyquist array (INA) and principal gain and phase (PGP)), to the methods taken in this thesis and demonstrates that the CL and INA design methdologies do not ensure robust controller designs and that the PGP analysis is not able to determine the robustness of important classes of systems and model errors.

7.2 Conclusions and Suggestions for Future Research

A systematic procedure for the design of robust feedback control systems is the ultimate goal of any analysis of the robustness properties of feedback systems. The impact of the analysis techniques developed in this thesis upon controller design is obviously not that of a new method for obtaining a controller given a model of the plant. Rather, this thesis has dealt primarily with the characterization of model uncertainty and how it affects current design methodologies.

The theoretical impact of this analysis consists of the following developments:

- the formulation of a new robustness theorem that exposes the fundamental character of all robustness tests which can be derived from it.
- the unification of various robustness tests by the classification of the type of model error they bound
- the derivation of new robustness tests based on alternate types of model error criteria not previously considered in the literature
- the fundamentally new characterization of model error, which requires only a partial knowledge of the model error, based on its projections onto certain subspaces.

The design impact of this analysis is not as clearly defined and future research to develop design techniques is necessary. However, the design developments that seem possible are:

- controller redesign based on the model error structural characterization of model errors critical to stability

- model improvement to reduce model errors critical to stability

The controller redesign and model improvement go hand in hand. Once an initial design has been accomplished and the model errors critical to system stability are identified, these model errors can be incorporated into a new model and a new controller design, using this new model, may be performed explicitly taking into account the characteristics of the new model critical to system stability.

Other directions in future research that might prove productive are tied to specific design methodologies. For LQG controllers, the development of procedures for producing robust low order compensators from robust high order compensators would be highly desirable. To produce a robust reduced order compensator, the loop transfer matrices corresponding to the high order and reduced order compensators must be nearly alike. More precisely, if $G_h(s)$ is the loop transfer matrix resulting from the use of the high order compensator and $G_\ell(s)$ is the loop transfer matrix resulting from the use of the reduced order compensator then $G_\ell(s)$ should approximate $G_h(s)$ in such a way that $\sigma_{min}(I+G_\ell(s)) \approx \sigma_{min}(I+G_h(s))$ at or below the crossover frequency range and $\sigma_{min}(I+G_\ell^{-1}(s)) \approx \sigma_{min}(I+G_h^{-1}(s))$ at or above the crossover frequency range. This is basically a model reduction problem with the objective of matching singular values and singular vectors of $G_\ell(s)$ and $G_h(s)$ rather than matching step responses or other typical model reduction approximation criteria.

The basic appeal of the frequency domain design methods, namely the characteristic loci (CL) and inverse Nyquist array (INA) methods,

is that they, in many cases, produce lower order and simpler dynamic compensators than the LQG approach. However, as was demonstrated in Chapter 6, they do not automatically produce robust compensators because they use diagonalizing matrices, V(s) and W(s), with possibly large condition numbers to diagonalize the open-loop plant $G_p(s)$. This implies that the gain and phase margins at the physical input and output of the system may be much smaller than those in the diagonal coordinate system. This difficulty would be eliminated if V(s) and W(s) could be guaranteed to have condition numbers near unity and represent stable finite dimensional linear time-invariant systems. If V(s) and W(s) are chosen as the diagonalizing matrices from the SVD of $G_p(s)$ then they are unitary and have condition numbers of unity. However, with these choices for V(s) and W(s), neither V(s) nor W(s) represent stable finite dimensional linear-time invariant systems. Therefore, approximations to this choice of V(s) and W(s) must be sought which approximately diagonalize $G_p(s)$. This is basically a problem in realization theory. Further research is necessary to determine whether sufficiently accurate approximations of V(s) and W(s) (so that $G_p(s)$ is almost diagonal) will produce compensators of lower order than compensators obtained by state space design methods such as the LQG methodology. If not, then these frequency domain techniques would seem to lose their original appeal.

The above problems (the design of low order robust compensators via the LQG method or the frequency domain CL or INA methods) assume that the robustness analysis of a control system can be carried out. The value of this analysis depends crucially on the control system designer's ability to characterize the uncertainty in the open-loop

nominal design model in a particular mathematical fashion. Often, the characterization of model error by its magnitude alone is insufficient to guarantee the stability of the perturbed feedback system by the robustness tests of Chapter 3. In this case, more detailed information about the possible structure of the error transfer matrix, E(s), is needed in order to guarantee stability of the feedback system. The robustness tests of Chapter 4 require that the magnitude of the projection of the error matrix, E(s), onto the subspace spanned by $\underline{u}_n(s)\underline{v}_n^H(s)$ also be known. It is thus necessary to determine what magnitude of $<\underline{u}_n(s)\underline{v}_n^H(s)$, E(s)> constitutes a physically possible type of model error. If this model error E(s) gives rise to a perturbed system $\check{G}(s)$ that violates the basic physics of the underlying physical process then E(s) can be eliminated from consideration. However, the control system designer does not usually have information about the projections of E(s) onto subspaces and what magnitudes of these projections are physically feasible. This projection information must be somehow deduced from the information that he does have or is able to obtain about the nature of the model error.

Similar model error characterization problems are encountered if the principal gain and phase (PGP) analysis is used. Again, the structure of the model error contained in the minimum and maximum principal phases of the error matrix must be known. These quantities, like subspace projections, are not the kind of information about modelling error structure usually possessed by the control system designer. Often the type of information available about model error is determined indirectly by the knowledge of the acceptable range of parameter variations in a

parameterized state-space model. Alternatively, it may be determined indirectly from an available set of SISO Nyquist or Bode plots of measured transfer functions for certain input and output variables of the physical system under a number of different operating conditions. This type of information does not directly provide the model error structure information needed in the robustness analysis. It is therefore necessary to devise methods for determining the required structural information about model error. This information might be obtained by using a more detailed class of models representing truth models of the physical system and determining if the resulting model errors for this class of more detailed models can ever have projections onto certain subspaces or ever have principal phases outside some given range. On the other hand, frequency domain measurements in certain input-output directions might obtained from the physical system to determine what model error projections or principal phases are possible. More experience with practical applications is needed in order to determine how particular types of model error structure information may be ascertained.

Another area for future research is the robustness properties and stability margins for time delay systems and multi-sampling rate digital systems. LQG based regulators for time delay systems of the form $\dot{x}(t) = A_0 x(t) + A_1 x(t-\tau) + Bu(t)$ can be determined from the solution of Riccati-like equations. It is not unlikely that these regulators will have some inherent robustness properties as does the standard LQ regulator. However, continuous-time delay systems are infinite dimensional and mathematically complex and hence it is not clear what type of robustness results for these systems can be obtained. A possible approach to these

type of problems is to first consider the optimal regulator for discrete time delay systems of the form $\underline{x}_{k+1} = A_0\underline{x}_k + A_1\underline{x}_{k-n} + B\underline{u}_k$. These systems are finite dimensional and can by state augmentation be formulated as standard discrete time systems of the form $\tilde{\underline{x}}_{k+1} = \tilde{A}\tilde{\underline{x}}_k + \tilde{B}\underline{u}_k$. Thus, the optimal regulator for a delay system can be reformulated as standard optimal regulator problem. The robustness properties of this augmented standard optimal regulator may then be related to those of the regulator of the time delay system. If this approach proves useful, the analogous type of results for optimal regulators of continuous-time delay systems may be possibly developed in spite of the fact that these systems are infinite dimensional.

The robustness properties of multirate discrete time systems are closely associated with those of discrete time-delay systems and the use of multiple sampling rates in discrete time control systems is occurring more frequently in practical applications. However, there is a lack of robustness theory for this type of control system and most design is done on a heuristic basis. Sampled data systems, give rise to mathematically complex continuous-discrete hybrid operators if an precise description of their continuous time behavior is desired. Simple approximations are needed to describe this behavior in order to make design use of the robustness results obtained in terms of these operators. It would be practically very useful to obtain a method for determining the sampling rate in terms of the desired stability margins.

The mathematical tools used in the analysis of the sampled data systems are largely the same as for nonlinear systems. In nonlinear system stability analysis, one of the basic problems is not being able

characterize the nonlinear systems in a sufficiently simple manner that is practically useful. There are many stability results like those mentioned in section 3.10 but these results use only the grossest characterization of the feedback system operators and hence are often conservative. To sharpen these results, finer characterizations of the feedback system operators must be determined and at present only a few results of this type are known. These stability results involve the concept of invariant limit sets (Lyapunov stability theory) or utilize phase plane analysis. They are not part of input-output stability theory to which the results and framework of this thesis are most similar. The extension of the robustness results for nonlinear systems analogous to the extension of the robustness results for linear systems by use of model error structure in Chapter 4 is not possible because there is no orthogonal decomposition such as the SVD available for nonlinear systems. Other means of determining structure in nonlinear systems must be developed and at present it is not clear to the author how this may be accomplished.

REFERENCES

1. H.H. Rosenbrock, Computer-Aided Control System Design, London: Academic Press, 1974.

2. H.H. Rosenbrock, "Design of Multivariable Control Systems Using the Inverse Nyquist Array," Proc. IEEE, Vol. 116, pp. 1929-1936, Nov. 1969.

3. H.H. Rosenbrock, "Multivariable Circle Theorem," in Recent Mathematical Developments in Control, D.B. Bell, Ed. London: Academic Press, 1974.

4. A.G.J. MacFarlane and I. Postlethwaite, "The Generalized Nyquist Stability Criterion and Multivariable Root Loci," Int. J. Control, Vol. 25, pp. 81-127, Jan. 1977.

5. A.G.J. MacFarlane and I. Postlethwaite, "Characteristic Frequency Functions and Characteristic Gain Functions," Int. J. Control, Vol. 26, pp. 265-278, Aug. 1977.

6. H.W. Bode, Network Analysis and Feedback Amplifier Design, New York: Van Nostrand, 1945.

7. M.G. Safonov, Robustness and Stability Aspects of Stochastic Multivariable Feedback System Design, Ph.D. Dissertation, MIT, Rpt. No. ESL-R-763, Cambridge, MA., Sept. 1977, also MIT Press, 1980.

8. M.G. Safonov, "Tight Bounds on the Response of Multivariable Systems with Component Uncertainty," in Proc. Allerton Conf. on Communication and Computing, Monticello, Illinois, Oct. 4-6, 1978.

9. I.M. Horowitz, Synthesis of Feedback Systems, New York: Academic Press, 1963.

10. G. Zames, "On the Input-Output Stability of Time-Varying Nonlinear Feedback Systems - Part I:Conditions Using Concepts of Loop Gain Conicity and Positivity," IEEE Trans. Automatic Control, Vol. AC-11, pp. 228-238, April 1966.

11. G. Zames, "On the Input-Output Stability of Time-Varying Nonlinear Feedback Systems - Part II: Conditions Involving Circles in the Frequency Plane and Sector Nonlinearities," IEEE Trans. Automatic Control, Vol. AC-11, pp. 465-476, July 1966.

12. C.A. Desoer and M. Vidysager, Feedback Systems: Input-Output Properties. New York: Academic Press, 1975.

13. J.C. Willems, The Analysis of Feedback Systems, Cambridge, MA., MIT Press, 1971.

14. J.C. Doyle, "Robustness of Multiloop Linear Feedback Systems," Proc. 1978 IEEE Conf. on Decision and Control, San Diego, CA, January 10-12, 1979.

15. R. DeCarlo and R. Saeks, "The Encirclement Condition an Approach Using Algebraic Topology," Int. J. Control, Vol. 26, pp. 279-287, 1977.

16. R. DeCarlo, J. Murray and R. Saeks, "Multivariable Nyquist Theory," Int. J. Control, Vol. 25, pp. 657-675, 1977.

17. R. Saeks and R. DeCarlo, "Stability and Homotopy," in Alternatives for Linear Multivariable Control, Eds. M. Sain, J. Peczkowski and J. Melsa, Chicago: National Engineering Consortium, 1978.

18. M.G. Safonov and M. Athans, "A Multiloop Generalization of the Circle Stability Criterion," Proc. of Twelfth Annual Asilomar Conf. on Circuits, Systems and Computers, Pacific Grove, Calif., Nov. 6-8, 1978.

19. A.J. Laub, "Computational Aspects of Singular Value Decomposition and Some Applications," Proc. Allerton Conf. on Communication, Control and Computing, Monticello, Illinois, Oct. 4-6, 1978.

20. H.H. Rosenbrock and P.D. McMorran, "Good, Bad, or Optimal?" IEEE Trans. Automatic Control, Vol. AC-16, pp. 552-553, December 1971.

21. R.E. Kalman, "When is a Linear Control Systems Optimal?", Trans. ASME Ser. D: J. Basic Eng., Vol. 86, pp. 51-60, March 1964.

22. B.D.O. Anderson and J.B. Moore, Linear Optimal Control. Englewood Cliffs, N.J.: Prentice-Hall, Inc., 1971.

23. B.D.O. Anderson, "The Inverse Problem of Optimal Control," Stanford Electronics Laboratories Technical Report No. SEL-66-038 (T.R. No. 6560-3), Stanford, Calif., April 1966.

24. J.B. Cruz, Jr., and W.R. Perkins, "A New Approach to the Sensitivity Problem in Multivariable Feedback System Design," IEEE Trans Automatic Control, Vol. AC-9, pp. 216-233, July, 1964.

25. M.G. Safonov and M. Athans, "Gain and Phase Margin for Multiloop LQG Regulators," IEEE Trans. Automatic Control, Vol. AC-22, pp. 173-179, April, 1977.

26. P.K. Wong, On the Interaction Structure of Multi-Input Feedback Control Systems, M.S. Thesis, M.I.T., Cambridge, MA., Sept. 1975.

27. P.K. Wong and M. Athans, "Closed-Loop Structural Stability for Linear-Quadratic Optimal Systems," IEEE Trans. Automatic Control, Vol. AC-22, pp. 94-99, Feb. 1977.

28. B.D.O. Anderson, "Stability Results for Optimal Systems," Electron. Lett., Vol. 5, p. 545, Oct., 1969.

29. S. Barnett and C. Storey, "Insensitivity of Optimal Linear Control Systems to Persistent Changes in Parameters," Int. J. Control, Vol. 4, pp. 179-184, 1966.

30. C.A. Harvey, "On Feedback Systems Possessing Integrity with Respect to Actuator Outages," In Recent Developments in the Robustness Theory of Multivariable Systems, Ed. N.R. Sandell, Jr., LIDS, Report No. LIDS-R-954, M.I.T., Cambridge, MA., Aug. 1979.

31. P. Molander and J.C. Willems, "Robustness Designs by State Feedback,"... in Recent Developments in the Robustness Theory of Multivariable Systems, Ed. N.R. Sandell, Jr., Laboratory for Information and Decision Systems, Report No. LIDS-R-954, M.I.T., Cambridge, MA., Aug. 1979.

32. M.G. Safonov and M. Athans, "Robustness and Computational Aspects of Nonlinear Stochastic Estimators and Regulators," IEEE Trans. Automatic Control, Vol. AC-23, pp. 717-725, Aug. 1978.

33. J.C. Doyle, "Guaranteed Margins for LQG Regulators," IEEE Trans. Automatic Control, Vol. AC-23, pp. 756-757, Aug. 1978.

34. A.E. Bryson, Random Problems in Control Theory, Stanford University, Report SUDAAR No. 447, Sept. 1972.

35. J.C. Doyle and G. Stein, "Robustness with Observers," IEEE Trans. Automatic Control, Vol. AC-24, Aug. 1979.

36. H. Kwakernaak, "Optimal Low-Sensitivity Linear Feedback Systems," "Automatica, Vol. 5, May, 1969.

37. J.R. Dowdle, Robust Observer Based Compensator, Ph.D. Phesis, M.I.T. Cambridge, MA., Aug. 1979.

38. B. Noble, Applied Linear Algebra, Englewood Cliffs, N.J.: Prentice-Hall, Inc., 1969.

39. C.L. Lawson and R.J. Hanson, Solving Least Squares Problems, Englewood Cliffs, N.J.: Prentice-Hall, Inc., 1974.

40. J.H. Wilkinson and C. Reinsch, Handbook for Automatic Computation, II, Linear Algebra, ed. F.L. Bauer, et.al., New York: Springer-Verlag, 1971.

41. M. Athans, "The Role and Use of the Stochastic Linear-Quadratic-Gaussian Problem in Control System Design," IEEE Trans. Automatic Control, Vol. AC-16, pp. 529-552, Dec. 1971.

42. J.B. Lewis, Automotive Engine Control: As Linear-Quadratic Approach, S.M. Thesis, Laboratory for Information and Decision Systems, M.I.T., Cambridge, MA., March, 1980.

43. J.C. Doyle and G. Stein, "Multivariable Feedback Design: Concepts for a Classical/Modern Synthesis", IEEE Trans. Automatic Control, Vol. AC-26, No. 1, Feb. 1981.

44. J.H. Wilkinson, The Algebraic Eigenvalue Problem, Clarendon Press, 1965.

45. P. Molander and J.C. Willems, "Synthesis of State Feedback Control Laws with a Specified Gain and Phase Margin", IEEE Trans. on Automatic Control, Vol. AC-25, No. 5, October 1980.

46. S.M. Chan, Small Signal Control of Multiterminal DC/AC Power Systems, Ph.D. Disseration, Laboratory for Information and Decision Systems, M.I.T., Cambridge, MA., June, 1981.

47. M.F. Barrett, Conservatism with Robustness Tests for Linear Feedback Systems, Ph.D. Dissertation, Unversity of Minnesota, June 1980.

48. N.R. Sandell, Jr., "Robust Stability of Systems with Application to Singular Perturbation Theory", Automatica, Vol. 15, No. 4, July, 1979.

49. A.J. Laub, "An Inequality and Some Computations Related to the Robust Stability of Linear Dynamic Systems", IEEE Trans. Auto. Control, Vol. AC-24, April 1979.

50. R.W. Brockett, Finite Dimensional Linear Systems, John Wiley and Sons, Inc., 1970.

51. N.A. Lehtomaki, N.R. Sandell, Jr. and M. Athans, "Robustness Results in Linear-Quadratic Gaussian Based Multivarable Control Designs", IEEE Trans. Automatic Control, Vol. AC-26, No. 1, Feb. 1981.

52. R.V. Churchill, Complex Variables and Applications, McGraw-Hill, New York, 1960.

53. V.C. Klema and A.J. Laub, "The Singular Value Decomposition: Its Computation and Some Applications", IEEE Trans. Automatic Control, Vol. AC-25, No. 2, April, 1980.

54. J.J. Dongarra et al., LINPACK User's Guide. Philadelphia, PA: SIAM, 1979.

55. G. Strang, Linear Algebra and Its Applications, Academic Press, New York, 1976.

56. A.G.J. MacFarlane and B. Kouvaritakis, "A Design Technique for Linear Multivariable Feedback Systems", Int. J. Control, Vol. 25, pp. 837-879, 1977.

57. I. Postlethwaite, J.M. Edmunds and A.G.J. MacFarlane, "Principal Gains and Phases in the Analysis of Linear Multivariable Feedback Systems", IEEE Trans. Automatic Control, Vol. AC-26, No. 1, Feb. 1981.

58. G. Stein and N.R. Sandell, Jr., Classical and Modern Methods for Control System Design, Notes of Course 6.291 offered in the Spring of 1979, Dept. of Electrical Engineering and Computer Science, MIT, Cambridge, MA.

59. D. Gangsaas, U. Ly and D.C. Norman, "Practical Gust Load Alleviation and Flutter Suppression Control Laws Based on a LQG Methodology", AIAA 19th Aerospace Sciences Meeting, St. Louis, Missouri, Jan. 1981, Paper 81-0021.